DESIGN PARADIGM

Air Sparging: Technology Transfer and Multi-Site Evaluation

ESTCP Project ER-9808

August 2002

Andrea Leeson, Ph.D.
SERDP/ESTCP

Paul C. Johnson, Ph.D.
Cristin L. Bruce, Ph.D.
Arizona State University

Richard L. Johnson, Ph.D.
Illa L. Amerson, Ph.D.
Oregon Health and Science University

Catherine M. Vogel
Noblis, Energy & Environmental Sustainability

Robert E. Hinchee, Ph.D.
IST

Michael Marley
XDD, LLC

Tom Peargin
Chevron Corporation

Christopher T. Coonfare
Rick D. Gillespie
Battelle Memorial Institute

This document has been approved for public release.

Environmental Security Technology Certification Program

TABLE OF CONTENTS

LIST OF TABLES III

LIST OF FIGURES III

ABBREVIATIONS AND ACRONYMS IV

ACKNOWLEDGEMENTS V

1.0 INTRODUCTION 2

2.0 BASIS, PHILOSOPHY, AND OVERVIEW OF THE AIR SPARGING DESIGN PARADIGM 4

3.0 SITE CHARACTERIZATION 5

4.0 AIR SPARGING APPLICATION: INITIAL SCREENING OF TECHNOLOGIES 8

4.1 QUESTION 1: DOES EXPERIENCE SUGGEST THAT AIR SPARGING COULD BE SUCCESSFUL AT THIS SITE? 8

4.2 QUESTION 2: FOR WHAT INJECTION WELL SPACINGS WOULD AIR SPARGING BE PRACTICABLE? 12

4.3 QUESTION 3: WHAT ARE REASONABLE PERFORMANCE EXPECTATIONS FOR THIS AIR SPARGING SYSTEM? 12

5.0 PILOT TESTING 15

5.1 PILOT TEST EQUIPMENT 17

5.2 PILOT TEST ACTIVITIES 17

5.2.1 Baseline Sampling (PT1) 19

5.2.2 Air Injection Flow Rate and Injection Pressure (PT2) 19

5.2.2 Air Injection Flow Rate and Injection Pressure (PT2) 19

5.2.3 Groundwater Pressure Measurements During Air Sparging Start-Up and Shutdown (PT3) 20

5.2.4 Helium Distribution and Recovery Test (PT4) 21

5.2.4.1 Tracer Test to Assess Recovery of Air Sparging Air by an SVE System 21

5.2.4.2 Tracer Test Procedure to Determine the Distribution of Air Sparging Air at the Water Table Without an SVE System (or with Co-Located SVE and Air Sparging Wells) 23

5.2.5 Soil Gas Monitoring (PT5) 23

5.2.6 Dissolved Oxygen Monitoring (PT6) 24

5.2.7 Other Qualitative Observations 24

5.2.8 Site-Specific Design Approach 25

5.2.8.1 SF_6 Distribution Test (PT7) 25

5.2.8.2 Geophysical Tests (PT8) 25

6.0 SYSTEM DESIGN 26

7.0 AIR SPARGING SYSTEM MONITORING 28

8.0 SUMMARY 29

9.0 REFERENCES 30

APPENDIX A: ADVANCES IN IN SITU AIR SPARGING/BIOSPARGING A-1

APPENDIX B: USE OF AN SF_6-BASED DIAGNOSTIC TOOL FOR ASSESSING AIR DISTRIBUTIONS AND OXYGEN TRANSFER RATES DURING IAS OPERATION B-1

APPENDIX C: A MULTI-TRACER PUSH-PULL DIAGNOSTIC TEST FOR ASSESSING THE CONTRIBUTIONS OF VOLATILIZATION AND BIODEGRADATION DURING IN SITU AIR SPARGING C-1

APPENDIX D: APPLICATION OF THE IN SITU AIR SPARGING DESIGN PARADIGM TO A BTEX SOURCE ZONE AT THE NAVAL BASE VENTURA COUNTY, PORT HUENEME SITE CALIFORNIA D-1

APPENDIX E. DIAGNOSIS OF IN SITU AIR SPARGING PERFORMANCE USING GROUNDWATER PRESSURE CHANGES DURING STARTUP AND SHUTDOWN E-1

APPENDIX F: HELIUM TRACER TESTS FOR ASSESSING AIR RECOVERY AND AIR DISTRIBUTION DURING IN SITU AIR SPARGING F-1

LIST OF TABLES

Table 1. Members of the Expert Panel on Air Sparging 2
Table 2. Sample Air Sparging Technology Screening Input Summary Table 9
Table 3. Summary of Pilot Test Activities 16

LIST OF FIGURES

Figure 1. Schematic Diagram of a Simplistic In Situ Air Sparging System Combined with Soil Vapor Extraction 3
Figure 2. Sequence of Activities During Implementation of the Air Sparging Design Paradigm 6
Figure 3. Cross-Section (A) and Plan (B) Views of a Sample Pilot Test Layout 18
Figure 4. Helium Tracer Test for Assessing Air Sparging Air Recovery in an Unstratified Setting (A) and a Stratified Setting (B) 22
Figure 5. Schematic Diagram Illustrating a Helium Tracer Test to Assess Air Distribution in the Absence of an SVE System 24

ABBREVIATIONS AND ACRONYMS

AFB	Air Force Base
AFRL/MLQE	Airbase and Environmental Technology Division
API	American Petroleum Institute
ASTM	American Society for Testing and Materials
bgs	below ground surface
BTEX	benzene, toluene, ethylbenzene, and xylenes
CFB	Canadian Forces Base
DNAPL	dense nonaqueous phase liquid
DO	dissolved oxygen
DoD	Department of Defense
DOE	Department of Energy
EAFB	Eielson Air Force Base
ECD	electron capture detector
ESTCP	Environmental Security Technology Certification Program
GC	gas chromatograph
HAFB	Hill Air Force Base
HNTS	hydrocarbon national test site
IAS	in situ air sparging
ID	inner diameter
MTBE	methyl tert-butyl ether
NAPL	nonaqueous phase liquid
NAVFAC	Naval Facilities Engineering Command
NAVFAC- ESC	U.S. Naval Facilities Engineering Service Center
NBVC	Naval Base Ventura County
NETDP	National Environmental Technology Demonstration Program
NETTS	National Environmental Technology Test Site
NEX	Naval Exchange
R&D	research and development
SCFM	standard cubic feet per minute
SERDP	Strategic Environmental Research and Development Program
SF_6	sulfur hexafluoride
SVE	soil vapor extraction
TCE	trichloroethene
TPH	total petroleum hydrocarbon
UHP	ultra-high purity
USEPA	U.S. Environmental Protection Agency
UST	underground storage tank
VOA	volatile organic analysis

ACKNOWLEDGEMENTS

The authors would like to thank John Wilson of the Robert S. Kerr Laboratory, U.S. Environmental Protection Agency, for the original idea for the development of this Design Paradigm. The authors also would like to thank the members of the Expert Panel for providing extensive input into this document. Members of the Expert Panel included:

Larry Acomb
Geosphere Inc.

David H. Bass
Fluor Daniel GTI

Brad Billings
Billings & Associates, Inc.

Jim Gonzales
AFCEE/ERT

Harley Hopkins
American Petroleum Institute

Minoo Havanmardian
Amoco Research Center

Lawrence Libelo
U.S. Air Force

Mike Marley
XDD, LLC

David McWhorter
Colorado State University

Colonel Ross N. Miller
U.S. Air Force

Sheldon Nelson
Chevron

Ed Payne
Mobil

Tom Peargin
Chevron

Neal Thomson
University of Waterloo

John Wilson
U.S. Environmental Protection Agency

This document is a product of the research and development efforts sponsored by the U.S. Air Force Armstrong Laboratory and the U.S. Naval Facilities Engineering Service Center. The field research and data analysis was conducted by Battelle Memorial Institute, Arizona State University, Oregon Graduate Institute, Parsons Engineering-Science, and Colorado State University.

AIR SPARGING DESIGN PARADIGM

This document is a product of the air sparging research and development (R&D) efforts sponsored by the U.S. Air Force Research Laboratory, Airbase and Environmental Technology Division, Tyndall Air Force Base (AFB), Florida. This project has been funded by the Airbase and Environmental Technology Division (AFRL/MLQE), the Strategic Environmental Research and Development Program (SERDP), the Environmental Security Technology Certification Program (ESTCP), and the U.S. Naval Facilities Engineering Service Center (NAVFAC-ESC).

The Airbase and Environmental Technology Division, an element of the Air Force Research Laboratory, is the Air Force's lead laboratory for airbase and environmental quality research and development. This Division provides technologies for Air Force commanders to improve airbase operability capabilities and to reduce environmental impacts and costs of ownership, while enhancing worldwide airbase and environmental quality.

SERDP and ESTCP are the Department of Defense's (DoD) corporate environmental R&D programs, planned and executed in full partnership with the Department of Energy (DOE) and the U.S. Environmental Protection Agency (USEPA), with participation by numerous other federal and non-federal organizations. Within their broad areas of interest, the Programs focus on cleanup, compliance, conservation, and pollution prevention technologies. The goal of ESTCP is to demonstrate and validate innovative, cost-effective, environmental technologies, and to implement and commercialize DoD-required technologies.

The NAVFAC-ESC is the Navy's center for specialized facilities engineering and technology. Products and services include shore, ocean, and waterfront facilities; environment; amphibious and expeditionary operations; and energy and utilities. As a member of the Naval Facilities Engineering command (NAVFAC) team, they provide worldwide support to Navy engineering activities, fleet and shore activities, Marine Corps, and other DoD agencies. NAVFAC-ESC provides solutions to problems through engineering, design, construction, consultation, test and evaluation, technology implementation, and management support.

The results from air sparging laboratory and field studies have been used to produce this Design Paradigm. An Expert Panel was formed composed of researchers from academia and industry who have extensive experience in air sparging. The members of the Expert Panel, shown in Table 1, have provided their input to the research and production of the Design Paradigm throughout this study.

The first draft of this document was based on field studies conducted at Port Hueneme, California, a national test location designated through SERDP as a SERDP National Environmental Technology Test Site (NETTS) location. The NETTS mission is to provide well-characterized locations for comparative demonstration and evaluation of innovative technologies performing environmental characterization, cleanup, and monitoring. This final document incorporates data from additional sites studied as part of the ESTCP-funded Multisite Air Sparging Study.

The Design Paradigm provides details on air sparging principles; site characterization; pilot testing; system design, installation, and operation; and system monitoring. The Design Paradigm provides guidance for both standard designs, as well as more complex designs, and provides decision points to help users choose the appropriate level of sophistication for their sites. Use of the Design Paradigm is illustrated

Table 1. Members of the Expert Panel on Air Sparging

Larry Acomb Geosphere, Inc.	David McWhorter Colorado State University
David H. Bass Fluor Daniel GTI	Colonel Ross N. Miller U.S. Air Force
Brad Billings Billings & Associates, Inc.	Sheldon Nelson Chevron
Jim Gonzales AFCEE/ERT	Ed Payne Mobil
Harley Hopkins American Petroleum institute	Tom Peargin Chevron
Minoo Havanmardian Amoco Research Center	Neal Thomson University of Waterloo
Lawrence Libelo U.S. Air Force	John Wilson U.S. EPA
Mike Marley XDD, LLC	

through presentation and interpretation of data collected from the field study sites, as well as from results of controlled physical model studies.

The following sections provide an overview of air sparging in general and this Design Paradigm specifically, followed by a discussion of site characterization, air sparging application, pilot testing, system design, and system monitoring.

1.0 INTRODUCTION

As shown in Figure 1, air sparging generally involves the injection of air into an aquifer through vertical or horizontal wells. In situations where contaminant vapor recovery is necessary (e.g., as required by regulation, or in situations where vapor migration could cause adverse impacts), air sparging systems are coupled with soil vapor extraction (SVE) systems. Historically, practitioners have installed air sparging systems to: (1) treat immiscible contaminant source zones at or below the capillary fringe; (2) remediate dissolved contaminant plumes; and (3) provide barriers to prevent dissolved contaminant plume migration. Air sparging systems are also now being incorporated into novel aquifer bioremediation schemes for the delivery of other gases (e.g., oxygen, hydrogen, propane), and they have also been used as a means of improving air distribution for bioventing applications targeting near-capillary fringe soils.

Some practitioners implement a variation of air sparging that they term “biosparging”. In practice, the term biosparging is frequently used to refer to air sparging systems when the intent is to operate without an SVE

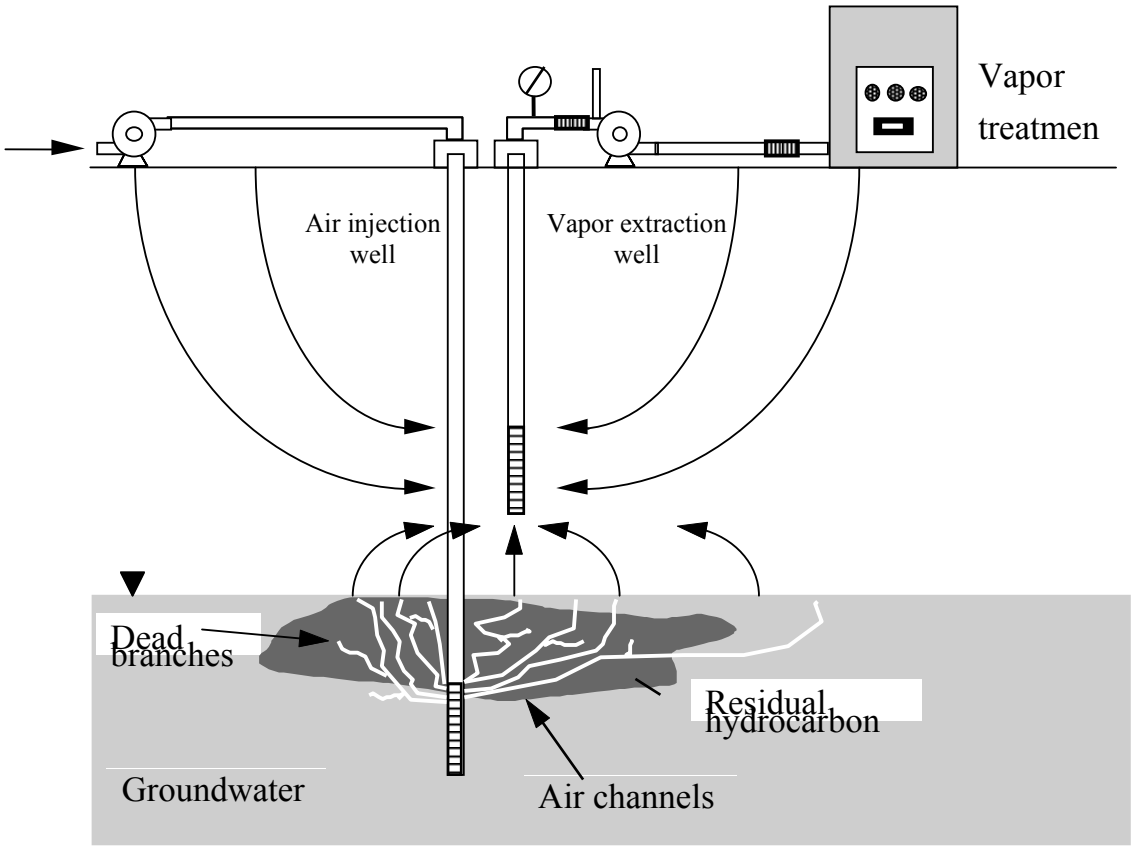

Figure 1. Schematic Diagram of a Simplistic In Situ Air Sparging System Combined with Soil Vapor Extraction

system. While some practitioners consider biosparging to be a unique technology that emphasizes biodegradation over volatilization, we consider it to be only a particular mode of air sparging operation. Air sparging/biosparging systems can be operated safely without accompanying SVE systems in many settings (e.g., remote locations, locations where sufficient vapor biodegradation occurs in the vadose zone, or locations where the volatilization rate is such that soil gas concentrations are below levels of concern). Practitioners, however, are cautioned that the potential consequences of improper vapor management are severe (e.g., explosions), and so the need for an SVE system should always be evaluated on a site-specific basis.

The use of air sparging has increased rapidly since the early 1990s. Based on informal surveys of underground storage tank (UST) regulators, it is now likely to be the most practiced engineered in situ remediation option when targeting the treatment of hydrocarbon-impacted aquifers. The feasibility assessment, pilot testing, design, and operation of air sparging systems has remained largely empirical, with variability in approaches by different practitioners (Bruell et al., 1997; Johnson et al., 1993; Johnson et al., 1997; U.S. EPA, 1992). Since the mid-1990s, much research has been devoted to gaining a better understanding of air sparging systems; however, as discussed in P.C. Johnson et al. (2000) (Appendix A), it appears that valuable knowledge gained from these studies has yet to be integrated into practice, and many of the current approaches to feasibility assessment, pilot testing, design, and operation show a lack of appreciation for the complexity of the phenomena and the sensitivity of the technology to design and operating conditions.

In the mid-1990s, the U.S. Air Force Research Laboratory, Airbase and Environmental Technology Division, Tyndall AFB initiated an air sparging project funded by the AFRL/MLQE, SERDP, and NAVFAC-ESC. This project was conducted by the authors of this article, with input and review from an expert panel consisting of practitioners, program managers, and members of academia (Table 1). Under this project, both laboratory- and field-scale experiments were conducted, and the results of the individual studies have been, and continue to be reported elsewhere (Amerson, 1997; Bruce et al., 2000a [Appendix B]; Amerson-Treat et al., 2000 (Appendix C); Bruce et al., 1998; Johnson et al., 1999; Rutherford and Johnson, 1996). The ultimate goal of this project, however, has been the development of a technically defensible and practicable Air Sparging Design Paradigm.

The following section provides a discussion of the basis for the Design Paradigm and a presentation of the general philosophy involved in the development of the guidance provided herein. In addition, an overview of the Design Paradigm is provided as guidance for utilizing this document.

2.0 BASIS, PHILOSOPHY, AND OVERVIEW OF THE AIR SPARGING DESIGN PARADIGM

P.C. Johnson et al. (2000) (Appendix A) reviewed air sparging-related studies appearing in the literature since the mid-1990s, identified some of the key lessons learned, and then discussed their implications for practice. Those lessons learned form the underlying basis for this Design Paradigm, and readers are referred to that article for a better appreciation of the range of air sparging studies and results that have been considered. Of particular note for this Design Paradigm are the following:

- The three most significant factors affecting air sparging performance are:
  - The air distribution in the target treatment zone
  - The distribution (location and concentration) of contaminants relative to the air distribution
  - The contaminant characteristics (composition and chemical properties).
- All other factors being equal, remediation is more effective in settings having a higher density of air channels in the treatment zone.
- Given current site assessment technologies and the sensitivity of air distributions to subtle changes in soil structure, it is unlikely that air distributions can be predicted, except in a gross sense for the most simple geologies (e.g., highly permeable and homogeneous settings, and settings with large macroscale heterogeneities such as clay layers in otherwise sandy soils).
- At this time, long-term air sparging performance (cleanup levels, cleanup times, etc.) cannot be predicted reliably from data collected during short-term pilot tests.

As a result, this air sparging Design Paradigm reflects the following philosophy:

- Given the importance of the air distribution and our inability to predict it, the actual air distribution in the target treatment zone should be characterized during the pilot-testing and full-scale implementation phases.

- The degree to which the air distribution is characterized at the pilot test-scale should be balanced by the system design. For example, a high degree of uncertainty in the air distribution at the pilot-scale level can be compensated for by a high density of air injection wells at the full-scale level. Conversely, distances between injection wells at the full-scale level can be optimized (and the number of wells minimized) when the air distribution is more fully characterized at the pilot-scale level.

- Pilot-scale testing activities should focus on looking for indicators of infeasibility (i.e., clear indicators that air sparging will not be successful), in addition to characteristics of the air distribution.

The sequence of activities involved in this Design Paradigm is presented in Figure 2. The overlying framework is similar to that generally used for other technologies in that there are site characterization, technology screening, pilot testing, design, and implementation steps. However, there are significant differences between this Air Sparging Design Paradigm and more traditional design approaches for other in situ technologies. For example, there are two parallel tracks that users may follow in the pilot testing and design stages. These are labeled the "Standard" and "Site-Specific" approaches. In the first, the user chooses to invest less in air distribution characterization at the pilot-scale level, but then compensates for this by installing a relatively dense network of closely spaced air sparging wells. In the second, the user performs a more detailed air distribution characterization at the pilot-scale level in the hopes of being able to relax the spacing between air sparging wells. Thus, a user has more flexibility in choosing the pilot-scale testing activities in this Design Paradigm; however, this comes with the responsibility of having to ensure that these are consistent with the degree of conservatism adopted in the final design.

In addition, this Air Sparging Design Paradigm reflects a combination of theory and empiricism, and the acceptance that, prior to full-scale implementation, there is significant uncertainty in the degree and rate of cleanup that might be achieved at any site. These differences in this Design Paradigm are simply a reflection of the complexity of the technology, its sensitivity to differences in subsurface conditions, and our inability at this time to confidently predict system performance.

3.0 SITE CHARACTERIZATION

Potential air sparging sites undergo one or more phases of site characterization. To minimize inefficiency, data collection should be focused on creating a defensible site conceptual model. This is often best communicated through a series of graphics (e.g., cross sections and plan view maps) showing the hydrogeologic setting (soil types, depth to groundwater, etc.), locations of key physical features (tanks, sewers, wells, etc.), and the approximate extent of source zone and dissolved plume contamination. The specific site characterization tools, sampling methods, and analyses are often dictated by regulatory guidance, and it is not our intent to review these here. Instead, we wish to focus on that information that is necessary for air sparging applications and data that might not be normally collected during site characterization.

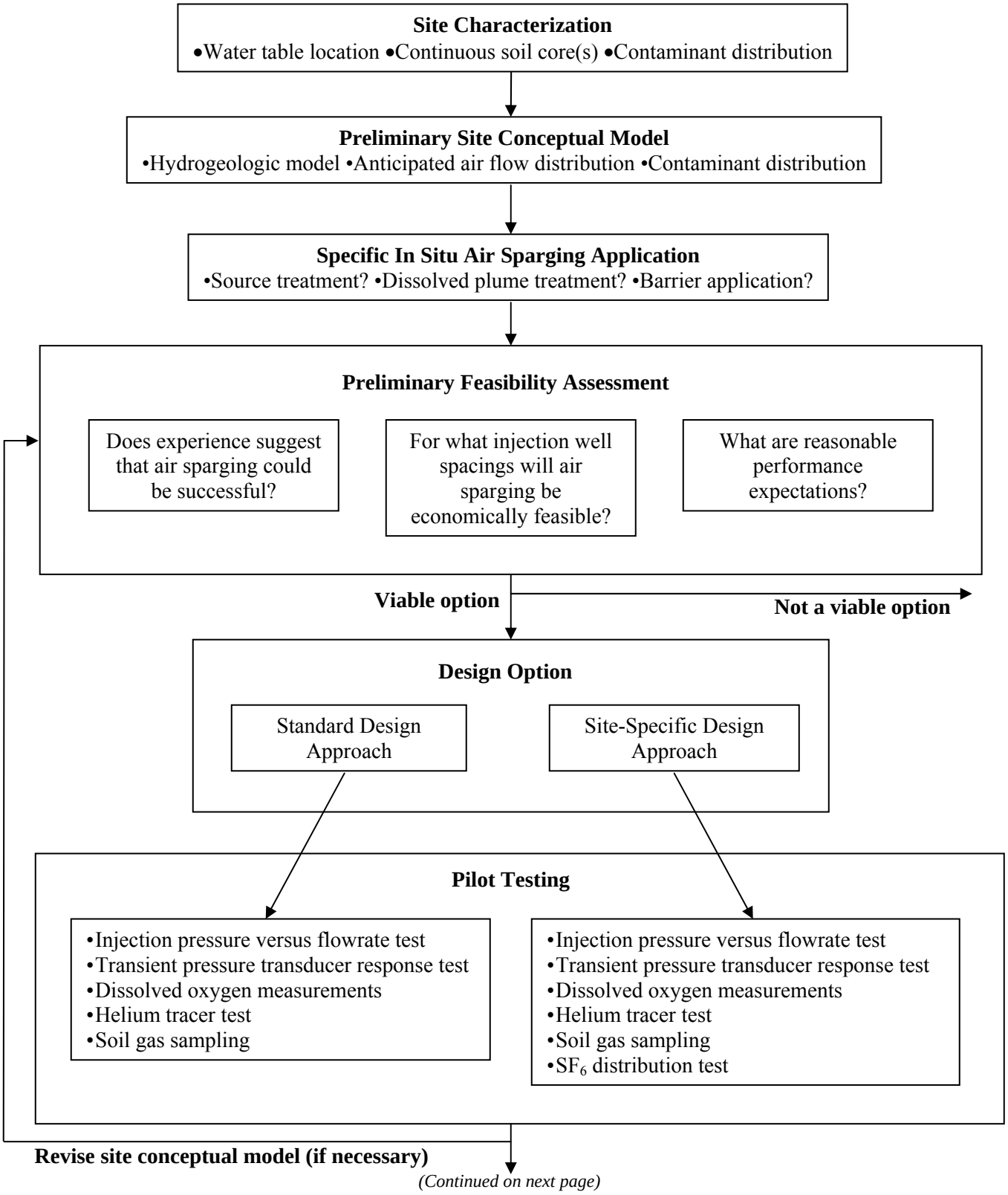

Figure 2. Sequence of Activities During Implementation of the Air Sparging Design Paradigm

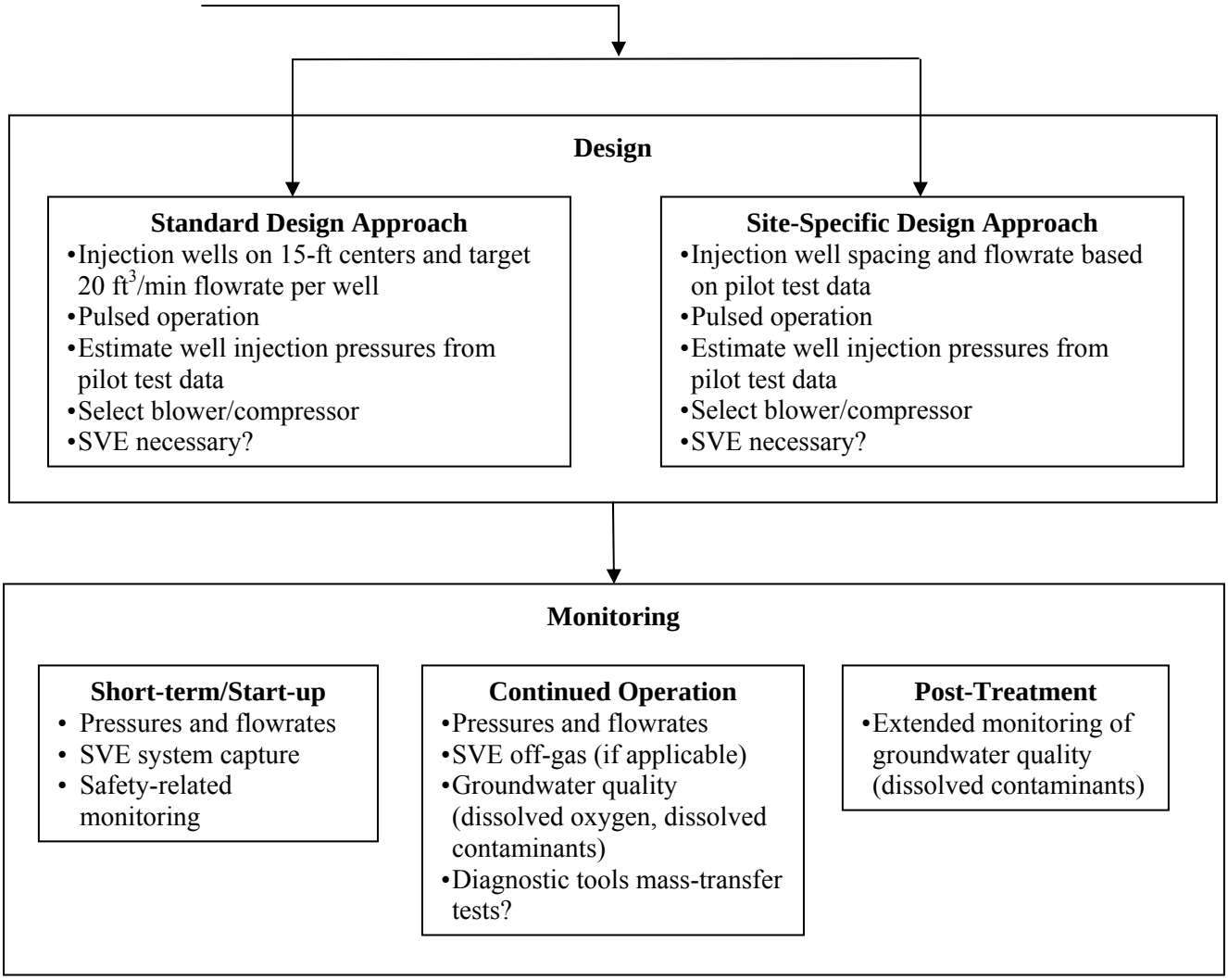

Figure 2. Sequence of Activities During Implementation of the Air Sparging Design Paradigm (continued)

For air sparging applications, it is critical to adequately characterize the subsurface from an air flow perspective. At a minimum, one or more continuous cores should be collected between the water table (or upper boundary of contamination) and the top of the anticipated screened interval of any air injection wells (usually placed 1 to 10 ft below the deepest contamination). Continuous cores should be logged and photographed; in some cases, determination of relevant quantitative characteristics (e.g., grain size distribution, permeability) of the soils is warranted. While prediction of actual air distributions is not practicable at this time, the gross features of air distributions can be anticipated for simple geologies (e.g., highly permeable and homogeneous settings and settings with large macroscale heterogeneities such as clay layers in otherwise sandy soils), and therefore, knowledge gained from visual review of soil cores is often invaluable for air sparging applications.

At the end of the site characterization phase and prior to the screening and pilot testing phases, site characterization data should be used to define a target treatment zone and to propose a conceptual model for the air distribution at the site. Users will find the work of Ji et al. (1993) and Lundegard and

LaBreque (1998), helpful in developing their intuition for anticipated air distributions in various hydrogeologic settings.

4.0 AIR SPARGING APPLICATION: INITIAL SCREENING OF TECHNOLOGIES

It is assumed at this point that a site characterization has been performed, and that it has been decided that some form of source zone treatment, dissolved plume remediation, or dissolved plume containment is needed. It is further assumed that air sparging is one of the technologies being considered, a target treatment zone has been defined, and a conceptual model for the air distribution at the site has been proposed. This section focuses on how one assesses if air sparging is a viable technology and if a pilot test is warranted.

As discussed above, it is important to recognize current limitations in predicting air sparging performance, and therefore, it is important to consider a wide range of input derived from both experience and theory. It is up to the user to decide how best to weigh these and other factors (e.g., political and regulatory issues) in their decision making. Users will find it efficient to focus on answering the following three basic questions:

Q1: Does experience suggest that air sparging could be successful at this site?

Q2: For what injection well spacings would air sparging be practicable?

Q3: What are reasonable performance expectations for this air sparging system?

These three questions are the focus of the discussion below. To better illustrate the initial technology screening phase, a hypothetical gasoline-spill site is also discussed, and the range of information considered when deciding air sparging applicability at that site is summarized in Table 2.

4.1 Question 1: Does Experience Suggest That Air Sparging Could Be Successful at This Site?

When assessing applicability, it is useful to first review what is known from experience (e.g., Bass and Brown, 1995; Bruell et al., 1997; Johnson et al., 1993; U.S. EPA, 1992). Air sparging has been successfully applied for source zone treatment at gasoline-release and smaller-scale chlorinated solvent spill sites (e.g., dry cleaners). Air sparging systems have also been implemented as barriers at larger-scale chlorinated solvent dissolved plume sites and for other more recalcitrant chemicals (e.g., methyl *tert*-butyl ether [MTBE]), although little performance data is available in the literature. Air sparging systems are generally not used for plume treatment or plume barriers when dealing with readily degradable compounds as the plume extent tends to be constrained by natural attenuation, and plume dissipation occurs relatively quickly once the source zone has been successfully remediated. Air sparging is not expected to be effective for treatment of inorganic chemicals and salts and chemicals that are both nonvolatile and nondegradable.

Hydrogeologic settings involving aquifers found at medium to shallow depths (<50 ft below ground surface [bgs]) and sandy/silty soils are typical candidates for air sparging application. Deeper aquifers, fractured treatment zones, highly stratified aquifers, and aquifers composed of soils that become finer with depth are also candidates but are expected to be much more challenging, and little data is available on treatment effectiveness in these settings. Air sparging is not expected to be effective in most clayey settings. On a site-specific basis, site characterization data (continuous cores) should be used to generate a conceptual

Table 2. Sample Air Sparging Technology Screening Input Summary Table

Site Characteristics and Application Goals	
Treatment goal (source zone, dissolved plume, barrier)?	Source zone treatment
Release scenario (attach plan view map)	Gasoline UST Leak
Target contaminants for treatment	Benzene, TPH[3]
Depth to groundwater (m bgs)	6
Hydrogeologic setting (describe qualitatively and attach cross section and photos of continuous core[s])	Relatively homogeneous, interbedded sands-silts
L - Approximate treatment zone length (m)	20
W - Approximate treatment zone width (m)	20
D - Approximate treatment zone thickness (m)	2 (6 to 8 m bgs)
Air distribution conceptual model for this site; see P.C. Johnson et al. (2000) (Appendix A) for a review and discussion on air distributions	Predominantly semi-conical homogeneous setting-type air distribution of limited lateral extent; some potential for air stratification and preferential flow direction
Qualitative and Empirical Assessment of Applicability	
(1) Are the target contaminants considered relatively volatile[1]?	Yes
(2) Are the target contaminants considered to be biodegradable aerobically[2]?	Yes
(3) Is this setting and contaminant "typical" of air sparging applications?	Yes
(4) What experiences have been reported for this type of setting and application?	Successful applications reported in literature (Bass and Brown, 1995)
(5) What are the challenges likely to be at this site (i.e., stratification, vapor control, well construction, etc.)	Number of injection wells required for close spacings

[1]$C_{v,max}$ >0.01 mg/L-vapor for removal rates >40 g/d (0.1 lb/d) at flowrates of about 100 ft^3/min (2,800 L/min)

[2]For aerobic biodegradation to be appreciable, reported aerobic biodegradation rates expressed as zero-order rates should be >1 mg/kg-soil/d; if expressed as first-order reaction, then rate constants need to be >0.001 d^{-1} (both quoted for well-oxygenated conditions).

[3]TPH = total petroleum hydrocarbon

Table 2. Sample Air Sparging Technology Screening Input Summary Table (continued)

Semiquantitative Assessment of Feasibility– Inputs	
$C_{T,i}$ - Approximate average contaminant soil concentration(s) in target treatment zone (mg/kg-soil) *(not applicable for barrier application assessment)*	10,000 (TPH) 300 (Benzene)
$C_{w,I}$ - Approximate average initial dissolved contaminant concentration(s) in target treatment zone (mg/L-water) *(or concentrations flowing to air sparging barrier treatment system)*	10 (TPH) 2.1 (Benzene)
ρ_b - Assumed soil bulk density (kg-soil/m^3-soil) (1,600 to 1,800 typical) *(not applicable for barrier application assessment)*	1,700
φ - Porosity of aquifer (L-pores/L-soil) (0.25 to 0.45 typical)	0.30
F - Assumed percentage of treatment zone directly affected by air distribution (%) (5 to 40% typical) *(not applicable for barrier application assessment)*	20
$C_{v,max}$ - Estimated maximum vapor concentration(s) (mg/L-vapor) (see Equation [1])	200 (TPH) 0.4 (Benzene)
V_{min} - Estimated minimum vapor volume requirement[4] for volatilization from channels (L-vapor/g-contaminant) *(not applicable for barrier application assessment))*	100
Q_{inject} - Approximate average total air injection rate (all wells) (L/min) (50 to 200 ft^3/min = 1,400 to 5,600 typical)	2,800 (100 ft^3/min)
B - Aerobic biodegradation rate estimate in air channels (mg/kg-soil/d) (1 to 10 typical for petroleum hydrocarbons based on Leeson and Hinchee, 1996) *(applicable only for source zone treatment)*	1 to 10
O - Approximate oxygen delivery rate to groundwater outside of air channels (mg-O_2/L-water/d) (10 to 100 based on Amerson-Treat et al., 2000)	10 to 100
U - Groundwater specific discharge (m/d) *(applicable only for barrier applications)*	NA
H - Maximum humidity change for air entering and leaving the aquifer (L-H_2O/L-air)	1×10^{-5}

[4]See Johnson et al. (1990a) for determination of this quantity.

Table 2. Sample Air Sparging Technology Screening Input Summary Table (continued)

Semiquantitative Assessment of Feasibility– Calculations	
Approximate number of injection wells required if placed on close-spacings (i.e., using the "Standard" design approach prescribed 15-ft spacings) (cost prohibitive?)	20 (not cost-prohibitive)
Minimum economically feasible injection well spacing (ft)	NA
$V_{soil} = L \times W \times D$ Volume of treatment zone (m^3)	800
$M_o = V_{soil} \times \rho_b \times C_{t,i} \times 10^{-6}$ kg/mg Initial mass of contaminant present (kg) *(not applicable for air sparging barrier treatment systems)*	1.4×10^4 (TPH) 420 (Benzene)
Flux = $U \times W \times D \times C_{w,i} \times 10^3$ L/m^3 $\times 10^{-6}$ kg/mg Contaminant flux to barrier (kg/d) *(only applicable for barrier treatment systems)*	NA
$R_{vc} = Q_{inject} \times C_{v,max} \times 10^{-6}$ kg/mg $\times$ 1,440 min/d maximum volatilization rate from within air channels (kg/d)	810 (TPH) 1.6 (Benzene)
$R_{Bc} = V_{soil} \times F \times \rho_b \times B \times 10^{-6}$ kg/mg Aerobic biodegradation rate from within air channels (kg/d)	0.3 to 3
$\tau_{min} = M_o \times 10^3$ g/kg $\times F \times V_{min}/Q_{inject} \times (1/1{,}440)$ d/min Minimum time necessary to achieve desired treatment in air channels by volatilization (d)	68
$R_{va} = Q_{inject} \times H \times C_{w,i} \times 10^{-6}$ kg/mg $\times$ 1,440 min/d Maximum volatilization rate from outside air channels due to water evaporation (kg/d)	4×10^{-4} (TPH) 8×10^{-5} (Benzene)
$R_{Bw} = V_{soil} \times \varphi \times O \times 10^3$ L/m^3 $\times 10^{-6}$ kg/mg $\times$ 0.33 kg-HC/kg-O_2 Estimated aerobic biodegradation rate in groundwater due to oxygen delivery to groundwater[5] (kg/d)	0.8 to 8
$R_{Bw} = V_{soil} \times \varphi \times O \times 10^3$ L/m^3 $\times 10^{-6}$ kg/mg $\times (C_{w,i}/9)$ Estimated initial volatilization rate from groundwater based on oxygen delivery rate estimate[6] (kg/d)	2.7 to 27 (TPH) 0.57 to 5.7 (Benzene)

[5]Assumes complete utilization of oxygen and complete mineralization of contaminant; assumes 3:1 oxygen/contaminant stoichiometry

[6]Assumes oxygen solubility in water is 9 mg/L, the driving force is the gradient in dissolved concentrations, and diffusion distances are similar for all chemicals

model of the projected air distribution through the target treatment zone. If the contact between the air distribution and the contaminant distribution is likely to be poor, then air sparging has a low probability of success.

4.2 Question 2: For What Injection Well Spacings Would Air Sparging Be Practicable?

At this point, if experience suggests that the air sparging application could be successful, then users should determine if the cost of injection well installation is likely to be prohibitive, and if so, what injection well spacing is economically feasible. The results of this analysis are not only used for feasibility assessment, but are also critical to the pilot test design. The Standard Design Approach path of this Design Paradigm calls for injection wells placed on 15-ft spacings, and users should first determine if the cost of that well spacing is cost-prohibitive. The 15-ft spacing recommendation stems from our understanding of air distributions in near-homogeneous and highly permeable settings; these are likely to yield the most spatially limited air distributions (generally the lateral extent is not much more than 10 ft in any direction away from the injection well). If that well spacing is cost-prohibitive, then the smallest well-spacing that is not cost-prohibitive should be determined.

4.3 Question 3: What Are Reasonable Performance Expectations for This Air Sparging System?

While our ability to confidently predict performance is limited at this time, it is possible to place some bounds on reasonable performance expectations. First, empirical summaries (e.g., Bass and Brown, 1995; Bruell et al., 1997) and experience suggest that many of the air sparging systems installed for source zone treatment at service station-scale sites are operated for periods of less than three years; however, it is not clear what criteria are being used to decide termination, and it may very well be a combination of asymptotic performance and regulatory closure criteria. Clearly, air sparging barrier control systems may be operated for longer (or shorter) time periods, dictated not by air sparging performance but by length of time that the migration barrier is needed.

Next, theory suggests that contaminant removal during air sparging occurs through a combination of volatilization and biodegradation. Thus, air sparging can be considered for any volatile and/or aerobically biodegradable chemical. Since many systems operate at or near a combined injection flowrate of 100 ft^3/min, a reasonable criterion for volatilization to be effective is that that the achievable vapor concentration must be >0.01 mg-contaminant/L-vapor. This corresponds to a removal rate of >40 g-contaminant per day (>0.1 lb/d). Which mechanism accounts for the greater amount of contaminant removal depends on the chemical properties, contaminant distribution, duration of air injection, and soil properties. Generally, volatilization dominates when systems are first turned on and, for aerobically degradable compounds, biodegradation can dominate in later phases of treatment. As mentioned above, air sparging may also be used to deliver gaseous-phase nutrients and cosubstrates, although this specific use of air sparging is not discussed in this document.

It is envisioned that a) air flows through discrete air channels in most settings; b) removal of contaminants from within the air channels behaves much like contaminant removal during soil vapor extraction (Johnson et al., 1990a; 1990b) and bioventing (Leeson and Hinchee, 1996); and c) contaminant removal from water-saturated regions lying outside the air channels is limited by liquid-phase mass-transfer processes. Thus, contaminant removal is most rapid from within the air channels and slowest from outside the air channels. Furthermore, air channels occupy at most 20 to 50% of the pore space, so typically most of the contaminant mass lies outside of the air channels.

To more quantitatively illustrate the factors, mechanisms, and rates affecting air sparging performance, we make use of the hypothetical example described in Table 2. There, air sparging is being considered for a 20 m-long × 20 m-wide × 2 m-deep source zone at a gasoline spill site. Using the values found in Table 1 for

the average soil concentration (10,000 mg-gasoline/kg-soil, 300 mg-benzene/kg-soil), the bulk soil density (1.7 kg-soil/L-soil), and the source zone dimensions, the initial masses of total hydrocarbons and benzene are estimated to be 14,000 kg and 420 kg, respectively. The volatilization and aerobic biodegradation rates discussed below correspond to a total combined air injection rate of 100 ft^3/min, a porosity of 0.30 m^3-pores/m^3-soil, and the assumption that the air channels occupy 20% of the soil volume in the treatment zone. While this is only a hypothetical example, the values selected are reasonable for typical air sparging applications.

Aerobic biodegradation rates in air channels have yet to be measured; however, reasonable estimates can be drawn from the bioventing literature (Leeson and Hinchee, 1996). Rates determined from bioventing in situ respirometry tests often fall in the 1 to 10 mg-hydrocarbon/kg-soil/d range for petroleum hydrocarbon spill sites. Therefore, for the hypothetical site, a cumulative aerobic biodegradation rate for all the air channels of 0.3 to 3.0 kg-hydrocarbon/d can be estimated (these and other calculations are detailed in Table 2).

Estimates of volatilization rates and remediation effectiveness inside the air channels can be generated using screening models such as those discussed by Johnson et al. (1990a; 1990b) for soil vapor extraction systems. As shown in Table 2, the maximum removal rate by volatilization for any compound can be estimated as the product of the air injection flowrate and the maximum achievable vapor concentration for that compound $C_{v,max,i}$ [mg-i/L]; the latter quantity being given by:

$$C_{v,max,i} = \frac{x_i \, M_{w_i} \, P_{v,i}}{R\,T} = H_i \, C_{w,i} \qquad (1)$$

Where x_i = mole fraction of compound i in immiscible phase (moles-i/total moles); $M_{w,i}$ = molecular weight of compound i (mg-i/mole-i); $P_{v,i}$ = vapor pressure of compound i (atm); R = gas constant (=0.0821 L-atm/mole-K); T = absolute temperature (K); H_i = Henry's Law Constant for compound i (mg-i/L-air/mg-i/L-water); and $C_{w,I}$ = dissolved concentration of compound i (mg-i/L-water).

The total removal rate is then the sum of all individual chemical removal rates. For example, Johnson et al. (1990b) estimate maximum total hydrocarbon vapor concentrations of roughly 200 to 1,300 mg/L-vapor and 3 to 9 mg/L-vapor benzene at gasoline spill sites. Using the lowest values for our hypothetical site and a total air injection rate of 100 ft^3/min yields initial removal estimates of 810 kg-total hydrocarbons/d and 1.6 kg-benzene/d. In this example, volatilization is clearly the dominant removal mechanism at the start of air sparging; however, if the vapor concentration of the contaminant declines to 0.1 mg/L with time, then the two removal mechanisms become comparable, and below that point aerobic biodegradation can be the more significant of the two.

The calculation above yields maximum volatilization removal rate estimates, but does not account for changing vapor composition with time due to composition and residual concentration changes. Johnson et al. (1990a) discuss a minimum volume of vapor required to achieve a given mass reduction by volatilization for any initial spill composition. The minimum time to achieve this degree of treatment (τ_{min} [min]) is calculated as follows:

$$\tau_{min} = \frac{M_o \times V_{min}}{Q_{inject}} \qquad (2)$$

where M_o is the initial mass of contaminant (g-contaminant); V_{min} is the minimum vapor volume requirement (L-air/g-contaminant); and Q_{inject} is the flowrate (L-air/min).

For example, in Table 2 it is assumed that 100 L-air is required per initial gram of residual gasoline to achieve a 90% reduction in initial mass (Johnson et al., 1990b). If about 20% of the initial gasoline mass is directly exposed to air channels, then this translates into τ_{min} = 68 d. Again, this is an idealized lower bound estimate on the treatment time for contaminants lying within the air channels, but the result of this example is consistent with data presented in Bruce et al. (2000b) (Appendix D) and other experience. Furthermore, this example reinforces the key points that a) in many settings (e.g., UST release sites, solvent spill sites), the air channels are remediated rapidly relative to the bulk of the target treatment zone and b) a large fraction of the contaminant mass lies outside the air channels and must be remediated by mechanisms other than direct biodegradation or volatilization.

Removal of contaminants lying outside the air channels can occur via a combination of transport to the air channels and subsequent volatilization plus oxygen delivery to the groundwater followed by aerobic biodegradation. Detailed comparative analysis of these mechanisms is beyond the scope of this document, but it can be found in Johnson et al. (1999). Here we consider each mechanism independent of the other to get rough estimates of removal rates expected from each of the mechanisms.

First, evaporation of water from the aquifer can transport dissolved contaminants to the air channels, where they are volatilized. For the injection of dry air into an aquifer at a temperature of about 15°C, and assuming 100% humidity leaving the aquifer, it is possible to evaporate about 0.5 L-H_2O/d per ft^3/min of air injection. This flow of water to the air channels then has the capacity to cause a removal rate equal to that flowrate of water multiplied by the dissolved concentration. In this example, an air injection rate of 100 ft^3/min has the potential to remove 4 x 10^{-4} kg/d of total hydrocarbons and 8 x 10^{-5} kg/d benzene due to water evaporation.

Loss due to diffusion and volatilization mechanisms, R_{diff} (mg/d), can be approximated with equations of the form:

$$R_{diff} = A\, D^{eff}\, \frac{C_W}{\delta} \qquad (3)$$

where A is the surface area of channels per unit volume of treatment zone (cm^2-area/cm^3-volume); D^{eff} is the effective porous media diffusion coefficient (cm^2/d); δ is the distance the contaminant must diffuse to reach the air channel (cm); and C_w is the dissolved contaminant concentration (mg-contaminant/cm^3-water).

Typical saturated-zone D^{eff} values are estimated to be approximately 0.1 cm^2/d, C_w is obtained from site data, A is highly uncertain and practicably immeasurable in situ, and δ increases with time. In this case, therefore, we rely on the few measurements reported in the literature. Amerson (1997) and Bruce et al. (2000a) (Appendix B) and Amerson-Treat et al. (2000) (Appendix C) report oxygen transport rates to groundwater of about 10 to 50 mg-O_2/L-H_2O/d from their use of a push-pull type diagnostic test and a gas tracer delivery test. For the hypothetical site, these oxygen transport rates are equivalent to aerobic biodegradation rates (outside the air channels) equal to 0.8 to 4 kg/d, assuming complete mineralization and stoichiometry typical of petroleum fuel hydrocarbons (3 mg oxygen required per mg hydrocarbon degraded) (Leeson and Hinchee, 1996).

Comparable measurements of volatilization rates from within air channels are not available; however, if we a) accept Equation (3) as a reasonable approximation, b) recognize that A is chemical-independent and that effective oxygen and contaminant diffusion coefficients are similar (within a factor of two in most cases), and c) assume that δ is similar for contaminants and oxygen, then it can be concluded that the contaminant volatilization rate should be roughly equivalent to the oxygen delivery rate multiplied by the ratio of dissolved contaminant and oxygen concentrations, as shown in Table 1. For our hypothetical scenario, this translates to estimated hydrocarbon and benzene volatilization rates of 3 to 15 and 0.6 to 0.3 kg/d, respectively. These values are roughly a factor of four greater than the aerobic biodegradation rate estimates.

In summary, the qualitative input for the hypothetical site indicates that it is a typical air sparging application scenario and that successful results have been reported for other similar sites. Closely spaced wells are not cost-prohibitive at this site as groundwater is relatively shallow and sandy soils are present. The semi-quantitative analysis shows that remediation of the air channels will be rapid, with slower treatment of the remainder of the treatment zone; furthermore, the estimated remediation rates are consistent with the 3- to 5-year remediation time frames typical of practice.

5.0 PILOT TESTING

Pilot tests are an important tool for improving our conceptual understanding of in situ air sparging behavior at a site. Unfortunately, prediction of long-term performance based on pilot tests has proved to be difficult (Johnson et al., 1997). Nevertheless, pilot tests have proven useful as a means of identifying "red flags" prior to installation of full-scale systems. In that context, air sparging pilot tests are most useful when designed to a) look for indicators of infeasibility, b) characterize the air distribution to the extent practicable, and c) identify any safety hazards to be addressed in the full-scale design.

Prior to planning the pilot test, the user should:

a) Define the target treatment zone (i.e., the depth interval and area which is to be treated by the air sparging system)

b) Propose a conceptual model for the air distribution in the treatment zone (e.g., based on site information, determine if the aquifer is homogeneous or stratified)

c) Determine if 15-ft well spacings are cost-prohibitive, and if so, determine the minimum injection well spacing that is not cost-prohibitive

d) Propose the depth, location, and construction specifics of a pilot test well, and

e) Determine the expected range of operating pressures for the injection well.

If, based on previous site activities, air sparging is chosen as the remediation technology for the site, it is recommended that the series of pilot test activities summarized in Table 3 (and discussed below) be conducted. If in the preliminary assessment it was determined that well spacings of 15 ft are cost effective, the first six activities in Table 3 (PT1 through PT6) should be conducted (Standard Pilot Test Approach). If a greater well spacing is required, additional site-specific activities should be conducted. These include the sulfur hexafluoride (SF_6)-distribution test (PT7) and possibly geophysical tests (PT8) to define the zone of aeration (Site-Specific Pilot Test Approach). In deciding whether or not to perform the additional SF_6-distribution and geophysical tests, the cost of the additional tests, the potential cost-savings

Table 3. Summary of Pilot Test Activities

	Activity	Question(s) Answered	Standard Pilot Test Approach	Site-Specific Pilot Test Approach
PT1	Baseline sampling • Dissolved Oxygen (DO) • Pressure • Soil gas • Geophysical[1]	What are aquifer conditions prior to air sparging start-up?	X	X
PT2	Injection pressure/ flowrate test	Is it possible to achieve desired flowrate at reasonable pressures?	X	X
PT3	Groundwater pressure response test	What are the general characteristics of the air distribution — is it likely to be more like the semiconical homogeneous-setting air distribution, or is there a significant degree of stratification?	X	X
PT4	Helium tracer test	What is the approximation of lateral extent of the air distribution? Are there indications of preferred directions?	X	X
PT5	Soil gas/off-gas sampling	What is the volatilization rate? Are there any obvious safety hazards?	X	X
PT6	DO measurements	What is the approximation of lateral extent of the air distribution? Are there indications of preferred directions?	X	X
PT7	SF_6 distribution test	What is the vertical and lateral extent of the air distribution in the target treatment zone? What are the oxygen transfer rates to groundwater?		X
PT8	Other geophysical tools	What is the vertical and lateral extent of the air distribution in the target treatment zone?		Optional

[1]Collect initial geophysical measurements if PT8 will be conducted.

of larger injection well-spacings, the impact of larger or smaller well-spacings on remediation performance, and the benefits of better understanding the air distribution should all be considered.

Users may also consider the use of geophysical tools for air distribution characterization, although their use has not been prescribed in this Design Paradigm. For example, use of neutron probes, capacitance probes, and electrical resistance tomography are reported in the literature (e.g., Acomb et al., 1995; Lundegard and LaBreque, 1998).

At the end of the pilot test, users should revisit and revise their answers to questions Q1 through Q3 described in Section 4.0 and again assess if air sparging is a feasible option for their site.

5.1 Pilot Test Equipment

The following equipment is needed to conduct the pilot test activities: a) at least one air injection well equipped with a well-head pressure gauge, flowmeter, and valve; b) an air supply compressor; c) one to three groundwater piezometers or monitoring wells; and d) several groundwater and vadose zone monitoring points. In addition, a vapor extraction system may be needed to reduce the potential for adverse vapor migration impacts (or it may be required by regulation).

The air injection well should be similar to that envisioned for full-scale implementation. A typical air injection well is a 1- to 4-inch-diameter vertical well having a 1- to 5 ft-long screened interval installed from 1 to 5 ft below the target treatment zone. Five feet below the target treatment zone is preferable; however, at some sites, 5 ft is not available due to site stratigraphy, and less than 5 ft will likely be acceptable. Most screened intervals are generally not placed deeper than 10 ft below the treatment zone as the risk of the air not reaching the target treatment zone increases with increasing separation. It is important to ensure a good annular air flow seal between the top of the screened interval and the water table.

The air injection compressor should be capable of providing at least 20 ft^3/min at pressures of up to 10 to 15 psig above the calculated hydrostatic pressure (see PT2 below). Additional description for sizing a compressor is provided in Section 5.2.

To the extent possible, existing groundwater monitoring wells and other monitoring installations should be incorporated into the pilot test design. A typical pilot test monitoring network consists of a) one to three groundwater piezometers or monitoring wells equipped with water-level pressure transducers, b) six or more groundwater sampling points, and c) six or more vadose zone sampling points. The piezometers and groundwater sampling points ideally should be screened only within the target treatment zone. Vadose zone sampling points should be screened over a narrow interval (1 to 2 ft maximum) and placed just above the capillary fringe. For shallow sites (<30 ft to groundwater), monitoring networks like these are often quickly and cost-effectively installed with direct-push methods. Small diameter (¼- to ⅜-inch) discrete (6- to 20-inch length) direct push implants are good candidates for the groundwater and vadose zone monitoring points. At deeper sites, or sites with access restrictions, practical considerations may dictate the use of fewer wells, multilevel samplers, and a heavier reliance on existing groundwater monitoring wells having screens that extend above the water table (these can be used to house pressure transducers and to collect groundwater and vapor samples).

A sample pilot test layout is shown in Figure 3. In choosing the monitoring layout, it is important to recognize that air distributions often have unpredictable preferred directions, and therefore a spatially distributed monitoring network is preferred over installations having monitoring points emanating out from the injection well in a line in one or two directions. Furthermore, the locations should reflect the hydrogeologic setting and the tentative well spacings as described in item (c) above. In near homogeneous settings, the monitoring network need not extend more than 20 ft out from the injection well. In cases where close well-spacings are prohibitive, the monitoring network should extend out at least a distance equal to one-half to three-fourths of the minimum non-cost-prohibitive well-spacing distance.

5.2 Pilot Test Activities

In most cases, the events outlined in Table 3 should be conducted in the sequence presented. In this section each of the activities will be discussed in greater detail. In a number of cases, a detailed protocol for the activities has been published and is cited when appropriate. The task-by-task discussion will be

A)

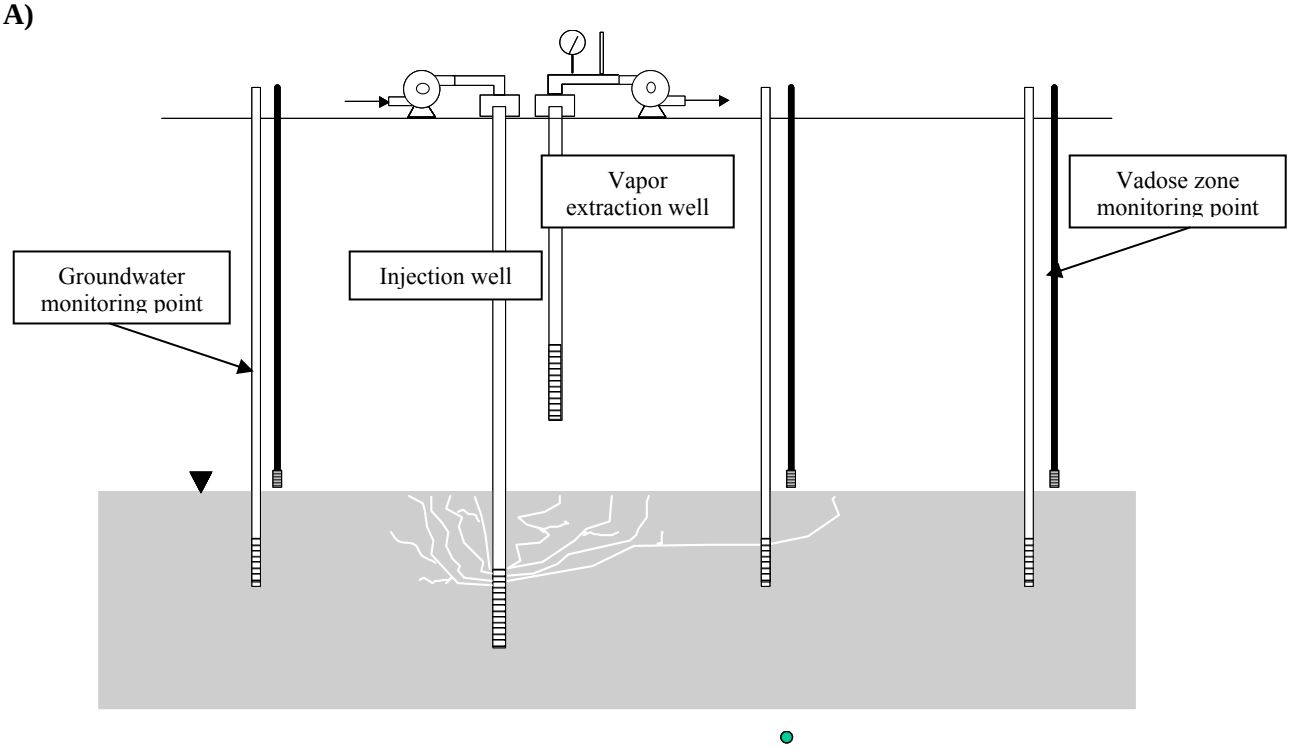

B)

Figure 3. Cross-Section (A) and Plan (B) Views of a Sample Pilot Test Layout

followed by a case history in which the various pieces of the pilot test are combined to interpret what is occurring at the site and assess if air sparging is appropriate at the site.

5.2.1 Baseline Sampling (PT1)

Baseline sampling represents a critical step in the pilot test process. For several of the parameters, it is important to collect data prior to any air sparging activity to ensure that initial conditions are understood. In particular, those parameters include dissolved oxygen (DO) concentrations and any geophysical measurements (if geophysical tests are to be conducted as part of the pilot test). It is also important to collect baseline pressure transducer data with a data-logger. The pressure data should be collected for a sufficiently long period to assess diurnal changes in water level (e.g., tidal fluctuations) if they are believed to be a significant.

If an SVE system is to be used in conjunction with the air sparging system, then the SVE system should be operated for a period of time prior to air sparging start-up primarily to ensure that the SVE system is operating properly to capture the initial high mass loading from air sparging. During this period, it may also be of interest to monitor SVE off-gas for the contaminants of interest in order to establish mass loading from volatilization from the vadose zone compared to volatilization from groundwater. Ideally, prior to initiating air sparging, the off-gas concentrations should have stabilized to the extent that changes in off-gas concentrations due to air sparging operation can be easily determined. In many cases it may be sufficient to monitor those off-gas concentrations with a hand-held field instrument, rather than requiring more sophisticated chromatographic analysis. If off-gas is regulated, regulatory requirements often will dictate which analytical method must be used.

If an SVE system is not part of the air sparging system, then soil gas concentrations (including both contaminant and oxygen concentrations) should be measured prior to air sparging start-up. The initial contaminant concentration in the vadose zone can be used to calculate roughly contaminant mass removal from groundwater via volatilization (see Section 5.2.5). Initial oxygen concentrations are useful for measuring bioactivity in the vadose zone. Hand-held instruments should be appropriate for this since soil gas concentrations of contaminants are rarely regulated.

5.2.2 Air Injection Flow Rate and Injection Pressure (PT2)

Prior to pilot test activities, it is important to evaluate the expected operating pressure for the air sparging system. This is important both for the selection of the correct air injection system and for the prevention of pneumatic fracturing of the aquifer. Outlined below is the general procedure for estimating the minimum pressure required to initiate sparging and the maximum pressures that should be exerted on the aquifer.

The operating pressure for an air sparging system will be determined by the depth of the air sparging well below the water table and the permeability of the aquifer. The minimum injection pressure necessary to induce flow (P_{min} [psig]) is given by:

$$P_{min}\,(\text{psig}) = 0.43\,H_h + P_{packing} + P_{formation} \tag{4}$$

The pressure at which fracturing of the aquifer can occur is given by:

$$P_{fracture}\,(\text{psig}) = 0.73\,D \tag{5}$$

where H_h = depth below the water table to the top of the injection well screened section (e.g., the hydrostatic head) (ft); $P_{packing}$ and $P_{formation}$ = air entry pressures for the well annulus packing material and the formation (psig); and D = depth below ground surface to the top of the air injection well screened interval (ft).

For typical air sparging wells and applications, $P_{packing}$ and $P_{formation}$ are small compared to the contribution from the hydrostatic head (air entry pressures are generally <0.2 psig for sands, <0.4 psig for silts, but may be >1.5 psig in some clayey settings). At start-up, it is not unusual for users to exceed P_{min} by as much as 5 to 10 psig to initiate flow quickly. The injection pressure then generally declines to about P_{min} as steady flow conditions are approached. Pressures in excess of $P_{fracture}$ can cause fracturing of the formation; however, as the pressure drops off rapidly away from an injection point, the extent of fracturing in most cases is expected to be limited to the area immediately surrounding the well.

In general, it is recommended that oil-less compressors be used for the pilot test (even if it is not chosen for operation of the full air sparging system) because they eliminate uncertainties relating to air flowrate and potential overheating. Other pumps may be used for air injection, but the practitioner may experience more operational difficulties, depending on site conditions.

As part of the initial shakedown of the air sparging system, the air injection system must be tested. During this process, it is important to measure both the air flowrate and the injection pressure to ensure that neither P_{min} nor $P_{fracture}$ are exceeded at the required air flowrate. There are two general approaches for the initial introduction of air into the subsurface. The first is to include a "vent valve" in the injection air line. This valve should be fully open to begin the test and then closed slowly while monitoring the increase in pressure and flowrate up to the desired flowrate. During this process, care should be taken not to exceed the upper pressure limit for the system (as determined by the calculations described above). In addition, if the air injection system requires some minimum airflow to provide cooling for the motor/pump, total air flow and system temperature should also be monitored.

A second approach for air sparging start-up is to determine the maximum pressure for air injection and to include an in-line pressure regulator in the air injection line. (This approach is best suited to oil-less compressors that do not require airflow for cooling.) In this case, the pressure can be set at the air sparging well head and flow allowed to increase as air pathways in the aquifer become developed. In general, when using this approach it will be necessary to make adjustments in the system to achieve the desired flowrate.

It is desirable to begin the test with an air injection flowrate of 20 ft^3/min if possible. The air injection pressure at the on-set of flow should be recorded, as well as pressures every 5 to 10 min until the pressure and flow stabilize.

5.2.3 Groundwater Pressure Measurements During Air Sparging Start-Up and Shutdown (PT3)

Once the flow and pressure conditions for sparging have been established (PT2), groundwater pressures during air sparging start-up and shutdown can be determined. The primary objective of this test is to assess the time required for airflow distribution to come to steady state. As discussed by Johnson et al. (2000a) (Appendix E), pressure measurements provide an easy and sensitive means of assessing if air sparging air is stratigraphically trapped below the water table. The pressure measurements can also provide a measure of site permeability, based on the magnitude of the response. In general terms, during air sparging start-up groundwater pressures will increase because air is being pushed into the formation faster than the water can move away from the air sparging well. Typically, as long as the volume of air below the water table is increasing, the groundwater pressure will remain above pre-air sparging levels. As a result, the time required for groundwater pressure to return to pre-air sparging values is a good

measure of the time required for the macro-scale air distribution to come to steady state. For media which are relatively homogeneous with respect to air flow (e.g., uniform sands), the time required for air sparging pressures to return to pre-air sparging values will generally be measured in tens of minutes to a few hours. If the site is stratified with lower-permeability layers, then the groundwater pressure may remain elevated for tens of hours to days.

The magnitude of the groundwater pressure response can be from millimeters to a few meters of water. In general, if the injection rate is on the order of 20 ft^3/min and the response is on the order of millimeters, the medium is very coarse (e.g., gravels). Pressure responses in sands are typically on the order of tens of centimeters and responses of a meter or more may occur in finer-grained media or in media where the air is stratigraphically confined.

Generally, at sites where groundwater pressures remain elevated by more than a few tens of centimeters for more than 8 hours, it can be assumed that the air distribution is controlled to a high degree by the structure of the aquifer, and it will be important to determine if the air is being delivered to the treatment zone in an effective manner.

5.2.4 Helium Distribution and Recovery Test (PT4)

Helium can be used in two primary ways as a tracer for air sparging systems (Johnson et al., 1996; Johnson et al., 2000b [Appendix F]). The first, if an SVE system is present, is to assess the effectiveness with which the SVE system is capturing the air sparging air. The second method is to identify the locations at which air sparging air moves from the groundwater zone to the unsaturated zone. Described in the following sections are the methods for assessing recovery of air sparging air by an SVE system and for evaluating air sparging air distribution at the water table. One of the strengths of the tracer test is that it can be easily repeated, usually with delays of only a few hours or so between them. This allows the effects of process changes (e.g., distribution of air flow from various wells) to be quickly assessed.

Helium is the most common tracer gas used, since it is relatively inexpensive, readily available, and analytical instrumentation is available for field use. Typical field instrumentation is a Marks Product helium detector. The detector can detect helium concentrations from 0.1% to 100%. It is factory-calibrated so it cannot be calibrated in the field, but checks should be made with helium standards to verify that the instrument is operating properly. Typically, vapor samples must be collected in Tedlar™ bags or canisters. The helium detector is then attached directly to the sample container for measurement. Alternatively, the helium detector can be modified to sample continuously. Continuous sampling is very convenient when measuring SVE off-gas where a continuous flow stream is available.

5.2.4.1 Tracer Test to Assess Recovery of Air Sparging Air by an SVE System. The tracer recovery tests described here are designed to be conducted on an air sparging system that is already operating and after the air flow patterns have stabilized. It can be conducted as part of a pilot test, or during full-scale operation. To be most useful, the air sparging and SVE wells should be co-located. The test is very simple to conduct and interpret. Basically, an inert tracer (usually helium) is introduced into the air sparging air at a constant, known rate and the concentration of tracer is monitored in the SVE off-gas air (Figure 4A). After some period of time (e.g., an hour or less for many systems), the concentration of the tracer in the off-gas begins to rise. It continues to rise and eventually reaches a stable plateau.

A)

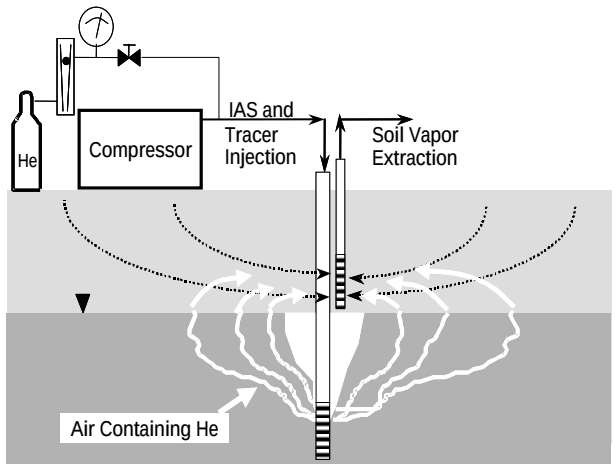

B)

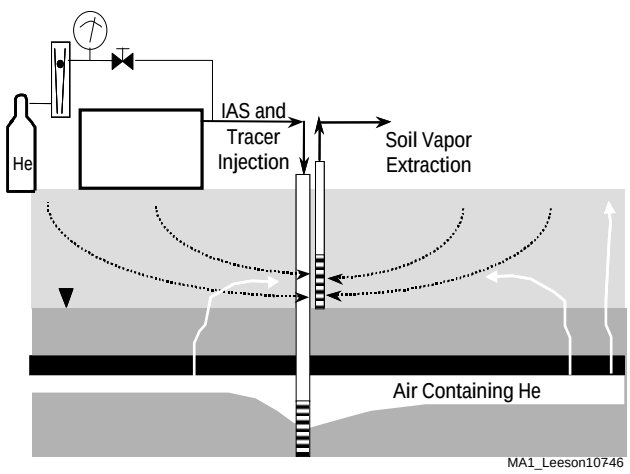

Figure 4. Helium Tracer Test for Assessing Air Sparging Air Recovery in an Unstratified Setting (A) and a Stratified Setting (B)

The percent of the air sparging air that is captured can be calculated by multiplying the SVE flowrate by the fraction of helium in the SVE air once the concentration has stabilized and dividing that number by the tracer injection rate as shown below.

$$\%\,\text{Recovery} = \frac{\text{SVE flowrate}}{\text{Trace injection rate}} \times \%\ \text{tracer in off - gas} \times 100 \qquad (6)$$

A more robust field technique for calculating recovery is to first measure the "100% recovery concentration" in the SVE off-gas by directly injecting the helium into the SVE manifold at the same rate

used for air sparging injection. (Care must be taken to ensure that the flow is the same in both cases since the back-pressures for the two systems are significantly different.) In this case the percent recovery of the air sparging air by the SVE system is simply the helium concentration measured in the SVE off-gas divided by the "100% recovery concentration."

If helium is used as the tracer, the injection concentration should be kept below 10% by volume to avoid buoyancy effects in the vadose zone. To ensure consistent helium flow under conditions of varying back-pressure, a calibrated direct-reading flow meter should be used along with a pressure gauge and a metering valve to provide a consistent, high back-pressure at the flow meter (Figure 4A).

The tracer recovery test is designed as a "red flag" for air sparging system performance. If the recovery of helium is low, then it is possible that air (and helium) is being trapped below the water table beneath lower-permeability strata (Figure 4B) and may be moving laterally beyond the reach of the SVE system. In some cases, it is possible that no helium will return to the well due to the presence of continuous layers. The presence of these layers should also be detectable by monitoring groundwater pressure during air sparging start-up and shutdown (Johnson et al., 2000a). Therefore, it is recommended that the helium recovery test be conducted in conjunction with groundwater pressure measurements.

If helium recovery is high (e.g. >80%), then the SVE system is performing well with regard to air sparging air recovery, and lateral migration of vapors is unlikely to be a problem. Additional information regarding the distribution of air based on the recovery tests can be obtained if vadose zone transport times are calibrated using a procedure similar to that presented by P.C. Johnson et al. (2000).

5.2.4.2 Tracer Test Procedure to Determine the Distribution of Air Sparging Air at the Water Table without an SVE System (or with Co-Located SVE and Air Sparging Wells)

If a number of discrete-depth vadose zone monitoring points (e.g., 6 to 12) are placed near the water table and distributed around the injection well, the tracer test described above can also be used to assess air sparging air distribution at the water table. In the absence of an SVE system (or with it turned off), the monitoring points are sampled every few minutes for the appearance of tracer. The presence of tracer at locations in the deep vadose zone within approximately 15 to 20 minutes of tracer startup indicates that air sparging air is reaching the vadose zone near that point (Figure 5). At times longer than 15 to 20 minutes, tracer transport by diffusion and/or advection reduces the utility of the test. With co-located air sparging and SVE wells, tracer reaching the water table will be drawn back towards the SVE well and appearance of the tracer at vadose zone monitoring points indicates that tracer reached the water table beyond that radial distance from the air sparging well.

5.2.5 Soil Gas Monitoring (PT5)

In the absence of an SVE system, soil gas samples should be collected for contaminant analysis during the pilot test. The observed values should be compared to the pre-air sparging concentrations to determine if a significant mass of contaminant is being pushed out of the groundwater. In general, it is difficult to assess the significance of this in a quantitative sense. However, if it is used in conjunction with the helium tracer data, the mass flux from the groundwater can be semiquantified. To accomplish that, it can be assumed that the soil gas samples that have concentrations of helium near the injection concentration will reflect the contaminant concentrations being removed from the groundwater zone. When those concentrations are multiplied by the flowrate, a rough estimate of the mass removal rate can be obtained.

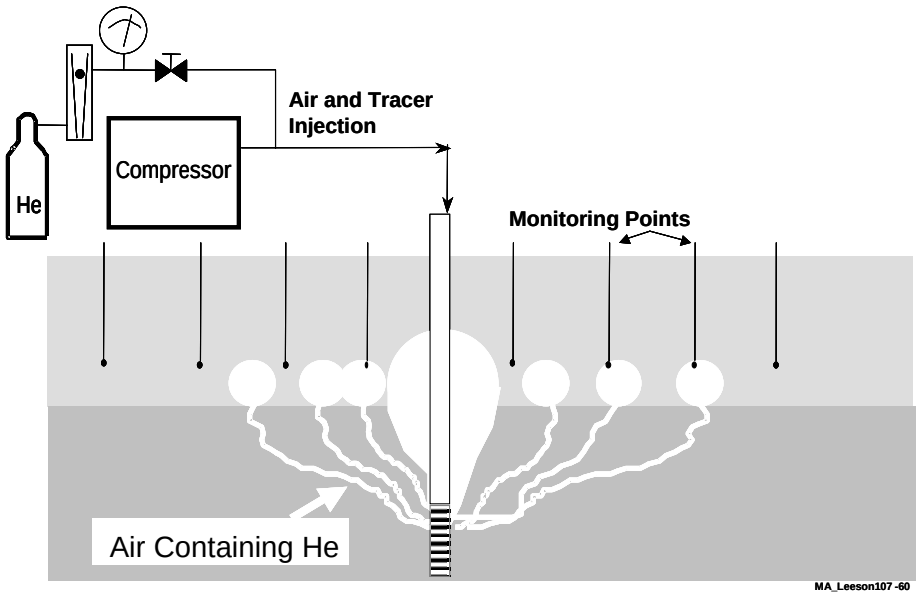

Figure 5. Schematic Diagram Illustrating a Helium Tracer Test to Assess Air Distribution in the Absence of an SVE System

A more quantitative estimate of mass removal can be obtained if the air sparging system is coupled with an SVE system. In this case, increases in contaminant concentrations in the off-gas, and the SVE extraction rate can be used to determine a mass removal rate. Of course, measurements made during the short duration of a pilot test are not indicative of long-term performance. However, it can generally be assumed that the pilot test data represent the maximum removal rate from the system. In that context, if mass removal rates during (e.g., at the conclusion) of the pilot test are too low, then there should be significant concern about the viability of air sparging at the site.

5.2.6 Dissolved Oxygen Monitoring (PT6)

Dissolved oxygen (DO) data has the potential to identify the zone where oxygen is being delivered by the air sparging system. If the preliminary measurements (PT1) showed low DO concentrations (e.g., less than 2 mg/L), it may be possible to identify areas where air sparging has resulted in increases in DO. To determine this, DO should be measured in all groundwater monitoring points immediately following the pilot test. Unfortunately, several factors can complicate the interpretation of DO. First, at many sites where active biodegradation is ongoing, there may be significant quantities of reduced species (e.g., Fe^{2+}) that act as rapid sinks for oxygen and that mask oxygen delivery to that region. Second, microbial activity may be high, effectively consuming oxygen as fast as it is delivered to the area. Finally, care must be taken to avoid artifacts caused by air entry into monitoring wells and preferential aeration within the well (Johnson et al., 1997). This is an important part of the reason that short-screened monitoring wells in the treatment zone are recommended for the pilot test.

5.2.7 Other Qualitative Observations

Often during pilot tests there are operational factors that are readily noticed and that are important to the viability of air sparging. It is important to note any qualitative indicators of air distribution, such as bubbling or gurgling noises in wells, water “fountaining” out of monitoring points, etc. It is also

important to be aware of odors due to the contaminants, noise due to the equipment, or other environmental factors. While these factors may not lessen the successful implementation of air sparging, they can make the system less feasible from a community impact perspective.

5.2.8 Site-Specific Design Approach

In cases where the Site-Specific Design Approach is being used, it may be appropriate to conduct one or both of the tests described in the following sections.

5.2.8.1 SF_6 Distribution Test (PT7). In this test, SF_6 is used as an analog for oxygen to determine the distribution of air in the groundwater zone (Johnson et al., 1996). SF_6 has a water solubility that is similar to oxygen; however, SF_6 has several advantages over oxygen and as a result the test can be both more sensitive and more quantitative. These advantages include: 1) it does not occur naturally, so background concentrations are essentially zero (unless it has been used at the site before); 2) SF_6 can be detected at extremely low concentrations in water and air, and thus is a much more sensitive tracer than oxygen; and 3) it is not biodegradable, so it acts as a conservative tracer to show where the air was delivered.

To conduct the test, SF_6 is blended with the injection air stream at a known concentration for a period of 12 to 24 h. The objectives in injecting for a short, known period are 1) to provide an opportunity for SF_6 transfer from the air to the groundwater without a significant amount of groundwater transport and 2) to allow an estimate of the mass transfer coefficient at various locations to be determined. The details of these procedures are discussed by Bruce et al. (2000a) (Appendix B). In overview, at the end of the SF_6 injection period, groundwater samples are collected and analyzed for SF_6. The duration of SF_6 injection and the cumulative volume of groundwater sample should be recorded. Based on the concentration of SF_6 in the injected air and the Henry's Law constant for SF_6, the percent saturation of SF_6 in the groundwater sample can be determined. In general, those concentrations can be divided into three groups. The first are values approaching saturation (e.g., >40% of theoretical solubility). These generally indicate that the sample location lies within the "zone of aeration" of the air sparging system. The second group are samples that contain low concentrations of SF_6 (e.g., <10%) and indicate that an air channel may be in the vicinity of the sampling location (e.g., it may be within the "zone of treatment"), but the air saturation in the aquifer at that point is probably low. The third group is composed of samples that have no SF_6 present. These samples are presumed to lie outside both the aeration and treatment zones.

In the context of site-specific pilot tests, to be sufficiently conservative, the spacing of the air sparging wells probably needs to be based on the size of the zone of aeration. Thus, for example, if high concentrations of SF_6 are observed at a distance of 15 ft, but not at 20 ft, then a well spacing of up to 30 ft might be appropriate, but greater than that would not be justified.

5.2.8.2 Geophysical Tests (PT8). Users may also consider the use of geophysical tools for identification of the zone of aeration (and thus well spacing), although their use has not been prescribed in this Design Paradigm. For example, use of neutron probes, capacitance probes, and electrical resistance tomography are reported in the literature (e.g., Acomb et al., 1995; Lundegard and LaBreque, 1998). These techniques generally have the ability to detect the presence of air in the subsurface at the "10% by volume" level. All of these techniques measure average properties over some roughly spherical volume. Depending on the specific technique, the diameters of those spheres over which air saturations are averaged range from 0.2 to 1 m. Once again, it is important to remember that all of these techniques require background (i.e., pre-air sparging) measurements.

6.0 SYSTEM DESIGN

When designing an air sparging system, the user must first:

- Define the target treatment zone
- Propose/revise a conceptual model for the air distribution in the aquifer
- Identify injection well spacings that ensure adequate air distribution throughout the target treatment zone and, if the Standard Design Approach is selected, use 15-ft well spacings
- Define the range of air injection operating pressures
- Determine if a soil vapor extraction system is necessary

Starting with a plan view map, air injection wells are then placed in locations consistent with the selected well-spacing. Injection well construction detail is discussed in Section 5.1 (Pilot Test Equipment). If a soil vapor extraction system is necessary, vapor extraction well locations are also selected. In some cases, it is convenient and cost-effective to co-locate the two in the same borehole. The piping and manifolding of the wells needs to be designed so that each well has its own dedicated pressure gauge and flow meter (rotameters are preferred as they provide rapid visual indication of flow). In addition, sampling access ports should be installed at least in the main manifold(s), if not in each individual line (this facilitates diagnostic tests discussed below).

Rotameters typically are calibrated at 77°F and 14.7 psia in accordance with American Society for Testing and Materials (ASTM) D 3195 Standard Practice for Rotameter Calibration. When the actual conditions during measurement of gas flow differ from the calibration conditions, the readings are affected both by the gas density and viscosity. Readings taken at other conditions should be corrected to the calibration conditions, if maximum accuracy is required. The rotameter manufacturer should be contacted to obtain a gas correction formula that accounts for the viscosity effect specific to the float design in their rotameter. In the absence of vendor specific information, the following correction formula presented in ASTM D 3195 may be used:

$$Q_S = Q_m \times \frac{T_s}{T_a} \times \frac{P_r}{P_s} \times \left(\frac{T_s}{T_a}\right)^{0.5}$$

where Q_m = measured flow (standard cubic feet per minute [SCFM]); Q_s = flow at standard conditions (SCFM); T_a = absolute temperature during measurement (°R); T_s = standard temperature (°R); P_r = absolute pressure in the rotameter during measurement (psia); and P_s = standard pressure (psia)

The temperature and pressure ratios correct for gas density, and the square root of the temperature ratio corrects for gas viscosity. For example, if a rotameter indicates a flow of 100 SCFM in a line at 10 psig and 80°F, the flow would be corrected to the flow rate at standard conditions as follows:

Q_m = 100 SCFM; Q_s = unknown; T_a = 80 + 459.67 = 539.67 °R; T_s = 77 + 459.67 = 536.67 °R; P_r = 10 + 14.7 = 24.7 psia; and P_s = 14.7 psia.

Therefore:

$$Q_S = 100 \times \frac{536.67}{539.67} \times \frac{24.7}{14.7} \times \left(\frac{536.67}{539.67}\right)^{0.5}$$

$$Q_S = 100 \times 0.9944 \times 1.68 \times 0.9972$$

Q_s = 167 SCFM

P.C Johnson et al. (2000) (Appendix A) recommend pulsed operation of banks of two to five injection wells for four reasons: a) the difficulty of controlling a multiwell air injection system increases as the number of wells manifolded together increases; b) the required system injection flow capacity is lower in this mode; c) studies suggest that performance can be improved by operating in a pulsed mode; and d) pulsed operation may be necessary in air sparging barrier applications to prevent groundwater bypassing due to water relative permeability reductions caused by air injection. Thus, the flow capacity of the system, Q_T (ft^3/min), is dictated by the number of wells in each well bank, the flow to each well, and the frequency at which each well bank is operated. For systems having identical numbers of wells in each well bank (N_{wells}), and equal flowrates to each injection well ($Q_{inject,i}$):

$$Q_T = N_{wells} \times Q_{inject,i} \times N_S \tag{7}$$

where N_S is the number of banks to be operated simultaneously.

For example, 100 ft^3/min flow capacity is sufficient to operate a system consisting of four banks of five wells each, with each well receiving 20 ft^3/min and each bank being operated individually for two h on a rotating basis (i.e., each bank is on for 2 h every 8 h). It is important that the blower(s) or compressor(s) are capable of providing the desired flow at the air injection pressure range determined in the pilot test.

To date, little effort has gone into determining how to choose pulsing frequencies (defined by on and off times) and therefore there is little fundamental basis for any guidance on this topic. SVE system off-gas data provides a direct measure of volatilization removal rates and, therefore, can be used to assess how changes in pulsing conditions affect volatilization rates. If aerobic biodegradation is the goal, simple calculations suggest that periods between injections (the off times) can be as long as several days as trapped air remains in the aquifer pores between injections. Some feel that the minimum active duration of injection (the on times) should be consistent with transient pressure transducer response data. Air injection needs to last at least as long as the time necessary to reach the peak in transducer response, and preferably as long as the time required to reach the asymptote. It is thought that these are representative of the times for air to emerge from the aquifer into the vadose zone and the times necessary to reach near-steady flow conditions (Johnson et al., 2000a) (Appendix E).

Well construction and compressor/blower details are not discussed further here. It should be noted that competent annular well seals are critical to successful air sparging operation. In their absence, the injected air will flow up along the well bore and the well will be ineffective. Compressor and blower selection should be discussed with a reputable manufacturer. It is important that the unit(s) are capable of providing the necessary flow capacity of clean air at the design pressures and of long-term steady operation.

7.0 AIR SPARGING SYSTEM MONITORING

Air sparging system monitoring plans should include startup, continued operation, and post-operation data collection activities. These are discussed briefly below.

At startup, and any time the operating conditions are changed, the following measurements should be conducted:

- The flow to and pressure at each injection well
- The on/off duration (timer sequence) for flows to each well.

In addition, to address safety concerns associated with air sparging system operation and to verify vapor extraction/capture system performance, if applicable), the following should be considered:

- Soil gas monitoring near locations of concern (nearby basements, sewers, etc.), if liberated contaminant vapor concentrations could be significant enough to be of concern from a health and safety standpoint
- A helium distribution test to assess distribution and migration of liberated vapors
- A helium recovery test to assess SVE recovery efficiency (if appropriate).

During continued operation, the following measurements should be made on a periodic basis (i.e., quarterly, semi-annually, etc.):

- Air sparging system injection flowrates (daily to weekly); if applicable, SVE system off-gas concentration and flowrate monitoring (daily to weekly)
- Groundwater quality monitoring: DO and contaminant concentrations (quarterly to semi-annually)
- Groundwater level measurements in wells unaffected by air injection (seasonal) to assess the position of the groundwater table relative to the injection and extraction wells screened intervals.

Finally, post-operation measurements should include:

- Groundwater quality monitoring: contaminant concentrations (quarterly for at least one year)
- Groundwater level measurements concurrent with the groundwater sampling.

In a recent survey of air sparging system design and operations at DoD facilities, the authors observed that many air sparging systems were poorly instrumented and monitored. Based on this work and other experience, it is not unreasonable to conclude that a significant fraction of existing air sparging systems are improperly instrumented and monitored. In particular, users should be aware of the following:

- It is critical that the system be properly instrumented so that flow to each individual air injection well can be verified and measured. It is the authors' experience that many systems do not have this level of instrumentation. Quite

frequently systems have a single flow measurement for an entire manifold of air injection wells. In those systems, one cannot determine the flow to each well, or even if there is flow to a given well in a multiple well system (unless only one well operates at a given time during normal system operation). It is the authors' experience that, in systems containing injection wells sharing a common manifold, all the air may be flowing to only a few of the manifolded wells. As discussed in P.C. Johnson et al. (2000) (Appendix A), it is the combination of variations in screened intervals, variations in soil properties, and the nature of air flow-injection pressure relationships that lead to this common problem. Thus, individual flow meters, pressure gauges, and valves are critical to proper air sparging system operation.

- As illustrated by Johnson et al. (1997), groundwater quality data obtained from conventional monitoring wells can be compromised by air sparging system operation. In such cases, practitioners often observe rapid increases in DO levels and rapid declines in dissolved contaminant concentrations. Then, after system operation, contaminant concentrations may rebound to near pre-treatment levels; in some cases, this rebound may occur over periods of 1 to 12 months. Thus, one must be cautious when interpreting monitoring well data at air sparging sites. To help minimize the potential for errors, Johnson et al. (1997) suggest a) long-term (12 months) monitoring following system shut-down, b) use of discrete (narrowly screened) sampling installations, or c) short-term (12 to 24 h) continuous slow-purging of conventional monitoring wells (or discrete sampling points) with time-series sampling. With respect to the latter, it has been observed that short-term continuous purging eventually yields samples that are more representative of formation conditions than in-well conditions, and that this might replace the need for longer-term groundwater quality monitoring.

During continued air sparging system operation, it is typically observed that volatilization removal rates decline to low (and often nondetect) levels (e.g., see Bruce et al., 2000b) (Appendix D). At that point it is difficult to assess real-time system performance via traditional measurements (e.g., groundwater monitoring and SVE off-gas sampling). In those cases, if real-time assessment is important, users should consider the tracer-based tests utilized by Bruce et al. (2000a) (Appendix B) and Amerson-Treat et al. (2000) (Appendix C).

8.0 SUMMARY

In situ air sparging is one of the most widely practiced aquifer remediation technologies today. This paper presents a feasibility assessment, pilot testing, design, and monitoring Design Paradigm developed by a group of researchers and practitioners who have been involved with air sparging for the past decade. The attached articles (Bruce et al., 2000a; Amerson-Treat et al., 2000; Bruce et al., 2000b; Johnson et al., 2000a; 2000b) (Appendices B through F, respectively) provide a thorough analysis of key aspects of the Design Paradigm and the research that was conducted to validate the Design Paradigm.

9.0 REFERENCES

Acomb, L.J., D. McKay, P. Currier, S.T. Berglund, T.V. Sherhart, and C.V. Benedicktsson. 1995. Neutron Probe Measurements of Air Saturation Near an Air Sparging Well. In *In Situ Aeration: Air Sparging, Bioventing, and Related Remediation Processes*. Pp. 47-61. (Hinchee, R.E., R.N. Miller, and P.C. Johnson, Eds.). Battelle Press: Columbus, Ohio.

Amerson, I. L. 1997. *Diagnostic Tools for the Monitoring and Optimization of In Situ Air Sparging Systems*. M.S. Thesis. Arizona State University.

Amerson-Treat, I.L, C.L. Bruce, P.C. Johnson, and R.L. Johnson. 2000. A Multi-Tracer Push-Pull Diagnostic Test for Assessing the Contributions of Volatilization and Biodegradation during In-Situ Air Sparging. Submitted to *Bioremediation Journal*.

Bass, D.H. and R.A. Brown. 1995. Performance of Air Sparging Systems - A Review of Case Studies. In: *Petroleum Hydrocarbons and Organic Chemicals in Ground Water: Prevention, Detection and Restoration*. Pp. 621-636. Ground Water Publishing Company: Dublin, Ohio.

Bruce, C.L., C.D. Gilbert, R.L. Johnson, and P.C. Johnson. 1998. Methyl *tert*-Butyl Ether Removal by In Situ Air Sparging in Physical Model Studies. In: Physical, Chemical, and Thermal Technologies. Pp. 293-298. (Wickramanayake, G.B. and R.E. Hinchee, Eds.). Battelle Press: Columbus, Ohio.

Bruce, C.L., I.L. Amerson-Treat, P.C. Johnson, and R.L. Johnson. 2000a. Use of SF_6 to Measure Air Distributions and Oxygen Mass Transfer Rates during In Situ Air Sparging. Submitted to *Bioremediation Journal*.

Bruce, C.L, P.C. Johnson, R.L. Johnson, and A. Leeson. 2000b. Application of the In Situ Air Sparging Design Paradigm to a BTEX Source Zone at the Construction Battalion Center, Port Hueneme, California. Submitted to *Bioremediation Journal*.

Bruell, C.J., M.C. Marley, and H. Hopkins. 1997. American Petroleum Institute Air Sparging Database. *J. Soil Contamination. 6*(2):169-185.

Ji, W., A. Dahmani, D. Ahlfeld, J.D. Lin, and E. Hill. 1993. Laboratory Study of Air Sparging: Air Flow Visualization. *Ground Water Monitoring and Remediation. Fall*:115-126.

Johnson, P.C., M.W. Kemblowski, and J.D. Colthart. 1990a. Quantitative Analysis for the Cleanup of Hydrocarbon-Contaminated Soils by In Situ Soil Venting. *Ground Water. 3*(28):413-429.

Johnson, P.C., C.C. Stanley, M.W. Kemblowski, D.L. Byers, and J.D. Colthart. 1990b. A Practical Approach to the Design, Operation, and Monitoring of In Situ Soil-Venting Systems. *Ground Water Monit. Rev.. 10*(2):159 - 178.

Johnson, P.C., R.L. Johnson, C. Neaville, E.E. Hansen, S.M. Stearns, and I.J. Dortch. 1997. An Assessment of Conventional In Situ Air Sparging Pilot Tests. *Ground Water. 35*(5):765-774.

Johnson, P.C., A. Das, and C.L. Bruce. 1999. Effect of Flowrate Changes and Pulsing on the Treatment of Source Zones by In Situ Air Sparging. *Environmental Science and Technology. 33*(10):1726-1731.

Johnson, P.C., R.L. Johnson, C.L. Bruce, and A. Leeson. 2000. Advances in In Situ Air Sparging/Biosparging. Submitted to *Bioremediation Journal*.

Johnson, R.L., R.R. Dupont, and D.A. Graves. 1996. *Assessing UST Corrective Action Technologies - Diagnostic Evaluation of In Situ SVE-Based System Performance*. EPA/600/R-96/041, 164p.

Johnson, R.L., P.C. Johnson, D.B. McWhorter, R.E. Hinchee, and I. Goodman. 1993. An Overview of In Situ Air Sparging. *Ground Water Monitoring and Remediation. 13* (4). Fall. 127-135.

Johnson, R.L., P.C. Johnson, T.L. Johnson, and A. Leeson. 2000b. Helium Tracer Tests for Assessing Air Recovery and Air Distribution during In Situ Air Sparging. Submitted to *Bioremediation Journal*.

Johnson, R.L., P.C. Johnson, T.L. Johnson, N.R. Thompson, and A. Leeson. 2000a. Diagnosis of In Situ Air Sparging Performance Using Groundwater Pressure Changes During Startup and Shutdown. Submitted to *Bioremediation Journal*.

Leeson, A., and R.E. Hinchee. 1996. *Soil Bioventing*. CRC Press: Boca Raton, Florida.

Lundegard, P.D., and D.J. LaBreque. 1998. Geophysical and Hydrologic Monitoring of Air Sparging Flow Behavior: Comparison of Two Extreme Sites. *Remediation. Summer*. 59 - 71.

Rutherford, K., and P.C. Johnson. 1996. Effects of Process Control Changes on Aquifer Oxygenation Rates during In Situ Air Sparging in Homogeneous Aquifers. Ground Water Monitoring and *Remediation. 16*(4):132-141.

U.S. Environmental Protection Agency. 1992. *A Technology Assessment of Soil Vapor Extraction and Air Sparging*. EPA/600/R-192/173. September.

APPENDIX A

Advances in In Situ Air Sparging/Biosparging

Paul C. Johnson[1], Richard L. Johnson[2], Cristin L. Bruce[1], and Andrea Leeson [3]

[1]Dept. of Civil and Environmental Engineering, Arizona State University, Tempe, Arizona; [2]Oregon Graduate Institute, Beaverton, Oregon; [3]Battelle Memorial Institute, Columbus, Ohio

In situ air sparging (IAS) is a technology commonly used for treatment of submerged source zones and dissolved groundwater plumes. The acceptance of IAS by regulatory agencies, environmental consultants, and industry is remarkable considering the degree of skepticism initially surrounding the technology in the early 1990s. Much has been learned and reported in the literature since that time, but it appears that practice has changed little. In particular, conventional pilot testing, design, and operation practices reflect a lack of appreciation of the complex phenomena governing IAS performance and the unforgiving nature of this technology. Many systems are poorly monitored and likely to be inefficient or ineffective. Key lessons-learned since the early 1990s are reviewed and their implications for practice are discussed here. Of particular importance are issues related to: a) the understanding of air flow distributions and the effects of geology and injection flowrate, b) the need to characterize air flow distributions at the pilot- and field-scale, c) how changes in operating conditions (e.g., pulsing) can affect performance improvements and reduce equipment costs, and d) how conventional monitoring approaches are incapable of assessing if systems are performing as designed.

INTRODUCTION

In its simplest form, IAS involves the injection of air into an aquifer with the intent to treat either trapped immiscible contaminants (source zones) or dissolved contaminant plumes. As the basic components of an IAS system are not complex (blowers/compressors, piping, and air injection wells) and because it is easily integrated with other remedial technologies (e.g., soil vapor extraction [SVE]), this technology has gained widespread use and acceptance. Based on informal surveys of underground storage tank (UST) regulators, it is now likely to be the most practiced engineered in situ remediation option when targeting the treatment of hydrocarbon-impacted aquifers. The rapid rate at which this technology has been embraced by regulatory agencies, environmental consultants, and industry is remarkable, especially when one considers the limited peer-reviewed published performance data available to date and the degree of skepticism surrounding the technology when it first gained attention in the early 1990s.

Biosparging is a term commonly heard when referring to certain types of IAS systems. Although the components are the same, biosparging is considered by some practitioners to be a different technology than IAS, distinguished by the emphasis on removal by aerobic biodegradation and, with some, lower air injection rates (<5 ft^3/min versus 10 to 20 ft^3/min per vertical well in typical IAS applications). It appears that some practitioners prefer to call their IAS systems "biosparging systems" (whether they truly are or not) in order to deflect questions concerning the fate of liberated contaminant vapors and to avoid the cost of installing and operating an SVE system along with their IAS system. With biosparging, the goal is to reduce the volatilization rate to a level where an SVE system is not necessary, with the hope that the resulting air injection rate is capable of maintaining a well-oxygenated treatment zone and a sufficient aerobic biodegradation rate. We consider biosparging to be a particular mode of IAS operation (not a separate technology), and also feel that such low air flowrate systems are inefficient and likely ineffective for treatment at many sites (as will be discussed in more detail below). We do agree, however, that some IAS systems can be operated safely without an accompanying SVE system, and that with time, the

dominant removal mechanism eventually becomes aerobic biodegradation at many hydrocarbon IAS sites.

In the early to mid-1990s, a number of IAS technology review articles appeared in the literature (Bass and Brown, 1995; Bruell et al., 1997; Johnson et al., 1993; Marley and Bruell, 1995; Reddy et al., 1995; U.S. Environmental Protection Agency [EPA], 1992). These gave a good perspective on the state-of-the-practice at that time, as well as performance expectations, and the understanding (or lack thereof) of the mechanisms and factors controlling air sparging performance. Of the data available then in the open literature (Johnson et al., 1993; U.S. EPA, 1992) and from American Petroleum Institute (API) member companies (Bruell et al., 1997; Marley and Bruell, 1995), most was associated with short-term feasibility pilot tests as opposed to long-term system operation. Few data sets included post-operation monitoring data. As a result, it was difficult to draw conclusions about what IAS could or could not achieve and there was much speculation concerning inherent limitations of the technology (e.g., mass transfer-limited removal). In what may be the most comprehensive performance data summary, Bass and Brown (1995) presented data for a number of IAS systems operated by the same environmental consulting firm. They noted observing rebound (dissolved concentration increases after the IAS system is turned off) at some sites and no significant rebound at others. In some cases, the concentration rebound was slow and occurred over a 12-month period. Mixed performance results were observed and Bass and Brown concluded that the data indicated that IAS was less effective at remediating petroleum hydrocarbon sites than chlorinated hydrocarbon sites. Bass and Brown's conclusion, however, may be an artifact of the types of IAS applications included in his study. At most of the petroleum-release sites, IAS was applied to remediate source zones, while dissolved plumes were typically the remediation target at the chlorinated solvent release sites.

Since the mid-1990s, much effort has gone into developing a better understanding of IAS performance and the factors and mechanisms that control it. This effort is reflected in the literature, where more than 50 peer-reviewed articles have been published on a wide range of topics, including flow visualization and air flow characterization (Acomb et al., 1995; Chen et al., 1996; Clayton, 1998; Elder and Benson, 1999; Hein et al., 1997; Ji et al., 1993; Lundegard and LaBreque, 1995, 1998; McKay and Acomb, 1996; Peterson et al., 1999; Roosevelt and Corapcioglu, 1998; Schima et al., 1996; Semer et al., 1998a); mass transfer studies in physical models (Adams and Reddy, 1999; Braida and Ong, 1998; Chao et al., 1998; Johnson et al., 1999; Reddy and Adams, 1998; Rutherford and Johnson, 1996; Semer and Reddy, 1998b); theoretical analyses of mass transfer and air distribution (Ahlfeld et al., 1994; Brooks et al., 1999; Clayton, 1999; Elder et al., 1999; Johnson, 1998; Lundegard and Andersen, 1996; Marley et al., 1992; McCray and Falta, 1996, 1997; Philip, 1998; Rabideau and Blayden, 1998; Unger et al., 1995; van Dijke et al., 1995,1998; Wilson et al., 1994, 1997), pilot testing (Johnson et al., 1997); design issues (Plummer et al., 1997); performance monitoring approaches (Amerson, 1997; Amerson et al., 2001); and results from field studies (Gordon, 1998; Johnston et al., 1998; Rabideau et al., 1999).

Unfortunately, it appears that the valuable knowledge gained from these studies has yet to be integrated into practice. While no formal surveys have been conducted, it is the authors' experience that the overall state-of-the-practice has changed little since the Marley and Bruell (1995) study. In brief, IAS system design remains largely empirical with an apparent lack of appreciation for the complexity of the phenomena and the sensitivity of the technology to design and operating conditions. In addition, performance monitoring seems to be limited to infrequent groundwater monitoring, and system optimization is rarely performed. Based on the authors' recent experiences gained from an Environmental Security Technology Certification Program (ESTCP)-sponsored multisite IAS evaluation project, it has been concluded that a) many IAS systems are being operated inefficiently or incorrectly and b) most site operators do not realize that their IAS systems are being operated inefficiently or incorrectly, because data collected from typical conventional monitoring plans are insufficient to make this deter mination.

The purpose of this article is to draw attention to some of the key lessons-learned since the early to mid-1990s, and to discuss the implications that this knowledge has for practice. The intent of this article is not to review or critique all the published studies or study areas but rather to focus on a few issues that the authors feel could have the most significant impact on practice at this time. The conclusions and results highlighted in this article also form the basis for the IAS Design Paradigm proposed by P.C. Johnson et al. (2001).

AIR DISTRIBUTION-RELATED ISSUES

As mentioned above, IAS involves the injection of air below the water table in the hope that it will cause volatilization and, in some cases, supply oxygen for aerobic biodegradation. The significance and degree to which each of these processes occurs depends on the air distribution resulting in the aquifer as well as the distribution and properties of the contaminants. In this section, we focus on air distribution-related issues.

Flow visualization and flow characterization experiments have provided valuable insight into IAS air distributions and how they are affected by geology and process conditions (flowrate, injection pressure, turning the system off and on, etc.). Three types of flow visualization and flow characterization experiments are reported in the literature: a) two-dimensional laboratory-scale visualization studies (Elder and Benson, 1999; Ji et al., 1993; Peterson et al., 1999; Roosevelt and Corapcioglu, 1998); b) "beach" sparging type studies (Leeson et al., 1995), and c) tomographic and other studies involving the use of geophysical tools (Acomb et al., 1995; Chen et al., 1996; Clayton, 1998; Elder and Benson, 1999; Lundegard and LaBreque, 1995; 1998, McKay and Acomb, 1996; Schima et al., 1996; Semer et al., 1998). In the first, the air distribution is viewed in cross section through plexiglass or glass walls. In the second, experiments are conducted at locations where the water table is at or slightly above ground surface (e.g., beaches and lagoons) and a plan view of the air distribution is inferred from the appearance of bubbles at ground surface. In the third, a three-dimensional picture of the air distribution is computed from in situ electrical resistivity measurements or is assessed through use of neutron probes, capacitance probes, or time-domain reflectrometry. A summary of the key results from these studies is given below, followed by a discussion of the important implications that these results have for practice.

Ji et al. (1993) conducted two-dimensional flow visualization studies in a 2 ft × 2 ft × 1 inch (approximately) transparent tank. The tank was packed with various sizes of glass beads, and model homogenous and heterogeneous subsurface hydrogeologic settings were simulated. The goal of the study was to observe how the injected air distributes itself beneath the water table, and how this distribution is affected by particle size, stratigraphy, and air injection flowrate. The reader is referred to the original publication for excellent pictures of the air distributions observed in their studies. Figure 1 illustrates key findings of that study that are discussed in the following paragraph.

As shown in Figures 1A through 1D, air distributions consisted of networks of distinct air channels for glass beads less than 1 mm in diameter. This is expected to be the type of behavior most often encountered in practice. For those settings having larger particle diameters (e.g., trenches back-filled with gravel), air could rise up through the formation in discrete bubbles. The Ji et al. (1993) conclusions have been confirmed by the subsequent studies reported by Elder and Benson (1999), Peterson et al. (1999), and Roosevelt and Corapcioglu (1998); these also provide more insight into air channel size and the extent of air saturation within the air flow zone.

Figures 1A and 1B illustrate effects of flowrate changes on the air distribution in a model homogeneous hydrogeologic setting. At low air flowrates, the buoyancy force dominates, and air flows vertically up from the air injection point in a few distinct air channels. The air distribution takes on a more bush-like

appearance as the air flowrate is increased. At some point, further increases in air injection flowrate do not yield further expansions of the air flow zone but rather cause increases in the density of air channels and an overall desaturation of water from within the established air flow zone (Rutherford and Johnson, 1996). Note that Figure 1B shows air flow paths that stopped growing before they reached the water table (these are labeled "dead branches" in Figure 1B), and it also shows there are zones within the boundaries of the air flow distribution where no air flows (these are labeled "bypassed regions" in Figure 1B). In Figure 1B, the maximum width of the air distribution is approximately equal to the depth of injection; however, readers are encouraged not to draw any generalized conclusions from this observation. It should be noted that these were two-dimensional studies, and that the injection depth was fixed and not a variable. For example, in the electrical resistance tomography field study of Lundegard and LaBreque (1998), the lateral extent of the air distribution (2 to 3 m) at a relatively sandy and homogeneous site was about half the depth to the screened interval of the air injection well.

Figures 1C and 1D correspond to low and high air flowrates, respectively, in a model-stratified geology. In this case, there are layers of 0.2-mm diameter glass beads within 0.75-mm diameter glass beads. As can be seen, the finer-grained layers impede the vertical movement of air so that stratified air layers are formed. Note that this happens even though the difference between the mean particle diameters is only a factor of three to four. Eventually, the air finds a route to the surface, either through a discontinuity in the finer-grained material, or through a build-up of pressure with time to the point where the air entry pressure of the finer-grained material is exceeded. As can be seen, increasing the air injection flowrate (and pressure) causes air to break through the finer-grained layers.

While one could argue that experiments conducted in small-scale, two-dimensional physical models are incapable of reproducing field-scale behavior, the results of Ji et al. (1993) are consistent with field-scale flow visualization studies reported in the literature. For example, beach sparging studies reported by Leeson et al. (1995) were conducted in a Florida lagoon underlain by relatively homogeneous sands. There, the majority of air channels appeared within 5 ft of the air injection point when it was driven first to 6 ft below ground surface and then to 10 ft. Increases in flowrate did little to expand the zone of air flow; instead they primarily increased the strength of flow in existing channels, and to some degree the density of air channels within the boundaries of the air flow region. Increasing the injection depth to 17.5 ft had the most pronounced effect, and the extent of air distribution expanded out to up to 16 ft from the injection point. The tomography results of Lundegard and LaBreque (1998) show air flow distributions in homogeneous and heterogeneous hydrogeologic settings that qualitatively resemble the flow distributions observed by Ji et al. (1993). The Lundegard and LaBreque (1998) results are reproduced in Figure 2. Figure 2A corresponds to a relatively homogeneous sandy setting, and the air distribution is roughly conical in shape with a maximum width of 2 to 3 m. Figure 2B corresponds to a glacial till setting, and in this case the air distribution is clearly stratified and anisotropic.

In addition, we know from theory that air flow distributions and air saturation are dependent upon the operating conditions and capillary pressure-related characteristics of the medium. While the intent of this article is not to discuss these in any detail (see Clayton, 1999, for example), it should be stated that a) for any porous material, air begins to flow only when the air entry pressure is exceeded and b) air saturations increase with increasing air pressure (for a fixed water pressure). Air entry pressures increase as a material becomes finer grained; typical air entry pressures for sands are a few cm-H_2O; for silty materials, they are in the tens of cm-H_2O and can be greater than hundreds of cm-H_2O for clays. Furthermore, at the same capillary pressure (air minus water pressure), the air saturation (or water desaturation) increases as the material becomes more coarser-grained.

To summarize, key results and conclusions from these and other air distribution studies include:

a. Air flow distributions are sensitive to relatively subtle changes in soil structure.

b. Air flow distributions may be irregular in shape, and there may be preferred directions of flow.
c. Low air flowrates generally yield less extensive and less effective air distributions.
d. Increasing air flowrate (and injection pressure) generally causes an increase in the density of the air flow network and can cause air to break through soil layers, under which it might normally be stratified at lower injection flowrates and pressures.
e. Air flow distributions resulting from vertical wells placed in homogenous and relatively permeable media tend to qualitatively resemble Figure 1B, where the areal extent of the air flow distribution is limited (<10 ft away from the injection point in many cases).
f. In more heterogeneous and layered settings, some degree of air stratification can be expected. Air stratification can be viewed as having both positive and negative implications for IAS performance. On one hand, it helps to achieve a broader air distribution; however, it also limits contact between the air lying below a finer-grained lens and contaminants that may have spread along the top of the lens (e.g., in dense, nonaqueous phase liquid [DNAPL] spill situations).

These observations have significant implications for practice. First, it is critical to adequately characterize a site from an air flow perspective to be able to assess the applicability of IAS at that site. Having said that, it should also be noted that, with even the most advanced site characterization tools currently available, air distributions are very difficult to predict. Certainly it is easiest for simple geologies (e.g., highly permeable and homogeneous settings and settings with large macroscale heterogeneities such as clay layers in otherwise sandy soils), but it is difficult for all other cases. Perhaps, therefore, the effort and resources spent on the initial site characterization should be better balanced with effort and resources allocated to characterization of the air distribution during the pilot-testing phase. Probably the single most important addition to a typical site assessment would be the requirement that one or more continuous cores be collected across the subsurface region bounded by the water table (or upper boundary of contamination) and the top of the anticipated screened interval of the injection well. These should be logged and photographed, and in some cases determination of relevant quantitative characteristics (e.g., grain size distribution) of the soils is warranted. Knowledge gained from a visual review of a continuous soil core is invaluable from an IAS air distribution perspective.

Following along this line of thinking, pilot testing and design strategies need to compensate for our inability to predict air flow distributions. This suggests that more effort needs to be focused on characterization of air flow distributions within the target treatment zone at the pilot- and full-scale, and the selection and placement of IAS wells needs to err on the side of over-design (e.g., more closely-spaced wells). R.L. Johnson et al. (2001a; 2001b; 2001c) and Bruce et al. (2001) have evaluated different air distribution characterization tools, and have found the use of pressure transducer responses and tracer gas (helium [He] and sulfur hexafluoride [SF_6]) monitoring to be practicable at the pilot- and full-scale.

Third, in characterizing and describing air flow distributions, the concept of a "radius of influence" should never be used. Practitioners should think in terms of three-dimensional air flow distributions (or "zone of air flow", or "extent of air flow") that are likely to be irregular in shape and likely to have a mixture of the characteristics exhibited by the model homogeneous and layered settings studied by Ji et al. (1993).

Finally, the air flow visualization results clearly show that low-injection-flowrate IAS systems (e.g., conventional biosparging systems) are likely to be inefficient (and possibly ineffective) for treatment. For example, consider the results of Bruce (2001) presented in Figure 3. They conducted an extended single-well air sparging pilot test in a relatively shallow and sandy gasoline-impacted aquifer. Figure 3 presents data from the vapor extraction system; here, cumulative mass removal is plotted as a function of air injection rate for air injection rates of 5, 10, and 20 ft^3/min. As can be seen, each successive increment in injection rate corresponds to an increment in cumulative mass removal at this site. Increasing the air

flowrate from 10 to 20 ft^3/min increased the cumulative mass removal by a factor of two to three. This is clearly reflective of air flow zone expansions and, at this site, is likely the result of behavior similar to the transition that occurs between Figures 1C and 1D. Thus, we suspect that conventional biosparging operating conditions are inefficient at many sites as these typically involve low-flowrate (<5 ft^3/min) air injection. The flow visualization results suggest that a much better strategy would be to operate these systems in a pulsed (on/off) mode, with short periods of higher intensity air flows. The data suggest that higher air flowrates yield better air distributions, and Rutherford and Johnson (1996) showed that trapped air remaining in the aquifer between injections continues to deliver oxygen to the aquifer while the system is off. Simple calculations show that the trapped gas (estimated at about 5% saturation of the pore space) can continue to deliver oxygen to groundwater for at least a day and probably longer, depending on the oxygen demand and groundwater flow velocity.

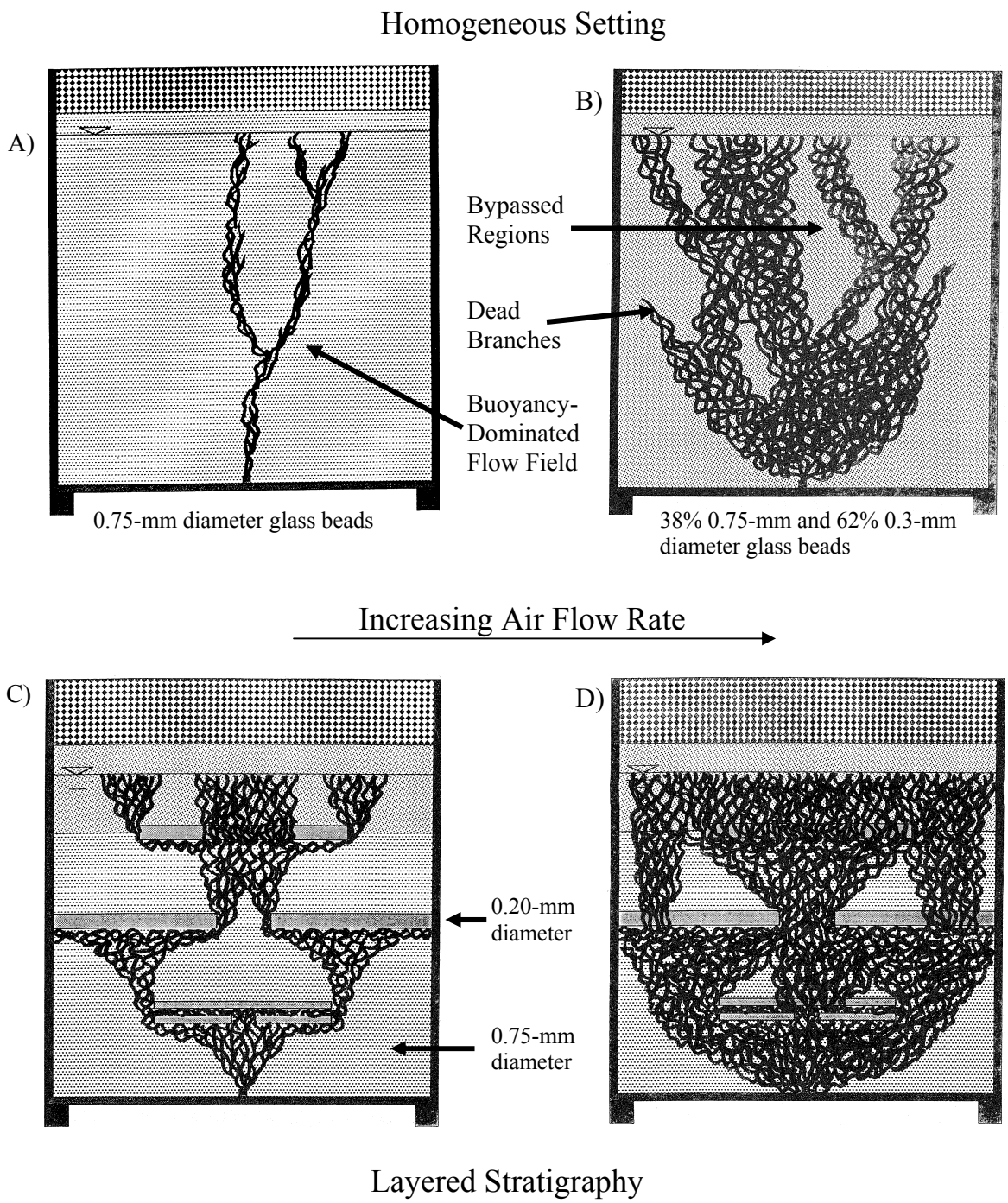

Figure 1. Effect of Air Flowrate Changes on Air Distribution in a Model Homogeneous Hydrogeologic Setting

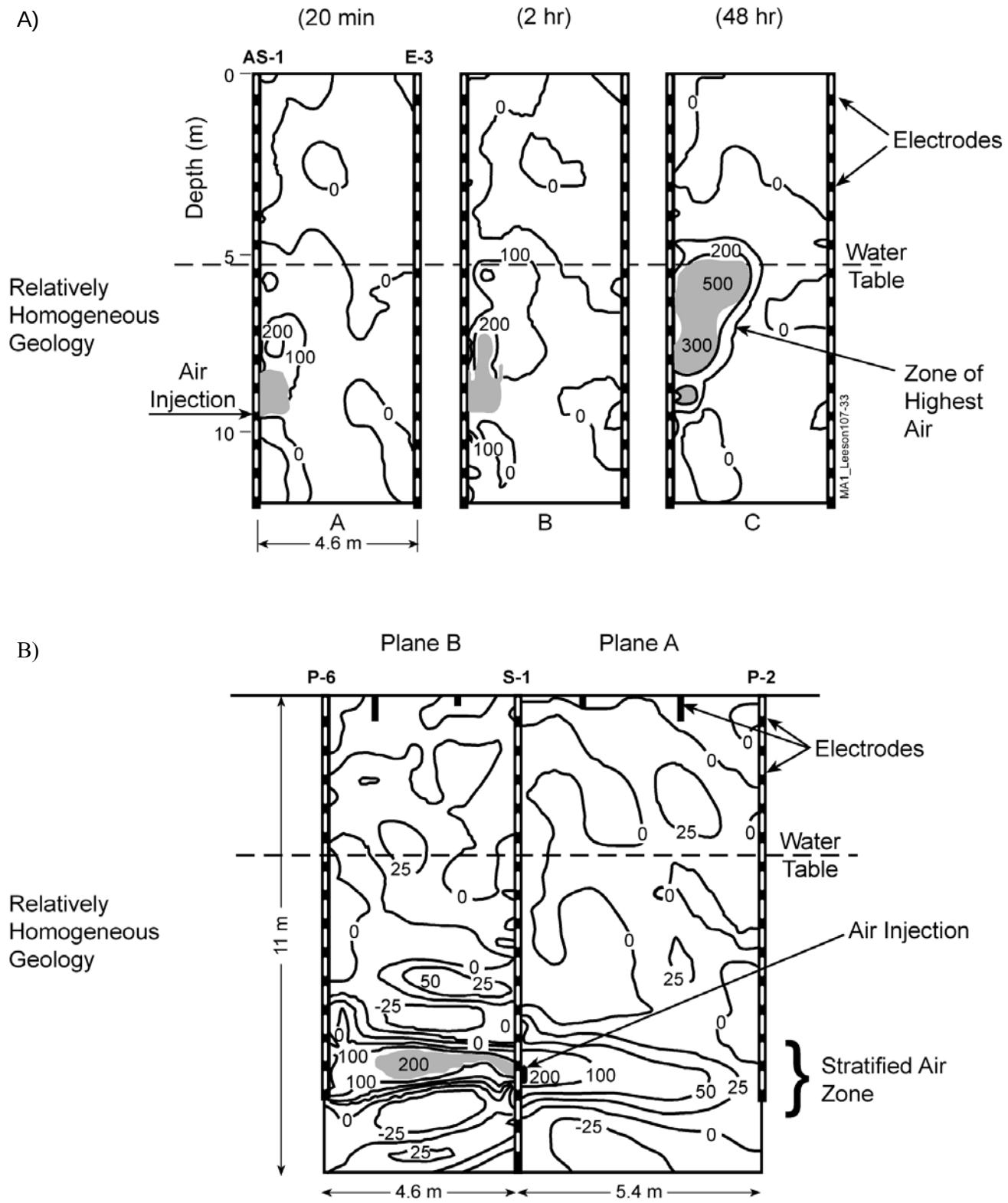

Figure 2. Air Flow Distributions in Homogeneous and Heterogeneous Hydrogeologic Settings

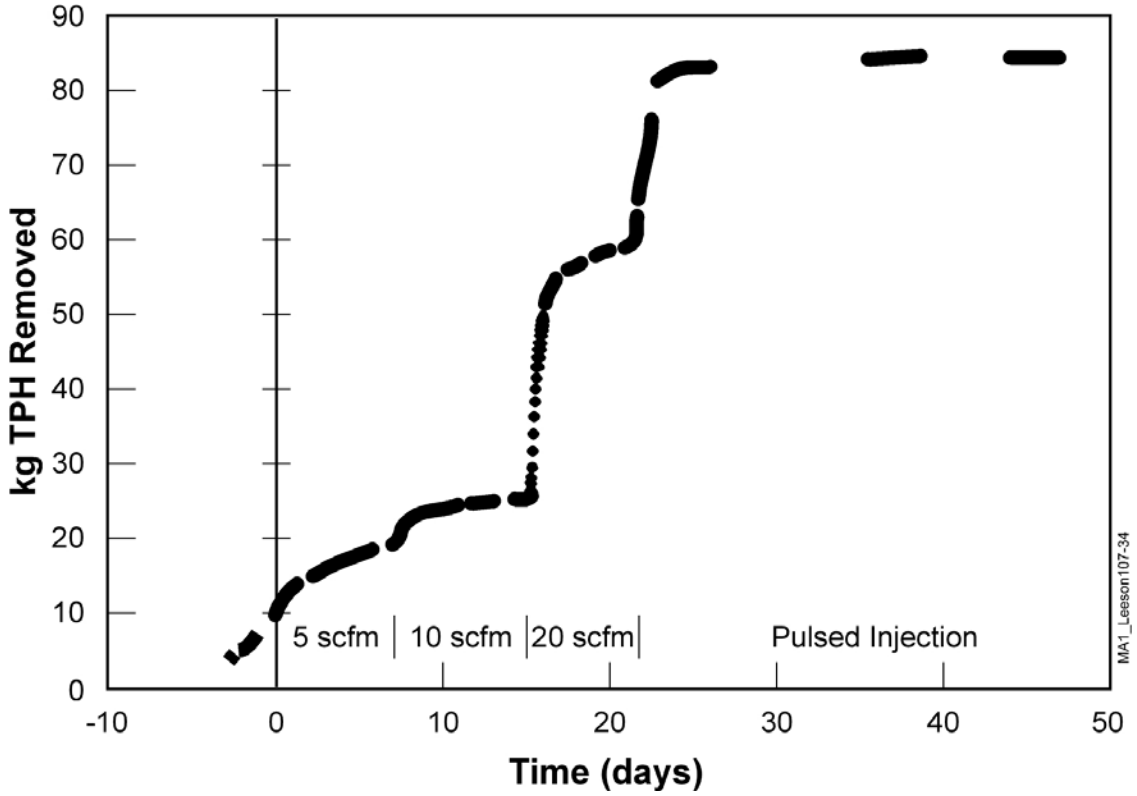

Figure 3. Cumulative Mass Removal Versus Time in SVE Off-Gas

CONTAMINANT REMOVAL-RELATED ISSUES

Developing an understanding of factors affecting contaminant removal during IAS begins with a conceptual model. Most authors have adopted one similar to that presented by Ahlfeld et al. (1994). In brief, it is acknowledged that a) air generally flows through discrete air channels in the aquifer; b) removal of contaminants from within the air channels behaves much like contaminant removal during soil vapor extraction (Johnson et al., 1990a; 1990b) and bioventing (Leeson and Hinchee, 1996); and c) contaminant removal from water-saturated regions lying outside the air channels becomes liquid-phase mass-transfer limited. Thus, we expect that the initial contaminant removal occurs from within the air channels. The volatilization contribution during this time frame can be estimated as the product of the air injection rate and the maximum equilibrium vapor concentration, with the latter being proportional to either a) the vapor pressure, molecular weight, and mole fraction for cases of source zone (immiscible phase-trapped nonaqueous phase liquid [NAPL]) treatment or b) the Henry's Law Constant and the dissolved concentration for dissolved plume treatment. An upper bound on the aerobic biodegradation contribution to treatment in the air channels can be estimated using reported biodegradation rates from bioventing systems, and these generally fall within the range of 1 to 10 mg-hydrocarbon/kg-soil/d. The use of this type of approach for estimating initial volatilization removal rates has been verified in a number of physical model studies (e.g., Johnson et al., 1999), while aerobic biodegradation rates in air channels have yet to be confirmed.

There is less agreement and more uncertainty in our understanding of the longer-term contaminant removal that occurs from outside the air channels. In the early 1990s, it was speculated that IAS system performance was inherently limited by aqueous-phase diffusion, and therefore, substantial removal would only ever occur from those areas directly impacted by air channels. Based on data now available from field studies (e.g., Johnston et al., 1998) and other empirical evidence (e.g. Bass and Brown, 1995), it appears that substantial removal of contaminants found outside the air channels must occur.

Investigators have used a range of approaches to gain a better understanding of contaminant removal, including fundamental microscale modeling (Johnson, 1998; Unger et al., 1995; Wilson et al., 1994; 1997), empirical lumped-parameter modeling (Elder et al., 1999; Rabideau and Blayden, 1998), physical model experiments (Adams and Reddy, 1999; Braida and Ong, 1998; Chao et al., 1998; Johnson et al., 1999; Rutherford and Johnson; 1996; Semer and Reddy, 1998) and field-scale studies (Johnston et al., 1998). Results and conclusions drawn from these studies sometimes appear to conflict, and this is often the result of differences in the scenarios studied, the experimental designs, and biases inherent in the analyses methods. First, readers need to note that some modeling and experimental studies focus on the treatment of source zones (regions containing trapped immiscible-phase contaminants), whereas others have focused on the treatment of dissolved contaminant plumes. Second, with the laboratory-scale experiments, there are differences in operating conditions, and some studies have been conducted under conditions not representative of most IAS applications (e.g., very large particle sizes and very high air flowrates per unit volume of aquifer). Third, there are differences in the approaches used for data analysis. In the following, we attempt to summarize some of the key findings from these studies and discuss the implications for practice.

First, for both source zone and dissolved plume treatment, the microscale modeling studies suggest that long-term removal rates are limited by liquid-phase mass transfer processes. Mathematical models based on this assumption are capable of predicting the qualitative features of the observed mass removal behavior, and they have proven to be useful for understanding the significance of various processes and chemical properties. However, none have been shown to be particularly useful as predictive tools because they require inputs that are impracticable to determine a priori (air distribution network characteristics such as air channel spacing, air channel surface area, etc.). Many have assumed that water-phase diffusion is the limiting process, but both Unger et al. (1995) and Johnson (1998) have suggested

that the evaporation of water into the air channels could result in the significant advection of dissolved contaminants towards the air channels.

In brief, results of the mathematical and mechanistic studies have the following implications to practice:

a. Removal in the short-term (days to weeks) is dominated by removal of contaminants found within air channels, and volatilization and aerobic biodegradation contributions to these removal rates are SVE- and bioventing-like and can be estimated as discussed above. Given that the air only occupies a fraction of the pore space (20 to 40% of the pore space within the air flow zone), removal rates measured in short-term pilot tests are not likely to be very representative of removal rates in the long term.
b. Removal in the long term is dominated by removal of contaminants found outside the air channels, and is limited by liquid-phase mass-transfer processes. Most have assumed that water-phase diffusion is the limiting process, but evaporation of water into the air channels could result in the significant advection of dissolved contaminants towards the air channels.
c. For aerobically biodegradable compounds, biodegradation due to oxygen delivery during continuous-injection IAS has the potential to become the dominant process (relative to volatilization) only when dissolved hydrocarbon concentrations are less than 1 mg/L-H_2O (Johnson, 1998). For pulsed systems, the analysis is more complex as the pulse frequency adds an additional variable, and it is difficult to set down definitive conclusions. As the downtime between air injections increases relative to the injection duration, the significance of aerobic biodegradation increases relative to volatilization; however, in decreasing the volatilization, the cumulative removal for a given time may also decrease.
d. All other things being equal, removal is more efficient under conditions having a higher density of air channels.
e. Most mathematical models suggest that long-term removal should become aqueous-phase mass transfer-limited. When this is the case, the removal rate becomes independent of the chemical properties normally associated with volatilization processes (i.e., vapor pressure and Henry's Law constant). Instead, the removal rate is expected to be proportional to the dissolved contaminant concentration, and the rate of change in removal with time decreases with increased soil residual concentrations (Johnson, 1998). In general, therefore, we expect dissolved plumes to remediate faster than source zones; Johnson (1998) also expects IAS to be as effective at removing chemicals with low Henry's Law constants as it is at removing more highly volatile chemicals (benzene, trichloroethene [TCE], etc.).

Some find the conclusions in (e) to be counter-intuitive based on experiences with aboveground water-treatment processes. To better support conclusions (a), (b), and (e), consider the data from Bruce et al. (1998). In those experiments, a NAPL mixture containing six hydrocarbons was spilled into a large (2 m wide x 2m tall x 5 m long) physical model, and then the water table was raised and lowered to create a source smear zone. This was followed by continuous air injection and monitoring of the off-gas vapors. A reference SVE-like experiment was also conducted; the only difference between the two experiments being that the water table was lowered below the smear zone for the SVE-like simulation and the water table was maintained above the smear zone for the IAS simulation. The results from the SVE- and IAS-simulations are presented in Figures 4A and 4B, respectively. The SVE simulation shows removal behavior consistent with typical SVE expectations; that is, it is dominated primarily by differences in vapor pressures (order of vapor pressures: isopentane > methyl *tert*-butyl ether [MTBE] > benzene > isooctane > toluene > xylenes) and the vapor composition reflects preferential removal of the more volatile compounds. Figure 4B, corresponding to the IAS-simulation, shows quite different behavior. In the short-term, initial removal rates were comparable with those measured initially in the SVE-simulation, consistent with conclusion (c) above. Differences between Figures 4A and 4B become noticeable after about 200 minutes. There, the longer-term IAS removal rate versus time behavior is quite similar for all

compounds, despite significant differences in Henry's Law Constants (e.g., the Henry's Law Constant for benzene is about ten times the value for MTBE).

A)

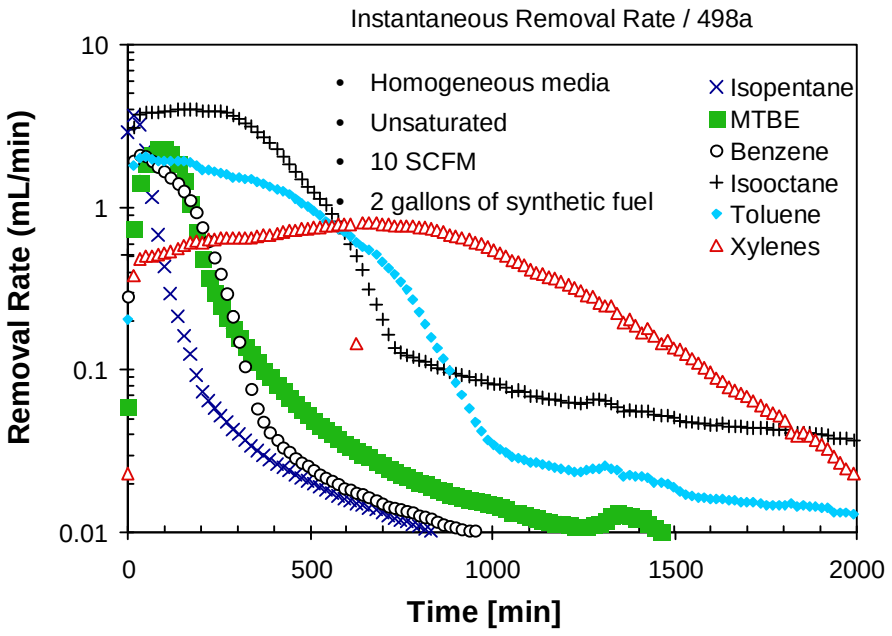

B)

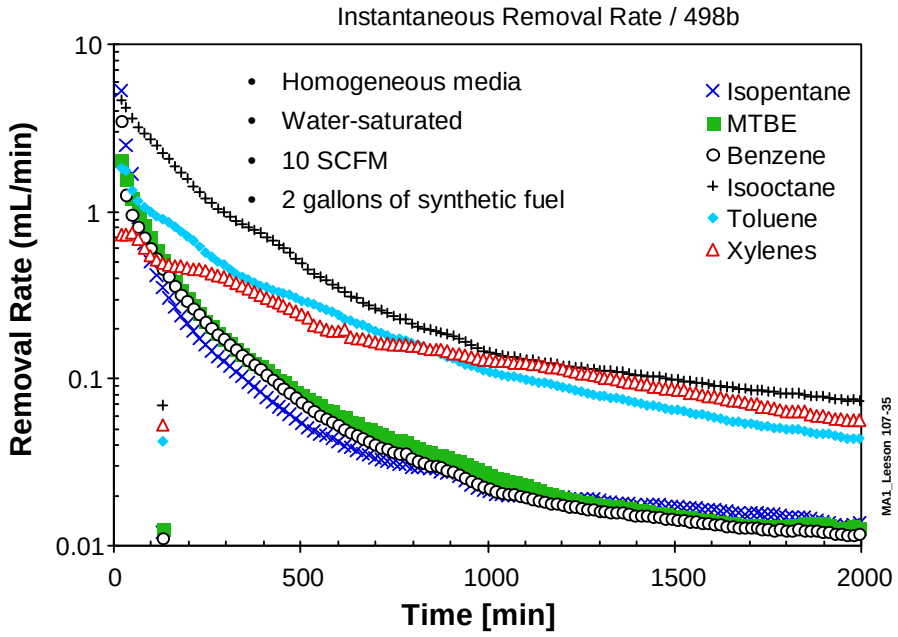

Figure 4. Removal of Contaminants Under Simulated (A) SVE Conditions and Under (B) Air Sparging Conditions

IAS MONITORING RELATED ISSUES

Monitoring IAS systems at the pilot- and full-scale level is frequently minimal. Changes in dissolved oxygen in groundwater monitoring wells are used as indicators of the extent of the air distribution at the pilot-scale level. Full-scale monitoring plans generally contain only those activities necessary to comply with regulatory compliance requirements. This usually translates to quarterly (or less frequent) groundwater monitoring and off-gas contaminant concentrations and flowrates if an SVE system is being operated.

Relative to the amount of effort devoted to understanding air distribution and contaminant removal mechanisms, less effort has been focused on assessing and developing monitoring approaches appropriate for IAS systems. Johnson et al. (1997) conducted a comparison of conventional and alternative monitoring approaches at a service station site. They concluded that the conventional monitoring approaches were likely to be misleading in many cases; specifically, contaminant concentration data collected from conventional monitoring wells was suspect. At best, groundwater monitoring well data could be used to assess the lateral extent of the air distribution. In addition, they recommended the use of tracer tests and more depth-discrete monitoring at the pilot- and full-scale levels.

Recently, there has been much activity in the development and assessment of "diagnostic tools" for IAS pilot testing and full-scale performance monitoring. The results of these studies are just now appearing in peer-reviewed publications. For example, R.L. Johnson et al. (2001a; 2001b; 2001c) and Bruce et al. (2001) have evaluated different air distribution characterization tools, and have found the use of pressure transducer responses and tracer gas (He and SF_6) monitoring to be practicable at the pilot- and full-scale levels. Some have also discussed the utility of in-well temperature measurements as an indicator of air flow distributions.

As noted by Lundegard and LaBrecque (1998) and R.L. Johnson et al. (2001b), the qualitative behavior of transient water-level pressure transducer responses measured in piezometers during start-up often reflects the gross features of the air distribution. For example, pressure transducer responses associated with air distributions like that shown in Figure 1B tend to be significantly different from transient pressure transducer responses associated with air distributions like that shown in Figure 1C. Thus, the transient pressure transducer data is a good indicator of the general nature of the air distribution and is a good tool for identifying the presence of significant stratified air. More information on the mechanics and data interpretation of this test is given by R.L. Johnson et al. (2001b).

Details on the use of helium during pilot testing can be found in R.L. Johnson et al. (2001a). In this case, helium is blended with the injection gas, and its appearance in soil gas monitoring points placed immediately above the capillary fringe is used as an indicator of the lateral extent of the air flow. As described in Amerson (1997) and Bruce et al. (2001), SF_6 can also be blended in with the injection air; in this case its appearance in groundwater in the target treatment zone is used to characterize the air distribution.

Amerson et al. (2001) note that groundwater quality monitoring is incapable of providing measures of system performance in the short term and therefore is of little use from a system optimization standpoint. For this reason, they report on the development and evaluation of two diagnostic tests (Amerson, 1997; 2001; Bruce et al., 2001). One is a push-pull type test involving the injection of a multitracer solution into the target treatment zone through a monitoring well, piezometer, or drive point. The injected solution is initially deoxygenated and contains a) a nondegradable, nonvolatile conservative tracer; b) one or more nondegradable, volatile chemicals; and c) a biologically degradable, nonvolatile compound. After some predetermined hold time, an excess quantity of groundwater is extracted from the same injection point,

and then changes in the concentrations of the tracer compounds are measured. Volatilization and oxygen consumption rates are then estimated from mass balances on the tracer components. A second complementary approach involves the blending of SF_6 into the injection air for a 12- to 24-hour period, and then determining its concentration in groundwater at monitoring points placed in the target treatment zone. The data is then used to estimate the rate of oxygen delivery to the aquifer. One attractive feature of this second diagnostic tool is that it yields both air distribution and oxygen delivery information from the same test.

DESIGN AND OPERATION ISSUES UNIQUE TO IAS SYSTEMS

The complex nature of the underlying phenomena controlling IAS performance creates some unique issues associated with IAS system operation and design. Three of the more critical operation and design issues are discussed here; these include the operation of IAS systems in a pulsed mode, operating considerations for contaminant migration barrier applications, and issues associated with the operation of air injection wells on a common manifold.

Operating IAS Systems in a Pulsed Mode

First, there has been much debate concerning the effect of air injection pulsing on IAS performance. Here, "pulsing" refers to a mode of operation where the air injection is periodic with some preset duration of injection times and downtimes (e.g., 4 hours on followed by 8 hours off). In the early 1990s, it was speculated that pulsing could cause macroscale mixing in the aquifer and might also change the air flow distribution, and that this in turn would help to overcome the expected aqueous-phase mass transfer limitations. Results of air distribution studies (e.g., Ji et al., 1993; Leeson et al., 1995) suggest that significant changes in air distributions are not effected by pulsing, and there has been no data presented to date to support the assertions of significant macroscale aquifer mixing. Nevertheless, contaminant removal studies conducted in physical models by Reddy and Adams (1998) and Johnson et al. (1999), and field data from Bruce (2001) have shown contaminant removal improvements resulting from pulsed operation. The field data of Bruce (2001), already presented in Figure 3, shows about a 30% increase in cumulative removal resulting from pulsed operation versus steady injection.

There are also other technical and practical reasons for operating in a pulsed mode. If oxygen delivery is the goal (versus volatilization), oxygen transfer can be as efficient under pulsed conditions as continuous injection because trapped air left in the aquifer continues to provide oxygen between injection cycles (Rutherford and Johnson, 1996). More important to some, perhaps, is the effect that pulsing can have on the economics of IAS systems. Capital costs for compressors begin to increase significantly with increases in flow capacity for flowrates in excess of about 100 standard cubic feet per minute (SCFM). Thus, one can connect more air injection wells to a given compressor and operate each at higher injection rates when wells are not operated simultaneously but are operated in an alternating pattern around the site, resulting in a pulsed mode.

The Use of IAS Systems as Contaminant Migration Barriers

In some cases, IAS systems are deployed as contaminant migration barriers. Air injection wells are generally placed in a line (or multiple lines) perpendicular to the direction of groundwater flow, with the goal of creating a treatment zone that prevents further down-gradient migration of a dissolved contaminant plume. In this case, one must balance the benefits of high air injection rates (improved air distributions) with the reductions in permeability to water flow that result from the increased air saturations in the IAS treatment zone. As the permeability reduction increases, there will be a greater tendency for groundwater to flow around and under the treatment zone. At this time, it is not clear how to best achieve this balance, as conventional methods for determining groundwater flow paths (e.g., monitoring the migration of conservative water soluble tracers) typically require long time frames (months) and measuring aquifer water permeability changes during air injection can be problematic. One option for reducing the possible impact of permeability reductions is to operate air injection in a pulsed mode, with the frequency of pulsing being linked somehow to the groundwater flowrate and contaminant concentration reduction desired. Further study in this area is clearly needed at this time.

Issues Associated with Operating Multiple Air Injection Wells

A critical concept typically overlooked in practice concerns the operation of multiple air injection wells connected to a common manifold. To understand this issue, it is necessary to review two important features of air injection. First, air begins to flow only after reaching a threshold pressure; this threshold pressure is the summation of the hydrostatic head of groundwater above the top of the air injection screen plus the air entry pressures of the well screen, well annulus packing, and the formation. Typically, the hydrostatic head is the largest of the contributions to the threshold pressure (several feet of H_2O of hydrostatic head versus less than 1 ft-H_2O of air entry pressure for sandy soils). Second, once steady air flow is achieved, relatively small changes in injection pressure (10 to 20%) can cause significant increases in air injection flowrate (2X to 10X). For example, the flowrate versus pressure data shown in Figure 5 is qualitatively representative of our observations at IAS field sites. This data comes from two-dimensional physical model studies (Rutherford and Johnson, 1996). Two different flow versus injection pressure regimes are observed. In the first, air injection is initiated at a pressure of about 40 inches-H_2O, and then the flowrate increases two orders of magnitude across an increase in injection pressure of only 20 inches-H_2O. Rutherford and Johnson (1996) report that across this injection pressure range, increases in air injection pressure cause visual changes in the extent and density of the air distribution. In the second regime, further increases in injection pressure correspond to less substantial changes in flowrate. For pressure increases above this range, Rutherford and Johnson (1996) report that the extent of the air distribution did not change, but increases in air saturation were observed.

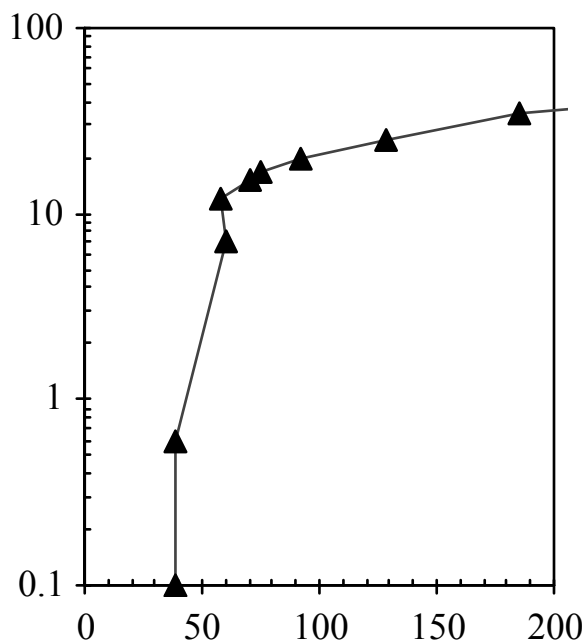

Figure 5. Flowrate Versus Pressure from Two-Dimensional Physical Model Studies

To fully appreciate the implications of this in practice, consider the following thought example involving a conventional IAS system comprised of multiple air injection wells connected to a common manifold having one main flow meter between the blower and the manifold. There are pressure gauges connected to each individual air injection line. As in practice, there are differences between the actual depths of well screens and design depths (as much as 12 inches at most sites). At start-up, the air injection pressure is increased and air flow is observed to begin once a threshold pressure is reached. At this point, the

operator notes that all wells have identical wellhead pressures and many would assume that this indicates that air is flowing to all wells. What goes undetected is the fact that air is flowing only to one well, the well that has the lowest threshold air pressure (probably the one with the shallowest screen—the likelihood of two wells having identical characteristics is small). Now the operator increases the injection pressure incrementally, and the manifold flowrate is observed to increase substantially. Soon, however, the operator reaches the maximum capacity of the compressor and the manifold final flowrate and air injection wellhead pressures are noted. It would not be unusual at this point for the operator to assume that all wells have flow, and it would also not be unusual for the system to be operated in this mode indefinitely. Again, what cannot be detected by this setup is that flow into the first well probably increased substantially, and perhaps, the manifold pressure increased enough that air now flows into a second or third well; however, there are also likely to be some wells that have no flow at this point. Based on the authors' experiences reviewing existing IAS systems, it is likely that many IAS systems are currently operated in a similar manner. At one site having 20 "identical" wells connected to a common manifold, air was flowing into fewer than half the wells, and this condition went undetected for over a year.

There are two lessons to be learned from this thought example and our experiences. First, given the relatively low cost of flow meters, it seems foolish to continue to operate and monitor IAS systems without dedicated flow meters and flow control valves on each air injection well. Second, even with dedicated flow meters, users will find it very difficult to balance air injection flows to more than two to five wells at one time because of the nonlinearity in the flowrate versus air injection pressure behavior and the normal differences in actual air injection well constructions at any given site. Therefore, practitioners will find it easier to balance the flows to banks of maybe two to five wells at once and to cycle the air injection to various well banks across the site. This mode of operation fits in well with the previous recommendation to operate IAS wells in a pulsed mode. For example, one service station-scale IAS system is composed of 18 air injection wells connected in four banks of wells (two banks of five wells and two banks of four wells). Air is injected at a rate of approximately 20 ft^3/min into each well. The compressor runs continuously, but only one well bank is active at any one time, and each receives air flow for two hours every eight hours.

These same observations have implications for the use of horizontal IAS wells. In this case, there is the risk that all of the air will preferentially exit through a small portion (or portions) of the entire screen length. Designers of horizontal wells have to compensate for variations in depth and soil properties along the length of the horizontal well. The first can be accomplished by designing the well such that the pressure drop across the well screen material is large compared to the variations in depth of the well. The second, however, is more challenging as it requires large injection pressures just outside the well screen, and these are not easy to achieve while taking measures to compensate for variations in depth.

SUMMARY AND FUTURE APPLICATION

Much has been learned about IAS since the early 1990s; however, it appears that practice has changed little. In particular, conventional pilot testing, design, and operation practices reflect a lack of appreciation of the complex phenomena governing IAS performance and the unforgiving nature of this technology. Many systems are poorly monitored and likely to be inefficient or ineffective, but the monitoring plans are insufficient to determine if that is in fact the case. In this paper, some of the key lessons-learned since the early 1990s have been reviewed, with an emphasis on those that we feel could make significant impacts in practice. Specifically, it is important for practitioners to gain a better understanding of a) air flow distributions and the effects of geology and injection flowrate, b) the need to characterize air flow distributions at the pilot- and field-scale levels, c) how changes in operating conditions (e.g., pulsing) can affect performance improvements and reduce equipment costs, and d) how conventional monitoring approaches are incapable of assessing if systems are performing as designed.

It is important for all to develop a good understanding of IAS, as it will continue to be widely applied at UST petroleum-release sites and because we are now beginning to see the incorporation of IAS systems into other innovative technologies. For example, Salanitro et al. (1999) report on the use of IAS for oxygen delivery in their MTBE bio-augmentation process, and others have considered using IAS systems for gas delivery (hydrogen, propane, etc.) in other aquifer bioremediation schemes.

REFERENCES

Acomb, L.J., D. McKay, P. Currier, S.T. Berglund, T.V. Sherhart, and C.V. Benedicktsson. 1995. Neutron Probe Measurements of Air Saturation Near an Air Sparging Well. In: *In Situ Aeration: Air Sparging, Bioventing, and Related Remediation Processes*. pp. 47-61. (Hinchee, R.E., R.N. Miller, and P.C. Johnson, Eds.). Battelle Press: Columbus, Ohio.

Adams, J.A., and K.R. Reddy. 1999. Laboratory Study of Air Sparging TCE-Contaminated Saturated Soils and Groundwater. *Ground Water Monitoring and Remediation. 19*(3):182-190.

Ahlfeld, D.P., A. Dahmani, and W. Ji. 1994. A Conceptual Model of Field Behavior of Air Sparging and Its Implications for Application. *Ground Water Monitoring and Remediation. 14*(4):132-139.

Amerson, I.L. 1997. *Diagnostic Tools for the Monitoring and Optimization of In Situ Air Sparging Systems*. M.S. Thesis. Arizona State University.

Amerson, I.L., C.L. Bruce, P.C. Johnson, and R.L. Johnson. 2001. A Multi-Tracer Push-Pull Diagnostic Test for In Situ Air Sparging Systems. *Bioremediation Journal*, *5*(4):349-362.

Bass, D.H., and R.A. Brown. 1995. Performance of Air Sparging Systems—A Review of Case Studies. In: *Petroleum Hydrocarbons and Organic Chemicals in Ground Water: Prevention, Detection and Restoration.* pp. 621-636. Ground Water Publishing Company: Dublin, Ohio.

Braida, W.J. and S.K. Ong. 1998. Air Sparging: Air-Water Mass Transfer Coefficients. *Water Resources Research. 34*(12):3245-3253.

Brooks, M.C., W.R. Wise, and M.D. Annable. 1999. Fundamental Changes in In Situ Air Sparging Flow Patterns. *Ground Water Monitoring and Remediation. 19*(2):105-113.

Bruce, C.L. 2001. *Performance Expectations for In Situ Air Sparging Systems*. Ph.D. Dissertation. Arizona State University.

Bruce, C.L., I.L. Amerson, R.L. Johnson, and P.C. Johnson. 2001. Use of an SF_6-Based Diagnostic Tool for Assessing Air Distributions and Oxygen Transfer Rates during IAS Operation. *Bioremediation Journal*, *5*(4):337-347.

Bruce, C.L., C.D. Gilbert, R.L. Johnson, and P.C. Johnson. 1998. Methyl *tert*-Butyl Ether Removal by In Situ Air Sparging in Physical Model Studies. In: *Physical, Chemical, and Thermal Technologies*. pp. 293-298. (Wickramanayake, G.B., and R.E. Hinchee, Eds.). Battelle Press: Columbus, Ohio.

Bruell, C.J., M.C. Marley, and H. Hopkins. 1997. American Petroleum Institute Air Sparging Database. *J. Soil Contamination. 6*(2):169-185.

Chao, K.P., S.K. Ong, and A. Protopapas. 1998. Water-to-Air Mass Transfer of VOC's: Laboratory-Scale Air Sparging System. *J. Environ. Engineering. 124*(11):1054-1060.

Chen, M.R., R.E. Hinkley, and J.E. Killough. 1996. Computed Tomography Imaging of Air Sparging in Porous Media. *Water Resources Research. 32*(10):3013-3024.

Clayton, W.S. 1998. A Field and Laboratory Investigation of Air Fingering during Air Sparging. *Ground Water Monitoring and Remediation. 18*(3):134-145.

Clayton, W. 1999. Effects of Pore Scale Dead-End Air Fingers on Relative Permeabilities for Air Sparging in Soils. *Water Resources Research. 35*(10):2909-2919.

Elder, C.R., and C.H. Benson. 1999. Air Channel Formation, Size, Spacing, and Tortuosity during Air Sparging. *Ground Water Monitoring and Remediation. 19*(3):171-181.

Elder, C.R., C.H. Benson, and G.R. Eykholt. 1999. Modeling Mass Removal During In Situ Air Sparging. *Journal of Geotechnical and Geoenvironmental Engineering. 125*(11):947-958.

Gordon, M.J. 1998. Case History of a Large-Scale Air Sparging/Soil Vapor Extraction System for Remediation of Chlorinated Volatile Organic Compounds in Groundwater. *Ground Water Monitoring and Remediation. 18*(2):137-149.

Hein, G.L., J.S. Gierke, N.J. Hutzler, and R.W. Falta. 1997. Three-Dimensional Experimental Testing of a Two-Phase Flow-Modeling Approach for Air Sparging. *Ground Water Monitoring and Remediation. 17* (3):222-230.

Ji, W., A. Dahmani, D. Ahlfeld, J.D. Lin, and E. Hill. 1993. Laboratory Study of Air Sparging: Air Flow Visualization. *Ground Water Monitoring and Remediation. Fall*:115-126.

Johnson, P.C. 1998. Assessment of the Contributions of Volatilization and Biodegradation to In Situ Air Sparging Performance. *Environmental Science and Technology. 32*:276-281.

Johnson, P.C., A. Das, and C.L. Bruce. 1999. Effect of Flow Rate Changes and Pulsing on the Treatment of Source Zones by In Situ Air Sparging. *Environmental Science and Technology. 33*(10):1726-1731.

Johnson, P.C., R.L. Johnson, C. Neaville, E.E. Hansen, S.M. Stearns, and I.J. Dortch. 1997. An Assessment of Conventional In Situ Air Sparging Pilot Tests. *Ground Water. 35* (5):765-774.

Johnson, P.C., M.W. Kemblowski, and J.D. Colthart. 1990a. Quantitative Analysis for the Cleanup of Hydrocarbon-Contaminated Soils by In Situ Soil Venting. *Ground Water. 3* (28):413-429.

Johnson, P.C., A. Leeson, R.L. Johnson, C.M. Vogel, R.E. Hinchee, M. Marley, T. Peargin, C.L. Bruce, I.L. Amerson, C.T. Coonfare, and R.D. Gillespie. 2001. A Practical Approach for the Selection, Pilot Testing, Design, and Monitoring of In Situ Air Sparging/Biosparging Systems. *Bioremediation Journal*, *5*(4):267-282.

Johnson, P.C., C.C. Stanley, M.W. Kemblowski, D.L. Byers, and J.D. Colthart. 1990b. A Practical Approach to the Design, Operation, and Monitoring of In Situ Soil-Venting Systems. *Ground Water Monit. Rev.. 10* (2):159-178.

Johnson, R.L., P.C. Johnson, T.L. Johnson, and A. Leeson. 2001a. Helium Tracer Tests for Assessing Contaminant Vapor Recovery and Air Distribution During In Situ Air Sparging. *Bioremediation Journal*, *5*(4):321-336.

Johnson, R.L., P.C. Johnson, T.L. Johnson, N.R. Thomson, and A. Leeson. 2001b. Diagnosis of In Situ Air Sparging Performance Using Transient Groundwater Pressure Changes During Startup and Shutdown. *Bioremediation Journal*, *5*(4):299-320.

Johnson, R.L., P.C. Johnson, I.L. Amerson, T.L. Johnson, C.L. Bruce, A. Leeson, and C.M. Vogel. 2001c. Diagnostic Tools for Integrated In Situ Air Sparging Pilot Tests. *Bioremediation Journal*, *5*(4):283-298.

Johnson, R.L., P.C. Johnson, D.B. McWhorter, R.E. Hinchee, and I. Goodman. 1993. An Overview of In Situ Air Sparging. *Ground Water Monitoring and Remediation. 13* (4):127-135.

Johnston, C.D., J.L. Rayner, B.M. Patterson, and G.B. Davis. 1998. Volatilization and Biodegradation during Air Sparging of Dissolved BTEX-Contaminated Groundwater. *J. Contaminant Hydrology. 33* (3-4):377-404.

Leeson, A., and R.E. Hinchee. 1996. *Soil Bioventing*. Boca Raton: CRC Press.

Leeson, A., R.E. Hinchee, G.L. Headington, and C.M. Vogel. 1995. Air Channel Distribution during Air Sparging: A Field Experiment. In: *In Situ Aeration: Air Sparging, Bioventing, and Related Remediation Processes*. pp. 215-222. (Hinchee, R.E., R.N. Miller, and P.C. Johnson, Eds.). Battelle Press: Columbus, Ohio.

Lundegard, P.D., and G. Andersen. 1996. Multi-Phase Numerical Simulation of Air Sparging Performance. *Groundwater. 34* (3):451-460.

Lundegard, P.D., and D.J. LaBreque. 1995. Air Sparging in a Sandy Aquifer (Florence, Oregon, USA): Actual and Apparent Radius of Influence. *J. Contaminant Hydrology. 19* (1):1-27.

Lundegard, P.D., and D.J. LaBreque. 1998. Geophysical and hydrologic monitoring of air sparging flow behavior: comparison of two extreme sites. *Remediation. Summer*:59-71.

Marley, M.C., L. Fengming, and S. Magee. 1992. The Application of a 3-D Model in the Design of Air Sparging Systems. *Ground Water Management. 14*:377-392.

Marley, M.C., and C.J. Bruell. 1995. *In Situ Air Sparging: Evaluation of Petroleum Industry Sites and Considerations for Applicability, Design, and Operation*. API Publication 4609. American Petroleum Institute. Washington, D.C.

McCray, J.E., and R.W. Falta. 1996. Defining the Air Sparging Radius of Influence for Groundwater Remediation. *J. Contaminant Hydrology. 24* (1):25-52.

McCray, J.E., and R.W. Falta. 1997. Numerical Simulation of Air Sparging for Remediation of NAPL. *Ground Water. 35* (1):99-110.

McKay, D.J., and L.J. Acomb. 1996. Neutron Moisture Probe Measurements of Fluid Displacement during In Situ Air Sparging. *Ground Water Monitoring and Remediation. 16* (4):132-141.

Peterson, J.W., P.A. Lepczyk, and K.L. Lake. 1999. Effect of Sediment Size on Area of Influence during Groundwater Remediation by Air Sparging: A Laboratory Approach. *Environmental Geology. 38* (1):1-6.

Philip, J.R. 1998. Full and Boundary-Layer Solutions of the Steady Air Sparging Problem. *Journal of Contaminant Hydrology. 33* (3-4):337-345.

Plummer, C.R., J.D. Nelson, and G.S. Zumwalt. 1997. Horizontal and Vertical Well Comparison for In Situ Air Sparging. *Ground Water Monitoring and Remediation. 17* (1):91-96.

Rabideau, A.J., and J.M. Blayden. 1998. Analytical Model for Contaminant Mass Removal by Air Sparging. *Ground Water Monitoring and Remediation. 18* (4):120-130.

Rabideau, A.J., J.M. Blayden, and C. Ganguly. 1999. Field Performance of Air Sparging System for Removing TCE from Groundwater. *Environmental Science and Technology. 33* (1):157-162.

Reddy, K.R., and J.A. Adams. 1998. System Effects on Benzene Removal from Saturated Soils and Ground Water Using Air Sparging. *Journal of Environmental Engineering. 124* (3):288-299.

Reddy, K.R., J. Zhou, and S. Kosgi. 1995. A Review of In Situ Air Sparging for the Remediation of VOC-Contaminated Saturated Soils and Groundwater. *Hazard. Waste Hazard. Mater. 12* (2):97-118.

Roosevelt, S.E., and M.Y. Corapcioglu. 1998. Air Bubble Migration in a Granular Porous Medium: Experimental Studies. *Water Resources Research*. *34*(5):1131-1142.

Rutherford, K., and P.C. Johnson. 1996. Effects of Process Control Changes on Aquifer Oxygenation Rates during In Situ Air Sparging in Homogeneous Aquifers. *Ground Water Monitoring and Remediation. 16*(4):132-141.

Salanitro, J.P., P.C. Johnson, G.E. Spinnler, P.M. Maner, H.L. Wisniewski, and C.L. Bruce. 1999. Field-Scale Demonstration of Enhanced MTBE Bioremediation through Aquifer Bioaugmentation and Oxygenation. *Environmental Science and Technology. 34*(19):4152-4162.

Schima, S., D.J. LaBreque, and P.D. Lundegard. 1996. Monitoring Air Sparging Using Resistive Tomography. *Ground Water Monitoring and Remediation. 16* (2):131-138.

Semer, R., J.A. Adams, and K.R. Reddy. 1998a. An Experimental Investigation of Air Flow Patterns in Saturated Soils during Air Sparging. *Geotechnical and Geological Engineering. 16* (1):59-75.

Semer, R. and K.R. Reddy. 1998b. Mechanisms Controlling Toluene Removal from Saturated Soils During In Situ Air Sparging. *J. Hazardous Materials. 57* (1-3):209-230.

Unger, A.J.A., E.A. Sudicky, and P.A. Forsyth. 1995. Mechanisms Controlling Vacuum Extraction Coupled with Air Sparging for Remediation of Heterogeneous Formations Contaminated by Dense Nonaqueous Phase Liquids. *Water Resources Research. 31* (8):1913-1925.

U.S. Environmental Protection Agency. 1992. *A Technology Assessment of Soil Vapor Extraction and Air Sparging.* EPA/600/R-192/173. September.

Van-Dijke, M.I.J., S.E.A.T.M. Van der Zee, and C.J. Van Duijn. 1995. Multi-Phase Flow Modeling of Air Sparging. *Advances in Water Resources. 18* (6):319 - 333.

Van-Dijke, M.I.J. and S.E.A.T.M. Van der Zee. 1998. Modeling of Air Sparging in a Layered Soil: Numerical and Analytical Approximations. *Water Resources Research. 34* (3):341-353.

Wilson, D.J., C.L. Gomez, and J.M.M. Rodriguez. 1994. Groundwater Cleanup by In Situ Air Sparging: VIII. Effect of Air Channeling on Dissolved Volatile Organic Compound Removal Efficiency. *Separation Science and Technology. 29* (18):2387-2418.

Wilson, D.J., A.N. Clarke, K.M. Kaminski, and E.Y. Chang. 1997. Groundwater Cleanup by In Situ Air Sparging. XIII. Random Air Channels for Sparging of Dissolved and Nonaqueous Phase Volatiles. *Separation Science and Technology. 32* (18):2969-2992.

APPENDIX B

Use of an SF_6-Based Diagnostic Tool for Assessing Air Distributions and Oxygen Transfer Rates During IAS Operation

Cristin L. Bruce[1], Illa L. Amerson[2], Richard L. Johnson[2], and Paul C. Johnson[1]

[1]Department of Civil and Environmental Engineering, Arizona State University
[2]Department of Environmental Science and Engineering, Oregon Graduate Health Sciences Institute

ABSTRACT

A diagnostic test designed to assess air distribution and oxygen delivery rate to the aquifer during in situ air sparging (IAS) is described. The conservative tracer gas, sulfur hexafluoride (SF_6), is added upstream of the air injection manifold during steady IAS operation and groundwater samples are collected from the target treatment zone after some time period (usually 4 to 24 h). The appearance of SF_6 in groundwater is used to characterize the air distribution in the target treatment zone, while the SF_6 concentration increase with time is used to assess oxygen transfer rates to the target treatment zone. Conversion from SF_6 concentration to oxygen mass transfer rate involves correcting the SF_6 concentration increase over time for differences in the relevant chemical properties and injection air concentration. Data presented from a field demonstration site illustrate the utility of this test for identifying air distribution details not readily identified by deep vadose zone helium and groundwater pressure transducer response tests. Oxygen transfer rates at this site ranged from 0 to 20 mg-O_2/L-H_2O/d. Finally, a comparison of short-term SF_6 test data with longer-term dissolved oxygen (DO) data illustrated this test's utility for anticipating long-term DO distribution.

INTRODUCTION

IAS is used for the treatment of contaminated aquifers. It has been employed as a source zone and a dissolved plume treatment option, a chemical migration barrier, and as a component of other remediation systems requiring gas delivery of oxygen, nutrients, or other reactants. It is most commonly employed at petroleum hydrocarbon spill sites but is also used frequently at chlorinated hydrocarbon spill sites. IAS systems are often coupled with soil vapor extraction (SVE) systems for capture of liberated contaminant vapors. A detailed summary of published IAS studies can be found in P.C. Johnson et al. (2001a).

The complexity of the processes involved makes it difficult to anticipate IAS performance (P.C. Johnson et al., 2001a). For example, performance is strongly dependent on air distribution in the target treatment zone, and air distribution is very sensitive to subtle changes in soil structure. Recognizing this, P.C. Johnson et a1. (2001b) propose a design paradigm that emphasizes characterization of air distribution at the pilot- and full-scale level, as well as use of diagnostic tools for full-scale performance assessment and optimization.

Air distribution can be inferred qualitatively from indirect measurements, such as transient pressure responses (R.L. Johnson et al., 2001a) and deep vadose zone helium measurements (R.L. Johnson et al., 2001b). It can also be assessed directly at discrete points with the use of DO measurements. However, Johnson et al. (1997) point out that short-term test (<24 h) oxygen measurements can be misleading, as measurable increases in DO levels sometimes occur only after periods of days to weeks due to oxygen demand within the aquifer. Given the advantages and limitations of each individual test, it has been

recommended that a suite of techniques be used to assess air distribution (P.C. Johnson et al., 2001b; R.L. Johnson et al., 2001b). The approach described here is complimentary to the methods identified above. Like DO measurement, it provides a direct measurement of air distribution in the target treatment zone at discrete points. This method is a modification of the approach presented by Johnson et al. (1996). It uses a tracer compound and is more sensitive than DO measurement as it can identify areas where oxygen delivery is occurring even though DO levels are unchanged in the short term.

With respect to performance monitoring and IAS system optimization, conventional monitoring plans provide little opportunity for the real-time performance assessment and optimization called for in the design paradigm mentioned above. Practitioners currently rely on quarterly (or less frequent) groundwater monitoring, and then performance is judged by changes in the dissolved concentrations over periods of months to years. With only this data, optimization of IAS systems is impracticable because conclusions regarding performance can only be drawn after collecting data over time intervals that are comparable to the overall remediation time frame (months to years). Without system optimization, many systems may operate longer than is necessary, and many systems may be terminated prior to achieving their full potential for remediation. In fact, the overall performance of IAS systems has been quite variable to date, and there is little evidence that system optimization is a component of conventional practice (Bass and Brown, 1995).

One of the attractive features of the SF_6 method described here is that it has dual utility. It can be used to assess air distribution and it can also be used to provide near real-time measurements of oxygen transfer rate. Knowledge of oxygen transfer rate is especially important when treating aerobically biodegradable contaminants; rates can be used to estimate remediation time frames, and it is desirable to maximize these rates throughout the target treatment zone. Oxygen transfer rates can be determined within 4 to 24 h with this method, so it can be used for system performance assessment and optimization. The authors are unaware of any other diagnostic tools for uses such as this, other than the complementary push-pull diagnostic test described by Amerson et al. (2001).

DIAGNOSTIC TOOL METHODOLOGY

Overview

Application of the SF_6 diagnostic tool is illustrated schematically in Figure 1. During either IAS pilot-test or full-scale operation, a nonreactive gas tracer is metered into the air injection manifold at a constant rate. As the air-tracer mixture flows through gas channels in the aquifer, tracer partitions into groundwater and moves away from the air channel-groundwater interface through the combination of diffusion and dispersion/advection. After a period of constant injection (usually 4 to 24 h), groundwater within the target treatment zone is sampled at locations of interest and dissolved tracer concentrations (C_{tracer} [mg/L]) are measured.

Dissolved tracer concentration in equilibrium with the injection air stream (C^{max}_{tracer} [mg/L]) is also measured. This is accomplished by bubbling a slip-stream of the injection air/tracer mixture through a groundwater sample as shown in Figure 1, and then measuring the dissolved tracer concentration in that sample.

Data Reduction

Given the short duration of the test, the presence of tracer in a groundwater sample is interpreted qualitatively to be an indication of the presence of gas channels within the sampling volume. Higher concentrations might also be interpreted to suggest a higher density of air flow channels.

Oxygen and tracer are delivered to the subsurface in the injected air stream, and then they both partition to groundwater. Differences in delivery rates occur as a result of differences in concentration in the injected gas stream and differences in chemical properties. Theory suggests that the delivery rate is limited by water-phase diffusion processes (e.g., Ahlfeld et al., 1994; Johnson, 1998). In this case one can approximate the mass transfer rate for a chemical i $<m_i>$ [mg-i/d]:

$$< m_i > = A \left(\frac{D_i}{\delta} \right) C_i^{max} \tag{1}$$

where A is the interfacial area [m^2], D_i is the diffusion coefficient for the chemical in water [m^2/d], d is the diffusion path length [m], and C_i^{max} [mg/m^3] is the dissolved chemical concentration in equilibrium with the gas phase concentration at the air-water interface.

As A and d should be the same for all chemicals, we use Equation (1) to write:

$$\frac{< m_o >}{< m_{tracer} >} = \left(\frac{D_o}{D_{tracer}} \right) \left(\frac{C_o^{max}}{C_{tracer}^{max}} \right) \tag{2}$$

The subscripts "o" and "tracer" refer to oxygen and the tracer, respectively. This expression can be rearranged for the case where $<m_{tracer}>$ is known and $<m_o>$ is desired:

$$< m_o > = \left(\frac{D_o}{D_{tracer}} \right) \left(\frac{C_o^{max}}{C_{tracer}^{max}} \right) < m_{tracer} > \tag{3}$$

Using experimental data, the time-averaged tracer transfer rate to a given sampling volume is calculated from the measured concentration increase C_{tracer} [mg/L] and the sampling volume V [L]:

$$< m_{tracer} > = \frac{C_{tracer} \, V}{T} \tag{4}$$

Therefore, the time-averaged oxygen mass transfer rate to the sampling volume can be written:

$$< m_o > = \left(\frac{C_{tracer}}{C_{tracer}^{max}} \right) \left(\frac{D_o}{D_{tracer}} \right) \frac{C_o^{max} \, V}{T} \tag{5}$$

The mass transfer rate can also be expressed as a rate per unit volume m* [mg-O_2/L-H_2O/d]:

$$m^* = \frac{< m_o >}{V} = \left(\frac{C_{tracer}}{C_{tracer}^{max}} \right) \left(\frac{D_o}{D_{tracer}} \right) \frac{C_o^{max}}{T} \tag{6}$$

Diffusion coefficients in water for some chemicals are tabulated, and others can be estimated from empirical relationships (Bird et al., 1960). Given the approximate nature of this theoretical analysis and the observation that many diffusion coefficients in water fall in the range of 1 to 2 × 10^{-5} cm^2/s, the ratio of diffusion coefficients in water can be treated as unity.

In summary, this analysis is based on the assumption that oxygen and SF_6 transfer processes are similar and that the rates are proportional to the equilibrium air channel-groundwater interface concentration and the molecular diffusion coefficient in water. This calculation also assumes that both species are nonreactive, whereas oxygen is likely to be consumed at sites where aerobic biodegradation reactions occur. Thus, it can be argued that this calculation might underestimate the actual time-averaged oxygen delivery rates to an aquifer as the driving force for mass transfer (concentration gradients) would be higher under conditions where a chemical was being consumed. Furthermore, it is important to note that the rate estimate obtained from this methodology is a time-averaged quantity, and, consequently, mass transfer rate estimates will be greatest for data from shorter tests when the concentration difference between C_{tracer} and C^{max}_{tracer} is large. Admittedly, this method of analysis is simplistic, but we believe that the approach should provide reasonable order-of-magnitude estimates of oxygen delivery rates. Other than the push-pull test described by Amerson et al. (2001), this is the only tool currently available for obtaining this information.

Tracer Selection

SF_6 was the tracer initially selected for testing this diagnostic tool. SF_6 is a gas at standard conditions; it is also a nondegrading and a nonreacting compound at typical environmental conditions. It is commonly used to trace leaks in ventilation and mine-face systems, and has also been applied to groundwater and geothermal investigations. It is sparingly soluble in water and has a Henry's Law constant much greater than unity (approximately 150 mg/L-air/mg/L-H_2O; Amerson et al., 2001). SF_6 is detectable in the low parts-per-trillion by volume (ppt_v) range with the use of a specialized SF_6 detector (Lagus Applied Technologies, Torrance, California) or other gas chromatograph (GC) equipped with an electron capture detector (ECD). SF_6 was selected for this work because its large Henry's Law constant makes analysis from groundwater samples relatively simple and because it can be detected at such low concentrations. It can be added at low parts-per-million by volume (ppm_v) concentrations to the air injection manifold and this greatly reduces the volume of tracer gas required for the test. Both oxygen and SF_6 partition to trapped gas in aquifers to a similar degree and both partition to nonaqueous phase liquid (NAPL). The effect of partitioning to NAPL on the results of this test is not understood at this time.

Diagnostic Test Procedures

A sample test protocol is given below. It is followed by a discussion of procedures and calculations specific to the use of SF_6. The test is conducted only after the IAS system is operating at steady conditions.

1. Determine the desired groundwater extraction volume based on how large a volume of aquifer is to be assessed about each sampling point. In this work groundwater samples were obtained from small volume discrete-depth samplers and the volume was typically <1 L.
2. Prior to tracer injection, collect groundwater samples for baseline tracer concentration measurements. At least one well-borehole volume is purged prior to sampling. It is critical that groundwater samples be collected without causing gas bubbling through the sample as this can affect dissolved tracer concentrations. DO concentrations can also be measured at this time.
3. Based on the baseline tracer concentrations, determine the target tracer concentration in the injection air. To be consistent with the mathematical analysis and to ensure a reasonable dynamic measurement range, the injection air tracer concentration should be high enough that C^{max}_{tracer} is at least 100 times greater than the baseline concentration.
4. Attach the tracer gas line to the air injection at least 10 pipe diameters upstream of the manifold connecting all air injection wells to allow adequate mixing.
5. Initiate flow of tracer at the target injection rate; use a back-pressure valve to adjust the tracer gas pressure at the flow meter to at least 15 psig above the pressure in the air line to minimize effects of air injection line pressure fluctuations on the tracer delivery rate.

6. Using the slip-stream valve on the air injection manifold (see Figure 1), bubble the air stream vigorously through a 40-mLvolatile organic analysis (VOA) vial containing initially tracer-free groundwater for about 2 minutes, then analyze and compare with the target C^{max}_{tracer} value. Adjust the tracer injection rate as necessary and repeat this step until the target concentration is achieved.
7. Allow the tracer gas to flow at a constant rate into the air injection line and keep the IAS system running 4 to 24 h.
8. Collect the desired volume of groundwater from the sampling points/wells, mix, and then fill a VOA vial (allowing no headspace in the sample) with a sample from this larger volume.
9. Analyze dissolved tracer concentrations for all samples and analyze data as discussed above (see Equation (6)).

SF_6 – Specific Methods and Procedures

Groundwater SF_6 concentrations are determined using a headspace technique coupled with GC-ECD analysis. In brief, groundwater samples are collected in zero-headspace 40-mL VOA vials. Using two syringes, a volume V_W (usually 1 mL) of the groundwater sample is removed into one syringe by pressure displacement using a second syringe containing SF_6-free water. The groundwater sample is then injected into a sealed and empty 40-mL VOA vial that has been purged with ultra-high purity (UHP) nitrogen and sealed. An additional 5 mL of UHP nitrogen is added through the septum and the vial is shaken vigorously. Then 5 mL of the headspace is withdrawn and injected into the GC-ECD for analysis. The large Henry's Law constant for SF_6 ensures essentially complete partitioning of the SF_6 from groundwater into the vial headspace (>99.9% for these conditions). The original dissolved concentration C_{tracer} and the measured headspace concentration C_{HS} are related by:

$$C_{tracer} = \frac{V_{HS}}{V_W} C_{HS} \qquad (7)$$

Where V_{HS} and V_W denote the headspace volume and volume of water in the nitrogen-purged vial. It is possible to analyze one groundwater sample approximately every 5 minutes with this approach.

It is important to note that the vial purge steps are extremely important as the concentration of SF_6 in ambient air increases during the test and this can cause cross-contamination of samples. Also, in some areas, industry emissions of SF_6 are significant enough that ambient air contains SF_6 at concentrations in the low ppb_v range.

As mentioned above, the target injection rate for SF_6 into the IAS injection air stream is determined based on the baseline SF_6 concentrations in groundwater. Instrument detection limits also need to be considered. In this work a specialized SF_6 detector (Lagus Applied Technologies, Torrance, California) having a linear response range of about 0.01 to 50 ppb_v was used. To make best use of the instrument's dynamic range and to avoid saturating the detector, it was decided that the SF_6 injection rates should be adjusted so that maximum measured headspace SF_6 concentration C^{max}_{tracer} would be about 10 ppb_v.

Knowledge of the baseline tracer concentration in groundwater, the target maximum headspace concentration, and Equation (7) determine the minimum ratio V_{HS}/V_W to be used in the analysis. The target SF_6 injection rate Q_{SF6} [ft^3/min] is calculated using Equation (7) and Henry's Law:

$$Q_{SF_6} = Q_{air}\ H\ C^{max}_{HS}\ [ppb_v] \left(\frac{V_{HS}}{V_W}\right) \times 10^{-9} \qquad (8)$$

where C^{max}_{HS} is the maximum target headspace concentration [ppb_v]; Q_{SF6} is the injection rate of SF_6 [ft^3/min]; Q_{air} is the total injection rate of SF_6 + air [ft^3/min]; H is the SF_6 Henry's Law constant [150 (mg/L-air)/(mg/L-H_2O)]; V_W is the volume of groundwater used in analysis [mL]; and V_{HS} is the volume of headspace used in analysis [mL].

For example, for an IAS system with a total injection rate of Q_{air}=100 ft^3/min, a target headspace concentration of C^{max}_{tracer}=10 ppb_v, V_W=1 mL and V_{HS}=39 mL, the target injection rate of SF_6 is Q_{SF6}=165 mL/min [=0.006 ft^3/min].

Finally, it should be noted that if one wishes to conduct multiple tests separated by relatively short periods of time (e.g., days to weeks), then it is prudent to conduct the initial test at a lower target concentration and then increase the target concentration by about an order of magnitude or more for each successive test.

APPLICATION OF THE DIAGNOSTIC TEST

Field Site Description

The diagnostic test was initially applied at the Hydrocarbon National Test Site (HNTS) located at the U.S. Naval Construction Battalion Center in Port Hueneme, California. At the HNTS, groundwater had been impacted by a relatively large gasoline release from the Base service station. The push-pull test was applied to a 20-m × 20-m IAS study area located within a larger (approximately 50 m × 300 m) residual immiscible hydrocarbon source zone. This study area was equipped with an extensive monitoring network, and the site hydrogeology and contaminant distribution were already well characterized.

A plan-view schematic diagram of the test site monitoring network is shown in Figure 2. The monitoring system included 12 multilevel monitoring installations, each containing a bundle of 15 0.32-cm inner diameter (ID) (1/8-inch) color-coded, stainless steel sampling lines with ports at 0.6, 1.2, 1.8, 2.4, 3.0, 3.4, 3.7, 4.0, 4.3, 4.6, 4.9, 5.2, 5.5, 5.8, and 6.1 m (2, 4, 6, 8, 10, 11, 12, 13, 14, 15, 16, 17, 18, and 19 ft) below ground surface (bgs). The groundwater table was at approximately 3-m (10-ft) bgs, and the immiscible hydrocarbon smear zone extended from approximately 3 to 4 m (10 to 13 ft) bgs. Dissolved total hydrocarbon concentrations in the smear zone generally exceeded 1 mg/L. The IAS well was screened from 5.8 to 6.1 m (18 to 20 ft) bgs. Previous studies have shown that the air distribution in the aquifer is nonuniform about the air injection, exhibiting tendencies to flow along the axis defined by MP6, MP12, MP3, and MP9 well (R.L. Johnson et al., 2001b).

The SF_6 diagnostic test was applied during the pilot study at an IAS air injection flow rate of 570 standard L/min (20 standard cubic feet per minute[SCFM]).

Assessing Air Distribution

Table 1 presents the dissolved SF_6 concentrations resulting after 24 h of SF_6 injection. The concentrations are expressed as saturations (=$C_{tracer}/C^{max}_{tracer}$ × 100%). While measurements have been made and are reported from 3.0 – 5.8 m bgs, the target treatment zone at this site is the 3.0 to 4.0 m bgs interval.

Overall, the SF_6 data set shows a nonsymmetrical and irregular air distribution. High saturations at MP1, MP2, and MP3 suggest that air leaving the IAS well initially flows upward within 1.5 m of the injection well as it moves towards the water table. This behavior is to be expected in relatively homogeneous sandy aquifers (P.C. Johnson et al., 2001a). What is unusual is that some of the air flow becomes stratified at a depth of about 4 to 4.5 m bgs, and it moves preferentially along the axis roughly defined by MP9 and MP12. This hypothesis is supported by the high saturations at MP3, MP6, MP9 and MP12 in the upper part of the aquifer (3 to 4 m bgs) and low saturations at other points. For reference, the air

distribution at the water table suggested by this data is similar to the distribution inferred from deep soil gas helium data at this site (R.L. Johnson et al., 2001b).

Oxygen Mass Transfer Rates

Table 2 contains the 24-h average oxygen mass transfer calculated from the data in Table 1. The oxygen mass transfer rates range from about 0 to 20 mg-O_2/L-H_2O/d. Assuming a stoichiometry of 3 mg-oxygen required per mg of hydrocarbon, the IAS system can support aerobic biodegradation rates ranging from 0 to 7 mg-hydrocarbon/L-H_2O/d, with these rates being spatially distributed as shown in Table 2.

Comparison of Short-Term SF_6 Distribution with Longer-Term Dissolved Oxygen Distribution

DO measurements were made after 7 d of 20 ft^3/min air injection. Prior to this, the pilot system had been operated for 14 consecutive days; 7 d at 5 ft^3/min and 7 d at 10 ft^3/min. It is useful to compare the short-term SF_6 distribution with the longer-term DO distribution to gain some insight as to how well the short-term diagnostic test results relate to longer-term DO distributions.

Table 3 presents the DO concentrations expressed as saturations ($=C_o/C^{max}_o \times 100\%$). In comparing Table 1 and Table 3, we look for qualitative similarities in the spatial distributions and not quantitative agreement with the saturations. Overall, both suggest asymmetric air distribution, with little oxygen delivery in the treatment zone at MP1, MP5, MP7, MP10, and MP11.

With respect to differences between the two, oxygen increases have occurred in the target treatment zone at MP4 and MP8. Also of interest are the increases in DO levels below the treatment zone in areas that SF_6 data suggest are not directly affected by air flow. These DO increases could be the result of groundwater advection and vertical dispersion from areas of air flow combined with little oxygen demand (as this zone lies below hydrocarbon-impacted soils).

SUMMARY

In summary, a gas-tracer diagnostic test for IAS systems has been developed and tested. This test is attractive because of its dual nature; it is useful for assessment of air distributions and oxygen mass transfer rates. The test can be conducted in a relatively short period of time and therefore is useful for pilot test air distribution characterization and full-scale system optimization. By monitoring changes in dissolved SF_6 distributions and oxygen transfer rates with changes in system operation and design, IAS system performance can be optimized. To date, no other short-term diagnostic tools have been developed for IAS system optimization.

Data presented from the initial application illustrate its utility in identifying air distribution details not readily identified by deep vadose zone helium and groundwater pressure transducer response tests. Oxygen transfer rates at this site ranged from 0 – 20 mg-O_2/L-H_2O/d, and this information is valuable for assessing potential significance of contaminant removal via aerobic biodegradation. Actual aerobic biodegradation rates could not exceed rates calculated from the oxygen delivery rates. Measurements at other sites not discussed here have ranged from 0 to 150 mg-O_2/L-H_2O/d. Finally, a comparison of short-term SF_6 test data with the longer-term dissolved oxygen data illustrated the utility of this short-term test for assessing long-term dissolved oxygen distribution.

ACKNOWLEDGEMENTS

The authors would like to acknowledge and thank Harley Hopkins and the American Petroleum Institute Soil and Ground Water Technical Task Force for their financial support, project review, and many valuable suggestions. We would also like to thank the Strategic Environmental Research and Development Program (SERDP) and the Air Force Research Laboratory, Materials and Manufacturing

Directorate, Airbase and Environmental Technology Division (AFRL/MLQ), Tyndall AFB, Florida, for providing a field site for this project. Finally, the authors would like to thank Karen Miller, Ernie Lory, James Osgood, and Dorothy Cannon at the Naval Facilities Engineering Service Center at Port Hueneme for their assistance with the field portion of this research.

REFERENCES

Ahlfeld, D. P., A. Dahmani, and W. Ji. 1994. A Conceptual Model of Field Behavior of Air Sparging and Its Implications for Application. *Ground Water Monitoring and Remediation. 14* (4):132-139.

Amerson, I.L. 1997. Diagnostic Tools for the Monitoring and Optimization of In Situ Air Sparging Systems. M.S. Thesis. Arizona State University.

Amerson, I.L., C.L. Bruce, P.C. Johnson, and R.L. Johnson. 2001. A Multi-Tracer Push-Pull Diagnostic Test for In Situ Air Sparging Systems. *Bioremediation Journal*, *5*(4):349-362.

Bass, D.H., and R.A. Brown. 1995. Performance of Air Sparging Systems—A Review of Case Studies. In: *Petroleum Hydrocarbons and Organic Chemicals in Ground Water: Prevention, Detection and Restoration*, Houston, Texas, November.

Bird, R.B., W.E. Stewart, and E.N. Lightfoot. 1960. *Transport Phenomena*. John Wiley & Sons. New York. 780 pp.

Johnson, R.L., R.R. Dupont, and D.A. Graves. 1996. *Assessing UST Corrective Action Technologies: Diagnostic Evaluation of In Situ SVE-Based System Performance*. EPA/600/R-96/041, 164p.

Johnson, P.C. 1998. Assessment of the Contributions of Volatilization and Biodegradation to In Situ Air Sparging Performance. *Environmental Science and Technology. 32*:276-281.

Johnson, P.C., R.L. Johnson, C. Neaville, E.E. Hansen, S.M. Stearns, and I.J. Dortch. 1997. An Assessment of Conventional In Situ Air Sparging Tests. *Ground Water. 35* (5). 765 - 774.

P.C. Johnson, R.L. Johnson, C.L. Bruce, and A. Leeson. 2001a. Advances in In Situ Air Sparging/Biosparging. *Bioremediation Journal*, *5*(4):251-266.

Johnson, P.C., A. Leeson, R.L. Johnson, C.M. Vogel, R.E. Hinchee, M. Marley, T. Peargin, C.L. Bruce, I.L. Amerson, C.T. Coonfare, and R.D. Gillespie. 2001b. A Practical Approach for the Selection, Pilot Testing, Design, and Monitoring of In Situ Air Sparging/Biosparging Systems. *Bioremediation Journal*, *5*(4):267-282.

Johnson, R.L., P.C. Johnson, T.L. Johnson, N.R. Thomson, and A. Leeson. 2001a. Diagnosis of In Situ Air Sparging Performance Using Transient Groundwater Pressure Changes During Startup and Shutdown. *Bioremediation Journal*, *5*(4):299-320.

Johnson, R.L., P.C. Johnson, T.L. Johnson, and A. Leeson. 2001b. Helium Tracer Tests for Assessing Contaminant Vapor Recovery and Air Distribution During In Situ Air Sparging. *Bioremediation Journal,* *5*(4):321-336.

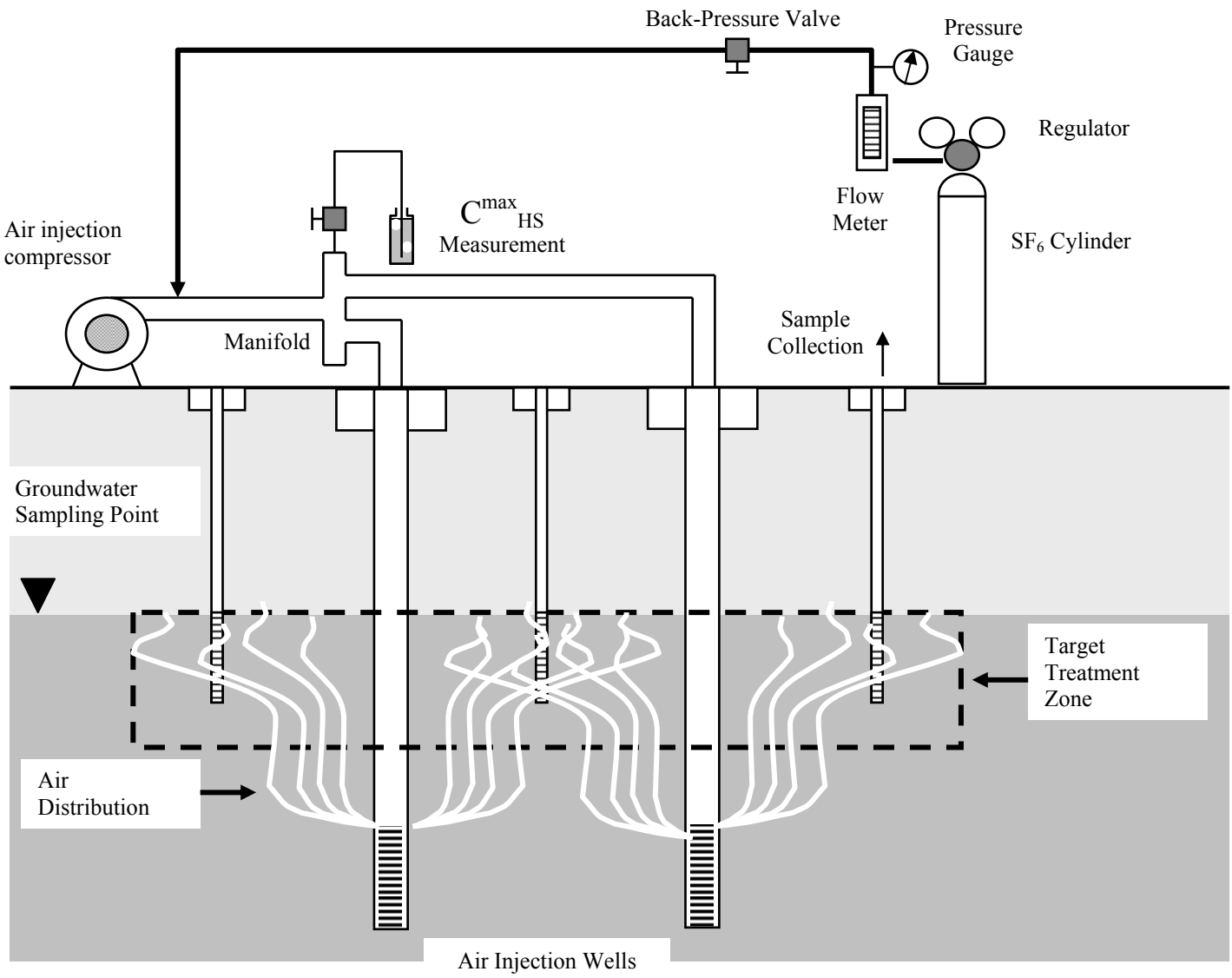

Figure 1. Schematic Diagram of Diagnostic Testing

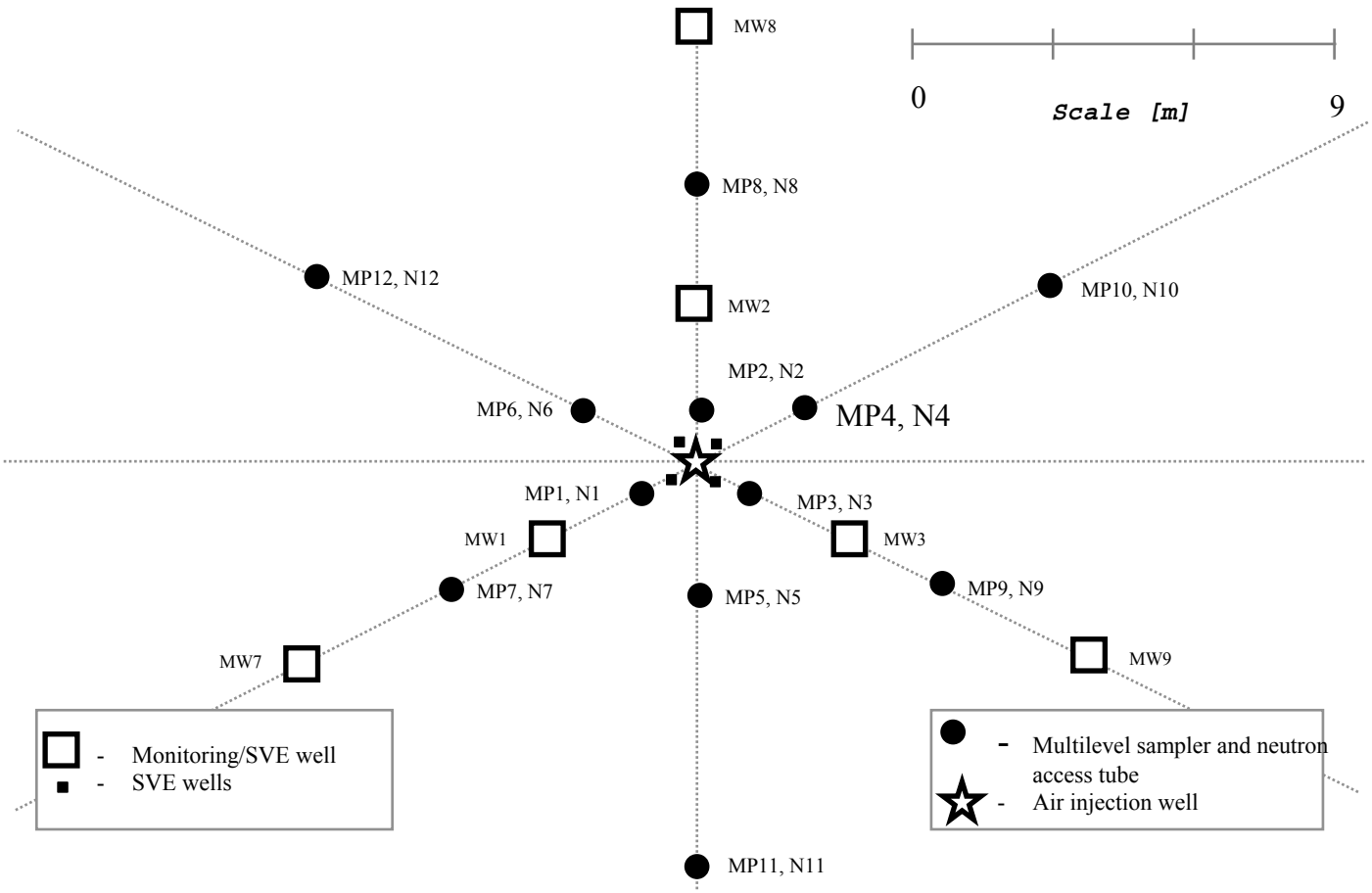

Figure 2. IAS Test Plot Setup at the HNTS Site, Naval Base Ventura County (NBVC), Port Hueneme Site, California

Table 1. SF_6 Saturations (%) After 24 Hours of Continuous SF_6 Injection During the 20 SCFM IAS Pilot Test (ns - groundwater samples not collected at this point as gas was recovered instead of water. Thus, the SF_6 saturation is assumed to be 100% at these points.)

Distance bgs (m)	MP1	MP2	MP3	MP4	MP5	MP6	MP7	MP8	MP9	MP10	MP11	MP12
3.0	4	90	0	1	0	31	0	0	72	0	0	2
3.4	6	100	2	2	0	54	0	1	82	1	0	1
3.7	1	58	31	6	0	ns	0	1	4	1	0	20
4.0	2	97	3	0	1	23	0	0	12	4	0	3
4.3	16	43	32	0	1	47	0	1	3	2	0	0
4.6	5	ns	22	5	4	38	0	1	0	0	0	0
4.9	2	36	16	0	0	0	0	2	0	1	0	ns
5.2	61	0	8	0	0	0	0	2	0	0	0	0
5.5	1	0	1	0	1	0	0	1	0	1	0	0
5.8	3	0	0	0	0	1	0	0	0	0	0	2
Distance from Sparge Well (m)		1.5			3			6			9	

Table 2. Oxygen Saturations (%) After 1 Week of Continuous Air Injection During the 20 SCFM IAS Pilot Test (0 values are assigned to all points where dissolved oxygen readings are <1 mg/L; points where gas was withdrawn from sampling point are labeled "air"; O_2 saturations are assumed to be 100% at these points.)

Distance bgs (m)	MP1	MP2	MP3	MP4	MP5	MP6	MP7	MP8	MP9	MP10	MP11	MP12
3.0	0	44	22	0	0	72	0	33	86	63	0	0
3.4	0	0	0	50	0	76	0	53	68	0	0	0
3.7	0	83	57	78	30	air	0	30	43	0	0	32
4.0	0	78	0	68	0	39	0	76	76	0	0	40
4.3	54	83	80	76	48	74	0	0	66	0	0	24
4.6	28	air	82	66	48	72	0	24	0	0	22	47
4.9	0	0	80	72	60	0	0	26	30	0	33	air
5.2	0	44	87	air	61	30	0	0	0	56	33	0
5.5	0	0	26	0	52	0	0	23	24	58	28	0
5.8	0	0	0	0	0	0	0	28	56	air	50	89
Distance from Sparge Well (m)		1.5			3			6			9	

Table 3. **24-hour Average Oxygen Mass Transfer Rates (mg-O_2/L-H_2O/d) inferred from SF6 data during the 20 SCFM IAS pilot test (ns - groundwater samples not collected at this point as gas was recovered instead of water. Thus, the oxygen mass transfer rates is assumed to be 19.2 mg/L/d at these points.)**

Distance bgs (m)	MP1	MP2	MP3	MP4	MP5	MP6	MP7	MP8	MP9	MP10	MP11	MP12
3.0	0.7	17.4	0.1	0.2	0.0	5.9	0.0	0.1	13.9	0.1	0.1	0.4
3.4	1.1	19.2	0.4	0.3	0.0	10.3	0.0	0.1	15.7	0.1	0.1	0.3
3.7	0.2	11.1	5.9	1.2	0.0	ns	0.0	0.2	0.7	0.1	0.0	3.8
4.0	0.3	18.6	0.6	0.0	0.1	4.4	0.0	0.0	2.2	0.7	0.1	0.6
4.3	3.2	8.3	6.2	0.0	0.1	8.9	0.0	0.1	0.6	0.3	0.0	0.0
4.6	0.9	ns	4.2	0.9	0.8	7.4	0.0	0.1	0.1	0.1	0.0	0.1
4.9	0.4	6.9	3.1	0.0	0.0	0.1	0.0	0.4	0.1	0.1	0.1	ns
5.2	11.7	0.0	1.6	0.1	0.0	0.0	0.0	0.4	0.0	0.0	0.0	0.0
5.5	0.2	0.0	0.2	0.0	0.3	0.1	0.0	0.2	0.0	0.3	0.1	0.0
5.8	0.5	0.1	0.1	0.0	0.1	0.1	0.0	0.1	0.0	0.0	0.1	0.4

Distance from Sparge Well (m): 1.5 (MP1–MP3), 3 (MP4–MP6), 6 (MP7–MP9), 9 (MP10–MP12)

APPENDIX C

A Multitracer Push-Pull Diagnostic Test for Assessing the Contributions of Volatilization and Biodegradation During In Situ Air Sparging

Illa L. Amerson[1], Cristin L. Bruce[2], Paul C. Johnson[2*], and Richard L. Johnson[1]

[1]Dept. of Environmental Science and Engineering, Oregon Graduate Institute of Science and Technology, Beaverton, Oregon; [2]Department of Civil and Environmental Engineering, Arizona State University, Tempe, Arizona

INTRODUCTION

In situ air sparging (IAS) involves the injection of air into a contaminated aquifer below the zone of contamination (Johnson et al., 1993; Marley and Bruell, 1995). The air injection promotes volatilization and biodegradation of aerobically biodegradable compounds. Based on a review of the literature (P.C. Johnson et al., 2001a), the rate and extent of these processes is dependent on the contaminant's chemical properties (e.g. vapor pressure, Henry's Law Constant, and solubility), the distribution of contaminants (e.g., NAPL or dissolved phase), and the spatial distribution of air in the aquifer relative to the spatial distribution of contaminants. The spatial distribution of air in the aquifer is known to be sensitive to subtle changes in aquifer material texture; the number, placement, and screened intervals of wells; and air injection flow rates.

While IAS systems have been used to successfully achieve closure at many sites, the overall performance has been variable (Bass and Brown, 1995). Based on the authors' experience, this can be attributed to several factors, including a) the unpredictability of saturated zone air distributions in many hydrogeologic settings, b) the range of empirical design and operating approaches found in practice, and c) limited real-time performance monitoring and lack of system optimization. As discussed below, this lack of real-time performance monitoring and optimization is a key motivating factor for this work, and therefore it is worthwhile to briefly review the state-of-the-practice for IAS system monitoring.

Monitoring plans for IAS systems often only include activities necessary to satisfy regulatory compliance requirements. When an SVE system is being operated, off-gas contaminant concentrations and flow rates are generally monitored; otherwise, performance monitoring is most often restricted to quarterly (or less frequent) groundwater monitoring. Performance is then judged by changes in the dissolved concentrations over periods of months to years. Of the conventional monitoring approaches, only SVE off-gas monitoring provides a real-time measure of remediation performance. Even then, it is an integrated measurement lacking in spatial resolution and the data reflects removal of contaminants from both above and below the groundwater table. Furthermore, this data is not available from those sites operated without SVE systems.

Given only these conventional options for system performance monitoring, optimization of IAS systems is impracticable because conclusions regarding performance can only be drawn after collecting data over time intervals that are comparable to the overall remediation time frame (months to years). Without system optimization, many systems may operate longer than is necessary, and many systems may be terminated prior to achieving their full potential for remediation. Both cases have economic implications, as costs usually increase with increased operation time, and costs may also increase with the use of additional follow-on technologies.

If IAS systems are to be optimized, there is a need for procedures, or "diagnostic tools" that provide more real-time IAS performance assessment. Diagnostic tools are not common in the remediation field. One good example is the bioventing respirometry test described by Hinchee and Ong (1992), in which soil gas oxygen concentrations are monitored over a period of one to two days following the cessation of steady air injection into the subsurface. The rate of oxygen concentration decline is used to calculate an aerobic biodegradation rate. Similar types of tests were considered in this work (i.e., monitoring dissolved oxygen level declines with time after cessation of air injection), but this route was not pursued because IAS introduces a significant mass of oxygen in the form of trapped gas in the aquifer, and it is difficult to account for this unknown, but significant, oxygen mass when interpreting dissolved oxygen changes with time. Furthermore, stratified gas pockets at some sites can continue to “off-gas” for hours to days following cessation of gas injection, further complicating the application and interpretation of a respirometry-type IAS test.

In this work, a multitracer push-pull diagnostic tool was studied in a controlled aquifer physical model and then applied at the U.S. Navy Hydrocarbon National Test Site (HNTS) in Port Hueneme, California. The multitracer diagnostic tool was designed to provide near real-time point-specific measures of contaminant volatilization and aerobic biodegradation rates during IAS operation. The diagnostic test involves injecting a solution containing multiple tracer compounds through a monitoring well, piezometer, or drive point and into the target treatment zone. The injected solution is initially deoxygenated and can contain a) a nondegradable, nonvolatile conservative tracer; b) one or more non-degradable, volatile chemicals; c) an aerobically biodegradable, nonvolatile compound; and d) a visible dye. After some predetermined hold time, an excess quantity of groundwater is extracted from the same injection point, and then changes in the concentrations of the tracer compounds are measured. Volatilization and oxygen utilization rates are estimated from mass balances on the tracer components. Because the results are specific to the tracers used, it is important to note that the results provide relative measures of biodegradation and volatilization and not the rates specific to the target contaminants. Thus, this is a diagnostic tool that should be used to assess spatial differences in biodegradation and volatilization rates across a given site and the effects of process changes on these rates. The tool can be used to identify zones of active treatment and can also be used to optimize system operation (flow rates, distribution of wells, etc.).

This approach differs from other IAS monitoring options in that interpretation of the measurements is made without pre-IAS test data and results are obtained relatively quickly. This tool is complementary to the inert tracer gas delivery diagnostic tool described by Bruce et al. (2001), Johnson et al. (1996), and Amerson (1997). The mechanics of this diagnostic test show some similarity to the push-pull tests described by Istok et al. (1997) and Schroth et al. (1998) for assessing microbial respiration during natural attenuation; however, the multitracer solution used and the data reduction approaches are different. These differences result from the objectives of each test (e.g., assessing anaerobic and aerobic activity versus assessing aerobic activity and volatilization), as well as the environmental conditions in the aquifer during the tests (e.g., natural conditions versus air injection).

OVERVIEW OF THE MULTITRACER PUSH-PULL DIAGNOSTIC TEST

The multitracer push-pull diagnostic tool is illustrated in Figure 1. During IAS operation, a deoxygenated aqueous solution containing multiple tracer compounds is injected through a monitoring well, piezometer, or drive point and into the desired zone of treatment. It is also injected into a nearby "background" point not affected by the IAS system; this location can be contaminated or uncontaminated. The injected solution contains a) a nondegradable, nonvolatile conservative tracer; b) a nondegradable, volatile conservative tracer; c) a readily aerobically biodegradable, nonvolatile compound; and d) a visible dye. The water is deoxygenated by nitrogen gas bubbling prior to addition of the tracers.

After some period of time, a greater volume of groundwater than the injected volume is extracted and concentrations of the tracer compounds are measured. Tracer volatilization and biodegradation rates are estimated from mass balances on the tracer compounds as discussed below

Selection of the multitracer solution injection volume is based on consideration of the monitoring well, piezometer, or drive point purge volume; the desired scale of the assessment; and other practical issues (e.g., solution storage and handling). For example, an injection volume of 1 L might be used to assess performance on a 10 cm scale about a drive point, while a 100-gallon injection volume could be used to assess performance on the scale of a few meters about a well. To estimate the necessary injection volume, one can use the following calculation:

$$V_{inject} = \frac{4\pi\theta R_{test}^3}{3} + V_{well}[\,for\,discrete\,points]$$

$$or \qquad (1)$$

$$V_{inject} = \pi\theta(R_{test} - R_{well})^2 L_{screen} + V_{well}[\,for\,wells]$$

where: V_{inject} = multitracer injection volume (mL); π = 3.14; R_{test} = radial distance about injection point desired to be assessed (cm); R_{well} = radius of the borehole (cm); L_{screen} = well screen interval (cm); θ = water content (approximately equal to the porosity) (mL-pores/mL-soil); V_{well} = volume of groundwater in the well and borehole that must be displaced (mL).

The first expression is used when the multitracer solution is delivered through drive rods or small discrete piezometers, while the second is used when delivering solution through conventional well installations. For example, multilevel samplers composed of bundled 0.32-cm ID stainless steel tubing were used in the initial field site application discussed below. In that case V_{inject} = 1 L and V_{well} <10 mL. This corresponds to assessing performance on the scale of about 10 cm about the injection point. The expressions given above are based on idealized spherical and cylindrical fluid distributions and are intended for estimation purposes; the actual multitracer solution distribution will reflect the aquifer structure near the injection point or well. Following injection of the tracer solution, one to three purge volumes of groundwater from the site should also be injected to displace the tracer from the well, piezometer, or drive-point.

The volume extracted at the end of the hold time is dependent on the groundwater velocity about the injection point, the in situ hold time, and the purge volume of the well, piezometer, or drive-point. Groundwater flow displaces the injected solution, so groundwater must be recovered from a larger volume of the aquifer than initially occupied by the tracer solution. That larger volume is pictured to be a cylinder having the same height as the volume initially occupied by the tracer, but with a larger radius equal to R_{test} plus the distance groundwater travels during the in situ hold time. For example, the initial field test was conducted in an aquifer having average linear groundwater velocities ranging from 0.1 - 1 ft/d across the aquifer thickness; the injected volume was 1 L; and the in situ hold time was 24 h. For those parameters, minimum extraction volumes were estimated to be about 4 L. Approximately 10 L were extracted, and the data showed that extracted volumes equal to four to five times the injected volume provided reasonable recovery (typically >80%) of the conservative tracer.

DATA REDUCTION

Data from the push-pull test are used to calculate tracer volatilization, oxygen utilization, and biodegradation rates. Required data include the tracer chemical concentrations in the injection solution (C_{inject} [mg/L]), the volume of tracer solution injected (V_{inject} [L]), tracer and dissolved oxygen (DO) concentrations in the solution extracted after the in situ hold time at the test and background locations ($C_{recovered}$ [mg/L] and $C_{recovered\text{-}background}$ [mg/L], respectively); the volume of groundwater extracted ($V_{recovered}$ [L]); and the in situ hold time ($T_{in\ situ}$ [d]). As mentioned previously, the background point location is not affected by the IAS system, and groundwater in this area can be contaminated or uncontaminated.

Measured tracer concentrations from extracted groundwater samples are first adjusted for losses caused by incomplete recovery of the injected aqueous solution (e.g., due to groundwater movement away from the injection point). Adjusted concentrations are calculated by dividing all other tracer concentrations by the fraction of conservative tracer recovered. For example, acetate (Ac) was the non-volatile aerobically degradable tracer used in this work, and bromide (Br) was the conservative tracer. Therefore:

$$C^*_{Ac-recovered} = \frac{C_{Ac-recovered}}{C_{Br-recovered} / C_{Br-injected}} \qquad (2)$$

where $C^*_{Ac\text{-}recovered}$ is the adjusted acetate concentration in the extracted groundwater.

Typical Br recoveries for the tests described later range from 0.8 to 1.0, but are sometimes as low as 0.5. In theory, tracer volatilization and biodegradation rates can be calculated for any level of conservative tracer recovery, but recoveries >50% are desirable. Confidence in the analytical data and interpretation of the results is low when the conservative tracer recovery is <25%.

A mass balance on the aerobically biodegradable tracer compound is used to calculate tracer-biodegradation rates and corresponding oxygen transfer rates. First, the mass of tracer degraded at the test and background locations is calculated by subtracting the recovered mass from the injected mass at each location. Then the mass loss at the background point is subtracted from the mass loss at the test location. This correction assumes that abiotic and anaerobic influences on tracer recovery are consistent between test and background areas, and therefore, any increase in mass loss at the test location is attributable to the IAS system. In summary:

$$\begin{aligned} M_{biodegraded} &= (C_{inject}\, V_{inject} - C^*_{recovered}\, V_{recovered}) - \\ &\quad (C_{inject}\, V_{inject} - C^*_{recovered-background}\, V_{recovered-background}) \\ M_{biodegraded} &= C^*_{recovered-background}\, V_{recovered-background} - C^*_{recovered}\, V_{recovered} \end{aligned} \qquad (3)$$

where C_{inject} = concentration of biodegradable tracer in injected mixed tracer solution (mg/L); V_{inject} = volume of mixed tracer solution injected into the monitoring location (L); $C^*_{recovered\text{-}background}$ = concentration in recovered solution at background point, after adjustment for conservative tracer recovery at that point (mg/L); $V_{recovered\text{-}background}$ = volume of solution recovered at background point (L); $C^*_{recovered}$ = concentration of biodegradable tracer in recovered solution at point of interest, after adjustment for conservative tracer recovery at that point (mg/L); $V_{recovered}$ = volume of solution recovered at point of interest (L).

The corrected mass of biodegradable compound lost ($M_{biodegraded}$) can be converted to an equivalent mass of oxygen consumed, $M_{oxygen\text{-}consumed}$, assuming complete mineralization. For example, for acetate (CH_3COO^-):

$$CH_3COO^- + H^+ + 2O_2 \rightarrow 2H_2O + 2CO_2 \tag{4}$$

Therefore, 2 moles of oxygen are required to degrade 1 mole of acetate, or 64 g of oxygen are required for degradation of every 59 g of acetate (1.08 g O_2/g acetate), and the mass of oxygen consumed ($M_{oxygen\ consumed}$ [g]) is calculated as:

$$M_{oxygen-consumed} = M_{lost} \times 1.08 \frac{g - O_2}{g - acetate} \tag{5}$$

An oxygen utilization rate $R_{oxygenation}$ (mg-O_2/L-water/d) can then be estimated by dividing $M_{oxygen\text{-}consumed}$ by the in situ hold time ($T_{in\ situ}$ [d]) and the tracer injection volume:

$$R_{oxygenation} = \frac{M_{oxygen\ consumed}}{T_{in\ situ}\ V_{inject}} \tag{6}$$

It should be noted that this manipulation might overestimate the actual oxygen delivery rate because it assumes that the entire biodegradable compound lost was completely mineralized. It might also underestimate the total oxygen delivery rate because other aquifer oxygen demands are being neglected (e.g., degradation of residual soil contamination and abiotic oxygen utilization).

To help assess the significance of oxygenation rates, they can be expressed as potential hydrocarbon aerobic biodegradation rates (mg-hydrocarbon/L-water/d) by dividing $R_{oxygenation}$ by an approximate stoichiometric conversion factor. For typical petroleum hydrocarbons of interest (e.g., benzene, toluene, xylenes), 3 mg-O_2/mg-hydrocarbon degraded is a reasonable value. Hydrocarbon biodegradation rates can also be converted to zero-order rates expressed as (mg-contaminant/kg-soil/d) by dividing by the soil bulk density (approximately 1.7 kg-soil/L-soil) and multiplying by the volumetric moisture content (approximately 0.3 L-water/L-soil).

A mass balance approach similar to that discussed above in Equation (3) is used to calculate volatilization rates from volatile tracer concentrations. The volatilization rate, $R_{volatilization}$, is expressed as a percent reduction per unit time (% loss/d), calculated as:

$$R_{volatilization} = \frac{M_{lost}}{T_{in\ situ}\ M_{initial}} \times 100 \tag{7}$$

where $T_{in\ situ}$ denotes the in situ hold time (d); M_{lost} is the mass of volatile, nonbiodegradable tracer lost after correcting for background losses (g); and $M_{initial}$ is the initial volatile tracer mass (g).

The volatilization rate is expressed in this way to emphasize its use as a relative (and not absolute) measure of volatilization induced by IAS. Actual volatilization rates of contaminants of interest will be different because of differences in concentrations and chemical properties. Fortunately, the goal is to use this tool for system optimization, and for that purpose we only need to be able to assess relative increases and decreases in $R_{volatilization}$ spatially and with changes in IAS process conditions and system design.

DEVELOPMENT OF THE PUSH-PULL DIAGNOSTIC TEST PROTOCOL

Starting with the conceptual and mathematical framework discussed above, the diagnostic tool development involved a sequence of steps, including a) tracer selection, b) protocol and analyses methods development, c) protocol evaluation in a three-dimensional laboratory-scale aquifer physical model, and finally, d) field evaluation. Complete details of the development studies can be found in Amerson (1997). The key points of steps (a) through (c) are summarized below, followed by a presentation of results from step (d) in the next section.

With respect to the selection and analyses of tracer compounds, some general comments are necessary before discussing the specifics of each tracer selected. First, it is important to recognize that solutions injected into an aquifer will be subject to regulatory approval, and therefore chemical toxicity, persistence in aquifer systems, and concentrations need to be considered. Second, this diagnostic tool is designed to be used for system optimization, and the goal is to assess increases and decreases in tracer biodegradation and volatilization rates with changes in system design and operation. Therefore, it is not critical that the tracer compounds volatilize or biodegrade at the same rates as the actual contaminants at the site. Also it is important to note that the tracer chemical volatilization and biodegradation rates are not used to determine actual volatilization and biodegradation rates of contaminants at the site.

With respect to the selection of specific tracer compounds:

- Nondegradable, nonvolatile conservative tracer: This should be a nonnutrient salt that is easily quantified (e.g., with an ion-specific electrode or by ion chromatography). It is important to use initial concentrations that are quantifiable at a minimum 10X dilution, but also to ensure that the initial concentration is not so high as to induce significant vertical density gradients in the aquifer (e.g. initial salt concentrations in the injected solution should be <100 mg/L). In this work, bromide (Br-) was selected because it is typically found only in trace quantities in groundwater systems and is easily measured, either with an ion chromatograph, a bromide-specific electrode, or a spectrophotometer (colorimetric assay).

  In this work, stock solutions of bromide were prepared using the KBr salt; the target injection concentration was 50 mg/L; and the analyses were performed using a Dionex DX500 Ion Chromatograph equipped with an Ionpac® AS12A analytical column, Ionpac®12A guard column and electrochemical and conductivity detectors. Using this method, concentrations above 1 mg/L are easily quantified.

- Biodegradable, nonvolatile tracer compound: This compound should be readily biodegradable aerobically, and should have the potential to biodegrade much faster aerobically than degradation via any other pathway during the time of the test. It also must not volatilize, so readily dissociated salts are desirable. As above, it is important to use initial concentrations that are quantifiable at a minimum 10X dilution, but not so high as to induce significant vertical density gradients in the aquifer (e.g., initial injected concentrations should be <100 mg/L). In this work, acetate (Ac^-) was selected because it is readily used as an energy source (electron donor) by a wide range of microbial organisms under aerobic growth conditions and because it is not a component of petroleum fuel mixtures.

  Stock Ac^- solutions were prepared using the NaAc salt; the target injection concentration was 50 mg/L; and the analyses were performed using the same ion chromatograph set-up described above for bromide analysis. Using this method, concentrations above 1 mg/L are easily quantified.

- Volatile, nondegradable tracer compound: This compound should be chemically stable for the duration of the test. Theory (Johnson, 1998) suggests that results of this test should be insensitive to specific values of chemical parameters related to volatilization (e.g., vapor pressure and Henry's Law Constant) as volatilization is expected to be diffusion-limited (not partitioning-limited). In this work, sulfur hexafluoride (SF_6) was chosen because it is sparingly soluble in water and it is easily detected in the low part per trillion by volume (ppt_v) range using a gas chromatograph (GC) equipped with an electron capture detector (ECD).

  As SF_6 is a gas at normal ambient temperatures and pressures, it was incorporated into solution using a closed loop gas recirculation system employing a peristaltic pump. This system continuously circulated 100 mL of headspace containing 10 ppm_v of SF_6 through the Br^-/Ac^- solution. A 1 L glass bottle containing 900 mL of tracer solution was sealed using a No. 5 rubber stopper, and 1 mL of 1,000 ppm_v SF_6 in N_2 was introduced to produce the desired headspace concentration of 10 ppm_v. The headspace was allowed to circulate for 30 to 40 min after the SF_6 was introduced.

  Dissolved SF_6 concentrations were determined by a method that takes advantage of the high SF_6 Henry's Law Constant (H>100 mg/L-vapor/mg/L-H_2O for SF_6). First, a 1-mL sample of water was injected into a sealed, nitrogen-purged 40 mL VOA vial and allowed to equilibrate with the headspace. This equilibration occurs within a minute when the vial is shaken. A 5-mL headspace gas sample was then analyzed for SF_6, using a Lagus Applied Technologies Autotrac analyzer equipped with an ECD. The dissolved SF_6 concentration was calculated from a mass balance using the known water and headspace volumes and the measured headspace calculation. The advantage of using such a high Henry's Law constant chemical is that >99% of the SF_6 mass is always found in the headspace, calibration to known aqueous standards is not necessary, and the analysis method is not sensitive to temperature changes.

- Visible dye: This tracer was used to visually assess when the volume of solution recovered from the aquifer is sufficient to have recovered a significant fraction of the injected solution. The dye can be degradable, provided that the degradation rate is slow compared to the test duration. Fluorescein was used because it produces a bright green color at low concentrations and is easily measured by spectrophotometry.

Initial experiments were conducted in a 1.2-m tall × 1.2-m wide × 2.4-m long (4 ft × 4 ft × 8 ft) aquifer physical model tank. Horizontal groundwater flow across the tank was induced using ports placed at the ends of the tank. Air was injected at the center of the tank near the bottom through a short 10-cm section of 2.54-cm ID PVC well screen. The tank was filled with unwashed fill sand, except 6-inches from each end where a more permeable ABC composite was placed to better distribute the groundwater flow. Unscreened stainless steel tubing (0.32-cm ID) sampling points were inserted vertically throughout the tank at sampling depths ranging from 0.3 to 1 m below the upper soil surface.

These initial experiments were conducted to assess the effects of in situ hold time and extracted volume, and to determine if the test was sufficiently sensitive to identify areas affected and unaffected by air sparging. Between 800 and 900 mL of the tracer solution was injected through selected sampling ports for hold times of 5 min, 1 h, 4 h, 24 h, and 48 h. Eight to 10 L of water were extracted in 1-L increments. The sampling points used were selected based on dissolved oxygen measurements following 24 h of air injection; sampling points showing significant (>4 mg/L) increases in dissolved oxygen (DO) were referred to as "affected" locations; and those where DO remained <1 mg/L were referred to as "unaffected" locations.

Figure 2a shows the recoveries of the three tracers in the affected and unaffected areas as a function of in situ hold time, and Figure 2b shows the difference in recoveries of the acetate and SF_6. These are representative results from this work and complete details of these experiments are given by Amerson (1997). The acetate and SF_6 recoveries presented have been adjusted for bromide recovery. As can be seen, bromide recovery is near 100% at both sampling points and all in situ hold times; >90% of the cumulative bromide tracer recovery occurred within the first 4-L extracted (an extracted volume approximately equal to 4 times the injection volume).

Acetate recovery was >80% at 1-h hold time, and declined with increasing in situ hold time at both the affected and unaffected sampling points. Complete disappearance of the acetate occurred within 48 h at both locations. Loss at the unaffected point was likely the result of anaerobic biodegradation as the tank was filled with water containing high sulfate concentrations (>100 mg/L). For short in situ hold times (<4 h), the adjusted recovery difference was about 10%. For longer in situ hold times, the adjusted recovery difference increased to about 30% at 24 h, and then declined to 0% at 48 h. It appeared that there was a 12–24 h window of in situ hold times for which the sensitivity to differences in acetate loss was maximized. It should be noted that the temperature of water in the physical model was high (27 to 33°C) relative to typical in situ conditions (15 to 20°C), and this might have induced higher acetate degradation rates than might occur in field settings.

Differences in adjusted SF_6 recovery ranged from –6% at 1 h to 23% at 48 h. The high Henry's Law Constant of SF_6 (>100 mg/L-vapor/mg/L-water) renders it difficult to use for this test. First, it requires the user to take special precautions when delivering and recovering solutions, since the SF_6 will completely partition into small volumes of gas. In this work, solutions were delivered from and recovered into gas-tight Tedlar™ bags to eliminate gases prior to injection and to capture any gases pumped up to ground surface. The SF_6 also has a strong tendency to partition into trapped aquifer gases (Fry et al., 1995), which in turn, hinders its recovery and decreases the sensitivity of the volatilization rate measurement. Based on this experience with SF_6, it is recommended that other tracer compounds having Henry's Law Constants in the range 0.1 to 1 (mg/L-vapor)/(mg/L-water) be tested. These are not expected to be significantly retained by trapped gas in the aquifer.

FIELD APPLICATION OF THE DIAGNOSTIC TOOL

The push-pull diagnostic tool was field-tested at the Hydrocarbon National Test Site (HNTS) located at the U.S. Naval Construction Battalion Center in Port Hueneme, California. At the HNTS, groundwater had been impacted by a relatively large gasoline release from the Base service station. The push-pull test was applied to a 20-m x 20-m IAS study area located within a larger (approximately 50 m x 300 m) residual immiscible hydrocarbon source zone. This study area was equipped with an extensive monitoring network, and the site hydrogeology and contaminant distribution were already well characterized.

A plan-view schematic diagram of the test site monitoring network is shown in Figure 3. The monitoring system included 12 multilevel monitoring installations, each containing a bundle of 15 0.32-cm ID (1/8-inch) color-coded, stainless steel sampling lines with ports at 0.6, 1.2, 1.8, 2.4, 3.0, 3.4, 3.7, 4.0, 4.3, 4.6, 4.9, 5.2, 5.5, 5.8, and 6.1 m (2, 4, 6, 8, 10, 11, 12, 13, 14, 15, 16, 17, 18, and 19 ft) below ground surface (bgs). The groundwater table was at approximately 3-m (10 ft) bgs, and the immiscible hydrocarbon smear zone extended from approximately 3 to 4 m (10 to 13 ft) bgs. Dissolved total hydrocarbon concentrations in the smear zone generally exceeded 1 mg/L. The IAS well was screened from 5.8 – 6.1 m (18 - 20 ft) bgs. Other studies at the HNTS IAS research site have shown that the air distribution in the aquifer is nonuniform about the air injection well (e.g., R.L. Johnson et al. 2001), exhibiting tendencies to flow along the axis defined by MP6, MP12, MP3, and MP9.

The diagnostic test was applied at several monitoring locations while the IAS air injection flow rate was 570 standard L/min (20 SCFM). Test locations within the target treatment zone were selected so that one to two locations from each radial distance away from the IAS well were used. All test points were located 3.4 m (11 ft) bgs in the hydrocarbon smear zone. In each case the injected concentrations of bromide and acetate were approximately 50 mg/L, the injected volume was 1 L, extracted volumes were at least 4 L, and the in situ hold time was 25 h. The experimental procedure was as follows:

1. Preparation of 11 L of a solution containing approximately 50 mg/L each of bromide and acetate, and 2 mL of a 10% fluorescein solution
2. De-oxygenation of this solution by N_2 gas bubbling until DO < 1 mg/L (15-20 min)
3. Addition of 1 ppm_v SF_6 to solution through gas bubbling and headspace recirculation
4. Collection of groundwater samples from the test points for a background ion analysis and measurement of DO, which was measured in an aboveground flow-through cell
5. Collection of a 40-mL sample from the multitracer stock solution carboy for analysis of initial tracer concentrations
6. Injection of 1-L of tracer solution into each test point with a peristaltic pump
7. Allowing the solution to remain in situ for 25 h
8. Extraction of 4 to 10 L of groundwater from each test point; visual observation of the color imparted by the fluoroscein served as the indicator to determine how much groundwater to withdraw (about 4 to 5 L)
9. Collection of 40 mL groundwater samples from each 1 L of extracted groundwater; this sample was preserved on ice for tracer analysis (Note that it would also have been sufficient to collect a single sample from a well-mixed vessel containing all of the extracted groundwater.)
10. Analysis of samples within 3 days of collection to ensure the validity of measured acetate levels; tests showed acetate concentration stability over approximately 7 d for samples stored on ice.

Results from the field test are presented in Table 1. In the data reduction, MP5 was taken to be the background point; as the adjusted acetate and SF_6 recoveries were 94% and 81%, respectively, the DO level remained <1 mg/L, and other air distribution studies at the site suggested that it was not within the area influenced by the air injection (R.L. Johnson et al., 2001).

The calculated oxygen utilization rates range from 0 to 51 mg-O_2/L-water/d. The oxygen utilization rates were used to calculate equivalent potential hydrocarbon aerobic biodegradation rates that ranged from 0 to 17 mg-hydrocarbon/L-water/d. This range is also equivalent to zero-order biodegradation rates of 0 to 3 mg-hydrocarbon/kg-soil/d, and these are comparable to the lower end of the range of rates reported for bioventing in situ respirometry tests (Leeson and Hinchee, 1996). In addition, this range of rates is comparable to that reported by Bruce et al. (2001) from use of a gas tracer diagnostic test at this site. The data suggest significant oxygen transfer at MP-1, MP-2, and MP-5 even though DO measurements remained ≤1 mg/L. For this to happen, oxygen must be utilized as fast as it is delivered at those locations.

Figure 4 presents oxygen utilization rates versus DO levels for the data appearing in Table 1 as well as data collected from other acetate-based push-pull diagnostic test applications at the HNTS IAS test site. As can be seen, most of the oxygen utilization rates fall in the 0 to 50 mg-O_2/L-water/d range, although one value is as high as 100 mg-O_2/L-water/d. The results also show little correlation between DO concentrations and oxygenation rates at each test point. This is an important finding as DO measurements are commonly used to define the zone of impact of an IAS system. These results suggest that significant oxygenation can occur at locations thought to be unaffected by IAS, as based on DO measurements alone. Alternatively, the discrepancy could be explained by differences in anaerobic degradation rates of acetate at the different points. However, the transfer of oxygen at points not showing elevated DO levels is

reported by Amerson (1997) and Bruce et al. (2001). In that work, a conservative tracer delivered in the gas injection stream was used to determine oxygenation rates at this site.

The adjusted SF_6 recoveries in the field tests ranged from approximately 51% to 124%, and therefore were generally much greater than the recoveries in the laboratory-scale physical model development studies. This could be caused by differences in trapped gas concentrations in the two settings. The estimated volatilization rates shown in Table 2 range from 0 to 47%/d, with most values being at or near zero. There appears to be little correlation between the estimated volatilization and oxygen utilization rates. This is unusual, as one would expect to see high oxygenation rates at locations having a higher density of air channels, and that volatilization rates would also be high in these locations. Confidence in these conclusions is low as the laboratory-scale development studies suggested a lack of sensitivity when SF_6 is used as the volatile tracer.

SUMMARY

The use of multitracer push-pull tests for IAS system diagnoses and optimization has several attractive features including: a) the relatively short response time (hours), b) its flexibility—the procedure is easily modified to assess performance over local (<1 ft radius) and larger scales—and c) the test is not dependent on knowing the initial site conditions and it can be applied at any time during IAS application.

The test would benefit from further development. In particular, identification and testing of alternate biodegradable/nonvolatile and volatile/nondegradable tracers would be beneficial. Acetate was used in these tests and it was discovered that data analysis and interpretation is confounded by the potential for significant anaerobic biodegradation. Conclusions regarding spatial variations in oxygenation are suspect if the degradable tracer biodegrades under anaerobic conditions and variability in anaerobic biodegradation rates is not well-characterized. Use of SF_6 identified difficulties in working with high Henry's Law constant tracers.

With respect to the use of acetate, laboratory-scale physical model tests suggest that there is an optimum in situ hold time; the test sensitivity is too low for shorter times and complete degradation via anaerobic pathways may occur for longer hold times. Acetate-loss based oxygenation rates from the field test site varied spatially from 0 to 40 mg-O_2/L-water/d. Assuming no spatial variability in anaerobic losses, one could conclude that significant oxygenation occurred at test points not exhibiting increased dissolved oxygen concentrations. If true, this is a significant observation as practitioners currently infer IAS treatment zones based on groundwater DO measurements. While the spatial variations in acetate loss could be due to spatial variations in anaerobic biodegradation rates, the work of Amerson (1997) and Bruce et al. (2001) supports the hypothesis that oxygenation occurred at points having sustained DO<1 mg/L. In their work, a gas tracer delivery diagnostic tool was used, and they report oxygenation rates similar to those from this work.

It is important to note that, in this work, the measured biodegradation and volatilization rates are specific to the tracers used. Therefore, the results only provide relative measures of biodegradation and volatilization processes at a given site, and not the rates specific to the target contaminants. Assuming that better tracers could be identified, this test does provide a tool that can be used to assess spatial differences in rates across a given site and the effects of process changes on these rates. Thus, the tool could be used to identify zones of active treatment and could also be used to optimize system operation (flow rates, distribution of wells, etc.).

It should also be noted that the oxygen utilization and aerobic biodegradation rates obtained from this push-pull diagnostic test might be regarded as upper-bound estimates of actual aerobic biodegradation rates because a) the tracer compound used here (acetate) is inherently more rapidly degraded than typical

contaminants of interest (e.g., petroleum compounds), and b) it is assumed that all acetate loss above background levels is due to aerobic biodegradation and that complete mineralization occurs. The test might also underestimate oxygenation rates as other oxygen demands in the aquifer are neglected. In addition, it should be noted that there are situations for which this test might not be useful; these include: a) the formation does not accept the tracer solution, or does not allow recovery, in a reasonable amount of time; b) there are high background levels of acetate, bromide, or SF_6; c) initial (pre-air sparging) groundwater DO > 5 mg-O_2/L-water; and d) the available monitoring point screen intervals or other well construction details cause impracticable volumes of tracer solution to be used (i.e. V_{well} is too large).

ACKNOWLEDGEMENTS

The authors would like to acknowledge and thank Harley Hopkins and the American Petroleum Institute Soil and Ground Water Technical Task Force for their financial support, project review, and many valuable suggestions. We would also like to thank the Strategic Environmental Research and Development Program (SERDP) and the Air Force Research Laboratory, Materials and Manufacturing Directorate, Airbase and Environmental Technology Division (AFRL/MLQ), Tyndall AFB, Florida, for providing a field site for this project. Finally, the authors would like to thank Karen Miller, Ernie Lory, James Osgood, and Dorothy Cannon at the Naval Facilities Engineering Service Center at Port Hueneme for their assistance with the field portion of this research.

REFERENCES

Amerson, I.L. 1997. Diagnostic Tools for the Monitoring and Optimization of In Situ Air Sparging Systems. M.S. Thesis. Arizona State University.

Bass, D.H., and R.A. Brown. 1995. Performance of Air Sparging Systems - A Review of Case Studies. In: *Petroleum Hydrocarbons and Organic Chemicals in Ground Water: Prevention, Detection and Restoration*, Houston, Texas, November.

Bruce, C.L., I.L. Amerson, R.L. Johnson, and P.C. Johnson. 2001. Use of an SF_6-Based Diagnostic Tool for Assessing Air Distributions and Oxygen Transfer Rates during IAS Operation. *Bioremediation Journal*, *5*(4):337-347.

Fry, V.A., J.D. Istok, L. Semprini, K.T. O'Reilly, and T.E. Buscheck. 1995. Retardation of Dissolved Oxygen Due to a Trapped Gas Phase in Porous Media. *Ground Water. 33*(3):391-398.

Hinchee, R. E., and S. K. Ong. 1992. A Rapid In Situ Respiration Test for Measuring Aerobic Biodegradation Rates of Hydrocarbons in Soil. *Journal of the Air & Waste Management Association. 42*:1305-1312.

Istok, J. D., M. D. Humphrey, M. H. Schroth, M. R. Hyman, and K. T. O'Reilly. 1997. Single-Well "Push-Pull" Test for In Situ Determination of Microbial Activities. *Ground Water. 35* (4):619 - 631.

Johnson, P.C. 1998. An Assessment of the Contributions of Volatilization and Biodegradation to In Situ Air Sparging Performance. *Environmental Science and Technology. 32* (2):276-281.

P.C. Johnson, R.L. Johnson, C.L. Bruce, and A. Leeson. 2001. Advances in In Situ Air Sparging/Biosparging. *Bioremediation Journal*, *5*(4):251-266.

Johnson, R. L., P.C. Johnson, D. B. McWhorter, R. E. Hinchee, and I. Goodman. 1993. An Overview of In Situ Air Sparging. *Ground Water Monitoring and Remediation. Fall*:127-135.

Johnson, R.L., R.R. Dupont, and D.A. Graves. 1996. *Assessing UST Corrective Action Technologies: Diagnostic Evaluation of In Situ SVE-Based System Performance*. EPA/600/R-96/041.

Johnson, R.L., P.C. Johnson, T.L. Johnson, and A. Leeson. 2001. Helium Tracer Tests for Assessing Contaminant Vapor Recovery and Air Distribution During In Situ Air Sparging. *Bioremediation Journal*, *5*(4):321-336.

Marley, M.C. and C.J. Bruell. 1995. *In Situ Air Sparging: Evaluation of Petroleum Industry Sites and Considerations for Applicability, Design, and Operation*. API Publication 4609. American Petroleum Institute. Washington, D.C.

Schroth, M. H., J. D. Istok, G. T. Conner, M. R. Hyman, R. Haggerty, and K. T. O'Reilly. 1998. Spatial Variability in In Situ Respiration and Denitrification Rates in a Petroleum-Contaminated Aquifer. *Ground Water*. *36* (6):924-937.

Leeson, A., and R. E. Hinchee. 1996. *Soil Bioventing.* CRC Press: Boca Raton, Florida.

Table 1. Sample Data for Field Implementation of the Push-pull Diagnostic Test (initial concentrations of bromide and acetate ions are 45.6±1.4 mg/L and 52.1±1.4 mg/L, respectively; in situ hold time is 25 h).

June-July 1997 Raw Data and Concentration Adjustments						
Monitoring Point	Cumulative Bromide Recovered (mg)	Fraction of Bromide Recovered (-)	Cumulative Acetate Recovered (mg)	Adjusted Acetate Recovered[1] (mg)	Cumulative SF_6 Recovery (%)	Adjusted Cumulative SF_6 Recovery[1] (%)
MP1-11	33.0	0.81	29.9	36.8	61.4	75.5
MP2-11	21.3	0.52	0.0	0	48.9	94.4
MP4-11	20.2	0.50	16.6	33.1	59.0	118
MP5-11	26.6	0.65	28.5	43.5	81.3	124
MP7-11	34.1	0.87	22.0	25.2	85.7	98.1
MP9-11	43.6	1.07	21.9	20.5	54.5	51.1
MP11-11	36.1	0.79	33.5	42.3	89.2	113

Data Reduction					
Monitoring Point	In Situ Hold Time (h)	DO (mg/L)	Oxygen Consumption Rate*, ** (mg-O_2/L-water/d)	Equivalent Aerobic Biodegradation Rate*** (mg-HC/L-water/d)	Volatilization Rate* (%/d)
MP1-11 (11 ft BGS)	25	<1	7.8	2.6	24
MP2-11 (11 ft BGS)	25	<1	51	17	5.4
MP4-11 (11 ft BGS)	25	4.5	12	3.9	0
MP5-11 (11 ft BGS)	25	<1	0 (background)	0	0
MP7-11 (11 ft BGS)	25	<1	20	6.7	1.8
MP9-11 (11 ft BGS)	25	6.1	27	9.0	47
MP11-11 (11 ft BGS)	25	<1	7.2	2.4	0

1 – "Adjusted" concentrations calculated from measured concentrations and bromide recovery using Equation (2)

* - Oxygen consumption rates calculated using Equations (3), (5), and (6) using adjusted concentrations and the data from MP-5 as the background point

** -Acetate-loss based oxygen consumption rate [1.0 mg-O_2/L-water/d = 1.08 mg-Acetate/L-water/d]

*** - Equivalent aerobic biodegradation rate calculated from the oxygen consumption rate assuming 3 mg-oxygen required per mg-hydrocarbon degraded

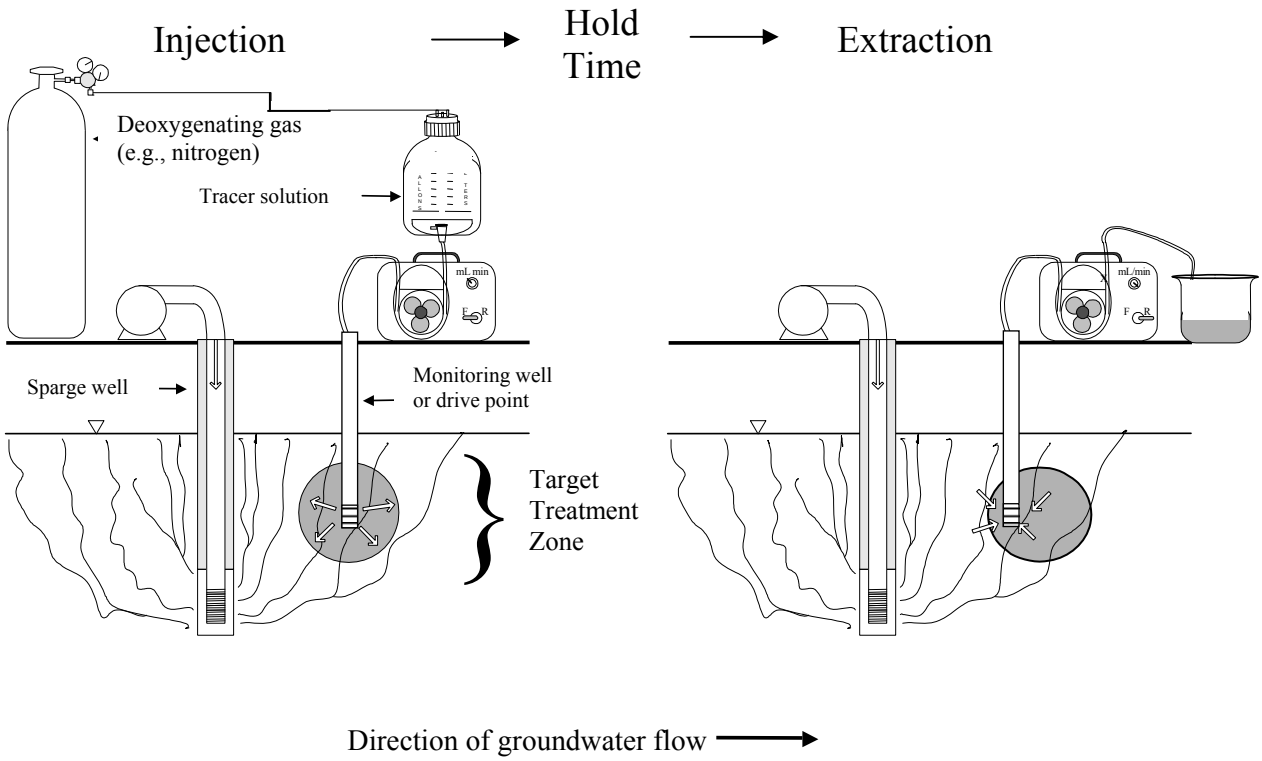

Figure 1. Schematic Diagram Illustrating Use of the Multitracer Push-Pull Test

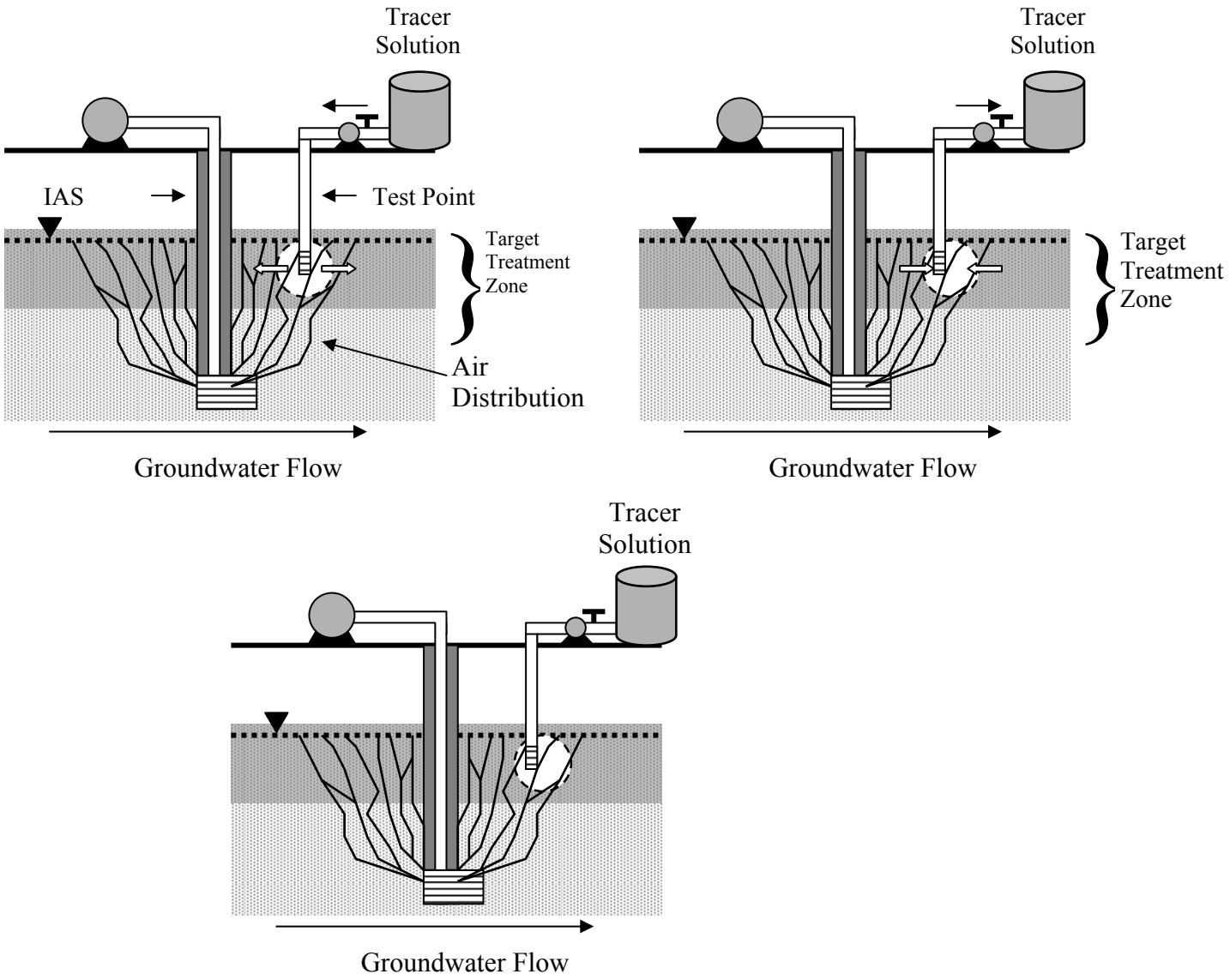

Figure 2. Recoveries from an Affected (Increased Dissolved Oxygen to >6 mg/L) and an Unaffected (Maintained <1 mg/L Dissolved Oxygen) Monitoring Point

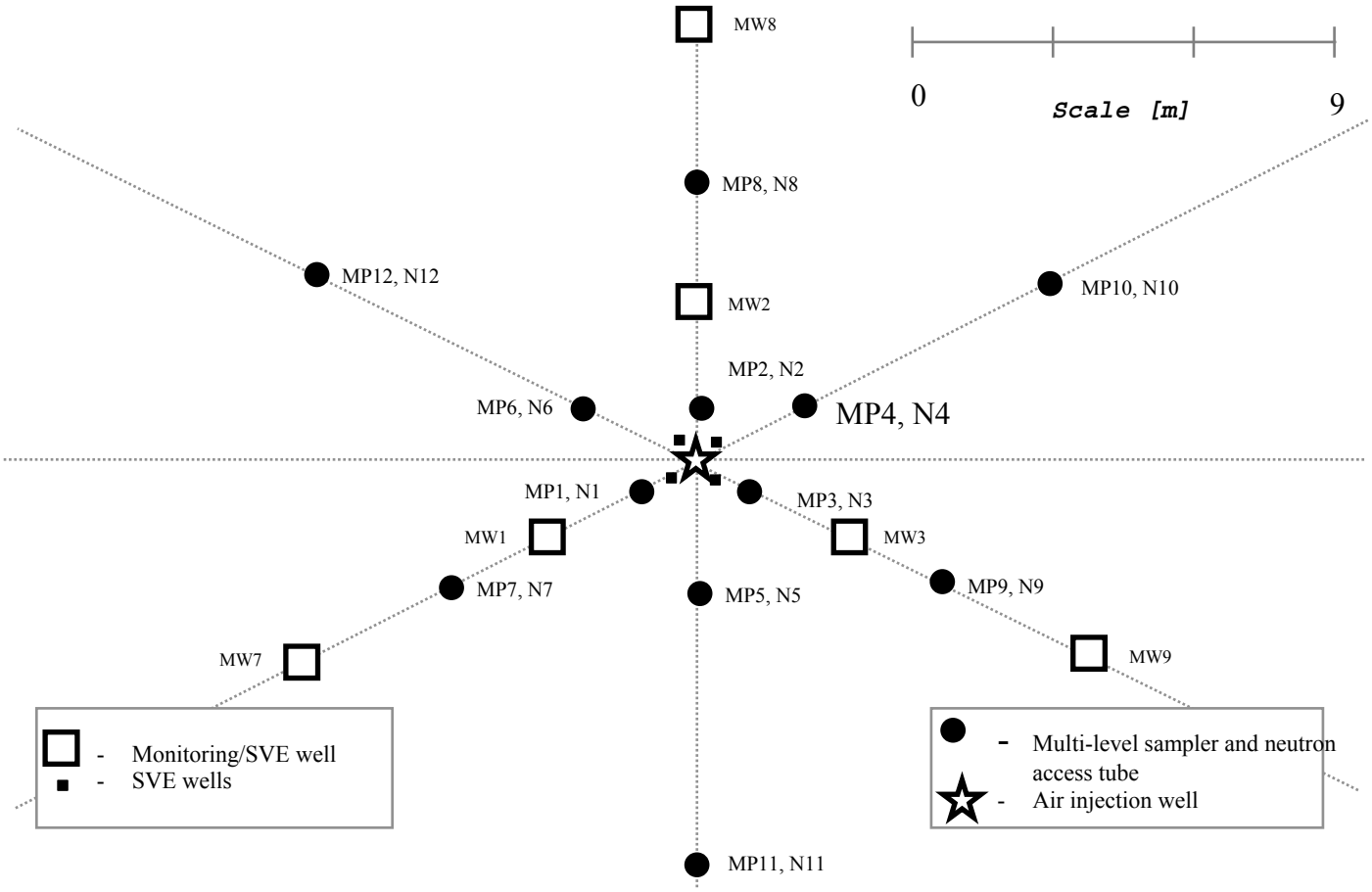

Figure 3. IAS Test Plot Setup

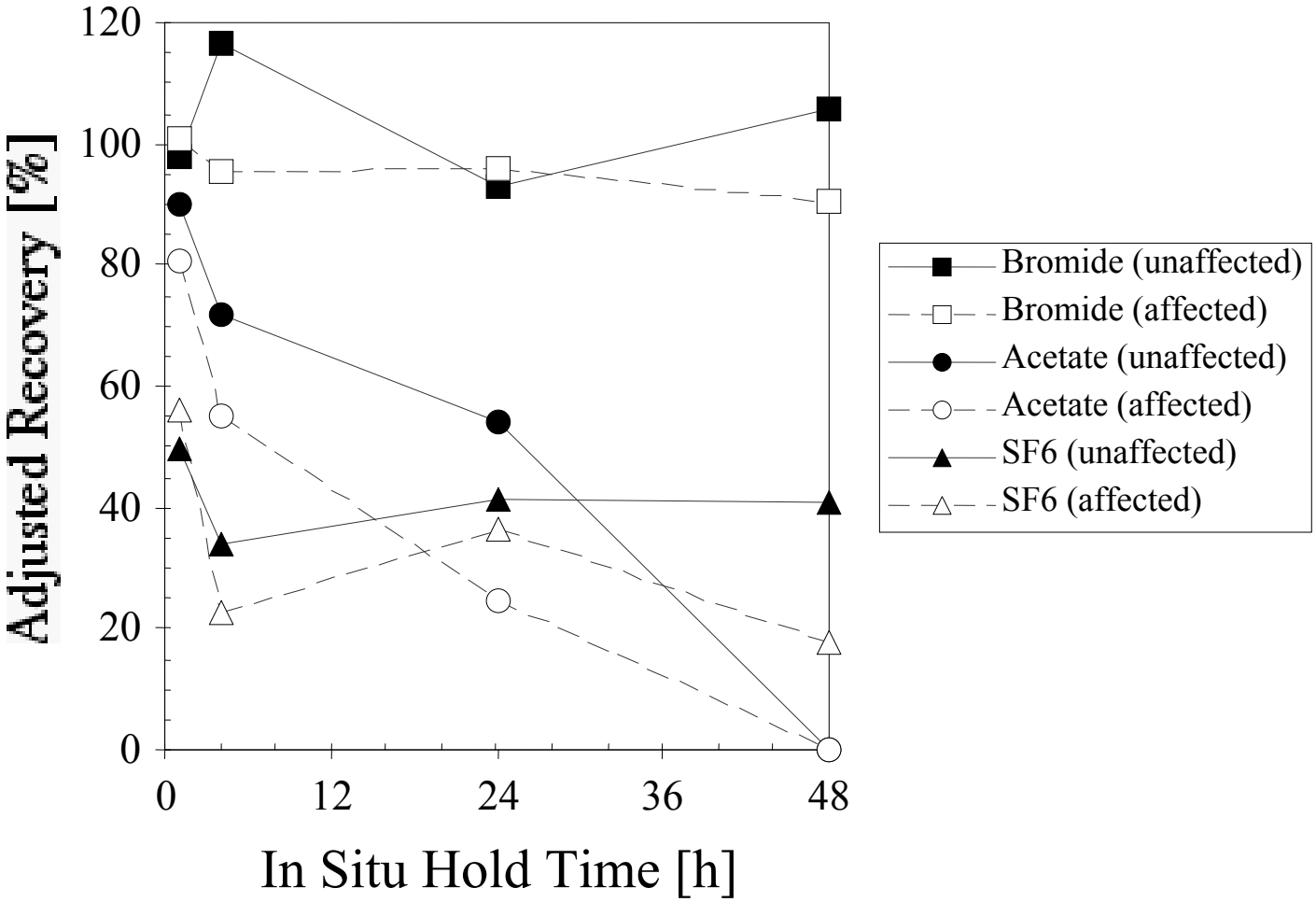

Figure 4. Percent Recovery Versus In Situ Hold Time for Various Tracers

APPENDIX D

Application of the In Situ Air Sparging Design Paradigm to a BTEX Source Zone at the Naval Base Ventura County, Port Hueneme Site, California

Cristin L. Bruce[1], Paul C. Johnson[1], Richard L. Johnson[2], and Andrea Leeson[3]

[1]Arizona State University, Box 875306, Tempe, AZ 85287-5306; [2]Oregon Graduate Institute, 20000 NW Walker Rd, Beaverton, OR 97006; [3]Battelle Memorial Institute, 500 King Road, Columbus, Ohio 43201

INTRODUCTION

An Air Sparging Design Paradigm has been created to answer the need for guidance on the implementation and evaluation of in situ air sparging systems (Johnson et al., 2000). Within this paradigm, the user has flexibility in choosing the pilot scale testing activities, depending on how conservative a final design they are willing to pursue. The Standard Design Approach calls for sparge wells to be placed on 15-ft centers throughout the treatment zone. This document illustrates the application of the Standard Design Approach (most conservative) design to a benzene, toluene, ethylbenzene, and total xylenes (BTEX) source zone at the Naval Base Ventura County (NBVC), Port Hueneme Site, California.

The three most significant factors affecting the efficiency of in situ air sparging (IAS) treatment are air distribution in the target treatment zone, distribution of contaminants relative to the air distribution, and contaminant characteristics. Subsurface air distributions, however, are so sensitive to soil variations that air distributions are unable to be predicted with any degree of accuracy (Ji, 1994). The paradigm asserts that the degree to which an air distribution is characterized should be balanced by the system design. In this case, however, the characterization of air distribution was much more detailed than would be expected of a standard design implementation.

Within the paradigm, pilot-scale testing activities focus on looking for indicators of infeasibility (signs that IAS will not be a successful treatment alternative) in addition to the characterization of the air distribution. One of the most important indicators of IAS applicability is whether air can be injected into the aquifer. Several air injection tests were performed at this site, but only the 10 standard cubic feet per minute (SCFM) injection data will be presented here.

SITE DESCRIPTION OF PORT HUENEME, CALIFORNIA

A site in Port Hueneme, California was chosen as the illustrative site for the application of the Standard Design Approach design. The NBVC, Port Hueneme Site, California, is designated a National Environmental Technology Test Site (NETTS) by the Strategic Environmental Research and Development Program (SERDP). As such, it is the location of a number of innovative technology demonstration programs designed to provide comparative demonstration and evaluation of innovative technologies performing characterization, cleanup, and monitoring. The Department of Defense (DoD) sponsors these programs through the National Environmental Technology Demonstration Program (D/NETDP) in order to evaluate new technologies for cost effectively treating hazardous waste that can be applied to restoring the habitats surrounding many DoD facilities.

Port Hueneme is located in Ventura County, California, on the coast 60 miles north of Los Angeles. The port was constructed in 1942 serve as a secondary port to San Pedro (in Los Angeles). It currently houses the Construction Battalion Center used by the Navy and Air Force for training civil engineers.

The plume of contamination originated from the Naval Exchange (NEX) Gasoline Station, located on the east side of the base at the intersection of Dodson Street and 23rd Avenue (Figure 1). The NEX station dispenses fuel and automotive maintenance services for employees of the base.

Free product was discovered in the area around the NEX station in December of 1984. By March of 1985 the source was determined to be leaks in two of the fuel delivery lines running from the underground storage tanks (UST) to the gas dispensers. According to a study performed by WESTEC Services, Inc., inventory records show that an estimated 10,800 gallons of leaded regular and premium unleaded gasoline were released between September 1984 and March 1985. It is unknown how much was spilled before that time. This gasoline reportedly contained methyl *tert*-butyl ether (MTBE) and 1,2-dichloroethane additives.

Site Characterization

Data collection for site characterization should focus on creating a technically defensible site conceptual model showing hydrologic settings, locations of key physical features, and the approximate extent of the source zone and dissolved plume contamination. The design paradigm suggests that, at minimum, data be collected to answer the following:

1. Characterize subsurface from an air flow perspective (one or more continuous soil cores between upper boundary of the contamination and the top of the anticipated screened interval of any air injection wells) to determine gross features of air distribution.
2. Target treatment zone defined and a conceptual model for air distribution should be created.

Continuous soil cores taken from the area show three distinct soil types: an upper fine-grained silty sand unit (3 to 6 ft bgs), an intermediate fine-to-coarse-grained sand unit (to ~24 ft bgs), and an underlying clay unit of gray sandy or silty clay (Figure 2).

The study site for the design paradigm demonstration is located approximately 400 ft west of the NEX station, within the BTEX source zone. The site measures 75-ft by 75-ft, is covered with asphalt and concrete, and has no known utility lines in the area (Figure 3).

Site Geology

Port Hueneme is situated on the Oxnard Plain and is underlain by unconsolidated sands, silts, and clays, with minor amounts of gravel and fill. These sediments are fluvial-deltaic in origin. Near- surface lithology in the Port Hueneme area was investigated by SCS and Landau Associates in 1985 (Leeson et al., 1996). Based on borehole cuttings, the unconsolidated deposits were characterized into three units. Tables 1 and 2 describe the chemical and physical properties of the semi-perched aquifer under the National Test Site. Figure 4 details a conceptual model of air distribution from a single air injection point at this site.

Figure 1. NBVC, Port Hueneme Site, California

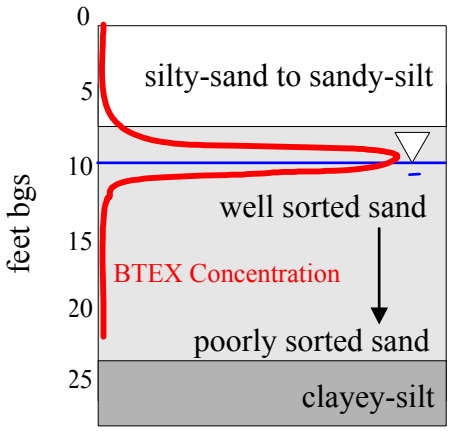

Figure 2. Soil Lithology and Contaminant Distribution at the Demonstration Site

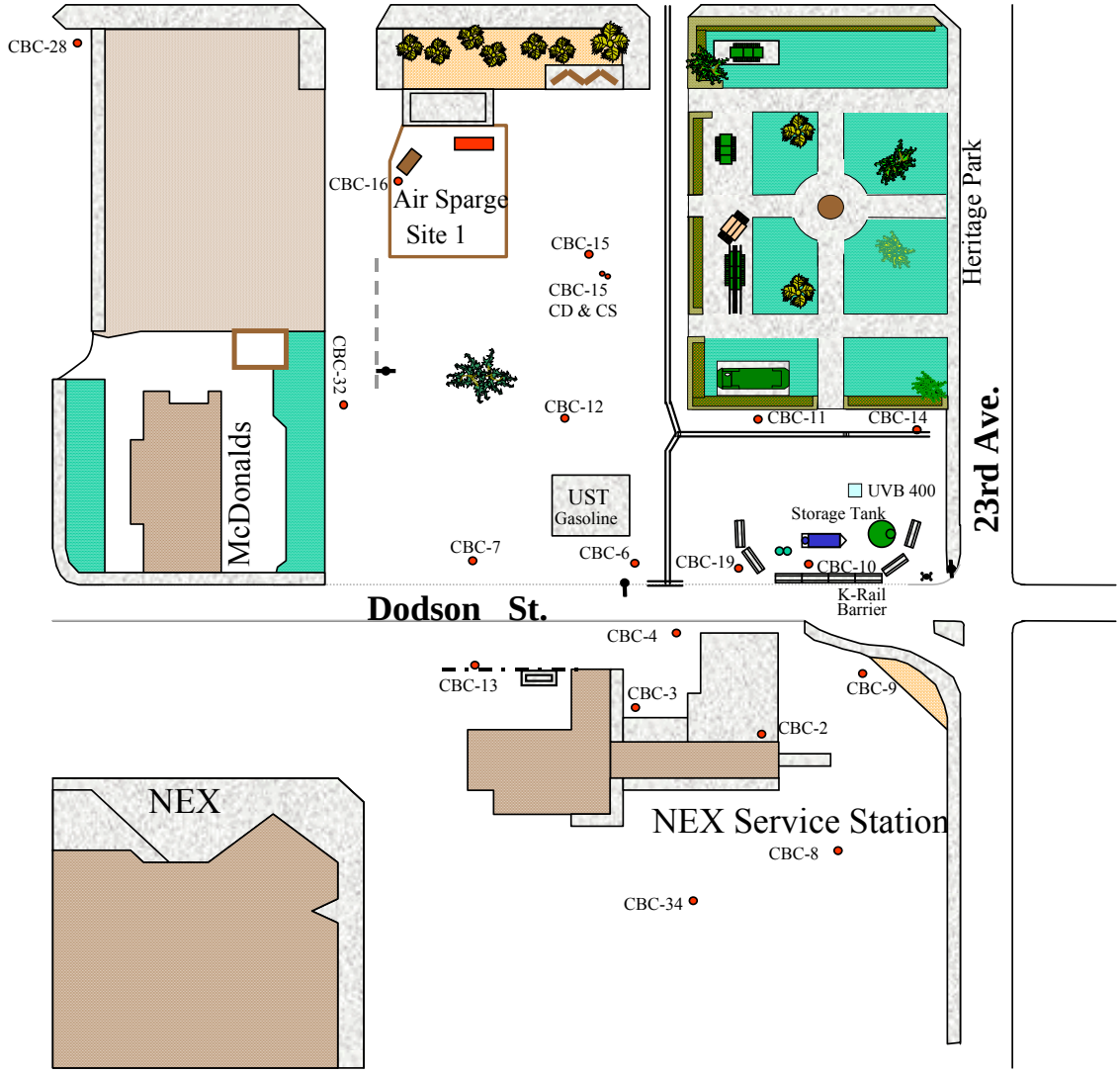

Figure 3. Air Sparging Demonstration Site

Table 1. Properties of the Semi-Perched Aquifer at Port Hueneme

Property	Units	Range or Value
Depth to groundwater	ft	8 – 9
Aquifer thickness	ft	10-15
Hydraulic gradient	ft/ft	0.0029
Groundwater flow direction	NA	Southwest
Porosity	%	30
Hydraulic conductivity	gpd/ft^2	1,300 – 3,000
Transmissivity	gpd/ft	300 – 45,000
Storativity	NA	0.001 – 0.05
Avg. linear groundwater flow	ft/yr	700 – 1,600

Table 2. Inorganic Chemical Properties at Port Hueneme

Component	Units	Range or Value
Total Dissolved Solids (TDS)	mg/L	1,212
Iron	mg/L	15
Manganese	mg/L	17
Nitrite	mg/L	
Salinity	mg/L	

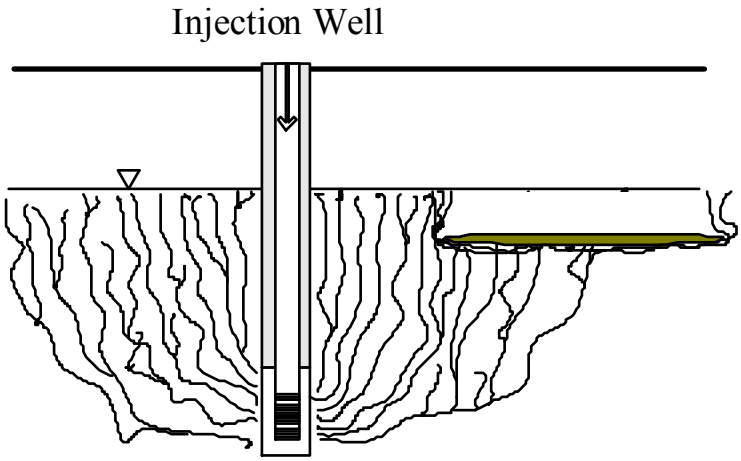

Figure 4. Conceptual Model of Probable Air Distribution at the Demonstration Site

INITIAL SCREENING OF TECHNOLOGIES

The next step is to determine whether IAS is a feasible technology to apply to the scenario at hand. Three straightforward questions are put forth in the design paradigm to address this issue:

1. **Does experience suggest that IAS will be successful at this site?**

The example site at Port Hueneme is contaminated with automotive fuel. IAS has been successfully applied for source zone treatment at gasoline release sites and smaller scale chlorinated solvent spill sites (Bass and Brown, 1995). The site isn't contaminated with chemicals that would impede the growth of indigenous organisms (i.e., pesticides). Aquifer depth is shallow (10 ft bgs) and the soils assayed are sandy to silty/sandy. Contact between contaminant and projected air distribution is good.

2. **For what injection well spacing would IAS be practicable?**

This is a demonstration of the Standard Design Approach design (15-ft centers). Closely spaced wells are not prohibitive at this site as groundwater is relatively shallow and sandy soils are present.

3. **What are the reasonable performance expectations for this IAS system?**

The Design Paradigm (Johnson et al., 2000) puts forth a series of prescriptive tables that an operator may fill out to determine reasonable IAS performance expectations.

PILOT TESTING

The pilot test is designed to look for indicators of infeasibility, characterize the gross features of air distribution, and identify any safety hazards that may result from application of IAS. Prior to implementation of the pilot test, the following details were completed:

1. Define target treatment zone
2. Propose conceptual model for the air distribution in the treatment zone
3. Determine if 15-ft well-spacing were cost-prohibitive
4. Propose depth, location, and construction specifics of a pilot test well
5. Determine the expected range of operating pressures for the injection well.

Monitoring Network Installation

Monitoring wells should be spatially varied because air distributions are often unpredictable in their preferred directions. A straight line of monitoring wells could miss the air-impacted zone entirely. The wells at Port Hueneme were installed via direct push according to the layout in Figure 5. Wells installed include a sparge well, four soil vapor extraction wells, six monitoring wells, and 12 multi-level sampling wells. The sparge well was installed in the center of the site and extended 20 ft bgs. It was constructed of 19 ft of PVC riser and was screened over the bottom 2 ft. Outside the well casing was filled with sand and a bentonite plug at the top to minimize short-circuiting around the well. Monitoring wells were installed similarly, with 6 ft of PVC riser and the bottom 15 ft screened. The multilevel sampling devices consisted of 14 1/8-in steel tubes inside of a 2-in PVC riser. The tubes terminate at 2, 4, 6, 8, 10, 11, 12, 13, 14, 15, 16, 17, 18, and 19 ft bgs within the PVC tube, where they sample through a "PVC-welded" 100-mesh stainless steel screen. These sampling wells were also installed via direct-push methods. Soil vapor extraction wells were 1-in-diameter PVC (6-ft casing, 5-ft screened interval)

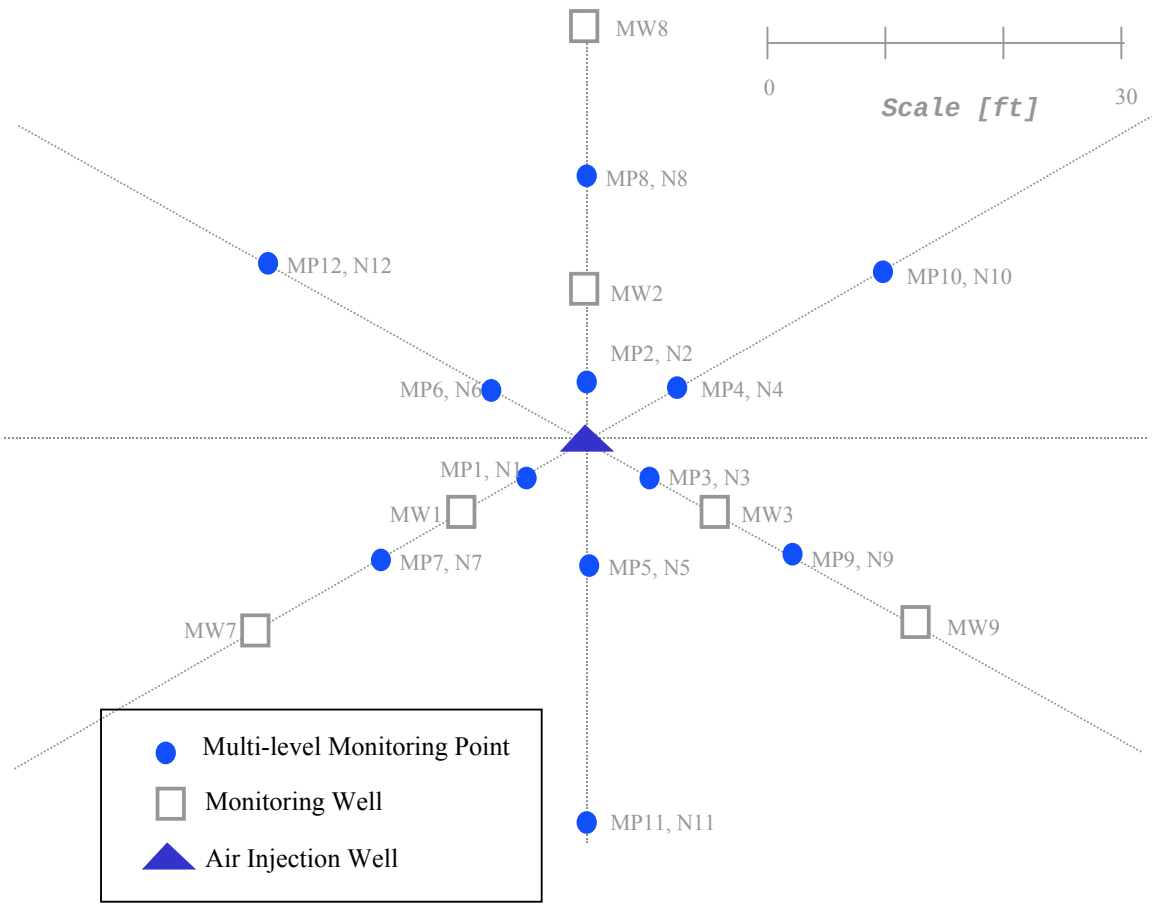

Figure 5. Well Layout for the Demonstration Pilot Test

installed to a depth of 10 ft bgs, and packed with sand and a top layer of bentonite as a plug. Figure 6 illustrates the locations of equipment at the demonstration site.

Baseline Sampling

A round of pre-sparge-test baseline sampling should be performed. The data may include dissolved groundwater oxygen and contaminant concentrations, and fluctuations in pressure readings. The data from Port Hueneme are below:

Groundwater Dissolved Oxygen. Dissolved oxygen (DO) concentrations at this site were generally below 2 mg-oxygen/L-water. Air saturation is frequently supposed to be related to measured DO. DO levels are also used as indicators of what type of microbial growth might be occurring in the subsurface. Table 3 shows the measured DO concentrations (in mg-oxygen/L-water) from the demonstration test site prior to the single-well air injection test.

Groundwater BTEX Concentrations. Hydrocarbon concentrations measured in the multilevel sampling wells before air injection are reported in Table 4.

Figure 6. The Single-Well Pilot Test Air Sparging Setup at Site 1

Table 3. Measured Pre-Sparge Dissolved Oxygen Concentrations (concentrations below 2 mg-oxygen/L-water were reported as 1)

(ft bgs)	MP1	MP2	MP3	MP4	MP5	MP6	MP7	MP8	MP9	MP10	MP11	MP12
10	1	1	1	1	1	NS	1	1	1	1	1	2.2
11	1	1	1	1	1	1	1	NS	1	1	1	2.3
12	1	2.8	1	1	1	1	1	1	1	1	1	1
13	1	2.8	1	4.3	1	1	1	3.3	1	1	1	1
14	1	1	4.2	5.1	1	1	1	1	1	1	1	3.2
15	1	1	1	1	1	1	1	1	1	1	1	2.2
16	1	1	1	2.4	1	1	1	1	1	1	1	NS
17	1	1	1	NS	1	1	1	1	1	1	1	2.5
18	1	1	1	2.1	1	1	1	1	1	1	1	2.5
19	1	1	1	NS	1	1	1	1	1	1	1	2.2

← 5 ft → ← 10 ft → ← 20 ft → ← 30 ft →

Distance from Sparge Well (ft)

Table 4. Measured Pre-Sparge MTBE and BTEX (in μg/L-water) Concentrations at the Demonstration Site

Location	Depth (ft)	MTBE (μg/L)	Benzene (μg/L)	Toluene (μg/L)	Ethylbenzene (μg/L)	Xylenes (μg/L)
MP-1	10	1500	290	2300	600	1500
MP-1	15	< 5	< 5	< 5	< 5	< 5
MP-1	19	< 5	< 5	< 5	< 5	< 5
MP-2	10	1200	< 5	6	< 5	< 5
MP-2	11	7300	< 5	97	7	< 5
MP-2	12	63	< 5	< 5	< 5	< 5
MP-2	13	< 5	< 5	< 5	5	< 5
MP-2	14	< 5	< 5	< 5	< 5	< 5
MP-2	15	< 5	< 5	< 5	< 5	< 5
MP-2	16	< 5	< 5	< 5	< 5	< 5
MP-2	17	< 5	< 5	< 5	< 5	< 5
MP-2	18	< 5	< 5	< 5	< 5	< 5
MP-2	19	< 5	< 5	< 5	< 5	< 5
MP-3	10	1200	< 5	< 5	< 5	< 5
MP-3	11	13000	110	< 5	< 5	< 5
MP-3	12	15000	< 5	< 5	< 5	< 5
MP-3	13	830	< 5	< 5	< 5	< 5
MP-3	14	< 5	< 5	< 5	< 5	< 5
MP-3	15	< 5	< 5	< 5	< 5	< 5
MP-3	16	< 5	< 5	< 5	< 5	< 5
MP-3	17	< 5	< 5	< 5	< 5	< 5
MP-3	18	< 5	< 5	< 5	< 5	< 5
MP-3	19	< 5	< 5	< 5	< 5	< 5
MP-4	10	390	< 5	46	< 5	< 5
MP-4	15	< 5	< 5	< 5	< 5	< 5
MP-4	18	< 5	< 5	< 5	< 5	< 5
MP-4	19	ns				
MP-5	10	9300	< 5	1200	1800	3500
MP-5	15	< 5	< 5	< 5	< 5	< 5
MP-5	19	< 5	< 5	< 5	< 5	< 5
MP-6	10	ns				

Table 4. Measured Pre-Sparge MTBE and BTEX (in μg/L-water) Concentrations at the Demonstration Site (continued)

Location	Depth (ft)	MTBE (μg/L)	Benzene (μg/L)	Toluene (μg/L)	Ethylbenzene (μg/L)	Xylenes (μg/L)
MP-6	15	< 5	< 5	< 5	< 5	< 5
MP-6	19	< 5	< 5	< 5	< 5	< 5
MP-7	10	5700	1700	3900	640	2800
MP-7	15	< 5	< 5	10	< 5	< 5
MP-7	19	< 5	< 5	10	< 5	< 5
MP-8	10	1200	< 5	< 5	< 5	< 5
MP-8	15	< 5	< 5	< 5	< 5	< 5
MP-8	19	< 5	< 5	< 5	< 5	< 5
MP-9	10	46	< 5	< 5	< 5	< 5
MP-9	11	430	< 5	15	61	< 5
MP-9	12	120	< 5	5	< 5	< 5
MP-9	13	< 5	< 5	< 5	< 5	< 5
MP-9	14	29	< 5	< 5	< 5	< 5
MP-9	15	< 5	< 5	< 5	< 5	< 5
MP-9	16	< 5	< 5	< 5	< 5	< 5
MP-9	17	< 5	< 5	< 5	< 5	< 5
MP-9	18	< 5	< 5	< 5	< 5	< 5
MP-9	19	< 5	< 5	< 5	< 5	< 5
MP-10	10	1700	150	4.85	420	< 5
MP-10	15	< 5	< 5	< 5	< 5	< 5
MP-10	19	< 5	< 5	< 5	< 5	< 5
MP-11	10	6600	5900	11000	1700	4300
MP-11	15	< 5	< 5	< 5	< 5	150
MP-11	19	< 5	< 5	< 5	< 5	< 5
MP-12	10	33000	510	190	520	2300
MP-12	15	< 5	< 5	< 5	< 5	< 5
MP-12	19	< 5	< 5	< 5	< 5	< 5

Pilot Test Sampling

Air Injection Pressure Monitoring. One of the most important indicators of feasibility of IAS is the ability to inject air into the subsurface. A pilot test should test if air flowrate of 20 SCFM is possible, and record injection pressure at onset of flow and subsequent pressures every 5 to 10 minutes until pressure and flow stabilize. At the example site, the pressure upon system startup was 25 psig, which decreased to 10 psig within 2 h (Figure 7). Reasonable air injection flow rates for IAS were found to be achievable.

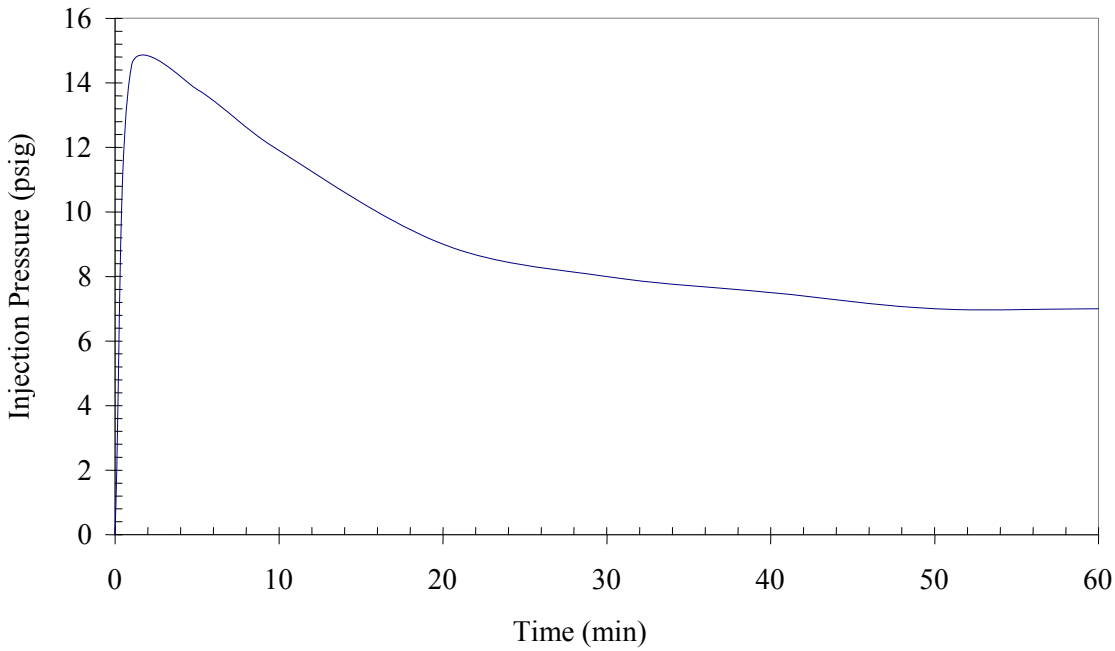

Figure 7. Air Injection Pressures Measured for a 10-SCFM Injection Flow Rate

Pressure Transducer Readings. Information about the probable air distribution within the aquifer can be obtained from the results of pressure transducer readings over the course of an air injection event. While it is difficult to glean specific data from these results, it can generally be said that the height of the peak associated with air injection can be correlated to the amount of air the aquifer accepted before a major release or vent opened. In the case of heavily stratified aquifers, this peak may continue to grow for hours to days. The level above the baseline at which the pressure levels off can be attributed to air trapped within the aquifer. Figure 8 details the pressure transducer readings measured (in feet of water) for a 10-SCFM air injection event.

Helium Distribution and Recovery Tests. Tracking the helium appearance and distribution shortly after its injection into the air stream allows an illustration of where the injected air is going (Table 5). Recovery and mass balance of injected tracers allow an assessment of capture efficiency of the SVE system. Soil gas samples were taken by purging 100 mL from the well, and then attaching a helium detector to the monitoring point. Figure 9 shows helium distribution results from the demonstration sparge test.

Soil Gas Monitoring. Soil off-gas measurements provide information useful to the determination of initial volatilization mass removal rates. Figure 10 shows the mass removal rates from volatilization at the demonstration site are quite high for the 30 h following the initiation of air injection, followed by a much lower, but still elevated rate.

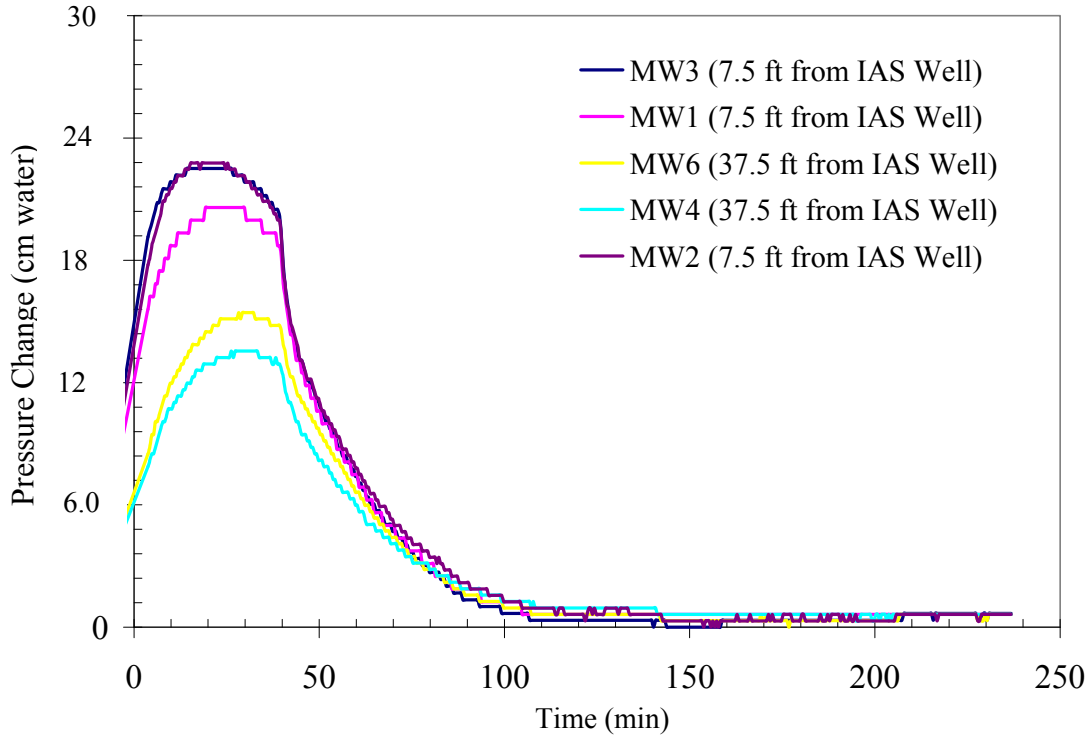

Figure 8. Pressure Transducer Reading from 10 SCFM Air Injection

Table 5. Helium Distribution in the Vadose Zone at 10 SCFM

(ft bgs)	MP1	MP2	MP3	MP4	MP5	MP6	MP7	MP8	MP9	MP10	MP11	MP12
2	0.0	0.8	0.1	3.1	0.0	1.2	0.0	0.0	0.0	0.0	0.0	0.0
4	0.0	1.8	0.4	4.2	0.0	1.5	0.0	0.0	0.1	0.4	0.1	3.0
6	0.0	2.0	0.4	3.9	0.0	2.8	0.0	0.0	0.1	1.3	0.1	4.3
8	2.9	2.7	0.0	4.7	0.0	3.5	0.0	0.0	0.3	2.1	0.1	4.4
	5 ft			10 ft			20 ft			30 ft		

Distance from Sparge Well (ft)

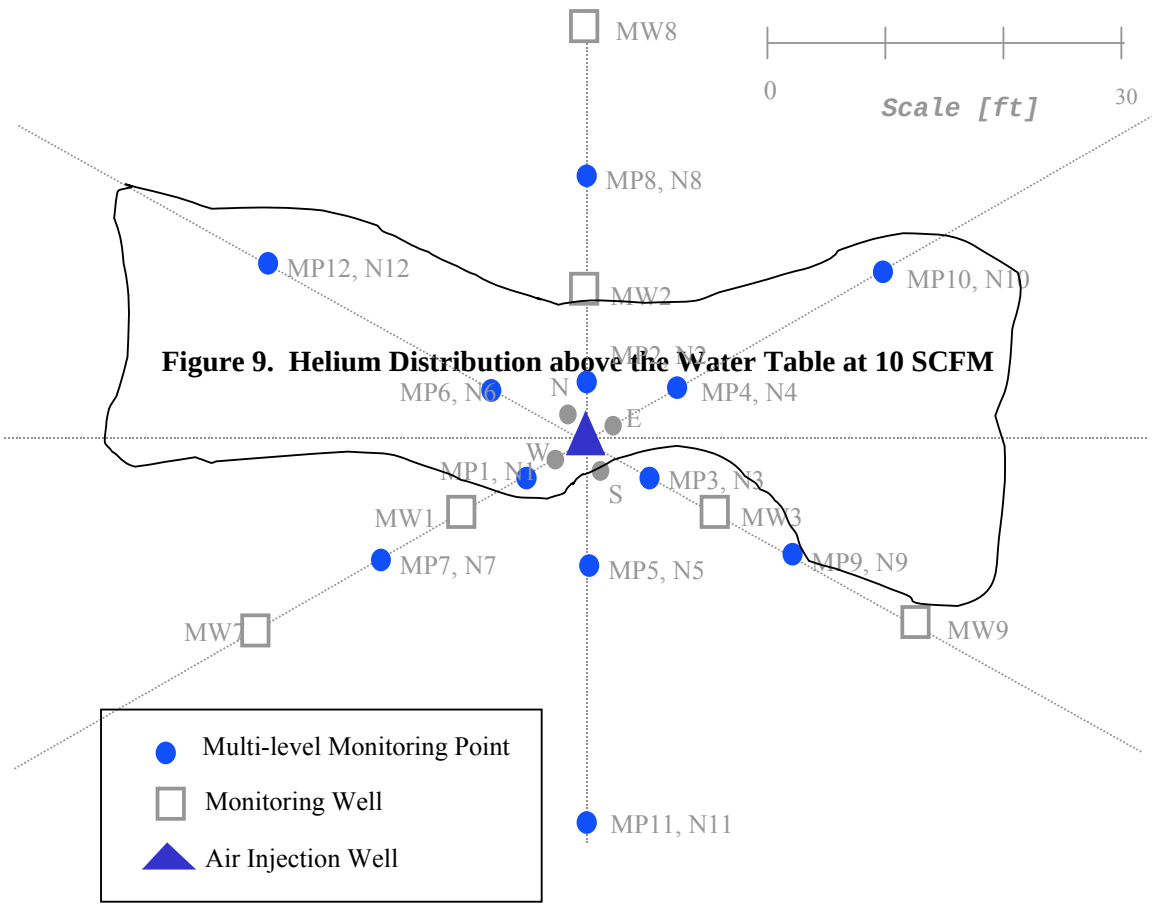

Figure 9. Helium Distribution above the Water Table at 10 SCFM

Figure 10. Mass Removal Rates from Volatilization at the Demonstration Site

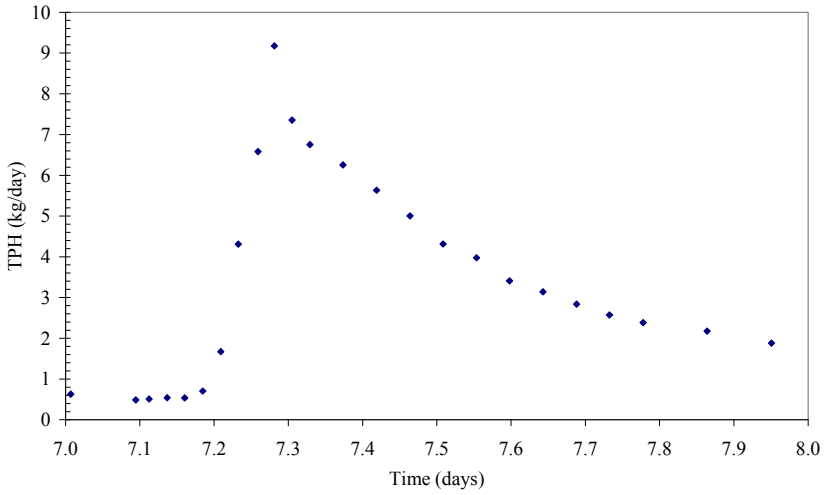

Dissolved Oxygen Monitoring. Air saturation is frequently supposed to be related to measured DO. DO levels are also used as indicators of what type of microbial growth might be occurring in the subsurface. Table 6 shows the results from the 10 SCFM single-well demonstration test.

Sulfur Hexafluoride Distribution Test. The appearance and distribution of nonreactive, fairly insoluble gas tracers injected with the sparge air provides insight into the subsurface air flow paths. Sulfur hexafluoride is a nonreactive volatile tracer with a low solubility that can be measured reliably in the low ppt. Soil gas samples were taken by purging the multilevel line for 100 mL, and then withdrawing 10 mL of soil gas for analysis on a Lagus SF6 detector. These data were collected at an air injection rate of 20 SCFM (Table 7).

SYSTEM DESIGN

Following the directive of the design paradigm, IAS wells were spaced at 15-ft intervals throughout the site. Seventeen wells were installed using the same method followed for the pilot test sparge well (Figures 11 and 12). Four banks of four or five wells were joined on a manifold, and each bank was run 2 hr on, 6 hr off, with each well injecting at 20 SCFM. Initially there was geysering from the monitoring wells on the easternmost portion of the site (Figures 13 and 14). After 24 hours, the geysering was only apparent from Monitoring Well #2.

SYSTEM MONITORING

Groundwater Concentration Reductions

The demonstration site was monitored quarterly (at depths of 10, 11, 12, and 15 ft bgs) for a year before air sparging commenced. In the concentration reduction graphs that follow, the ordinant shows the initial concentrations as determined by the average of these four data points, while the abscissa reports the measured concentration for the time indicated on the legend (Figures 15, 18, and 21). The line bisecting the chart indicates the expected concentration had no treatment taken place. Deviations below this line indicate a decrease in concentration. The dotted lines on either side of this line indicate a 90% concentration difference. Over time, concentrations generally decrease several orders of magnitude. Figures 16, 19, and 22 depict the mean, high, and low concentrations measured within the proposed zone of treatment (within 7.5 ft from the sparge well). Figures 19, 20, and 23 show the same results for monitoring wells outside the proposed treatment zone.

Soil Concentration Reduction Data

Soil samples were collected during installation of the multilevel samplers (prior to the pilot test) and analyzed for BTEX and TPH. Another series of soil samples were taken upon completion of the Standard Case IAS demonstration (15-month-long demonstration). The initial samples showed that the majority of the contamination was distributed from 7 to 12 ft bgs, with the most contaminated interval occurring between 10 and 12 ft bgs (Table 9).

Another series of soil samples was sampled and analyzed upon completion of the demonstration test. These samples show a significant decrease in the soil-associated contamination levels (Table 10), with more than 80% of the samples reading below the detection limit.

Table 6. Dissolved Oxygen Levels Measured at 10 SCFM (Reported as % Air Saturation)

(ft bgs)	MP1	MP2	MP3	MP4	MP5	MP6	MP7	MP8	MP9	MP10	MP11	MP12
10	10	28	69	10	10	ns	10	52	10	57	29	10
11	37	10	10	69	33	77	10	ns	39	36	10	32
12	10	82	62	74	10	ns	10	10	51	31	25	34
13	10	74	10	86	47	48	10	34	70	56	10	48
14	54	80	80	78	59	69	10	10	75	36	25	37
15	37	ns	82	70	79	68	10	10	36	39	10	52
16	29	26	78	76	70	10	26	40	53	10	10	ns
17	31	44	72	ns	64	37	38	40	69	ns	53	30
18	10	32	36	45	71	36	10	10	51	10	10	10
19	34	30	10	ns	10	10	10	28	10	ns	10	37

← 5 ft → ← 10 ft → ← 20 ft → ← 30 ft →

Distance from Sparge Well (ft)

Table 7. SF_6 Distribution in the Vadose Zone for IAS = 20 SCFM at the Demonstration Site (reported as % SF_6 in the injected air). The outlined cells are those that also had a DO concentration of greater than 4 mg-O_2/L-water

(ft bgs)	MP1	MP2	MP3	MP4	MP5	MP6	MP7	MP8	MP9	MP10	MP11	MP12
10	3.8	90.3	0.4	0.9	0.2	30.5	0.0	0.4	72.1	0.3	0.4	2.0
11	5.8	276.7	2.2	1.8	0.2	53.7	0.1	0.7	81.7	0.7	0.3	1.4
12	1.2	57.8	30.9	6.3	0.0	ns	0.1	0.8	3.9	0.5	0.1	20.0
13	1.8	96.9	3.1	0.2	0.5	22.7	0.1	0.2	11.5	3.5	0.4	3.3
14	16.4	43.3	32.3	0.2	0.7	46.5	0.0	0.7	3.0	1.5	0.2	0.2
15	4.5	ns	22.1	4.7	4.0	38.4	0.0	0.7	0.3	0.4	0.1	0.3
16	2.1	35.8	15.9	0.2	0.0	0.3	0.0	2.3	0.3	0.7	0.3	ns
17	60.9	0.1	8.1	0.4	0.1	0.2	0.1	2.0	0.1	0.0	0.1	0.2
18	1.1	0.2	1.0	0.0	1.4	0.3	0.1	0.9	0.1	1.4	0.4	0.1
19	2.5	0.3	0.3	0.0	0.3	0.7	0.1	0.4	0.1	0.2	0.4	2.2

← 5 ft → ← 10 ft → ← 20 ft → ← 30 ft →

Distance from Sparge Well (ft)

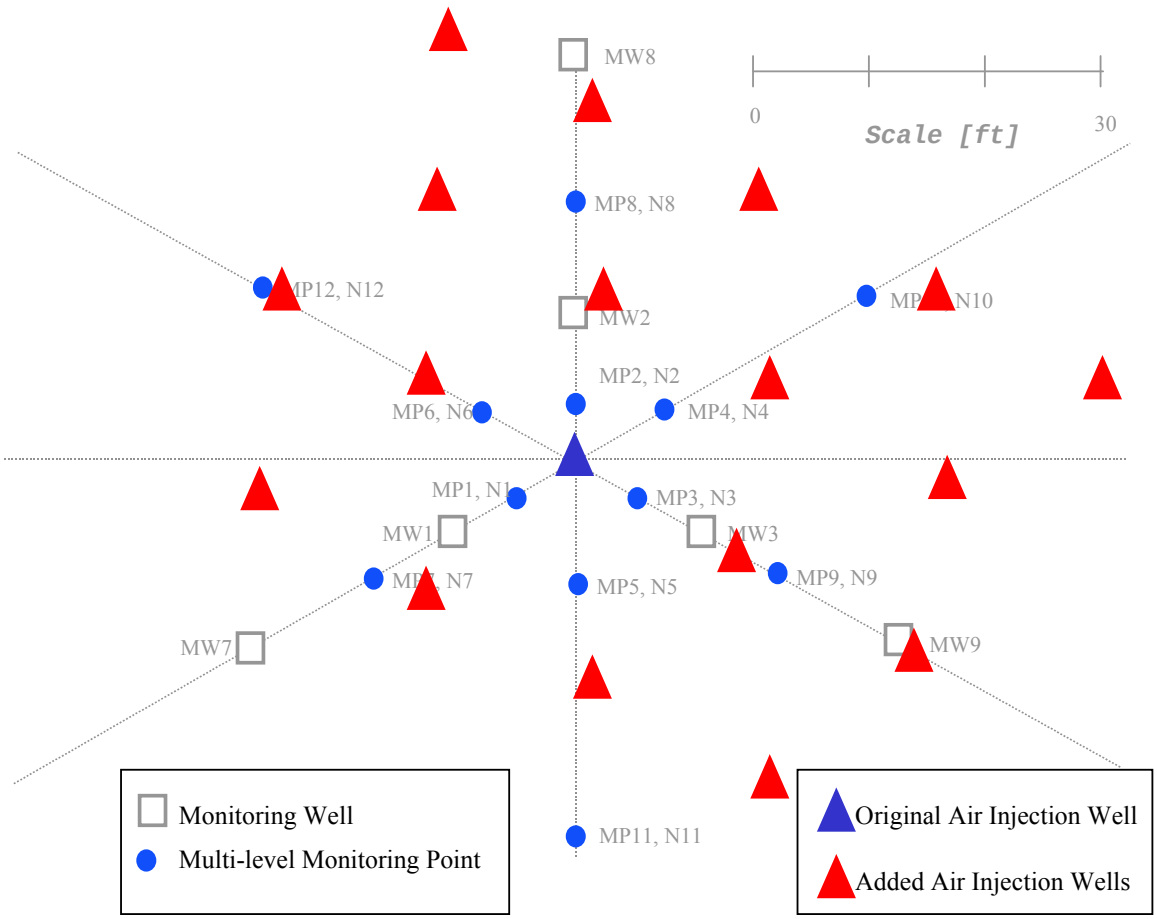

Figure 11. Plan View for Base Case Demonstration

Figure 12. Field View of a Standard Case Application

Figure 13. Evidence of IAS Impact

Figure 14. Geysering Effect Following an Increase in Air Injection Rate

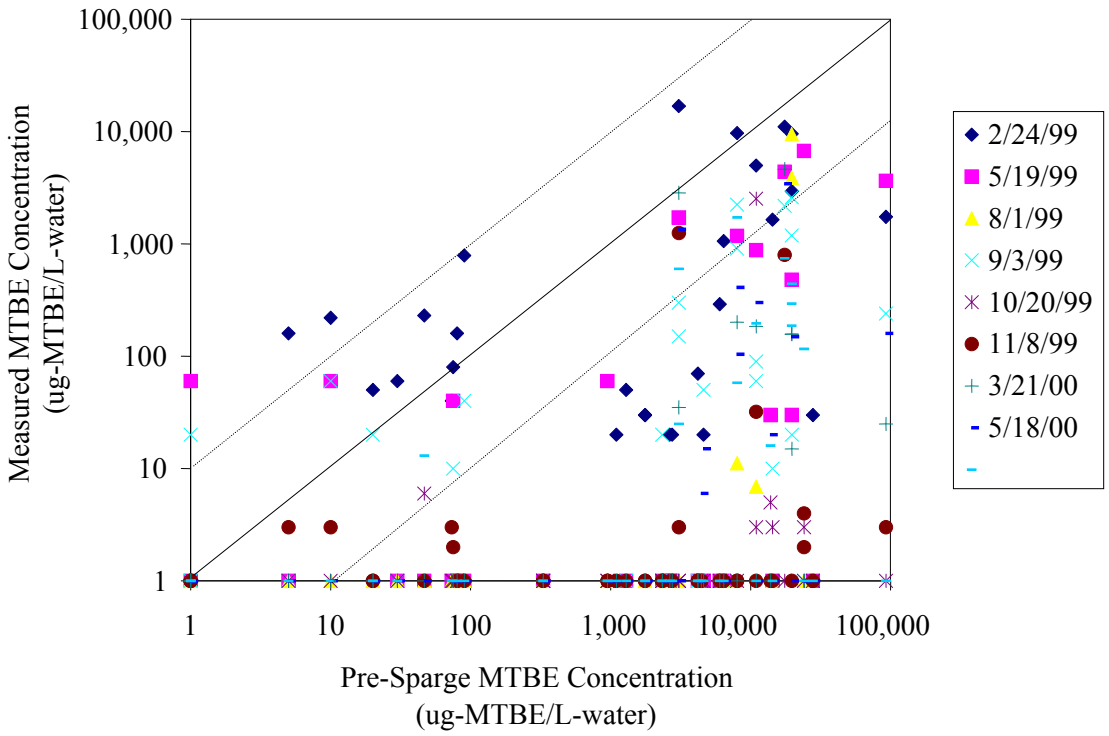

Figure 15. MTBE Concentration Reduction over the Course of IAS Treatment

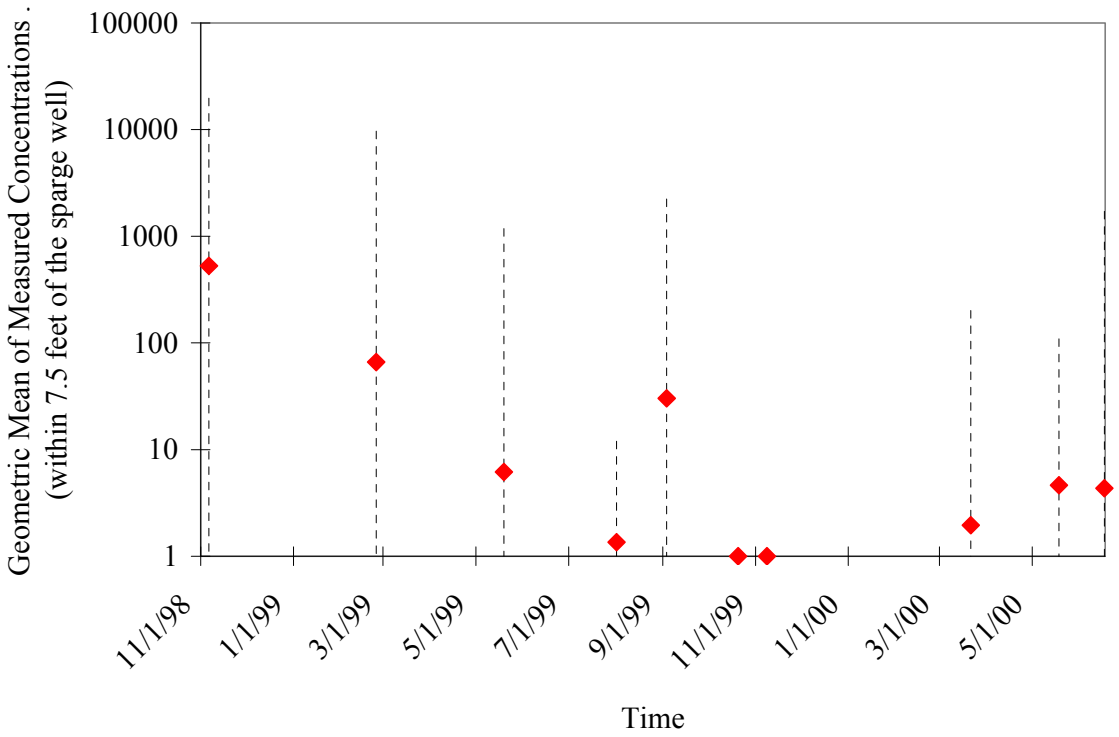

Figure 16. Geometric Mean of MTBE Concentrations within 7.5 ft of the Sparge Well

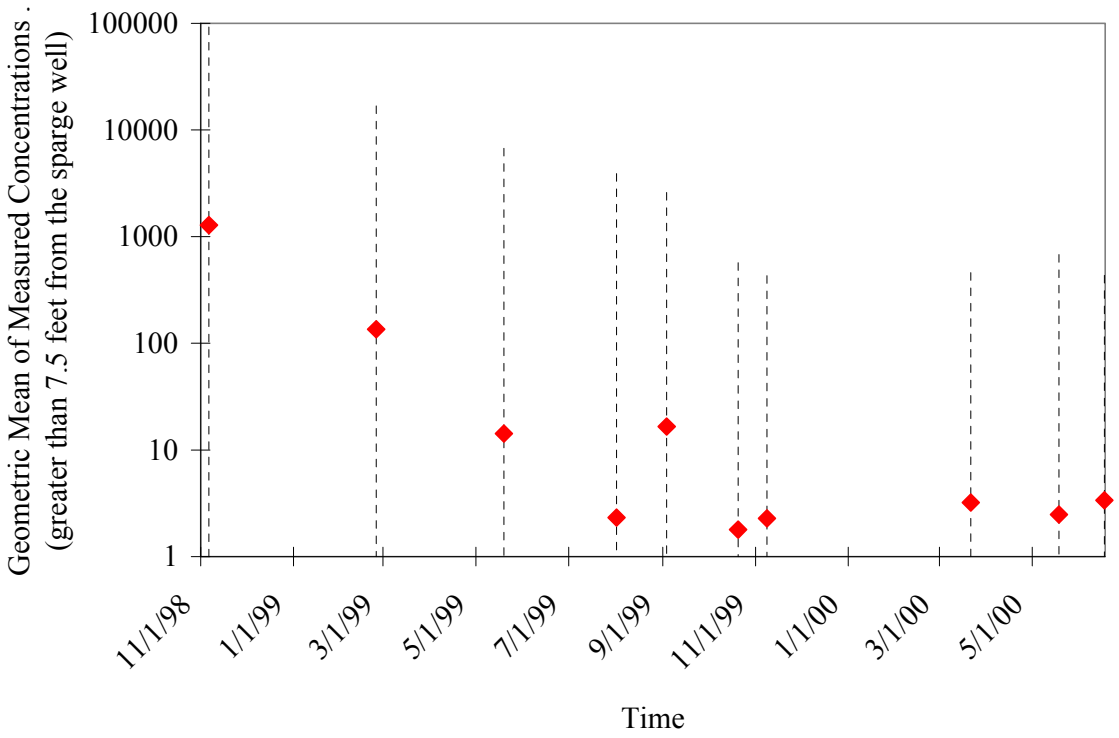

Figure 17. Geometric Mean of MTBE Concentrations at Greater Than 7.5 ft

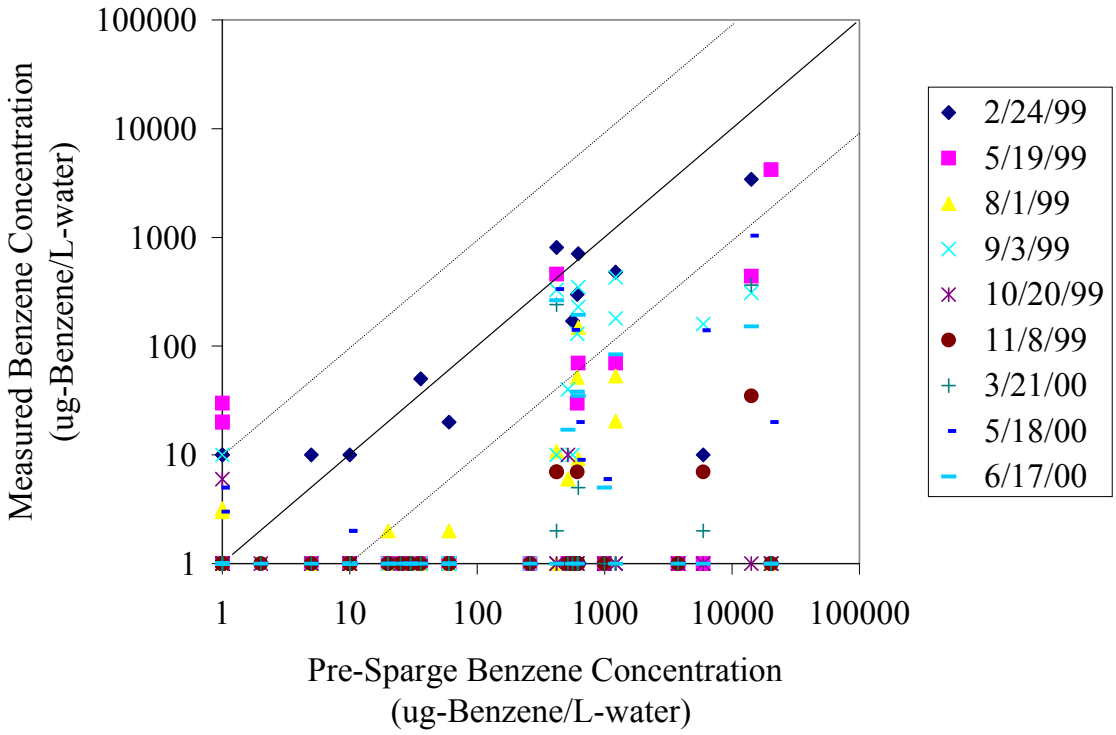

Figure 18. Benzene Concentration Reduction over the Course of IAS Treatment

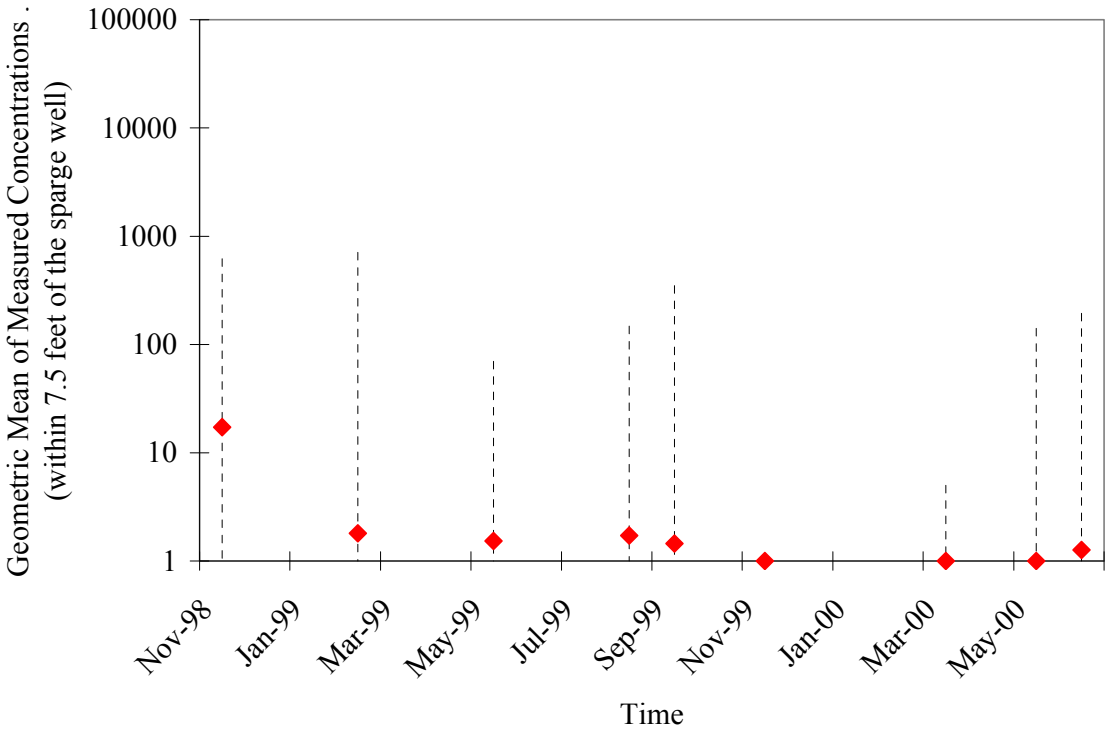

Figure 19. Geometric Mean of Benzene Concentrations within 7.5 ft of the Sparge Well

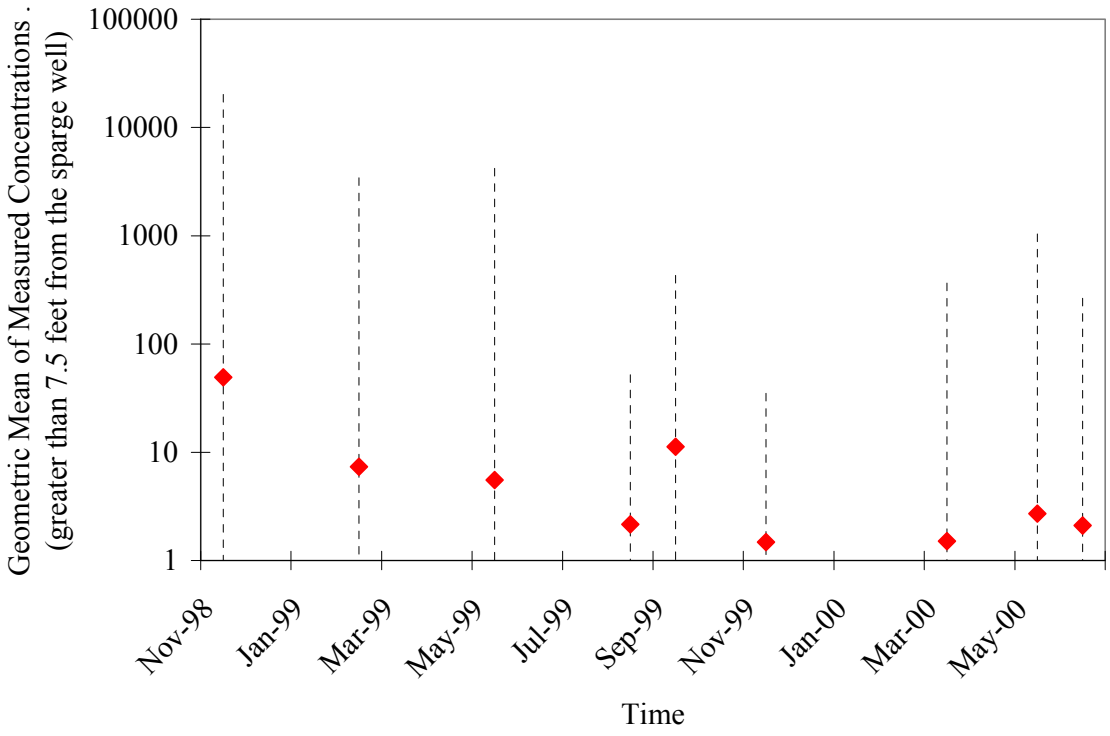

Figure 20. Geometric Mean of Benzene Concentrations outside 7.5 ft of the Sparge Well

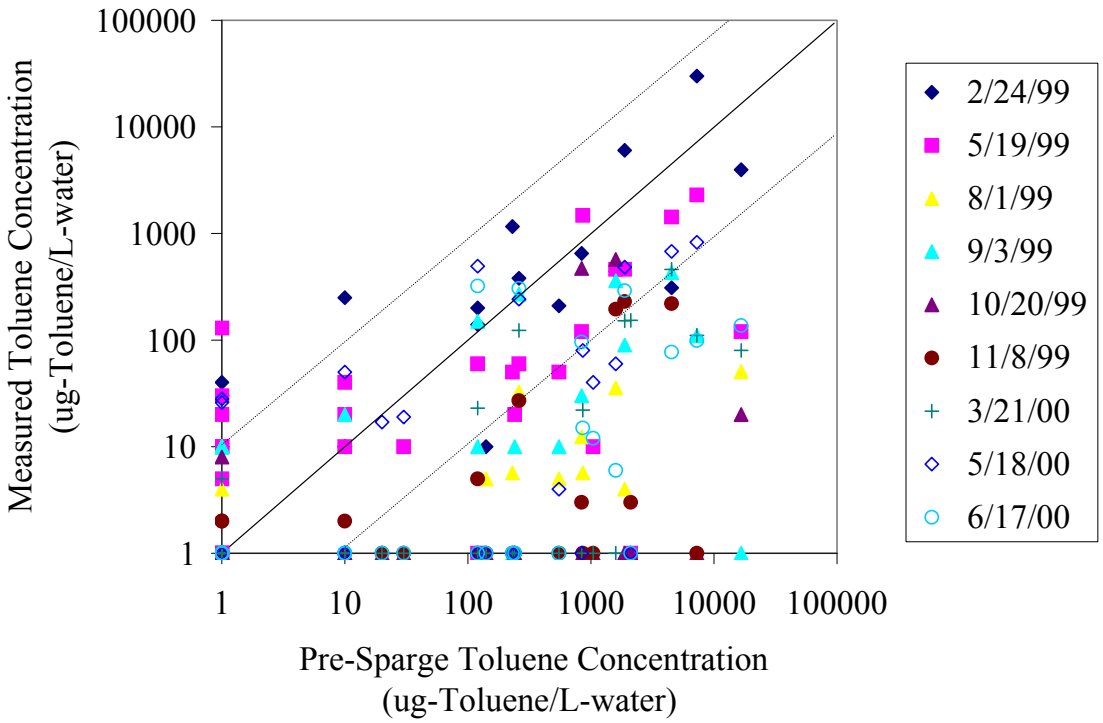

Figure 21. Toluene Concentration Reduction over the Course of IAS Treatment

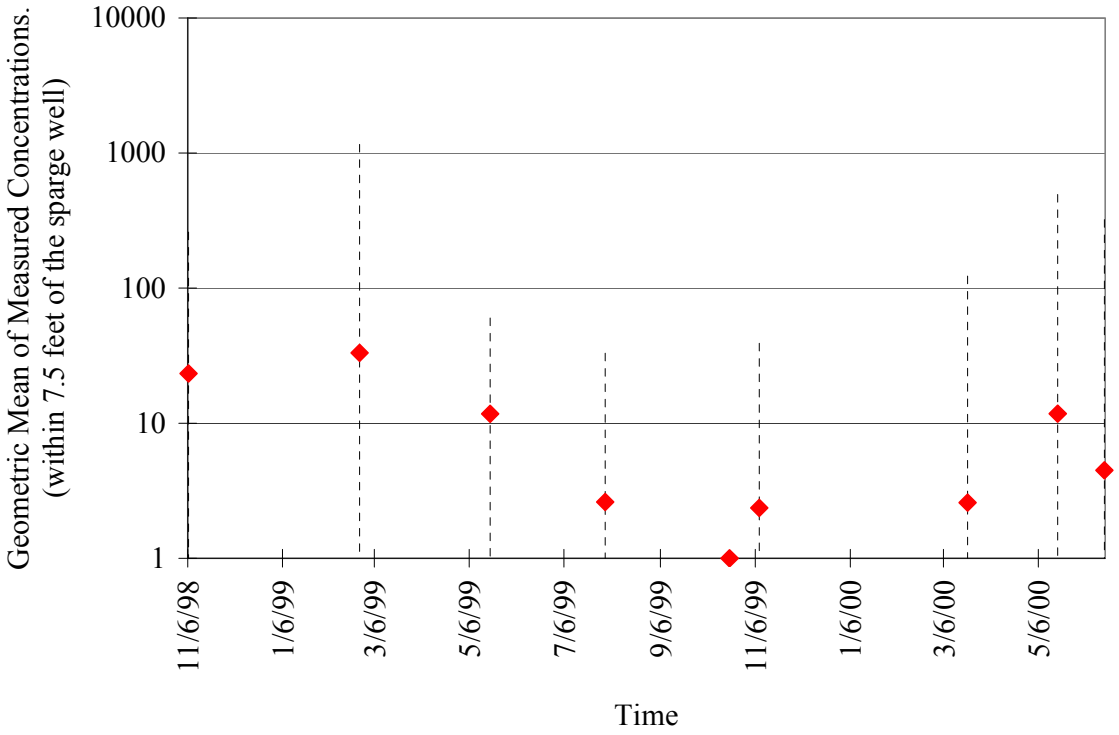

Figure 22. Geometric Mean of Toluene Concentrations within 7.5 ft of the Sparge Well

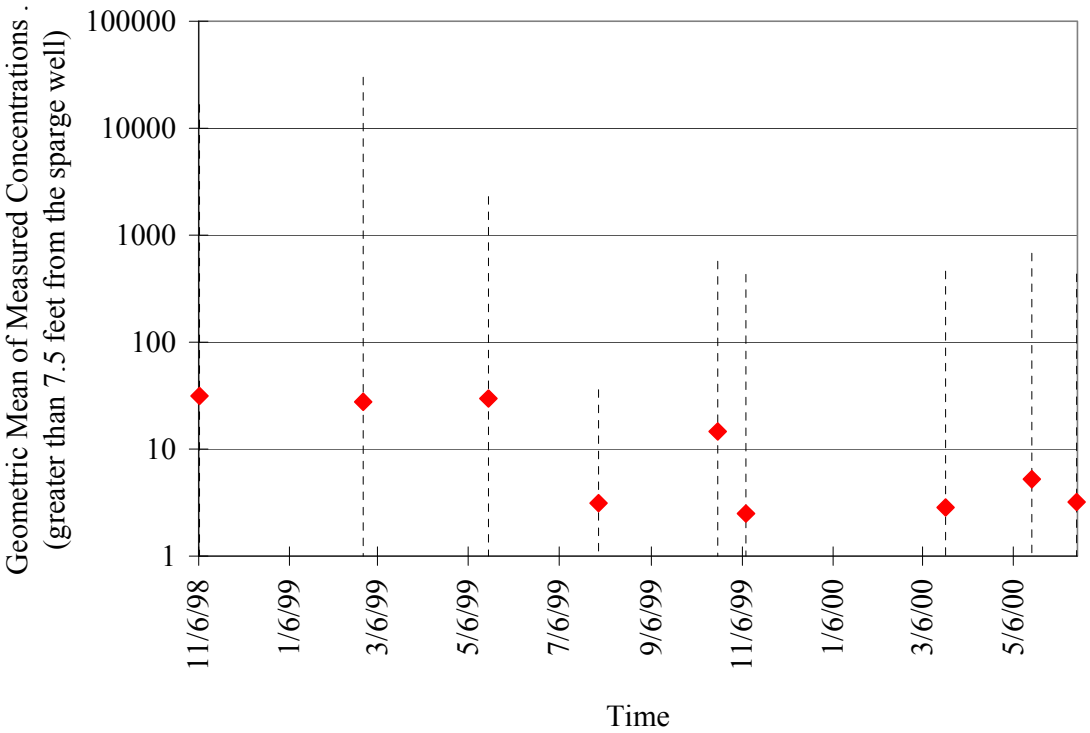

Figure 23. Geometric Mean of Toluene Concentrations outside 7.5 ft of the Sparge Well

Table 9. Soil Analyses from Site #1, Port Hueneme, Averaged by Depth (Pre-Sparge)

Depth (ft bgs)	Benzene (mg/kg)	Toluene (mg/kg)	Ethylbenzene (mg/kg)	Xylenes (mg/kg)	TPH (mg/kg)
4	< 0.0005	0.085	< 0.0005	0.0013	8.8
5	0.017	0.13	0.0022	0.11	5.4
6	< 0.0005	0.035	< 0.0005	< 0.0005	<10
7	1.4	3.5	7.7	45	690
8	.21	0.024	1.4	7.4	82
9	0.059	0.17	0.25	1.1	10
10	3.4	77	38	210	1600
11	13	200	93	480	3800
12	11	87	49	230	1900
13	1.7	10	6	31	200
15	0.023	0.16	0.069	0.37	<10
17	0.0058	0.053	0.017	0.091	<10
19	0.0018	0.028	0.0088	0.054	<10

Table 10. Soil Analyses from Site #1, Port Hueneme, Averaged by Depth (Post-Sparge)

Depth (ft bgs)	Benzene (mg/kg)	Toluene (mg/kg)	Ethylbenzene (mg/kg)	Xylenes (mg/kg)	TPH (mg/kg)
10	< 0.005	< 0.005	< 0.005	0.006	4.5
12	< 0.005	< 0.005	< 0.005	< 0.005	9.5
13	< 0.005	< 0.005	< 0.005	< 0.005	<1

SUMMARY

An in situ air sparging design paradigm has been created to provide guidance on the implementation and evaluation of in situ air sparging systems. This paradigm allows the user flexibility in choosing the pilot-scale testing activities, depending on how conservative a final design they are willing to pursue. The most conservative, or Standard Design Approach design, calls for sparge wells to be placed on 15-ft centers throughout the treatment zone. This paper presented results from an extensive pilot test, and an application of the Standard Design Approach design at a BTEX source zone in Port Hueneme, California.

According to the paradigm, pilot-scale testing activities focus on looking for signs that IAS will not be a successful treatment alternative in addition to the characterization of the air distribution. The pilot test at Port Hueneme showed no signs of infeasibility: air was injected at 5, 10, and 20 SCFM from the single sparge well with no difficulty. The soil cores taken from the site show a medium-to-coarse sand, with few variations in the treatment zone. Air-stimulated pressure transducer responses show no evidence of undue stratification or well-casement leaking (air breakthrough occurred between 30 min and 50 min for the air injection tests). Further air distribution tests, including the helium and sulfur hexafluoride tracer tests, showed that the injected air tended to follow a North-South pattern rather than a circle.

The distribution and characteristics of contaminants are also significant factors affecting the efficiency of IAS treatment. At the Port Hueneme test site the contaminant was primarily automotive fuel, which should to be treatable by IAS. The majority of contamination at this site was found to be between 10-12

ft bgs. There were no signs of layering that would impede the flow of air to this zone. Subsurface air distributions, however, are so sensitive to soil variations that air distributions are unable to be predicted with any degree of accuracy. The degree to which an air distribution is characterized should be balanced by the system design. In this case, however, the characterization of air distribution was much more detailed than would be expected of a Standard Design Approach design implementation.

REFERENCES

Bass, D.H., and R.A. Brown. 1995. Performance of Air Sparging Systems - A Review of Case Studies. Proceedings—Petroleum Hydrocarbons and Organic Chemicals in Ground Water: Prevention, Detection and Restoration. Ground Water Publishing Company. Dublin, O hio. 621-636.

Johnson, P.C., A. Leeson, R.L. Johnson, C. Vogel, R.E. Hinchee, M. Marley, T. Peargin, C.L. Bruce, and I.L. Amerson. 2000. A Practical Approach for the Selection, Pilot Testing, Design, and Monitoring of In Situ Air Sparging/Biosparging Systems. Submitted to *Bioremediation Journal*.

Leeson, A., R. Gillespie, P.C. Johnson, R.L. Johnson, R.E. Hinchee. 1996. Annual Report on Remediation of a Contaminated Aquifer. Submitted to AFRL/MLQE, Tyndall AFB, Florida.

Ji, W., A. Dahmani, D. Ahlfeld, J.D. Lin, and E. Hill. 1993. Laboratory Study of Air Sparging: Air Flow Visualization. *Groundwater Monitoring and Remediation*. Fall: 115-126.

APPENDIX E

Diagnosis of In Situ Air Sparging Performance Using Groundwater Pressure Changes During Startup and Shutdown

Richard L. Johnson[1], Paul C. Johnson[2], Tim L. Johnson[1], Neil R. Thomson[3] and Andrea Leeson[4]

[1]Oregon Graduate Institute, Center for Groundwater Research, Department of Environmental Science and Engineering, Portland, Oregon; [2]Arizona State University, Department of Civil Engineering, Tempe, Arizona; [3]University of Waterloo, Department of Civil Engineering, Waterloo, Ontario Canada; [4]Battelle Memorial Institute, Columbus, Ohio

BACKGROUND

The air distribution achieved during in situ air sparging (IAS) is governed by complicated multiphase flow processes that are very difficult to predict, even with extensive site characterization. As a consequence, a number of approaches for measuring air distribution during initial system operation have been proposed, the two most common being the use of dissolved oxygen measurements and transient pressure transducer responses measured in groundwater monitoring wells. It is the latter that is the focus of this manuscript.

In the last few years, it has become increasingly common to use pressure transducers (rather than water level tapes) to measure groundwater pressure changes during IAS operation. Water level pressure transducers are becoming a common piece of field equipment for many consulting firms, they are easy to employ in the field and allow nearly continuous data collection. As a result, pressure data are more frequently being used to provide insight to air distributions achieved during IAS (Lundegard and LaBrecque, 1998). As discussed below, transient groundwater pressure changes during start-up, and shutdown can be used to assess a) the time to reach near-steady air distributions, b) the cumulative volume of air channels, and c) qualitative features of the air distribution (e.g., significance of trapped air layers). Figure 1 presents a schematic diagram illustrating the use of pressure transducers to measure transient groundwater pressure changes during IAS startup.

Unfortunately, transient groundwater pressure data can also be misinterpreted. For example, it is common for practitioners to equate the lateral distance at which pressure changes are measured with the extent of the IAS treatment zone. This leads to over-estimation of the IAS treatment zone because: a) although pressure attenuates with distance, it can theoretically propagate an infinite distance, while the air distribution is finite, and b) water level pressure changes tend to propagate in a more radially symmetric manner than the air actually does. In addition, water level rises (and drops) in piezometers have often incorrectly been equated to formation water level changes, rather than simply being measurements of groundwater pressure change.

This manuscript focuses on the use of transient groundwater pressure measurements as a diagnostic tool for characterization of air distributions during IAS operation. To help develop insight into the use and limitations of this tool, a simplistic conceptual model is first presented followed by examples of measurements collected during IAS start-up and shutdown at four field sites.

Current Conceptual Model of IAS Startup in a Near-Homogeneous Aquifer

During IAS start-up and shutdown, there are a number of operational parameters that can be controlled, including the injection well pressure and air flowrate. In the following discussion, it is assumed that the

injection well pressure is being set at some predetermined value that is sufficient to achieve air flow into the aquifer.

A simple conceptual model for IAS start-up in homogeneous media is shown in Figure 2. As the air injection pressure is increased in the air injection well, groundwater is displaced from the well into the formation. Once the air injection pressure exceeds the hydrostatic head of groundwater above the top of the well screen, air flows out into the formation and continues to displace groundwater. Because groundwater is flowing away from the air injection well, a pressure gradient directed away from the air injection point is established; therefore increases in groundwater pressure are observed, with the pressure changes attenuating with distance away from the air injection well. The extent and rate of the groundwater pressure rise reflects the permeability of the aquifer and the air injection pressure (and air flowrate).

After a very short period of more-or-less outward flow, buoyancy forces will cause the air to migrate upward (as well as possibly continuing to move outward). The volume of air found below the water table will continue to increase until the air reaches the water table and is "vented" to the vadose zone. At this point, the groundwater pressure passes through a maximum value and begins to drop back towards the pre-sparge hydrostatic level. In some cases, there is probably also a "deflating" of the air zone below the water table, as the injected air now only follows those paths that are continuous between the injection well and the vadose zone. After some period of time (probably minutes in a homogeneous isotropic aquifer), a balance is reached between the volume of air being injected and the flow to the vadose zone. At a macroscopic scale, this would correspond to steady-state air flow.

Conceptual Model of IAS Start-Up in a Stratified Aquifer

In stratified media, the upward movement of air to the water table is likely to be impeded or stopped by the presence of lower permeable layers (Figure 3). In these cases, there can be a significant accumulation of air below finer-grained strata, and this accumulation can be transient or permanent. As accumulation of air occurs, the groundwater pressure continues to rise. The extent to which this pressure rise is measured depends upon the locations of the measurement points relative to this injection well and the strata. At some point, the volume of air flowing through or going around those confining strata will become equal to the injection rate, and the macroscopic air distribution will reach steady state. This decline to pre-start-up conditions generally occurs at a much slower rate than in near-homogeneous settings.

Conceptual Model of IAS Behavior During Shutdown

Whenever air injection is stopped, water will spontaneously begin to displace the air out of the groundwater zone (Figure 4). As groundwater is now flowing towards the air injection well and there must be a groundwater pressure gradient towards the well, the groundwater pressure decreases and remains below the initial hydrostatic pressure while the air volume is decreasing. As with system start-up, the magnitude and rate of the hydrostatic pressure change in the formation is related to permeability (and the initial volume of displaced groundwater). For a near-homogeneous aquifer, this process is usually completed in minutes to a few hours. For a stratified aquifer, the process can go on for several hours or even days. At the conclusion of the process, there will be some residual air remaining in the formation as the result of entrapment by various mechanisms.

TRANSIENT GROUNDWATER PRESSURE MEASUREMENTS AS A DIAGNOSTIC TOOL FOR IAS AIR DISTRIBUTIONS

Because IAS involves complex, two-phase processes, and because there are a wide range of subsurface conditions found at contaminated sites, it is difficult to predict the subsurface air distribution, and the best approach is to use a suite of diagnostic tools. The transient pressure diagnostic tool described here

complements other field measurement techniques (e.g., helium tracer tests, dissolved oxygen measurements, or geophysical measurements) and can be used both as "red flag" indicators of IAS infeasibility during pilot tests and to assess changes in system operation.

The complexity of the processes governing air distributions and their sensitivity to subtle changes in subsurface conditions makes quantitative analysis of transient pressure transducer response data difficult at best. However, the experience at field sites discussed below leads us to conclude that this data can still be valuable, even if detailed quantitative analysis is not possible at this time. For example:

- The length of time over which the groundwater pressure remains above the pre-sparge hydrostatic value after IAS start-up provides valuable insight to qualitative features of the air distribution. If the groundwater pressure remains above the pre-sparge hydrostatic value for many hours or days, this indicates that a significant volume of air is accumulating beneath lower-permeability strata and significant lateral air migration may be occurring. Conversely, a very short transient pressure response (e.g., minutes) may indicate that air flow is occurring within a fairly limited distance of the injection well, or even short-circuiting up the injection well annulus. As a result, in either case, air may not be reaching the desired treatment zone and/or lateral migration may carry contaminants to off-site receptors.
- The duration of elevated groundwater pressure can also help to establish the time frame for pulsing of air in the IAS well. As part of the Design Paradigm described by P.C. Johnson et al. (2001), pulsed air flow is recommended for IAS operation. Pulsed air flow has been demonstrated to improve contaminant mass removal from groundwater via volatilization (P.C. Johnson et al., 2001). The pattern of pressure response immediately after IAS start-up provides a good indication of the length of time required for a pulse of air to propagate through the treatment area, thereby providing the practitioner a starting point for determining a pulse cycle.
- The magnitude of the groundwater pressure pulse can also be used to assess subsurface conditions. In general, small, short-duration increases in pressure during start-up indicate that the permeability of the aquifer is high, while higher-pressure values generally suggest lower permeability. The magnitude and duration of pressure pulses can be used together to assess air distribution. For example, if both the magnitude and duration of pressure increases are small, this can indicate a limited radius of influence of the air around the well. Conversely, pressures approaching the overburden pressure that are sustained for hours are a clear indication that the air is stratigraphically trapped. In this case, the potential exists for extensive lateral migration of the air or even pneumatic fracturing. Most sites fall somewhere between these two examples, and the practitioner must evaluate the pressure data together with data from other air distribution indictors to determine whether IAS is feasible.

RESULTS AND DISCUSSION

IAS start-up and shutdown transient groundwater pressure data for four sites is examined here. The sites span a range of operating conditions (e.g., one to four IAS wells and injection rates from 5 to 20 standard cubic feet per minute [SCFM]). Most sites are located in relatively permeable media that ranges from homogeneous sands and gravels to a site with extensive clay strata. The sites (in approximate order of increasing stratification) include 1) Eielson Air Force Base (AFB), Alaska; 2) Port Hueneme, California; 3) Canadian Forces Base (CFB) Borden, Ontario, Canada; and 4) Hill AFB, Utah.

Example 1: Eielson AFB, Alaska

The lithology of the Eielson AFB site consists of a layer of sandy loam overlying a 200- to 300-ft thick sequence of sand and gravel. In the vicinity of the IAS well, the thickness of the sandy loam is approximately 8 ft, which is also the depth to groundwater. IAS wells were installed at two depths at the site. The top of the well screen for the shallow well was approximately 4 ft below the water table, and for

the deep well it was approximately 10 ft below the water table. Monitoring wells were installed at distances of 10, 20, and 30 ft from the well. Each was screened from the water table to a depth of 10 ft. A schematic diagram of the Eielson AFB test plot is shown in Figure 9. Air was injected at 5 SCFM in the shallow well and 10 SCFM in the deeper well.

The groundwater pressure response to the injection of air into the shallow IAS well at a rate of 5 scfm is shown in Figure 10A. The pressure changes are very small (e.g., <1 cm water), indicating a very high permeability at that depth. Injection at 10 SCFM into the deeper well (Figure 10B) shows an order of magnitude larger pressure increase than at the shallow depth; however, the absolute value is still relatively small (e.g., <10 cm of water), indicating that the aquifer is relatively permeable. Groundwater pressure curves for IAS shutdown at the two flowrates (Figures 10C and 10D) are similar in magnitude to the start-up values. Also, the pressure data return to near-hydrostatic values within about an hour of start-up and shutdown. This suggests that there was minimal stratification in the aquifer and that lateral migration of air will probably not be a problem at this site. However, pressure data alone cannot assess the lateral extent of the air distribution at this or most other sites. As a consequence, the pressure data are best used in conjunction with other diagnostic data.

Example 2: Port Hueneme, California

The pressure data reported here for Port Hueneme was collected at a site that is similar to and located approximately 100 m from the site described in Bruce (2001). The unconfined aquifer at the site consists of mildly stratified sands with hydraulic conductivities ranging from approximately 0.002 to 0.02 cm/s (Figure 7). The sparge well for these tests was screened from 4.8 to 5.1 m below ground surface (bgs). The water table at the site ranges from about 2.4 to 3 m bgs. Groundwater pressure data were collected from four 2-inch water table monitoring wells with screen intervals at approximately 1.5 to 6 m bgs and located at distances of 4.6 to 9.1 m (15 and 30 ft) from the sparge well (wells MW1, MW2, MW4, and MW5 in Figure 8). The air injection rate was approximately 0.27 m^3/min (10 scfm).

Pressure measurements following system startup and shutdown for two of the wells are shown in Figure 7. As can be seen, pressure fluctuations were on the order of tens of centimeters of water, and the durations of the changes were on the order of 100 min, suggesting that steady flow had been established by that time. As a result, the IAS system at the site was operated in a pulsed mode with a cycle of 3 h on and 3 h off. The pressure response in the four groundwater monitoring wells during pulsed operation is shown in Figure 8[1]. As shown, the pulse cycle of 3 h on, 3 h off, allows for pressure measurements to return to near hydrostatic measurements before initiation of the next pulse cycle.

Example 3: CFB Borden, Ontario

As described in Tomlinson et al. (2002), a range of IAS diagnostic tests was conducted at the CFB Borden site. The site consists of medium sand (average hydraulic conductivity of approximately 0.005 cm/s) and is composed of many small-scale beds or lenses with dimensions of a few centimeters in thickness and a few meters in areal extent. Unlike the other sites examined here, the vadose zone at the site had been removed so that the water table was just above ground surface. Air was injected into one of three IAS wells (Figure 11) and the pressure was monitored with pressure transducers in five piezometers.

---

[1] It is useful here to comment on pressure responses in water table monitoring wells and piezometers. Piezometers reflect actual pressure changes in the groundwater at the depth of the well screen. Pressure responses in water table monitoring wells are more complicated in that water can move between the capillary zone and the well; thus pressure changes do not necessarily reflect groundwater pressure changes and can reflect actual transient changes in water table level in the immediate vicinity of the well.

The pressure data in Figure 12 were collected when air was injected into IAS2 at a rate of 5 SCFM (0.135 m^3/min). As can be seen in the figure, the pressure quickly increased by up to 40 cm of water. The pressure remained significantly elevated for 6 hours until airflow was stopped. This indicated that during that period the volume of air was continuing to increase in the subsurface. Because the water table was above ground surface, the arrival of air at the water table could be observed as bubbles in the standing water. No significant air flow at the surface occurred for the first 30 min after sparging was initiated.

It is instructive to examine in detail the pressure changes during the first 30 min of sparging. Figure 13 shows that the pressure at all of the monitoring points began to rise in the first minute or two. For the point closest to the sparge well (P3-1), the pressure reached a maximum and began to fall after about 7 min (even though no air had reached the water table, which is in contrast to the conceptual model discussed above). The monitoring points that were 10 ft (3 m) away (P4-1 and P4-2) also reached a maximum in that same interval but decreased at a slower rate. This was particularly true for the deeper point (P4-2), which had decreased only about 20% from the maximum value after 30 min. The two points at 20 ft (P5-1 and P5-2) did not go through a maximum during the first 30 min, but continued to rise over the whole interval. These data point out the complexities associated with interpreting pressure data in stratified media, particularly in the absence of other corroborating information. Nevertheless, the period over which the pressure is elevated does clearly indicate that a substantial volume of air was accumulating below the water table.

Following cessation of air injection, the groundwater pressure dropped and remained below the hydrostatic value for approximately 4 h. During that period, air continued to flow out of the saturated zone (as evidenced by bubble flow at the surface). Prior to cessation, the air flow at the surface appeared quite steady, and when injection stopped, the flow to the water table continued with little if any change. The air flowrate at the water table was estimated as a function of time following cessation and is shown in Figure 14. Based on that data, the volume of trapped air was estimated to be approximately 28 m^3, which corresponds to about 200 min of injection at 5 SCFM. At this site, the entrapped air may have had a significant impact on hydraulic conductivity at the local scale (Tomlinson et al., 2002)

Example 4: Hill AFB, Utah

The water-bearing zone at Operable Unit (OU)-6, Hill AFB is composed primarily of sands and silty sands. It is overlain by silt with beds of sand and clay. The interface between these two is near the current water table at approximately 105 ft bgs (Figure 15). A line of four sparge wells with co-located soil vapor extraction (SVE) wells was placed across a portion of a dissolved trichloroethene (TCE) plume that was exiting the base boundary (Radian, 1995). In addition, nests of monitoring wells were distributed around the treatment zone. The locations of the wells are shown in Figure 16. The total injection rate was approximately 50 SCFM for the four wells.

Groundwater pressure increases in excess of 300 cm were observed at the wells closest to the injection well. Pressure increases of nearly 200 cm were observed even at a distance of 130 ft (Figure 17). The pressures remained elevated for nearly two days, until the sparging system was turned off. This is indicative of an extensive layer that is effective at preventing upward migration of the air and is consistent with the helium tracer data for the site (R.L. Johnson et al., 2001). Vertical permeability was measured using intact soil cores from the site in a constant-head permeameter. The data are shown in Figure 18 and indicate that there is a very high conductivity layer at about 125 ft bgs and that the conductivity decreases by several orders of magnitude in the upper portions of the saturated zone. If the lower-permeability layer is extensive, then this permeability contrast would be sufficient to cause the stratigraphic entrapment of the air inferred from the pressure data.

At this site, the bulk of the contaminated groundwater lay below the confining layer so the sparge air was able to be reasonably effective at removing contaminants. However, the system was not capable of

lowering concentrations to the drinking water limit (5 μg/L for TCE in this case). Furthermore, there is some concern that the large volume of air trapped below the water table may have had a significant impact on the water permeability of the aquifer (as was seen, for example, at the CFB Borden site) and could have caused part of the plume to be diverted around the treatment zone.

CONCLUSIONS

For many sites, groundwater pressure responses during start-up and shutdown provide important insight into air movement below the water table. If lag times of hours to days are required for groundwater pressures to return to within a few cm of water of pre-sparge hydrostatic values, this indicates that there is significant stratigraphic trapping of air. Stratigraphic trapping can be either good or bad, depending where the confining layer is located relative to the zone to be treated and to risk pathways. For many sites, some degree of stratification is necessary to increase the width of the treatment zone to a scale that makes sparging practical. However, too much stratification can cause excessive lateral migration or it may prevent the sparge air from reaching the treatment zone.

In general terms, the magnitude of pressure responses during start-up and shutdown can be viewed as proportional to air flowrate and inversely proportional to aquifer permeability. However, there is currently no overall modeling framework that allows the magnitude of the pressure responses to be directly related to unique characteristics of the aquifer and/or air distribution.

Because pressure measurements are easy and rapid to collect, they are a useful component of pilot tests, where they can act as a "red flag" for IAS infeasibility. They are also useful for evaluating system operating parameters (e.g., pulse cycle times, air flowrates) because the tests can be repeated quickly following changes in system parameters. In either case, the pressure data are best used in conjunction with other diagnostic tools, which collectively can present an overall picture of IAS performance.

REFERENCES

Bruce, C.L. 2001. *Performance Expectations for In Situ Air Sparging Systems*. Ph.D. Dissertation. Arizona State University.

Johnson, P.C., R. L. Johnson, C. Neaville, E. E. Hansen, S. M. Stearns, and I. J. Dortch. 1997. An Assessment of Conventional In Situ Air Sparging Pilot Tests. *Ground Water. 35*(5):765-774.

Johnson, P.C., A. Leeson, R.L. Johnson, C.M. Vogel, R.E. Hinchee, M. Marley, T. Peargin, C.L. Bruce, I.L. Amerson, C.T. Coonfare, and R.D. Gillespie. 2001. A Practical Approach for the Selection, Pilot Testing, Design, and Monitoring of In Situ Air Sparging/Biosparging Systems. *Bioremediation Journal*, *5*(4):267-282.

Johnson, R. L., R.R. Dupont, and D.A. Graves. 1996. *Assessing UST Corrective Action Technologies—Diagnostic Evaluation of In Situ SVE-Based System Performance*. EPA/600/R-96/041, 164p.

Johnson, R.L., P.C. Johnson, T.L. Johnson, and A. Leeson. 2001. Helium Tracer Tests for Assessing Contaminant Vapor Recovery and Air Distribution during In Situ Air Sparging. *Bioremediation Journal*, *5*(4):321-336.

Lundegard, P.D., and D.J. LaBreque. 1998. Geophysical and Hydrologic Monitoring of Air Sparging Flow Behavior: Comparison of Two Extreme Sites. *Remediation. Summer*:59 - 71.

Radian International. 1995. *Interim Report on the IAS/SVE System at Hill AFB OU6*, 25 September 1995.

Tomlinson, D.W., N.R. Thomson, R.L. Johnson, and J.D. Redman. 2002. *In Situ* Air Distribution at CFB Borden during Air Sparging" Submitted to J. Contaminant Hydrology.

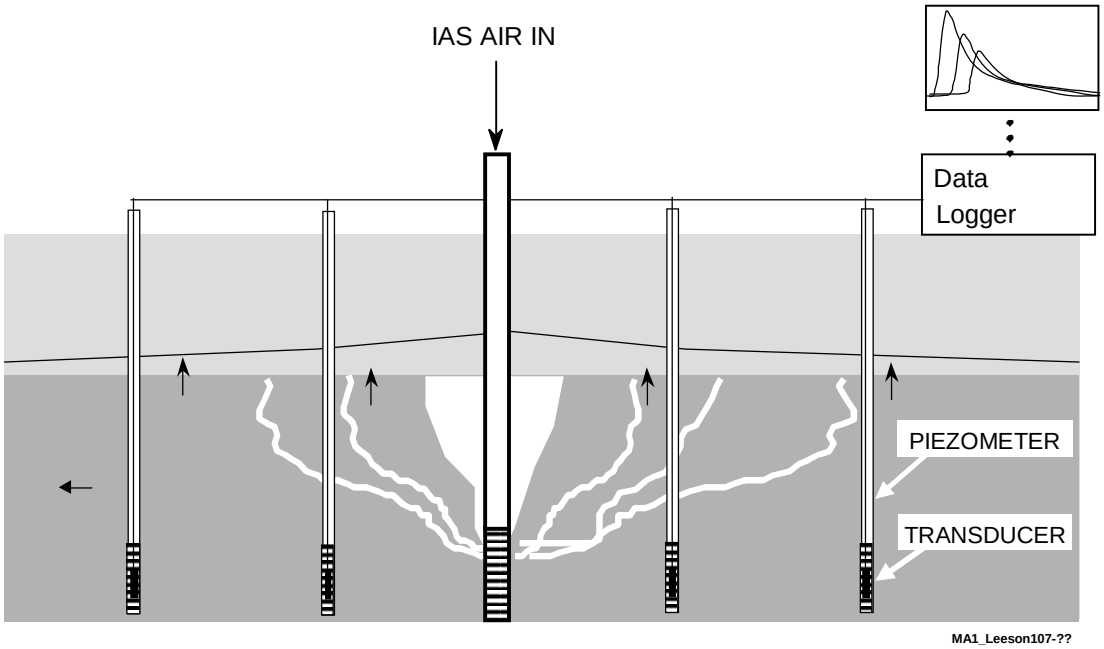

Figure 1. Use of Pressure Transducers to Measure Water Pressure During IAS Startup

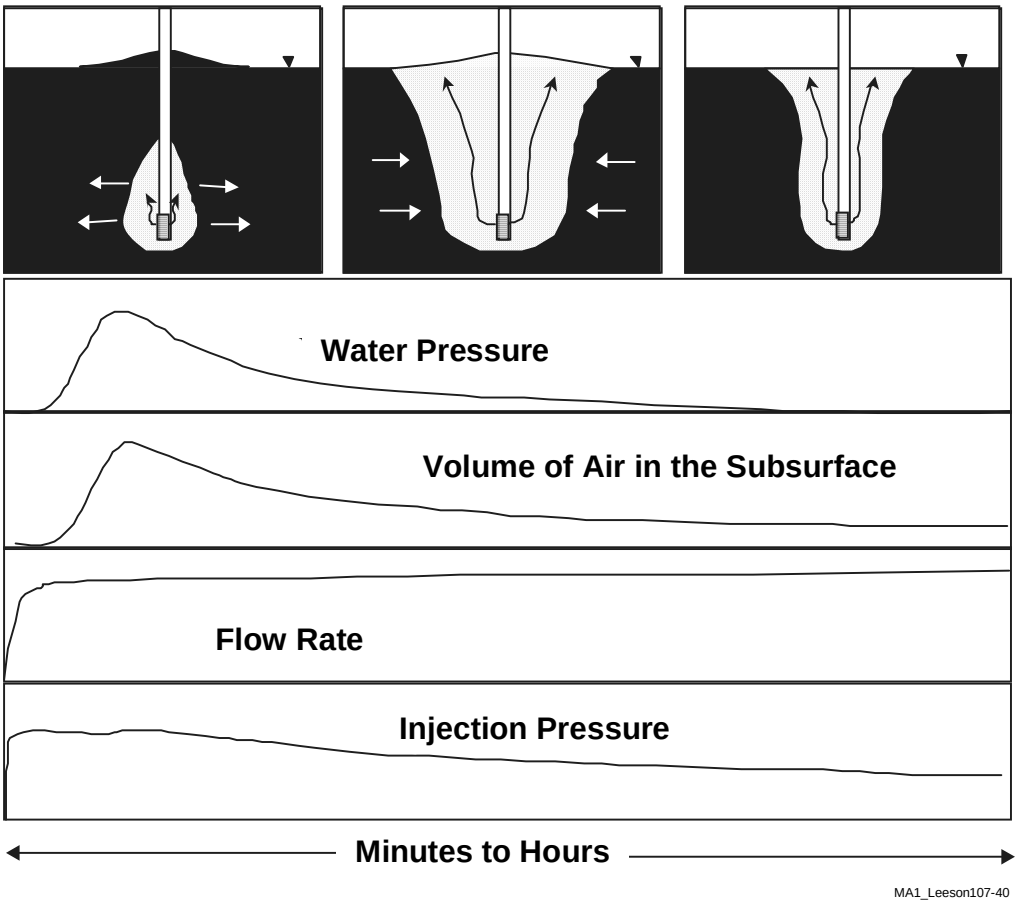

Figure 2. Simple Conceptual Model for IAS Startup in Homogeneous Media

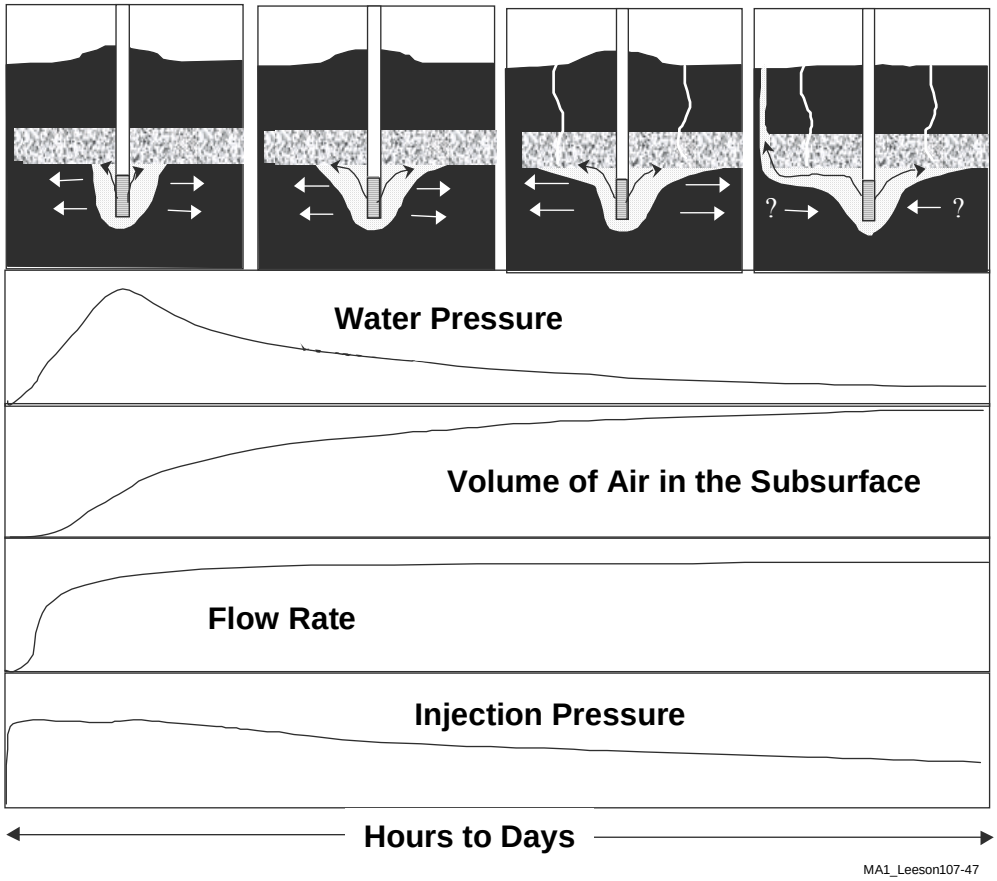

Figure 3. Simple Conceptual Model for IAS Startup in a Stratified Aquifer

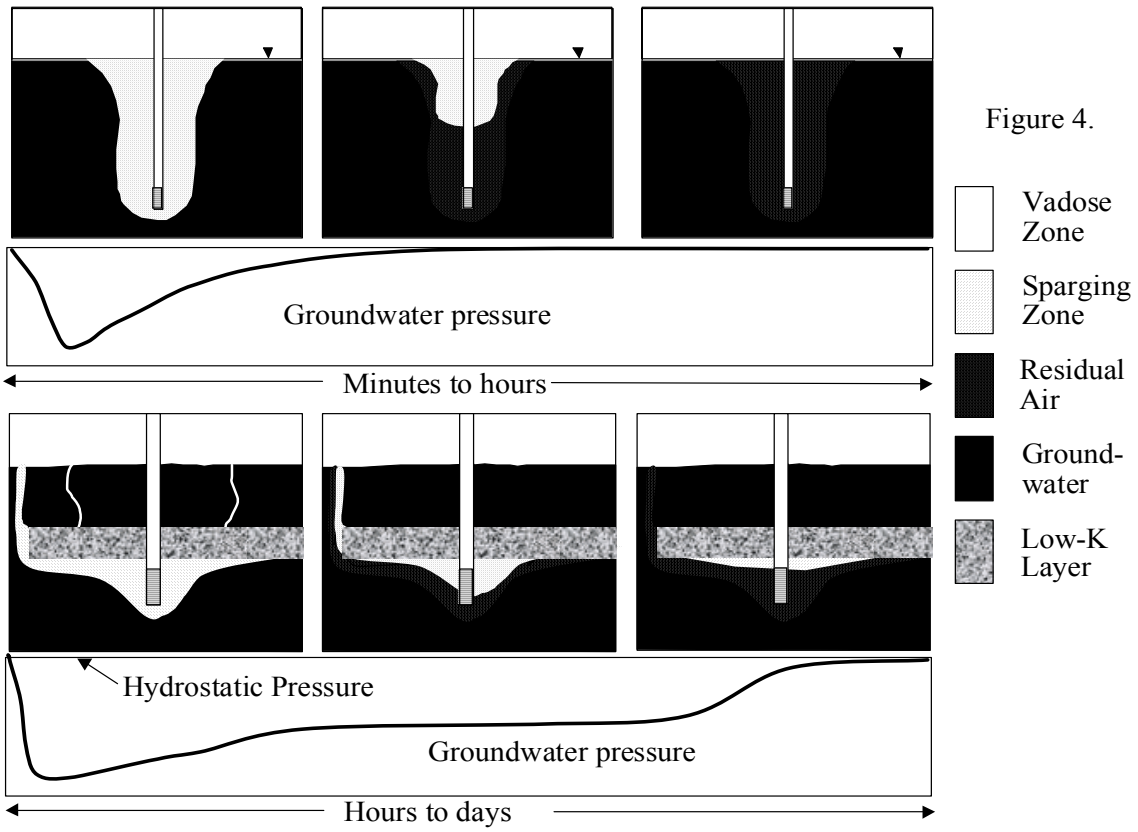

Figure 4. Conceptual Model of IAS Behavior During Shutdown

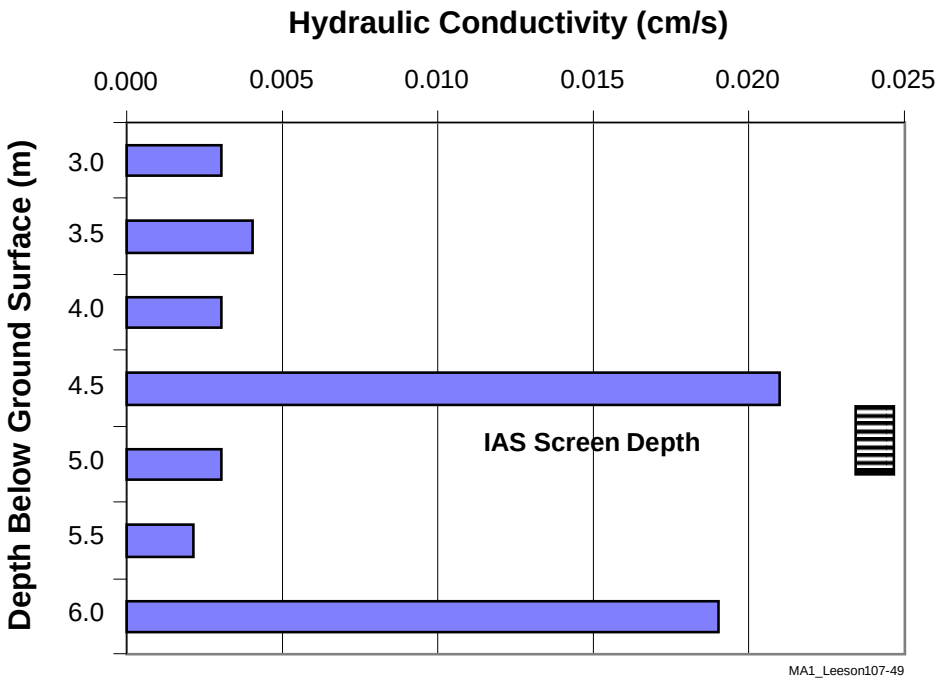

Figure 5. Hydraulic Conductivity Versus Depth, Port Hueneme, California

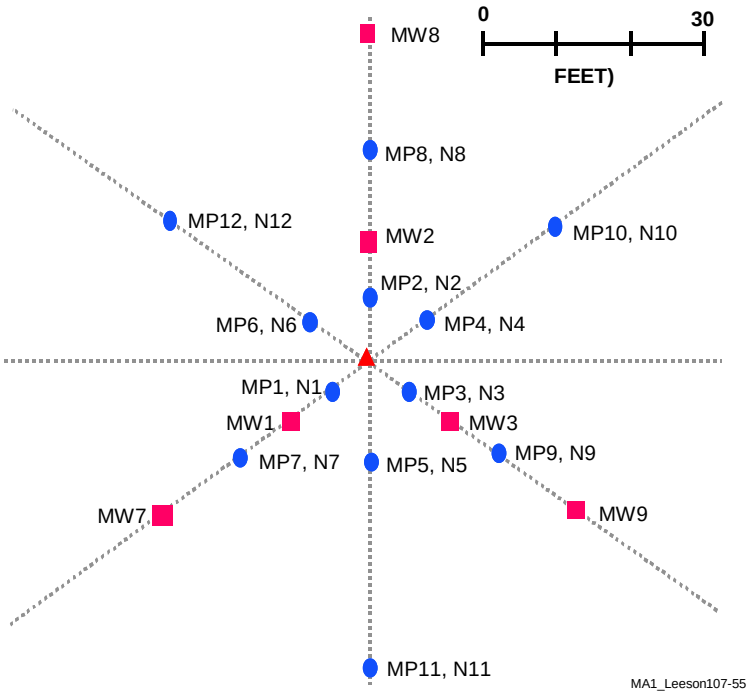

Figure 6. Site Layout, Port Hueneme, California

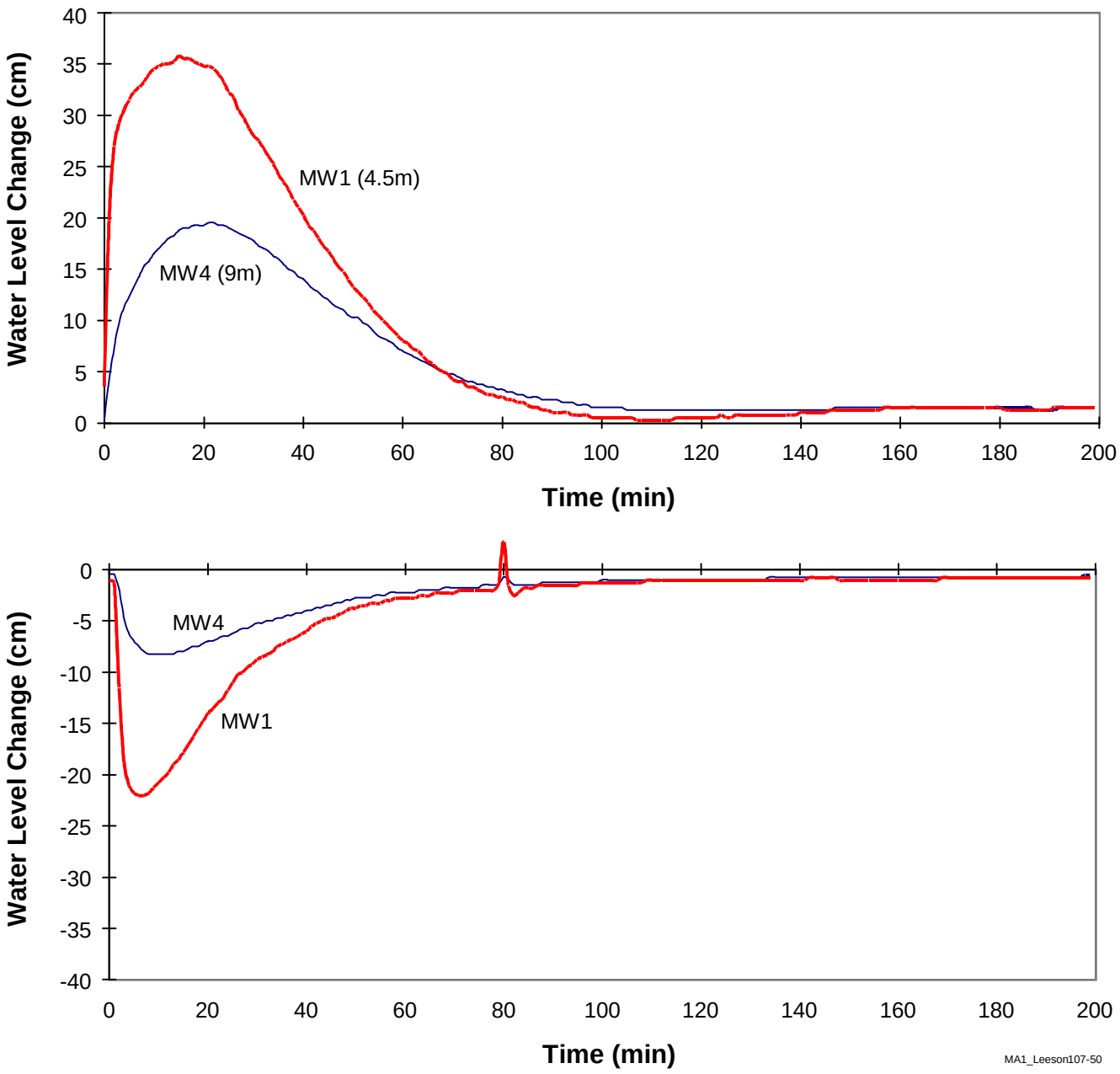

Figure 7. Pressure Measurements Following System Start-Up and Shutdown for Monitoring Wells MW1 and MW4, Port Hueneme, California

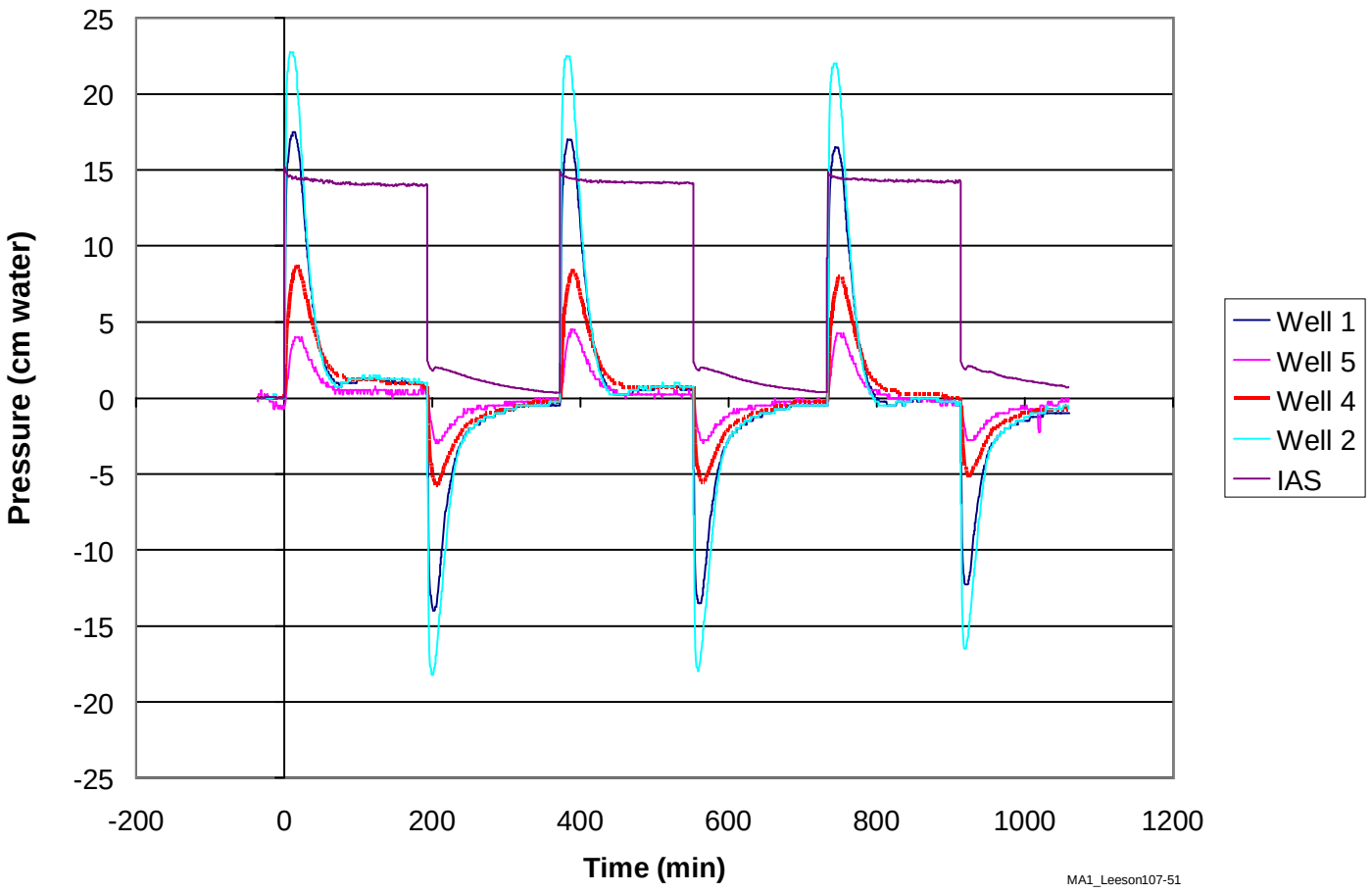

Figure 8. Pressure Measurements During Pulsed Operation, Port Hueneme, California

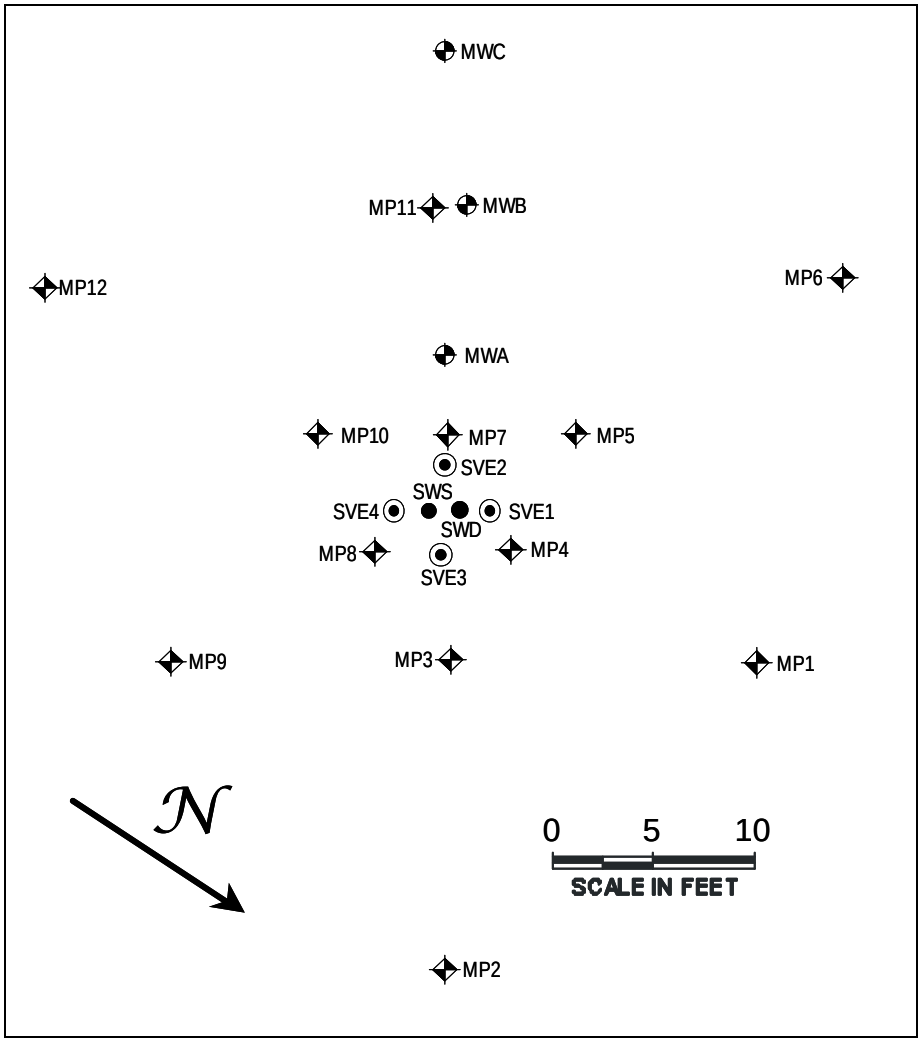

Figure 9. Schematic Diagram of the Test Plot, Eielson AFB, Alaska

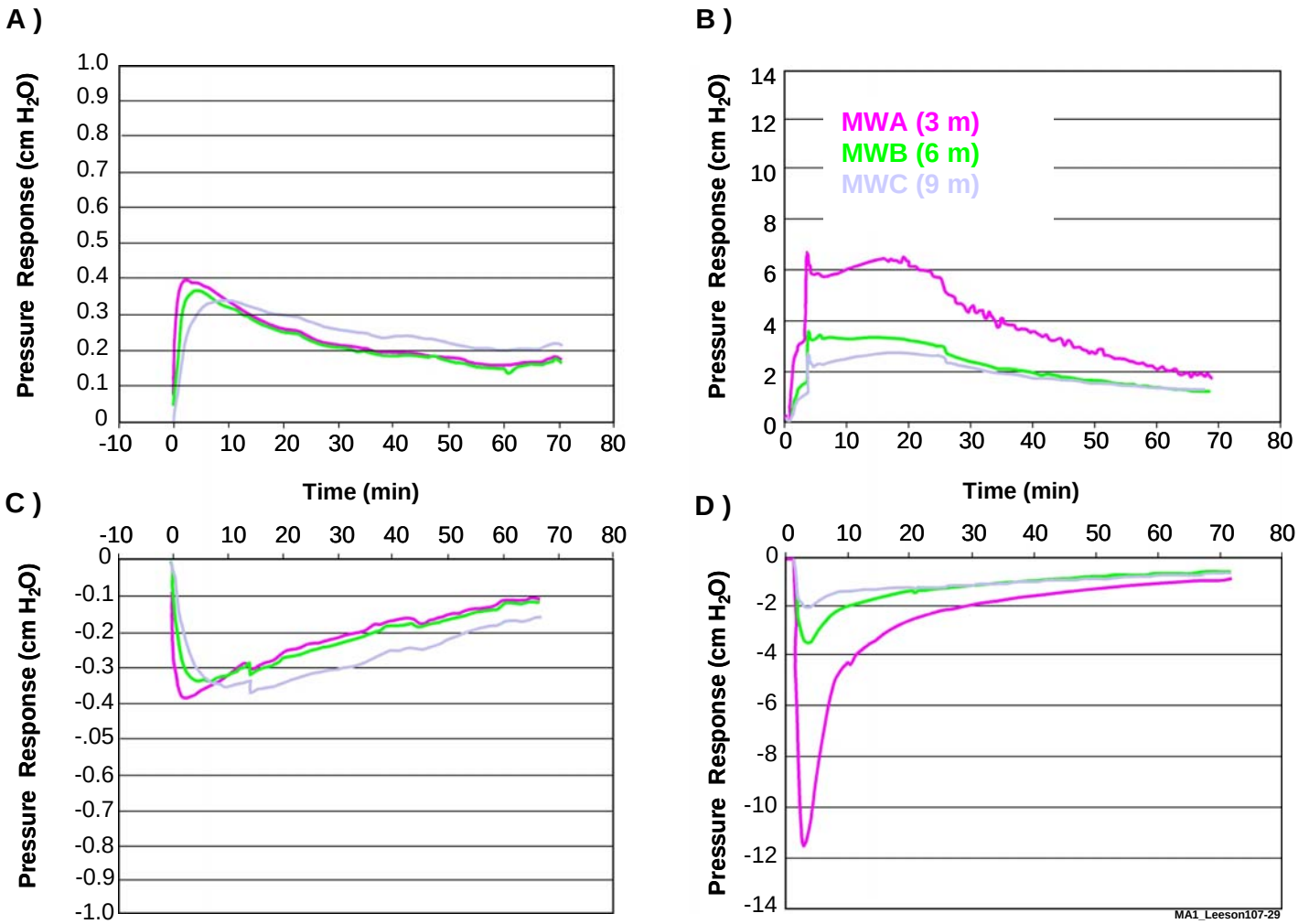

Figure 10. Pressure Testing: A) Pressure Response at Initiation of Air Injection into the Shallow Well; B) Pressure Response at Initiation of Air Injection into the Deep Well; C) Pressure Response at Discontinuation of Air Injection into the Shallow Well; D) Pressure Response at Discontinuation of Air Injection into the Deep Well; Eielson AFB, Alaska

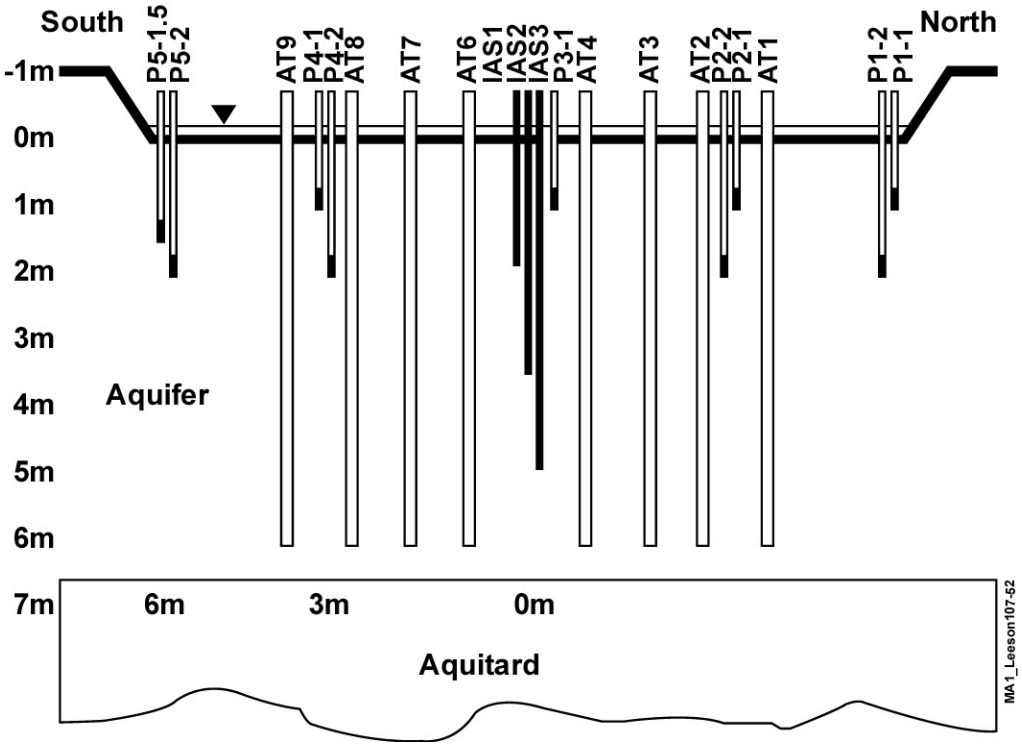

Figure 11. Site Layout at CFB Borden, Ontario

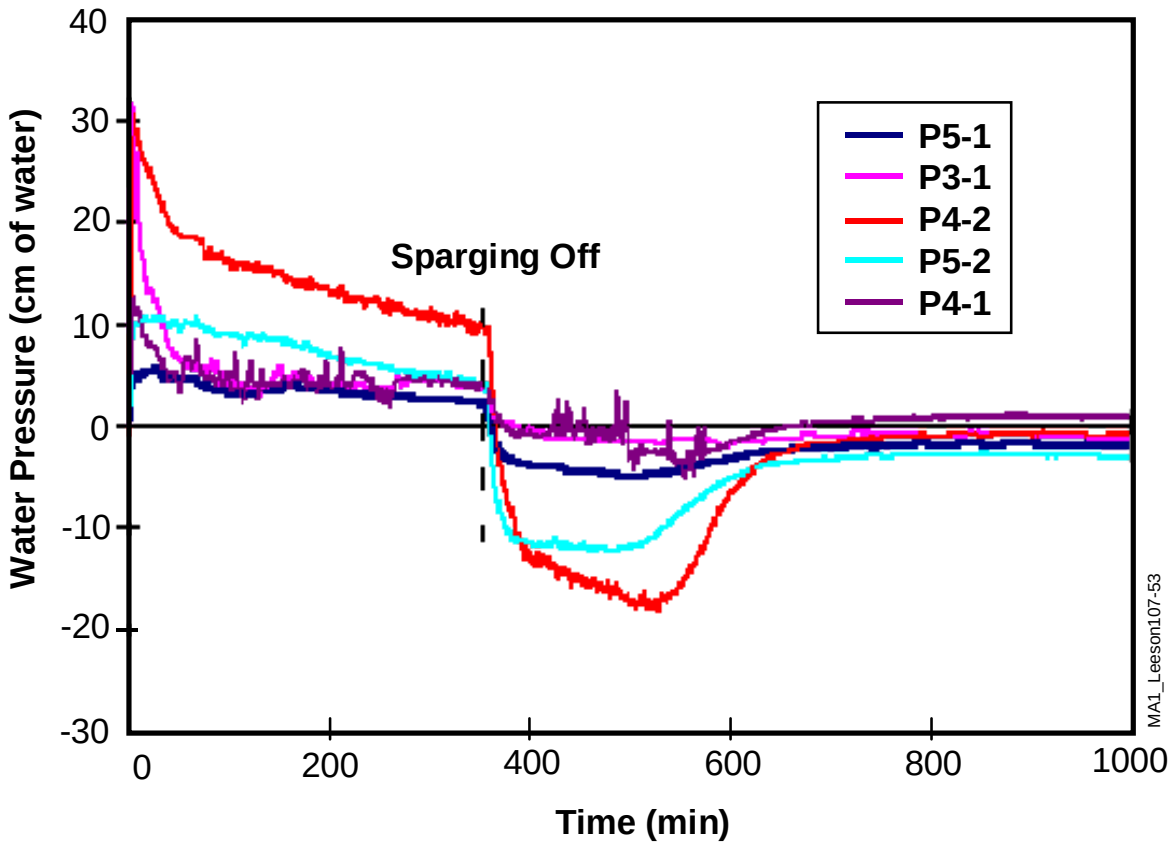

Figure 12. Pressure Response Versus Time, CFB Borden, Ontario

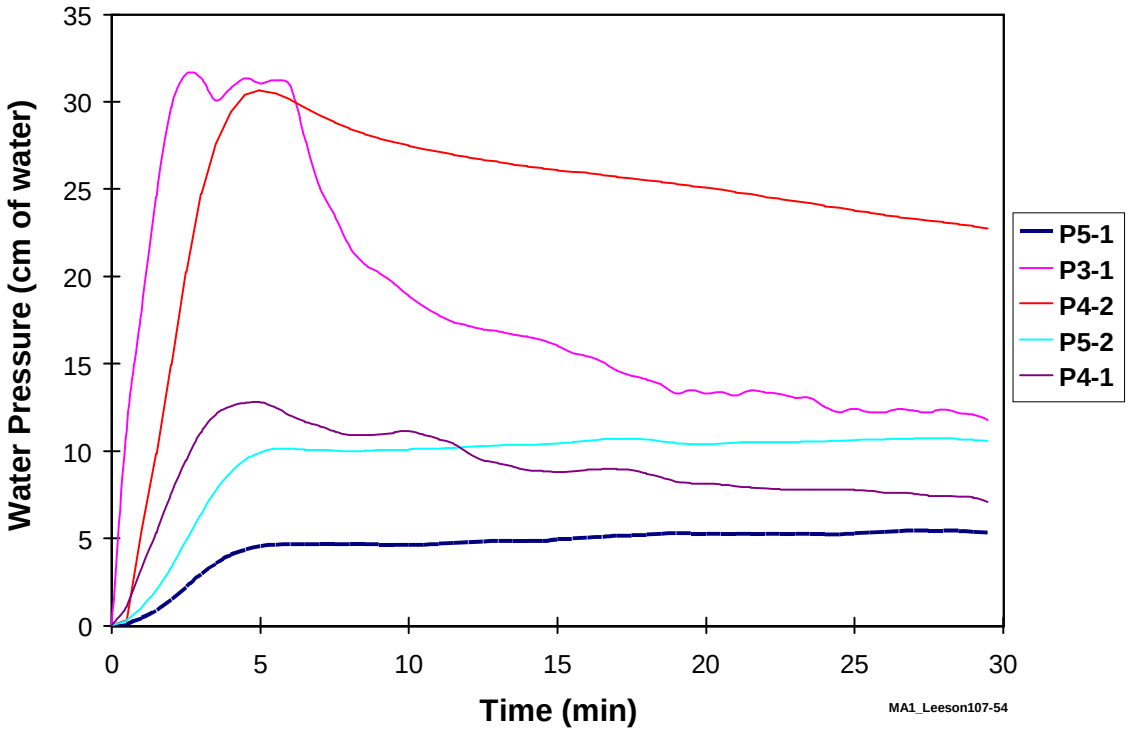

Figure 13. Pressure Response Versus Time During the First 30 min after Initiation of Air Injection, CFB Borden, Ontario

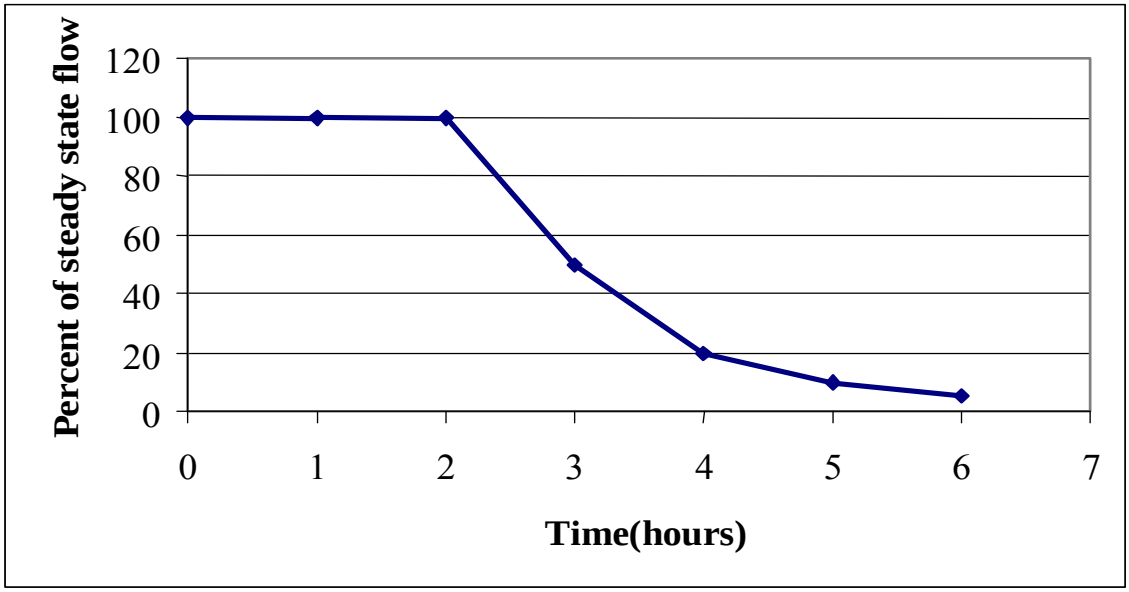

Figure 14. Air Flowrate at Water Table Versus Time, CFB Borden, Ontario

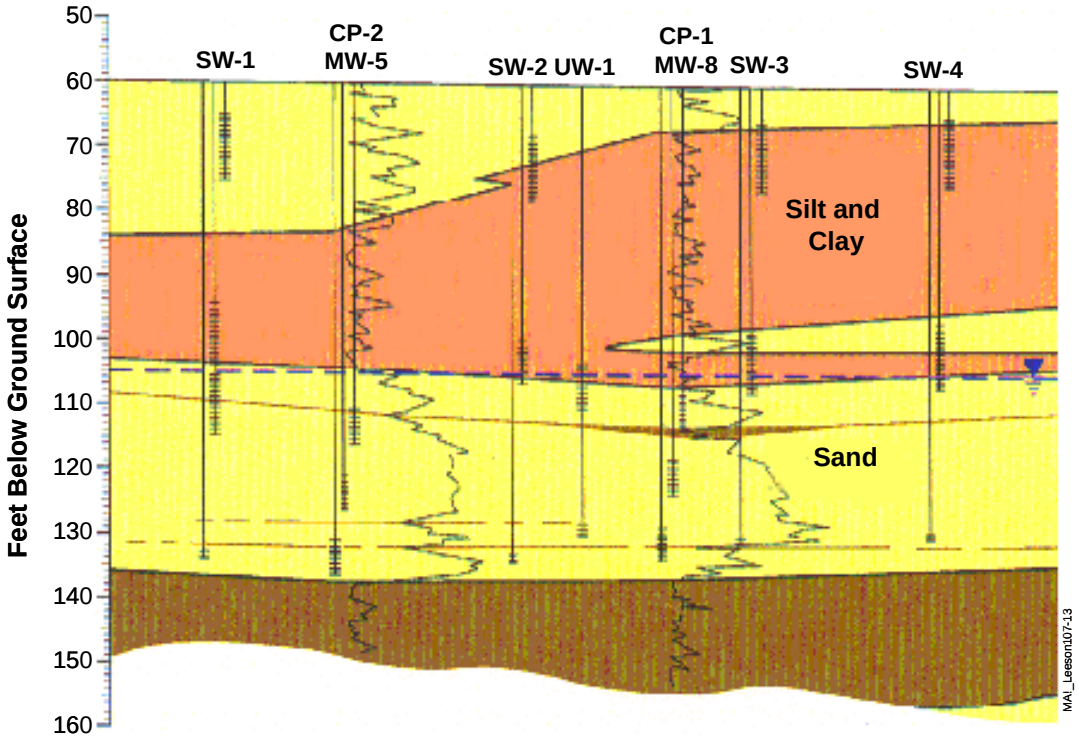

Figure 15. Site Hydrogeology, Hill AFB, Utah

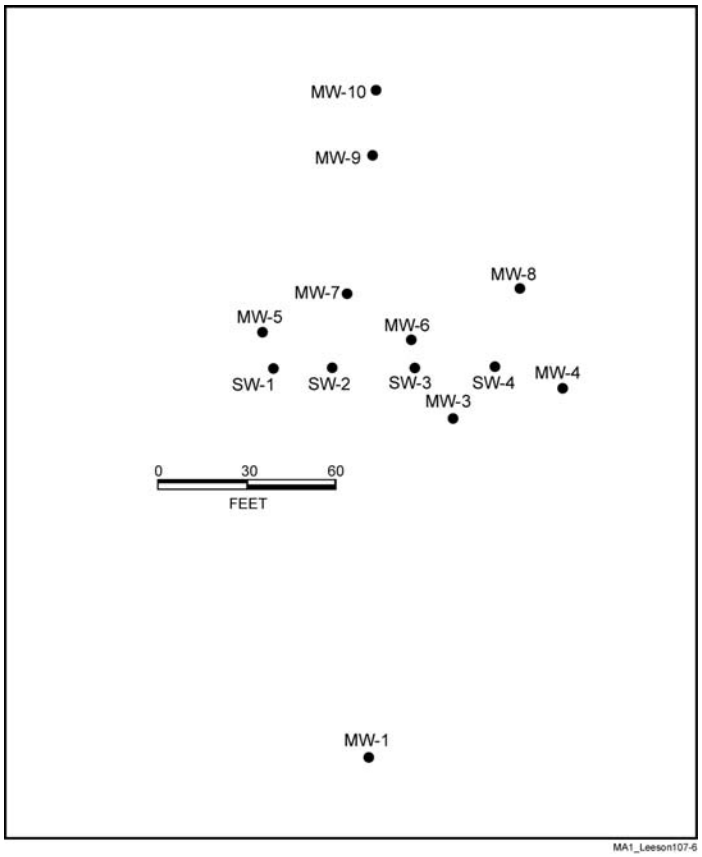

Figure 16. Site Layout, OU-6, Hill AFB, Utah

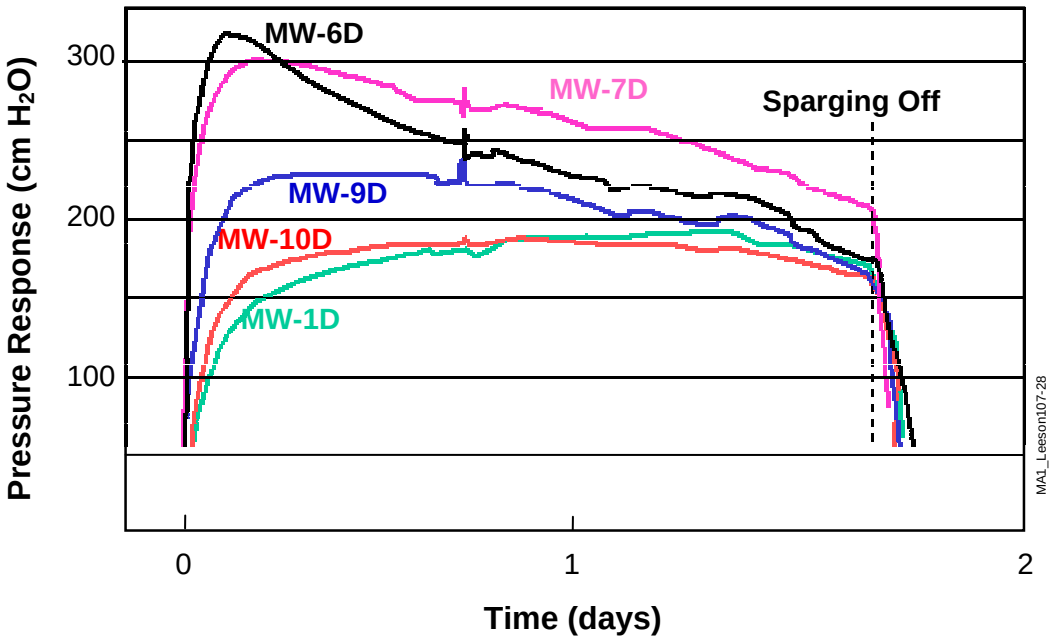

Figure 17. Pressure Response Versus Time, Hill AFB, Utah

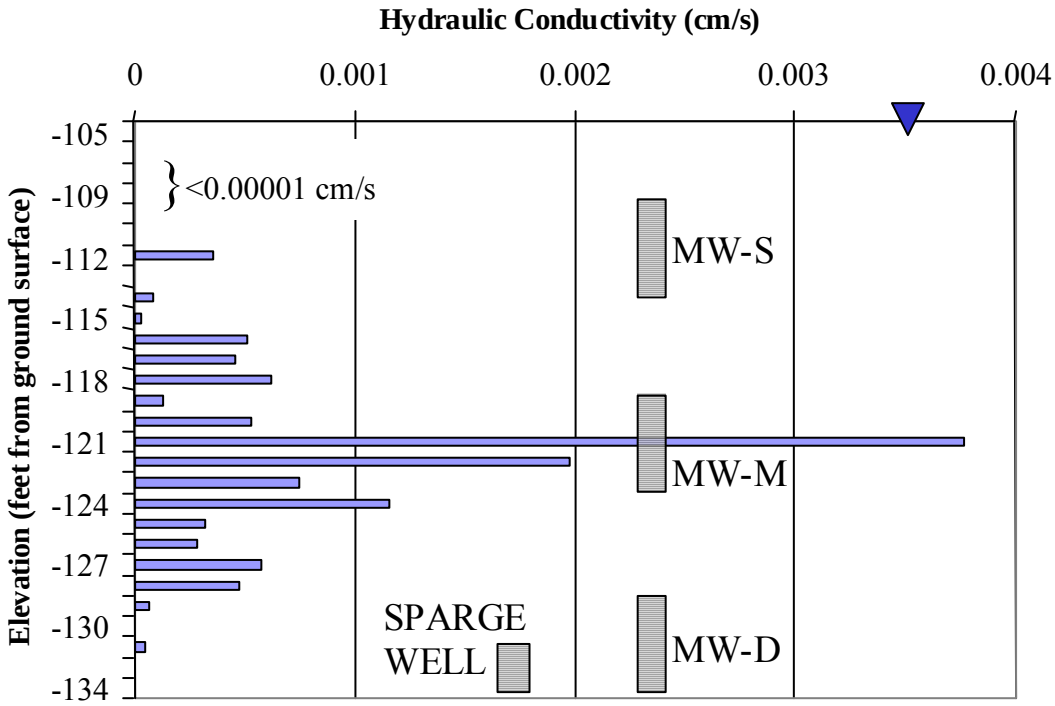

Figure 18. Hydraulic Conductivity Versus Depth, Hill AFB, Utah

APPENDIX F

Helium Tracer Tests for Assessing Air Recovery and Air Distribution During In Situ Air Sparging

Richard L. Johnson[1], Paul C. Johnson[2], Tim L. Johnson[1] and Andrea Leeson[3]

[1]Oregon Graduate Institute, Center for Groundwater Research, Department of Environmental Science and Engineering, Portland, Oregon; [2]Arizona State University, Department of Civil Engineering, Tempe, Arizona; [3]Battelle Memorial Institute, Columbus, Ohio

BACKGROUND

Uncontrolled migration of contaminant vapors liberated during in situ air sparging (IAS) can pose safety and health hazards to nearby receptors (e.g., via buildings, utility conduits, sewers, etc.). In cases where a risk pathway is present, soil vapor extraction (SVE) systems are frequently installed to mitigate that risk. In most cases, practitioners utilize vadose zone soil-gas pressure data to assess the ability of the SVE system to capture contaminant vapors. It is usually assumed that if sub-ambient soil-gas pressures are measured throughout the treatment area, then contaminant vapors are being captured. However, the fieldwork of Johnson et al. (1997) demonstrated that this approach does not ensure capture of the contaminant vapors. For example, a stratum present below the water table may cause the injected air to migrate laterally away from the IAS system and outside the SVE capture zone before it emerges from the saturated zone. At some sites, the vadose zone may be sufficiently stratified so that soil-gas measurements at one depth may not reflect the air flow field at other depths, while at other sites, the vadose zone may be sufficiently permeable that significant vapor flow away from the SVE system can occur without measurable positive soil-gas pressures.

As an alternative to soil-gas pressure measurements, Johnson et al. (1996, 1997) and others have used inert tracer gas tests to assess the effectiveness of SVE systems for capturing contaminant vapors liberated by IAS. These tests are simple to conduct and provide more direct and reliable measures than the soil-gas pressure measurement approach discussed above. In addition, the same tracer test can also provide valuable insight to the IAS air distribution below the water table by observing the appearance of the tracer in deep vadose zone soil gas (i.e., just above the water table) within a short time (e.g., minutes) after tracer injection is initiated. These data provide an indication of the spatial extent and directionality of the air distribution below the water table, information that can be critical for decisions about IAS well spacing. Helium tracer tests, along with transient pressure transducer measurements (Johnson et al., 2001b), are easily incorporated into short-term IAS pilot testing procedures (Johnson et al., 2001a). They can also be used for full-scale system diagnosis and optimization. One of the strengths of the tracer tests discussed here is that they can be easily repeated, usually with delays of only a few hours between tests. This allows the effects of process changes (e.g., distribution of air flow from various wells) to be quickly assessed.

EXPERIMENTAL METHODS

The methods for conducting the helium tracer tests to both determine SVE system capture efficiency and to evaluate air distribution during pilot- and full-scale IAS operation are described below. In addition, to help illustrate the utility of the test, sample data collected at three sites are presented and discussed. Helium is the most common tracer gas used for these tests, since it is relatively inexpensive, readily available, and easy-to-use field analytical instrumentation is available. For example, the Marks Product

model 9822 helium detector used in case studies discussed below is available for rental. It can detect helium concentrations from 0.01% to 100% and comes factory-calibrated. The detector has a built in sampling pump and can be used to measure helium concentrations in samples collected in gas sampling containers, or it can be configured to sample from a process slip-stream on regular timed intervals. In either case, it can also be connected to data-logging computers for data storage and semi-automatic sampling and analysis. Readers should be cautioned that the detector's response to helium can be affected by elevated carbon dioxide concentrations in soil gas, so that calibration checks may have to be done using actual soil gas from the site and not atmospheric air. The tests described below discuss the use of helium. While helium is recommended for these tests, other inert tracer gases and detectors could potentially also be used.

Tracer Test to Assess SVE Recovery of Contaminant Vapors Liberated by IAS

The tracer recovery tests described here are designed to be conducted on an operating IAS-SVE system after the IAS air flow patterns have stabilized. At most sites, these tests can be performed within a few hours of IAS start-up. The tests were originally developed for IAS pilot tests, but can also be conducted during full-scale operation to evaluate system performance and ensure that health and safety objectives have been met. To be most useful at the pilot-test scale, the IAS and SVE wells should be operated as envisioned during full-scale operation. At many sites the IAS and SVE wells are co-located, although this is not a requirement. It is important to note that the helium recovery test results are specific to the well configuration and operating conditions tested. Changes in either could lead to significantly different results and conclusions.

The helium tracer recovery test is simple to conduct and interpret. Figure 1A presents the basic test setup, and the general sequence of activities is as follows.

a) An inert tracer (usually helium) is introduced into the IAS air stream upstream of the IAS injection wellhead (if a single well is being tested) or the injection air manifold if multiple IAS wells are operating. Because these tests are rapid to conduct, it is recommended that recovery tests be conducted on individual IAS wells.
b) The tracer gas flow is maintained at a constant, known rate and the resulting tracer gas concentration in the injection air stream is measured. The helium injection concentration should be kept below 10% by volume to minimize buoyancy effects.
c) The concentration of tracer in the SVE off-gas stream is monitored with time. If more than one SVE well is operating, the tracer concentration should be measured downstream of the SVE well manifold and in the same location as the SVE cumulative flowrate measurement.
d) Over a period of minutes to hours, the helium concentration in the SVE off-gas will increase and eventually reach a stable plateau. Once this has been accomplished, the final helium concentration as well as the IAS and SVE air flow rates should be recorded.

Based on these data, the percent of the IAS air that is captured can be calculated by a simple steady-state mass balance, as follows:

$$\%\ \mathrm{Recovery} = \frac{Q_{SVE} \times C_{Off-gas}}{Q_{Tracer} \times C_{gas\ \tan k}} X\ 100 \qquad (1)$$

where Q_{SVE} is the SVE flowrate; $C_{off\text{-}gas}$ is the tracer concentration in the SVE off-gas; Q_{tracer} is the tracer flowrate (i.e., from the helium cylinder); and $C_{gas\ tank}$ = the tracer concentration in the gas tank (i.e., 100% for pure helium).

This equation, of course, assumes that all flowrates are measured accurately with flow meters that have been calibrated for appropriate gas at the flow rates and pressures used in the field. Unfortunately, this is rarely the case in practice, and therefore, an alternate field method is presented here. In the alternate method, the absolute values of the flow rates are not critical, only that the flow rates be held constant during the test. Rather than calculating a helium mass balance, the helium concentration in the SVE off-gas when all the tracer gas is captured as well as the concentration achieved during the actual operating conditions are determined. The ratio of these two values times 100 is equivalent to the "% Recovery" calculated by Equation (1):

$$\%\,\text{Recovery} = \frac{C_{Off-gas}}{C_{100\%\,recovery}} X\ 100 \qquad (2)$$

Where $C_{100\%\,recovery}$ is the tracer concentration of at which 100% of the tracer is recovered.

The procedure for determining percent recovery using the alternate field method is as follows:

- To determine the "100% tracer gas recovery concentration," the tracer gas injection line is connected directly to an SVE wellhead, and the helium concentration resulting from the dilution of the tracer gas in the SVE off-gas stream is determined. Because the tracer is going directly into the SVE recovery system, it is known that 100% of the tracer is being "captured." During this process, the helium flow meter reading and the pressure at the flow meter should be recorded.
- Once the 100% tracer gas recovery concentration measurement is made, the tracer gas injection line is then connected to the IAS air injection stream. Because the backpressures of the IAS and SVE are typically quite different, at this point it may be necessary to adjust the helium cylinder pressure and the downstream needle valve (Figure 1A) to obtain the same pressure and flowmeter reading observed in the previous step. As discussed above, to ensure a consistent tracer gas flowrate under conditions of varying back-pressure, the tracer gas direct-reading flow meter (e.g., rotameter) should be connected as shown in Figure 1A. The flow meter is placed next to a pressure gauge and both are upstream of a valve used to maintain a constant back-pressure at the flow meter. This backpressure provided by the needle valve should be kept large relative to the steady-state injection pressure (e.g., usually 20 to 40 psig above the injection pressure) to minimize the effects of changing back pressure on flow).
- Once the same flow rate has been achieved, the helium injection into the IAS system is allowed to continue until the concentration in the SVE off-gas has stabilized. Equation 2 can then be used to calculate the percent recovery.

If the recovery of helium is low (<30%), then it is likely that air (and helium) is being trapped below the water table beneath lower-permeability strata (Figure 1B) and may be moving laterally beyond the reach of the SVE system. In some cases it is possible that no helium will return to the well due to the presence of continuous layers. The presence of these layers should also be detectable by monitoring groundwater pressure during IAS start-up and shutdown (Johnson et al., 2001b). Therefore, it is recommended that the helium recovery test be conducted in conjunction with transient groundwater pressure transducer measurements at start-up.

If helium recovery is high (e.g. >80%), then the SVE system is performing well with regard to IAS air recovery, and lateral migration of vapors is unlikely to be a problem. However, it should be noted that this test does not provide any information on the actual concentrations of contaminant vapors at points in the subsurface. Therefore, low capture efficiencies do not necessarily indicate actual safety or health problems, and conversely, high capture efficiencies do not preclude the potential for high contaminant vapor concentrations at nearby locations of concern. Thus, at "high risk" sites, users should consider

augmenting this test with supplemental soil-gas analysis at any points of concern. Finally, it should be noted that achieving good capture during a pilot test does not ensure capture at full scale, and the tracer tests should be repeated at full-scale system start-up.

Tracer Test Procedure to Determine the Distribution of IAS Air at the Water Table

If a number of discrete-depth vadose zone monitoring points (e.g., with 6- to 12-inch screened intervals) are placed near the water table and distributed around the IAS well, then the tracer test setup and equipment described above can also provide useful information about the aerial distribution of IAS air below the water table. Generally, six or more vadose zone monitoring points will be required to develop a picture of helium distribution at the water table. This test can be completed in approximately 20 to 60 minutes and can be performed as part of the helium recovery test discussed above. The sequence of activities in this test is as follows:

1. Initiate IAS air injection
2. If an SVE system is present, it can be on or off. In either case, the procedure for conducting the test is the same. However, the interpretation of the results is somewhat different, as will be discussed below.
3. After the transient start-up period (usually this is a few hours or less and can be determined on a site-specific basis using the transient pressure transducer response test described in Johnson et al., 2001b), helium is blended into the injection air to readily measurable concentrations (e.g., about 5% by volume).
4. After approximately 5 min, and before 15 to 20 min, all the vadose zone soil-gas sampling points are sampled and concentrations of the tracer gas are measured and recorded along with the time of measurement/sampling. (This rapid sampling is best accomplished if purge times are kept small by using very-small-diameter direct push [e.g., Geoprobe] monitoring points.)

If an SVE system was not in operation, the presence of tracer at the deep soil gas monitoring points at concentrations near the injection concentration is indicative of IAS air emerging from the aquifer and entering the vadose zone near those points (Figure 2). It is critical that measurements be made relatively soon after tracer introduction in order to minimize the potential for tracer to arrive at a given vadose sampling point by diffusion and/or advection from some other point in the vadose zone. If a co-located SVE system was in operation, then elevated helium concentrations at monitoring points indicate that IAS air reached the water table at a distance beyond the monitoring point. In the examples discussed below, co-located SVE systems were in operation and the vadose zone measurements were made concurrently with the determination of percent helium recovery.

RESULTS AND DISCUSSION

The helium tracer tests described above have been conducted at a number of sites, most recently as part of a Department of Defense (DoD) multisite air sparging evaluation project funded through the Environmental Strategic Technology Certification Program (ESTCP). Three of those IAS sites will be examined here. One site is located in a mildly stratified sand (Port Hueneme, California [PH]); one is in a relatively homogeneous sandy gravel (Eielson Air Force Base [AFB], Alaska [EAFB]), and one is in a stratified sand and clay aquifer (Hill AFB, Utah [HAFB]). Two of the sites had single IAS sparge locations with co-located SVE systems and were evaluated as part of pilot tests (PH and EAFB). In both cases, two different injection depths were evaluated. Air injection rates for those two sites ranged from 5 to 20 SCFM (typical of many IAS systems). The depths of air injection at the first two sites were 6 to 10 feet (2 to 3 m) below the water table. The HAFB site had four IAS wells, each with co-located SVE wells. The injection rate there was approximately 12.5 SCFM per IAS well, and the depth of injection was approximately 23 ft (7 m) below the water table. System installations are described in more detail for

PH in Amerson (1997) and for EAFB and HAFB in Johnson et al. (2001b). In each case, additional data from other independent diagnostic measurements are also presented to help the reader assess the utility and reliability of the helium tracer results.

Port Hueneme, California

Helium tracer tests were conducted during IAS pilot tests in air injection wells at two different depths at Port Hueneme, California (Figure 3). In the first test, the IAS well was screened from 18 to 20 ft (5.4 to 6 m) below ground surface (bgs). At this site the water table is encountered at about 8 to 10 ft bgs (2.4 to 3 m), depending upon the season. The air injection rate was 5 SCFM and the co-located SVE system operated at 80 SCFM. Figure 4A presents the helium recovery percentage versus time results, and shows that only approximately 40% of the injected helium was recovered by the SVE system.

As a result of the low tracer recovery in the first test, a second test was conducted with the IAS well screen located at a depth of 15 to 17 ft bgs (4.6 to 5.2 m). The air injection rate for this test was 10 SCFM and the SVE system was again operated at 80 SCFM. Figure 4B presents the helium recovery versus time data for this pilot test; as can be seen, helium recovery was nearly 100%. Soil boring logs support the hypothesis that the significant change in helium recovery was largely due to the presence of a thin lower-permeability layer at 17 to 18 ft bgs. This data illustrates how small changes in soil structure and positioning of an IAS well can affect the resulting air distribution.

Concurrent with startup of the recovery tests described above, tracer concentrations in the deep vadose zone were monitored at the12 locations shown in Figure 3. Each was positioned approximately 1.5 ft (0.5 m) above the water table, and soil gas was extracted through an open-ended tube implanted at that depth in the vadose zone.

Figure 5A shows the deep vadose zone helium tracer distribution for air injection when the IAS well screen was placed at 18 to 20 ft bgs. Based on the tracer distribution, it appears that all of the injection air was traveling to the upper right-hand quadrant; furthermore, some of the injection air appeared to be traveling beyond the monitoring network. These observations are consistent with the measured 40% recovery of tracer in the SVE off-gas. Both observations are important for full-scale design since the full-scale system design would need to allow for both an asymmetrical air distribution and the potential for lateral migration away from the SVE system. Figure 5B presents the deep vadose zone tracer distribution for the case where the IAS well was screened from 15 to 17 ft bgs. As in Figure 5A, the tracer shows that most of the injected air is traveling to one quadrant of the plan view map. However, the lateral migration must be less because the SVE system is capable of achieving 100% capture in this case.

To further assess air distribution at the PH site, a sulfur hexafluoride (SF_6) tracer test (Johnson et al., 1996) was conducted to determine the distribution of IAS air below the water table. This test compliments the helium test because it provides a direct measure of the horizontal and vertical distribution of air below the water table. Briefly, the test involves injecting SF_6 along with the IAS air and then measuring the resulting concentration of dissolved SF_6 in the groundwater after a period of injection (e.g., 24 hours). (In these tests SF_6 acts as a conservative analog for oxygen.) SF_6 distribution data from the two pilot tests are shown in Figure 6. Like the deep vadose zone helium data, the IAS air distribution in groundwater data from the SF_6 test shows an asymmetric distribution, although the spatial extent and the preferred direction of flow in 5b are somewhat different than for helium in Figure 4b. However, from the perspective of IAS performance, both tests indicate the need for closely spaced (<20 ft) IAS wells at full-scale to compensate for the limited spatial extent and asymmetry of the air flow field.

Eielson AFB, Alaska

A series of pilot tests similar to those at Port Hueneme was conducted at Eielson AFB, Alaska. Helium tracer tests were conducted sequentially in two co-located IAS wells, one installed to a depth of 6 ft (2 m)

below the water table; the other installed at 10 ft (3 m) below the water table. Both wells had 1-ft (0.3 m) screens and were installed by "direct-push" equipment. Air injection rates were set at 5 SCFM for the shallow IAS well and 10 SCFM for the deep IAS well. An SVE system was co-located with the IAS wells. The vadose zone at the site was quite fine-grained, and the maximum SVE rate that could be achieved without excessive upwelling of water was a total flow 15 SCFM.

Figure 7 presents the results for the two recovery tests. In both cases, the tracer quickly appeared in the SVE wells and the tracer concentration rose to approximately 100% recovery. When helium injection was stopped, the concentration quickly dropped. These quick-response data suggest that most of the injected air is reaching the water table in the immediate vicinity of the IAS well. To evaluate this, as in the previous case, at the beginning of the recovery test, tracer concentrations in the deep vadose zone were monitored. At this site there were 12 vapor monitoring points distributed around the IAS wells at distances of 5,10, 20, and 30 ft (1.5, 3, 6, and 10 m). Each well was screened at a depth of 6 ft (2 m) (2 ft/0.6 m above the water table). For the shallow IAS well operated at 5 SCFM, helium was not observed at any of the deep vadose zone points, as shown in Figure 8a. This indicates that all of the air came up to the water table within a 5 ft (1.5 m) radius of the well. When air was injected at 10 SCFM into the deeper well screen, helium was observed at one vadose zone sampling location 10 ft (3 m) from the sparge well as shown in Figure 8b.

Hill AFB Operable Unit (OU)-6, Utah

HAFB OU-6 is a stratified site where the aquifer is composed primarily of sands and silty sands. The aquifer is overlain by silt with beds of sand and clay, and the interface between the sand and overlying silt near the current water table at approximately105 ft (32 m) bgs. A line of four IAS wells with co-located SVE wells was placed as a chemical migration barrier across a portion of the dissolved trichloroethene (TCE) plume at that site (Radian International, 1995). In addition, nests of groundwater monitoring wells were distributed around the treatment zone. The locations of the wells are shown in Figure 10.

Under normal operation, the total IAS injection rate for the four wells was approximately 50 SCFM and the extraction rate from the eight SVE wells was about 175 SCFM. A tracer recovery test was conducted at the site under steady conditions by injecting helium into the IAS wells at a total rate of 0.55 SCFM. The concentration in the air coming from the SVE system was measured as a function of time and that data are presented in Figure 11. After approximately 500 min of helium injection, a helium recovery rate of approximately 20% was measured.

During the test it was observed that air was flowing out of a number of the shallow groundwater monitoring wells that were screened 5 to 10 ft (1.5 to 3 m) below the water table. As a consequence, the air flow and helium concentrations from each of the wells were monitored during the test. In Figure 10, the upper number associated with each monitoring well is the total flow of air out of the well, the lower number is the flowrate of helium out of the well (i.e., helium concentration times total flowrate). As can be seen, approximately 75% of the injected helium was flowing out of groundwater monitoring wells 7 and 8, and not flowing up into the vadose zone. This type of behavior indicates that vertical air movement being restricted below the water table, presumably by some lower permeability layer. Thus the injected air accumulates below the lower permeability layer, and can only move laterally. At some point the growing air "pocket" encounters the groundwater monitoring wells and air begins to flow up and out of these wells. This hypothesis is supported by the transient groundwater pressure response data reported by Johnson et al. (2001b), which indicates the accumulation of air below the water table.

CONCLUSIONS

The helium air recovery tests discussed above can be used to quantify the efficiency of vapor capture during combined IAS and SVE operation, and can provide valuable insight to the areal distribution of IAS

treatment zones. The ease and speed with which these tests can be conducted and interpreted makes them well suited for IAS pilot tests (even 1-day tests). The helium tests can also be conducted on full-scale systems already in operation to confirm that SVE system performance meets project goals. In addition, the tests can be easily repeated, which allows system parameters to be modified and the impact of those modifications to be quickly assessed. The three case histories presented here were chosen to represent the kinds of conclusion that can be drawn from the tests. In many cases, when problems are identified, system operating parameters (e.g., injection depth) can be modified to yield better results. At some sites (e.g., HAFB) the helium tracer tests can identify "red flags" that may result in IAS not being used at the site. Finally, while the helium tests are very useful as stand-alone measurements, their diagnostic value is significantly increased when they are used in combination with the other diagnostic tools described in this issue (Johnson, 2001a, 2001b, 2001c)

REFERENCES

Amerson, I. L. 1997. Diagnostic Tools for the Monitoring and Optimization of In Situ Air Sparging Systems. M.S. Thesis. Arizona State University, Tempe, Arizona.

Johnson, P.C., R.L. Johnson, C. Neaville, E.E. Hansen, S.M. Stearns, and I.J. Dortch. 1997. An Assessment of Conventional In Situ Air Sparging Tests. *J. Ground Water, 35*:765-774.

Johnson, P.C., A. Leeson, R.L. Johnson, C.M. Vogel, R.E. Hinchee, M. Marley, T. Peargin, C.L. Bruce, I.L. Amerson, C.T. Coonfare, and R.D. Gillespie. 2001. A Practical Approach for the Selection, Pilot Testing, Design, and Monitoring of In Situ Air Sparging/Biosparging Systems. *Bioremediation Journal*, *5*(4):267-282.

Johnson, R.L., R.R. Dupont, and D.A. Graves. 1996. *Assessing UST Corrective Action Technologies: Diagnostic Evaluation of In Situ SVE-Based System Performance*. EPA/600/R-96/041, 164p.

Johnson, R.L., P.C. Johnson, I.L. Amerson, T.L. Johnson, C.L. Bruce, A. Leeson, and C.M. Vogel. 2001b. Diagnostic Tools for Integrated In Situ Air Sparging Pilot Tests. *Bioremediation Journal*, *5*(4):283-298.

Johnson, R.L., P.C. Johnson, T.L. Johnson, N.R. Thomson, and A. Leeson. 2001a. Diagnosis of In Situ Air Sparging Performance Using Transient Groundwater Pressure Changes During Startup and Shutdown. *Bioremediation Journal*, *5*(4):299-320.

Radian Corporation. 1995. *Interim IAS/SVE Test Technology Demonstration Report, Operable Unit 6, Hill Air Force Base, Utah*. 25 September 1995.

A)

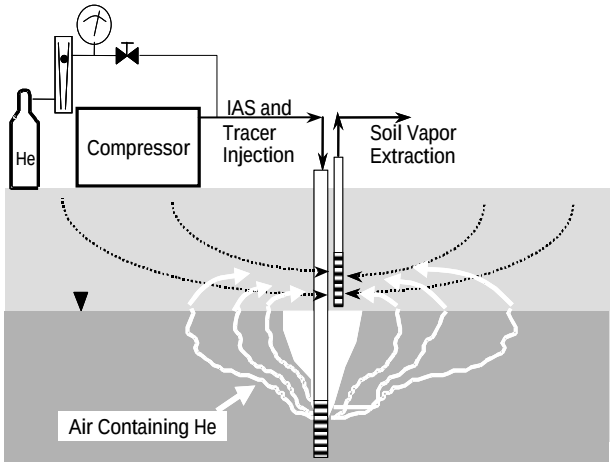

B)

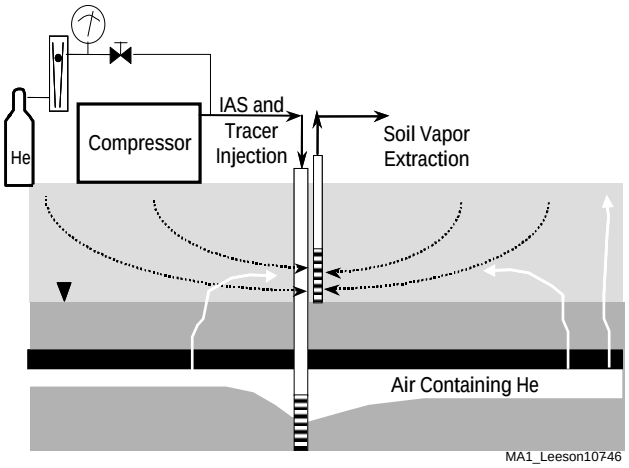

Figure 1. Helium Tracer Test for Assessing Air Sparging Air Recovery in an Unstratified Setting (A) and a Stratified Setting (B)

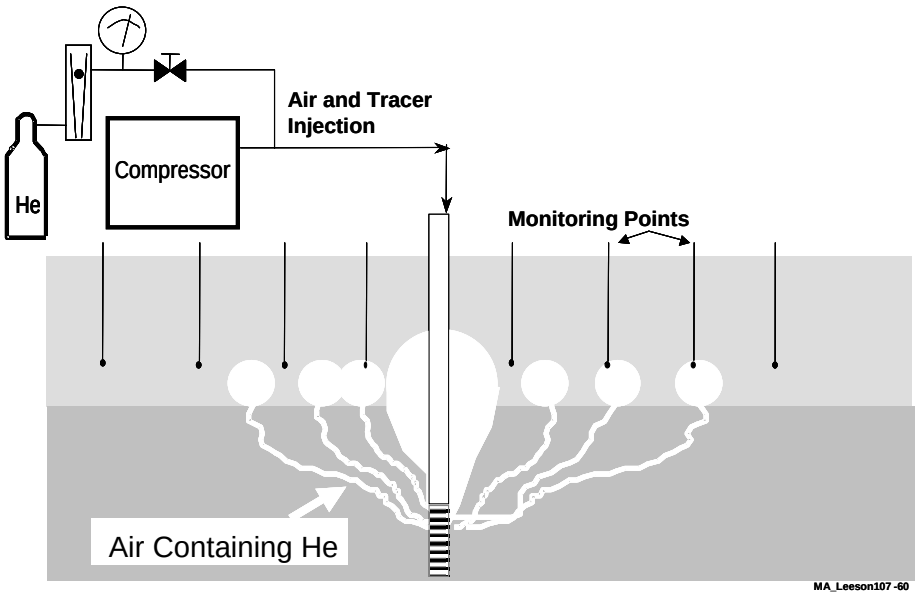

Figure 2. Helium Tracer Test Setup to Assess Air Distribution in the Absence of an SVE System

A)

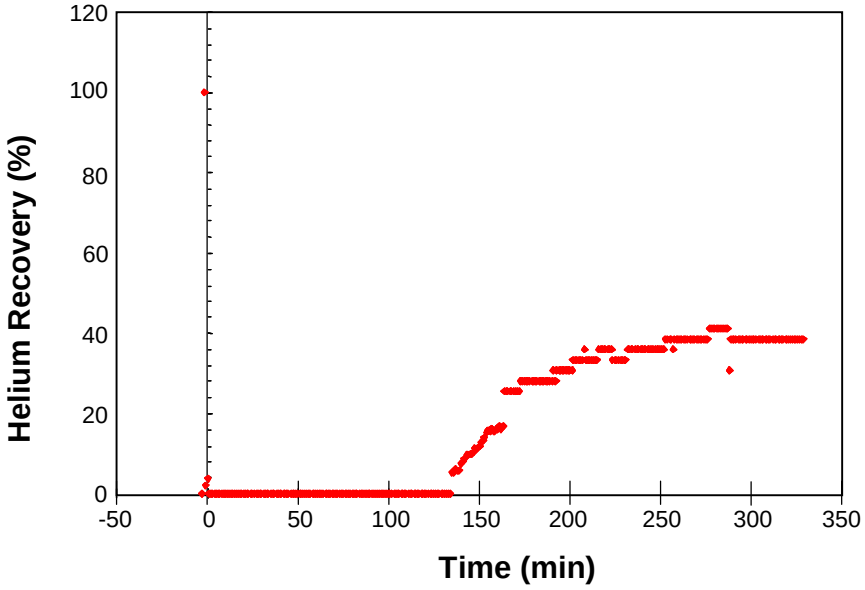

B)

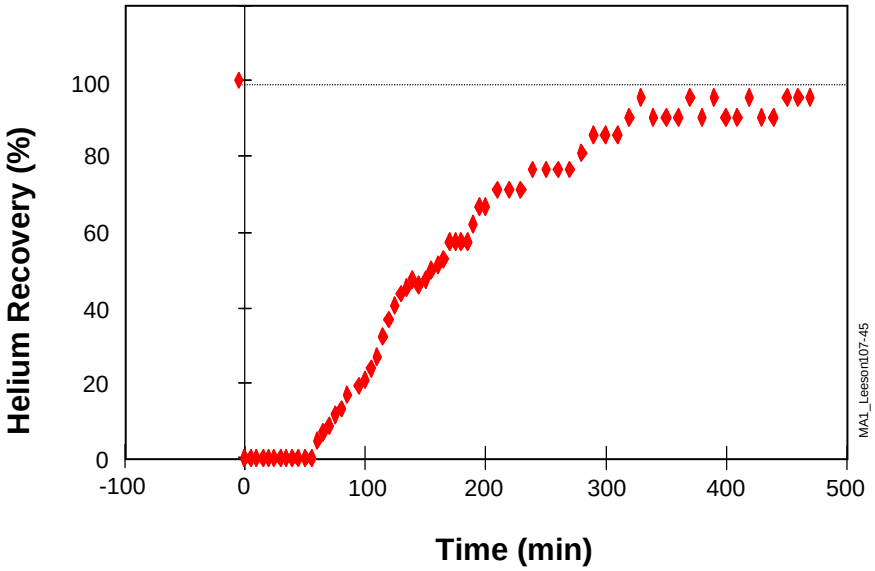

Figure 3. Helium Recovery at an Extraction Rate of 80 SCFM and (A) an Air Injection Rate of 5 SCFM and (B) an Air Injection Rate of 10 SCFM, Port Hueneme, California

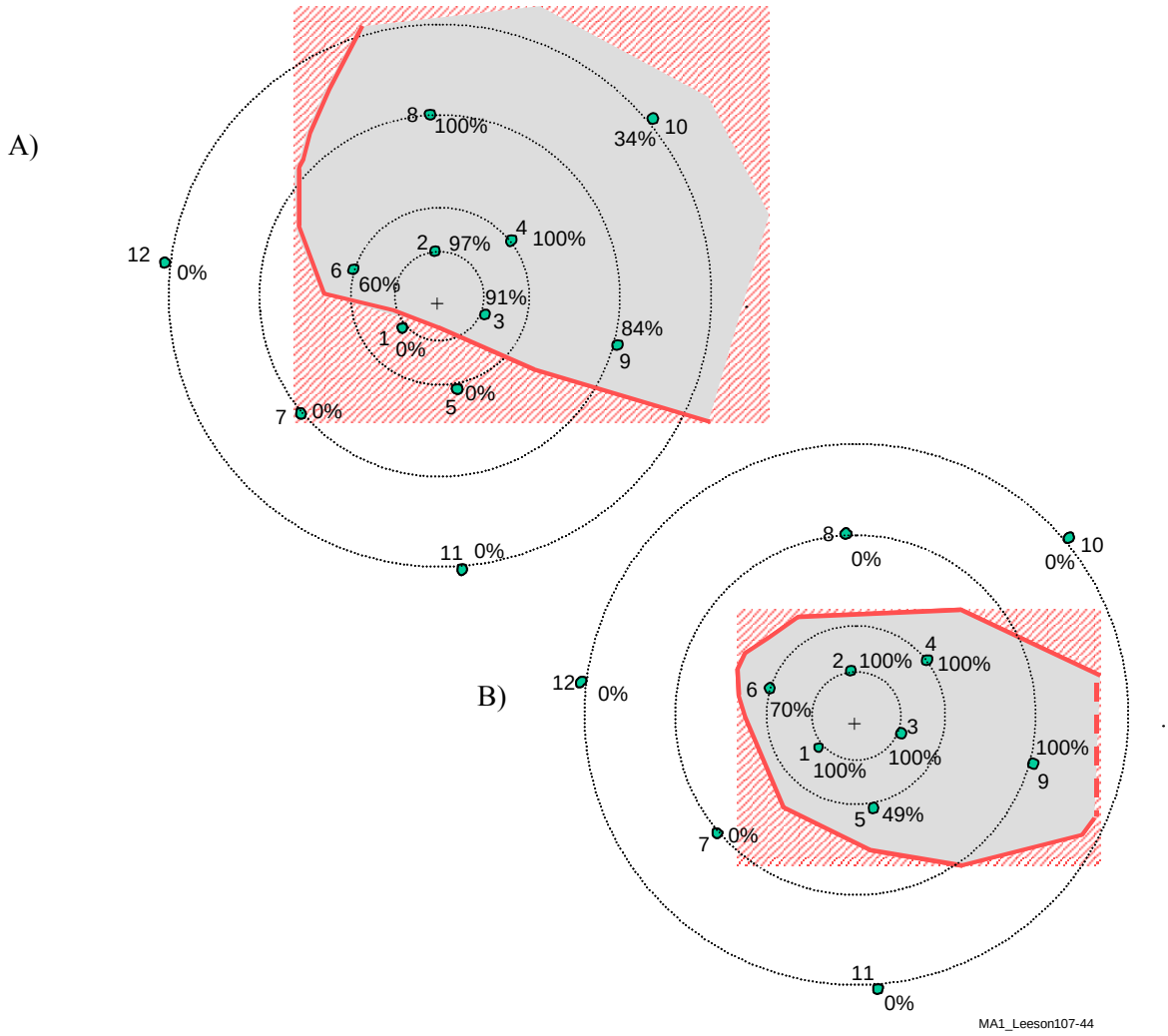

Figure 4. Plan View of Helium Concentrations at Deep Vadose Zone Monitoring Points at an Air Injection Depth of (A) 4.4 to 6 m bgs and (B) 3.8 to 4.1 m bgs, Port Hueneme, California

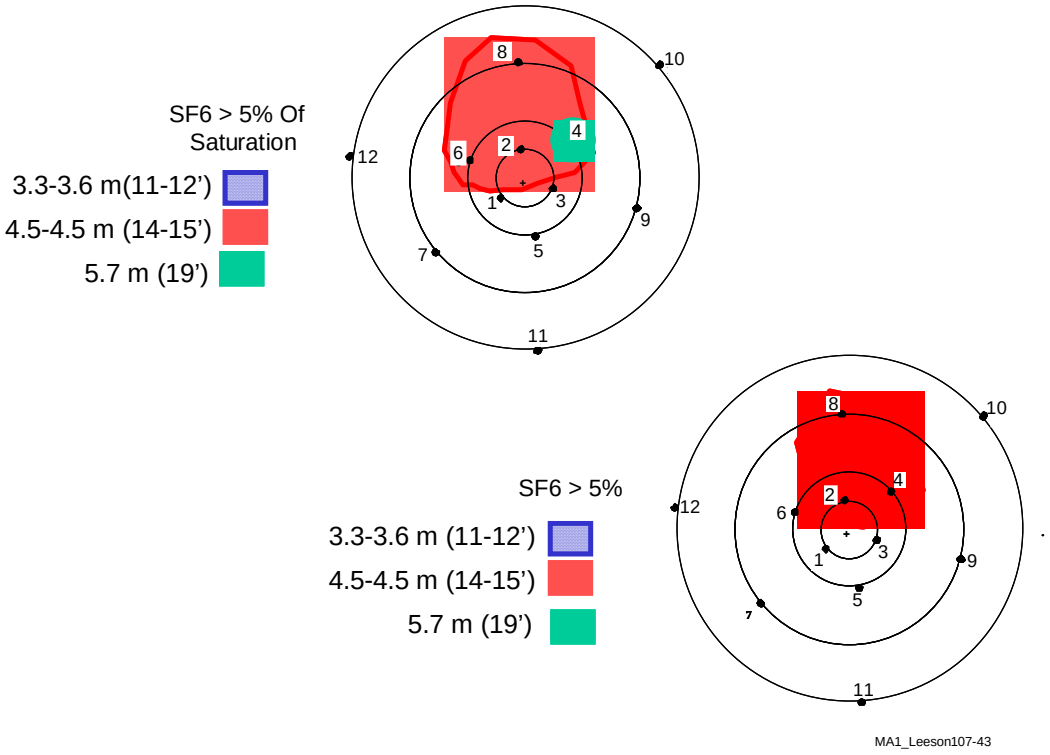

Figure 5. Appearance of SF_6 in Groundwater at an Injection Depth of (A) 4.4 to 6 m bgs and (B) 3.8 to 4.1 m bgs, Port Hueneme, California

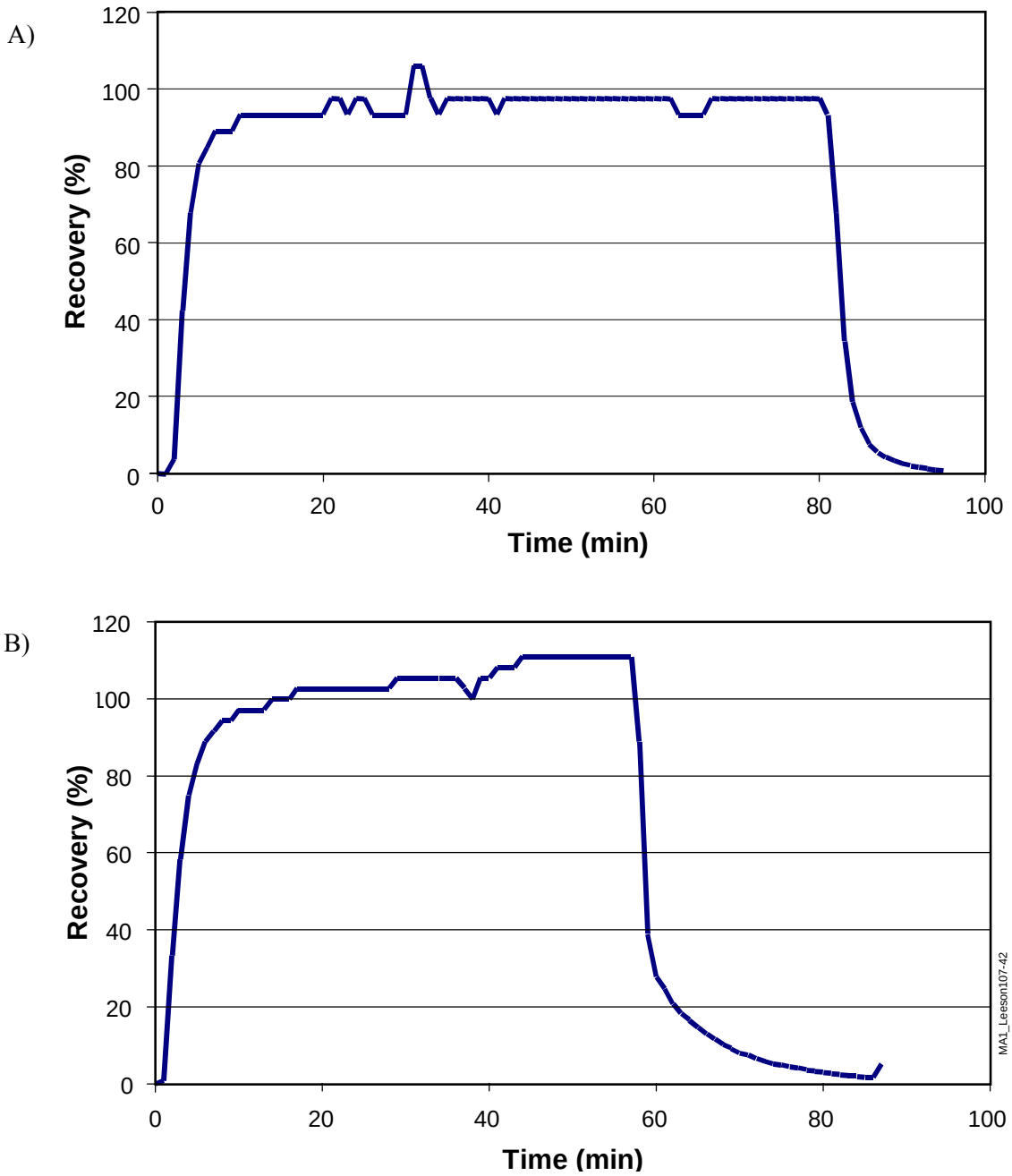

Figure 6. Helium Recovery versus Time During Injection into the (A) Shallow Injection Well and (B) Deep Injection Well, Eielson AFB, Alaska

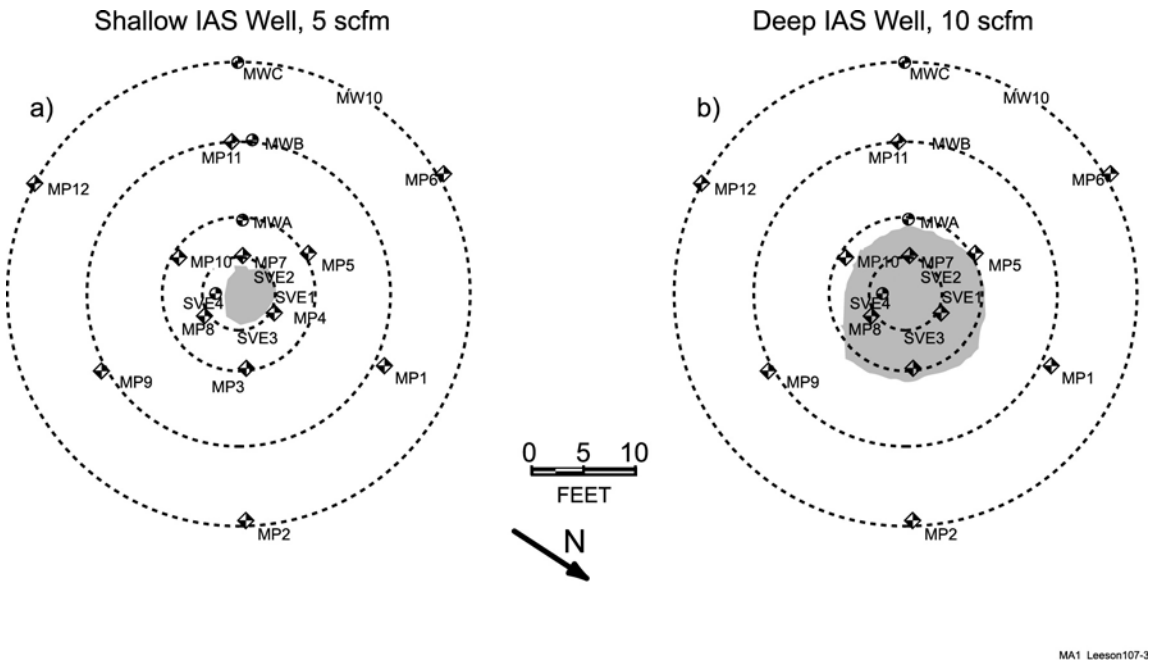

Figure 7. Plan View Showing Helium Appearance in the Deep Vadose Zone, Eielson AFB, Alaska

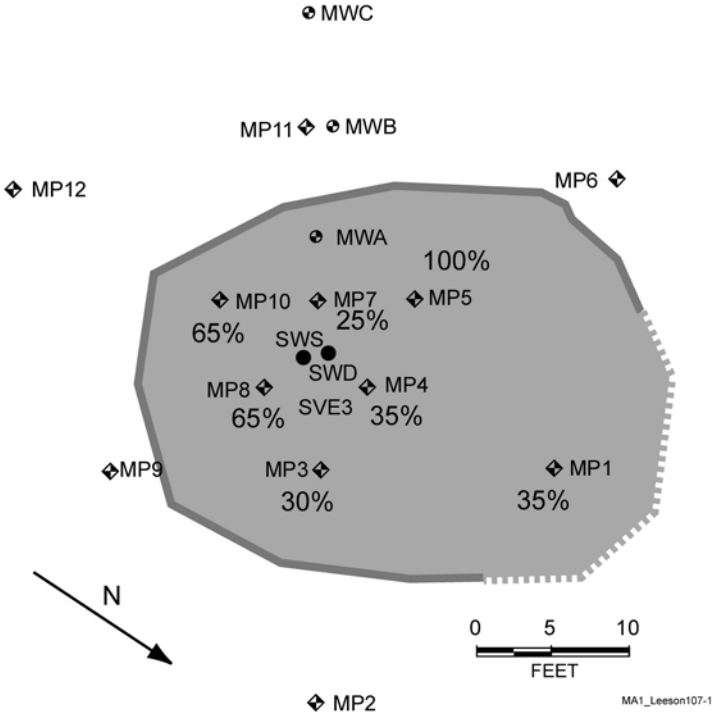

Figure 8. Plan View of SF_6 Distribution in Groundwater, Eielson AFB, Alaska

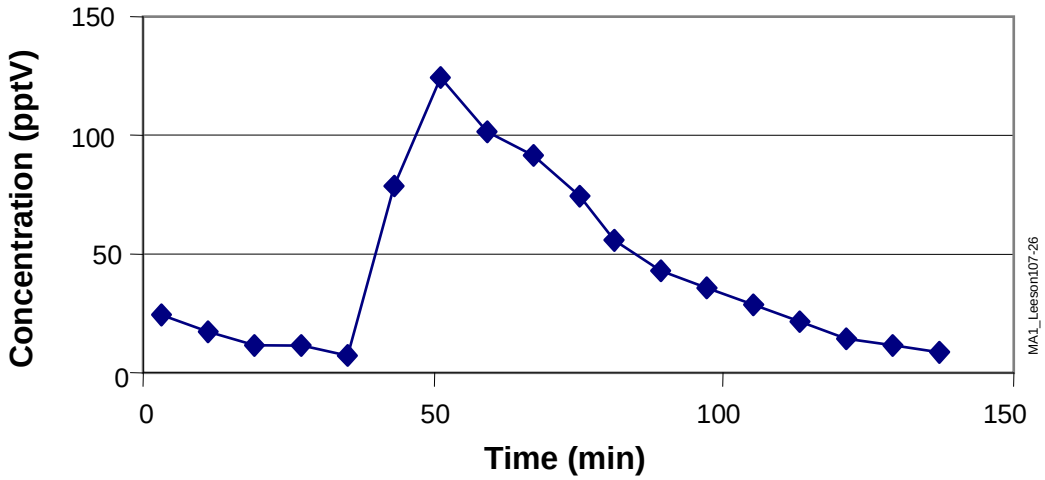

Figure 9. SF_6 Pulsed Tracer Test: Appearance of SF6 at an SVE Well, Eielson AFB, Alaska

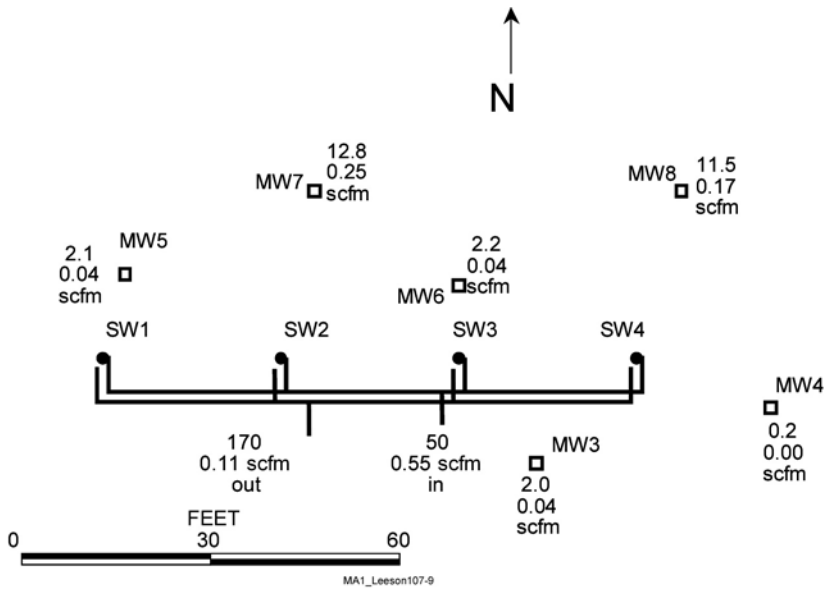

Figure 10. Location of Injection and Monitoring Wells and Results of Helium Tracer Data, Hill AFB, Utah

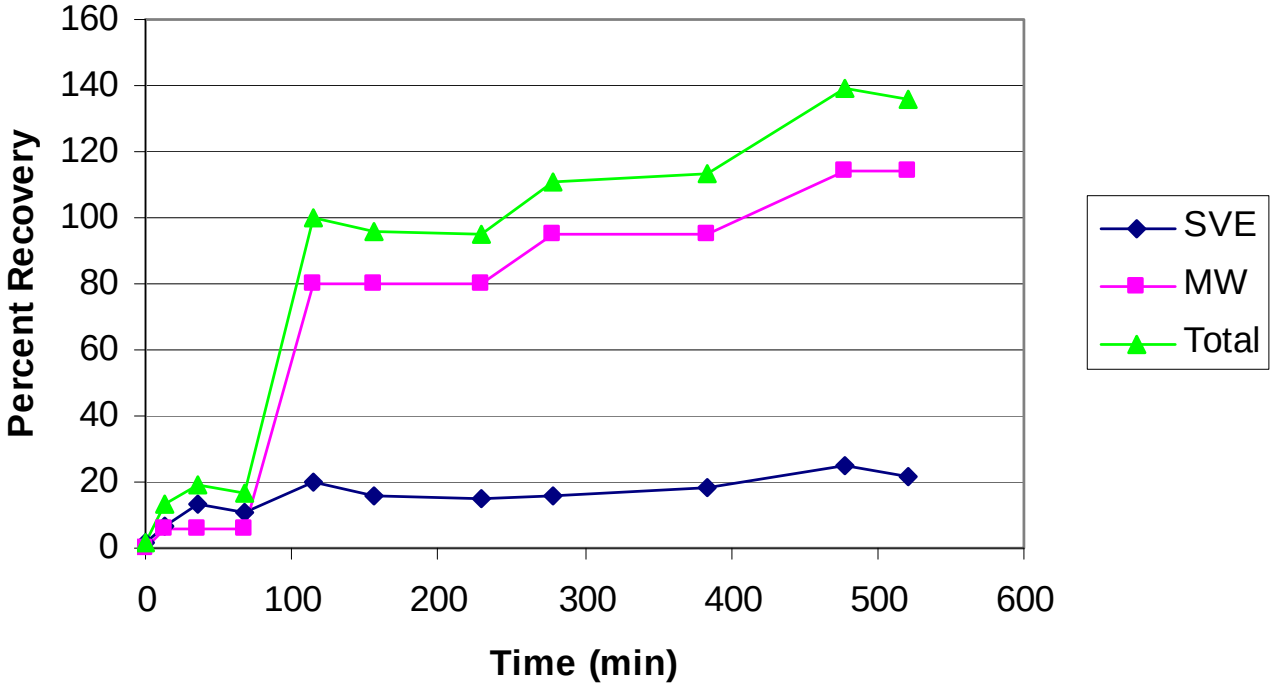

Figure 11. Helium Recovery versus Time, Hill AFB, Utah